U.S Department
of Transportation
**National Highway
Traffic Safety
Administration**

DOT HS 807 614
Final Report

December 1989

Development and Analysis of Intermediate Tripped Vehicle Rollover Model (ITRS)

The United States Government does not endorse products or manufactures. Trade or manufacturer's names appear only because they are considered essential to the object of this report.

Technical Report Documentation Page

1. Report No.	2. Government Accession No.	3. Recipient's Catalog No.

4. Title and Subtitle

DEVELOPMENT AND ANALYSIS OF INTERMEDIATE TRIPPED VEHICLE ROLLOVER MODEL (ITRS)

5. Report Date
DECEMBER 1989

6. Performing Organization Code

7. Author(s)
ANDRZEJ G. NALECZ, CLEVE BARE

8. Performing Organization Report No.
NALECZ - UMC - 1289

9. Performing Organization Name and Address

DEPARTMENT OF MECHANICAL & AEROSPACE ENGINEERING
UNIVERSITY OF MISSOURI-COLUMBIA
1006 ENGINEERING, COLUMBIA, MO 65211

10. Work Unit No. (TRAIS)

11. Contract or Grant No.
DTNH22-87-D-27174

12. Sponsoring Agency Name and Address

NATIONAL HIGHWAY TRAFFIC SAFETY ADMINISTRATION
U. S. DEPARTMENT OF TRANSPORATION
WASHINGTON, D.C. 20590

13. Type of Report and Period Covered
FINAL REPORT 88/89

14. Sponsoring Agency Code

15. Supplementary Notes

COTR: HOWELL K. BREWER/LLOYD H. EMERY

16. Abstract

This report describes the development of the Intermediate Tripped Rollover Simulation (ITRS) which can be used to investigate the rollover behavior of vehicles impacting a roadside curb. The eight degree-of-freedom ITRS model consists of sprung and unsprung masses interconnected through suspension elements. The ITRS model accounts for complete forward, lateral and directional dynamics and is capable of simulating vehicle's skidding motion, simultaneous and oblique impact of the front and rear wheels with a curb, and subsequent tripped rollover under a variety of initial conditions.

The ITRS vehicle model has been thoroughly examined for the energy exchanged between the vehicle components. Two energy based rollover functions were developed and examined to assess their ability to predict rollover. It has been shown that, if tripped rollover is to occur at critical speed, the dynamic criteria for rollover become satisfied when vehicle roll angles equal 9.5 and 11.5 degrees for impact angles of 0 and 25 degrees, respectively. The influence of all design parameters on vehicle rollover stability during both side and oblique impacts has been determined using the percentage sensitivity functions. The sensitivity results demonstrate that geometrical, mass and impact deformation characteristics have the largest influence on vehicle rollover propensity in tripped rollover situations.

17. Key Words	18. Distribution Statement
VEHICLE ROLLOVER VEHICLE DYNAMICS SENSITIVITY ANALYSIS	DOCUMENT IS AVAILABLE TO THE U.S. PUBLIC THROUGH THE NATIONAL TECHNICAL INFORMATION CENTER, SPRINGFIELD VIRGINIA 21161

19. Security Classif. (of this report)	20. Security Classif. (of this page)	21. No. of Pages	22. Price
UNCLASSIFIED	UNCLASSIFIED	206	

Form DOT F 1700.7 (8-72) Reproduction of completed page authorized

TABLE OF CONTENTS

TABLE OF CONTENTS (Concluded)

LIST OF FIGURES

LIST OF FIGURES (Continued)

LIST OF FIGURES (Continued)

Page

LIST OF FIGURES (Continued)

Page

LIST OF FIGURES (Concluded)

1. INTRODUCTION

The National Highway Traffic Safety Administration (NHTSA) has been increasingly concerned about the rising number of single vehicle rollover accidents. One of the primary reasons behind this concern is almost twice higher fatality rate associated with accidents involving rollover compared with those accidents which do not involve rollover (2.32% versus 1.21%) [1]. Rollover accidents are one of the most hazardous events based on both the frequency of occurrence and severity level of occupant injuries. According to data collected by the 1985 National Accident Sampling System (NASS) [2], over 20% of 18,400 fatalities occurred in rollover accidents, while these accidents accounted for 7% of all fatal accidents.

In general, vehicle rollover accidents can be classified into two distinct types, tripped rollover and untripped or maneuver-induced rollover. Vehicle tripped rollover occurs when a vehicle rolls over after striking a tripping device such as a rigid obstacle/curb, soft soil, or other similar terrain feature and untripped (maneuver-induced) rollover results when abrupt maneuvers and/or excessive driver inputs cause vehicle rollover. A large majority of single vehicle rollover accidents are classified as tripped rollovers.

Static analysis of vehicle rollover is frequently used to determine vehicle rollover propensity [4], [5]. Primarily, the Static Rollover Stability Factor (SRSF), defined as the ratio of half track width to CG height, is utilized to compare the rollover tendencies of various vehicles. In general, increasing SRSF (by increasing track width or decreasing vehicle CG height) will decrease a vehicle's rollover propensity. The determination of a vehicle rollover propensity should not be based solely on static analysis. Vehicle rollover is complex behavior which is dependent upon both static and dynamic factors. While a static analysis of vehicle rollover can provide valuable information, it still cannot completely determine the direct and indirect effect of all vehicle design characteristics on rollover. Dynamic couplings between motions, inertia forces, as well

as vehicle subsystem behavior (suspension, tires, ect.), all can have a significant influence on system response during rollover situations. In addition, assessment of rollover stability based solely on static considerations cannot accurately determine the likelihood of a vehicle to become involved in a rollover accident.

If one wishes to increase the rollover stability of a vehicle it is essential that he understands the influence of design parameters on rollover behavior. A number of studies have examined accident data in an attempt to find statistical correlations between different vehicle parameters and the likelihood of the vehicle involvement in a rollover accident. For example, a study conducted by the Texas Transportation Institute [3] has shown a strong correlation between vehicle curb weight (or interrelated parameters) and incidence of rollover. While these studies can provide useful information and point out areas for analytical investigation, they do have several limitations. First, studies such as these can only show how parameters relate to rollover involvement, and cannot provide any information as to the reasons behind the results. Secondly, parameters which are indirectly interrelated, such as wheelbase and vehicle weight (e.g. longer, larger vehicles are heavier) prevent such studies from making definitive conclusions into the influence of specific vehicle parameters on rollover propensity. Studies performed by the CALSPAN Corporation [1] have shown that wheelbase, curb weight, and track width are highly interrelated, especially among American-made cars.

An analysis of the dynamic response of a vehicle prior to, and during rollover can provide valuable information relating vehicle design and rollover safety. Dynamic rollover analysis can account for couplings of various interrelated vehicle motions. The influence of viscous and elastic suspension elements on rollover can be also found using dynamic analysis. In addition, a vehicle's dynamic response can be used to investigate the effectiveness of various rollover stability measures such as energy functions which are capable of incorporating both static and dynamic factors.

Systems Technology Incorporated (STI), under sponsorship of the NHTSA, developed the Vehicle Tripped Rollover Model [6] which simulates the dynamic response of a vehicle skidding laterally into a roadside curb. The eight degree of freedom model provides system response of a vehicle and is capable of finding a vehicle's critical rollover speed (the minimum speed required for vehicle rollover). The University of Missouri-Columbia (UMC) performed an investigation into the effects of vehicle design characteristics on rollover propensity using the STI model [7], [14]. Sensitivity methods developed by Dr. A. G. Nalecz at UMC [8] - [13] were utilized to perform a complete and efficient sensitivity analysis of all vehicle parameters. The concept of an energy based function for vehicle rollover prediction (Rollover Prevention Energy Reserve (RPER)) was a direct result of this project. The results obtained during the sensitivity analysis were reasonable and agreed with existing information concerning rollover behavior and propensity. However, some problems associated with STI's Vehicle Tripped Rollover Model prevented a complete investigation into vehicle rollover propensity. All forward dynamics were neglected within the model, preventing investigation of many rollover cases. Additionally, a number of dynamic couplings which can influence a vehicle's rollover behavior were ignored in the system's equations of motion. Finally, the limited range of heading angles which could be investigated using STI's model precluded investigation of many of tripped rollover situations.

The Intermediate Tripped Rollover Simulation (ITRS) project was initiated to correct the shortcomings in STI's Vehicle Tripped Rollover Model. The eight degree-of-freedom ITRS models a vehicle's skidding motion, impact of the front and rear wheels with a roadside curb, and the subsequent tripped rollover motion. Two masses, one sprung and one unsprung, are interconnected with spring-damper elements and a pin connection. The vehicle's unsprung mass has six translational and rotational degrees-of-freedom and its sprung mass is free to roll and heave relative to the unsprung

mass. The equations of motion for the ITRS model were derived by extending the Newton-Euler equations to allow the mass center to move relative to the non-inertial reference system. All dynamic couplings and mass properties were included in extended equations of motion in accordance with the mechanical representation of the physical system.

A non-linear vehicle/curb impact model has been developed which is capable of simulating plastic (permanent) and elastic (recoverable) deformations of the suspension elements, tires, and vehicle frame. Oblique curb impacts are modelled with longitudinal and lateral forces calculated separately for the front and rear wheel/suspension/axle subsystems. In addition, a tire/curb scrub force was included for impact situations with motion along the tire/curb interface.

Validation of the ITRS was performed by examining the vehicle's system response and the energy exchange between the vehicle subsystems. From the principles of work and energy for isolated systems, it is known that while energy can be exchanged between various system components, the total system energy must always decrease due to the dissipative forces which act on the system. All vehicle energies were examined individually and together in a number of different rollover and non-rollover situations.

During the analysis of ITRS simulation results, several energy functions were developed and investigated for their ability to assess rollover stability of vehicles. Kinetic energy, as well as elastic and gravitational potential energies were analyzed for their possible influence on vehicle rollover. Rollover prediction criteria for the energy functions was developed and verified using a number of different sets of initial conditions. The system response of the vehicle has been provided for each situation which was investigated. Finally, sensitivity analysis of all vehicle parameters on the rollover energy functions was performed. Oblique curb impacts, as well as lateral impacts were investigated and vehicle design characteristics

were ranked in order of importance in both rollover and non-rollover situations. The percentage sensitivity functions were utilized to provide the clearest physical interpretation of results and facilitate the ranking of the influence of various design and environmental characteristics on vehicle rollover propensity.

2. DEVELOPMENT OF ITRS TRIPPED ROLLOVER MODEL

2.1 PHYSICAL MODEL

The three-dimensional light vehicle model developed in this project (Figure 1) is a two mass model which has eight-degrees of freedom. One mass of the vehicle system is used to represent the combined unsprung masses of the front and rear suspension systems, the other mass represents the sprung mass of the vehicle chassis. These two masses are connected by pins at the front and rear of the vehicle and have the freedom to slide in vertical slots within the unsprung mass. In addition, four spring elements and viscous dampers are used to represent the front and rear suspension systems connecting the two masses. To allow complete modeling of any light vehicle, no planes

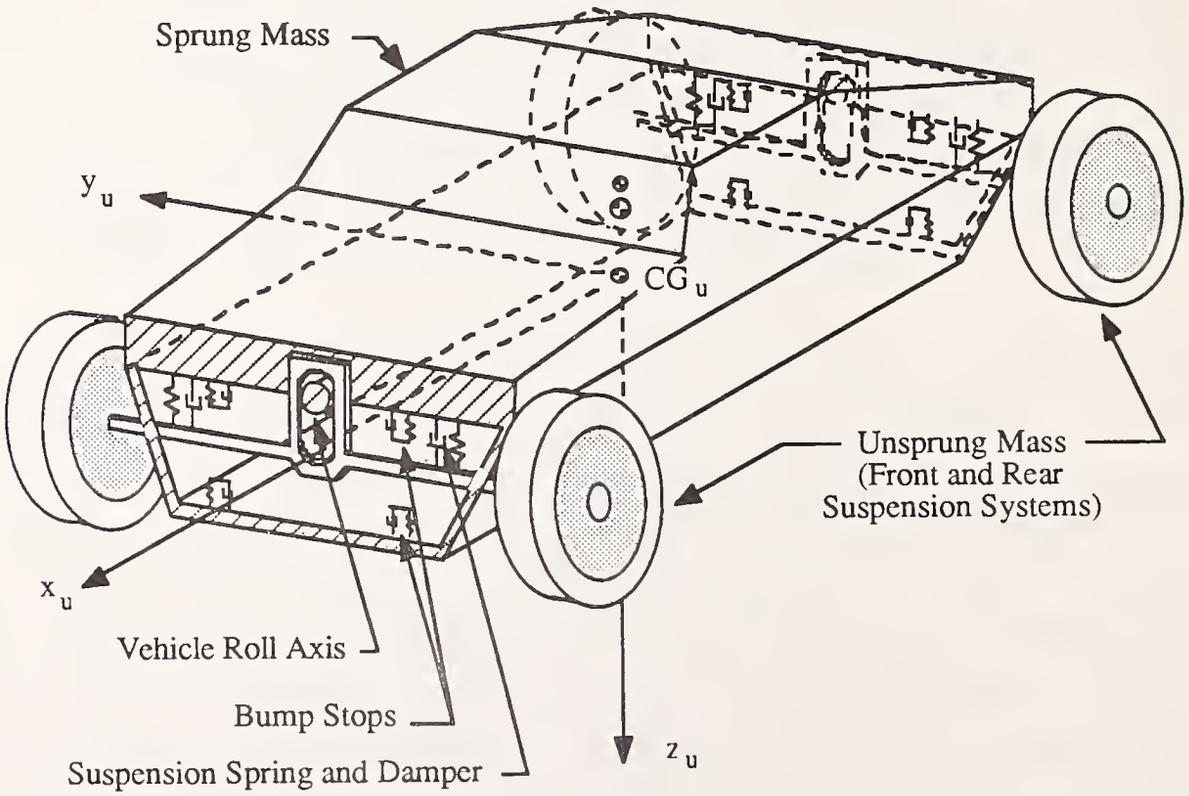

Figure 1. ITRS Vehicle Model.

of symmetry were assumed and all elements within the inertia tenser were included. The ITRS accounts for the three translational motions and three rotational motions for the unsprung mass and sprung mass roll and heave motions.

The following eight generalized coordinates were used to describe vehicle position.

$q_1 = x$ longitudinal position of the unsprung mass CG (in the inertial reference system)

$q_2 = y$ lateral position of the unsprung mass CG (in the inertial reference system)

$q_3 = z_u$ vertical position of the unsprung mass CG (in the inertial reference system)

$q_4 = z_s$ vertical position of the sprung mass pivot point (in the inertial reference system)

$q_5 = \phi_u$ absolute roll angle of unsprung mass

$q_6 = \phi_s$ absolute roll angle of sprung mass

$q_7 = \theta$ vehicle pitch angle

$q_8 = \psi$ vehicle yaw angle

One absolute and three non-inertial reference systems (NIRS) were utilized within ITRS (Figure 2) and are described below.

OXYZ - absolute reference system

oxyz - non-inertial reference system (NIRS) which yaws and translates with the vehicle and whose x and y axes are in the ground plane

$o_u x_u y_u z_u$ - non-inertial reference system (NIRS) fixed to the unsprung mass CG

$o_s x_s y_s z_s$ - non-inertial reference system (NIRS) fixed to the sprung mass CG

In order to simplify the appearance of the equations, throughout this report terms associated with coordinate system transformations are

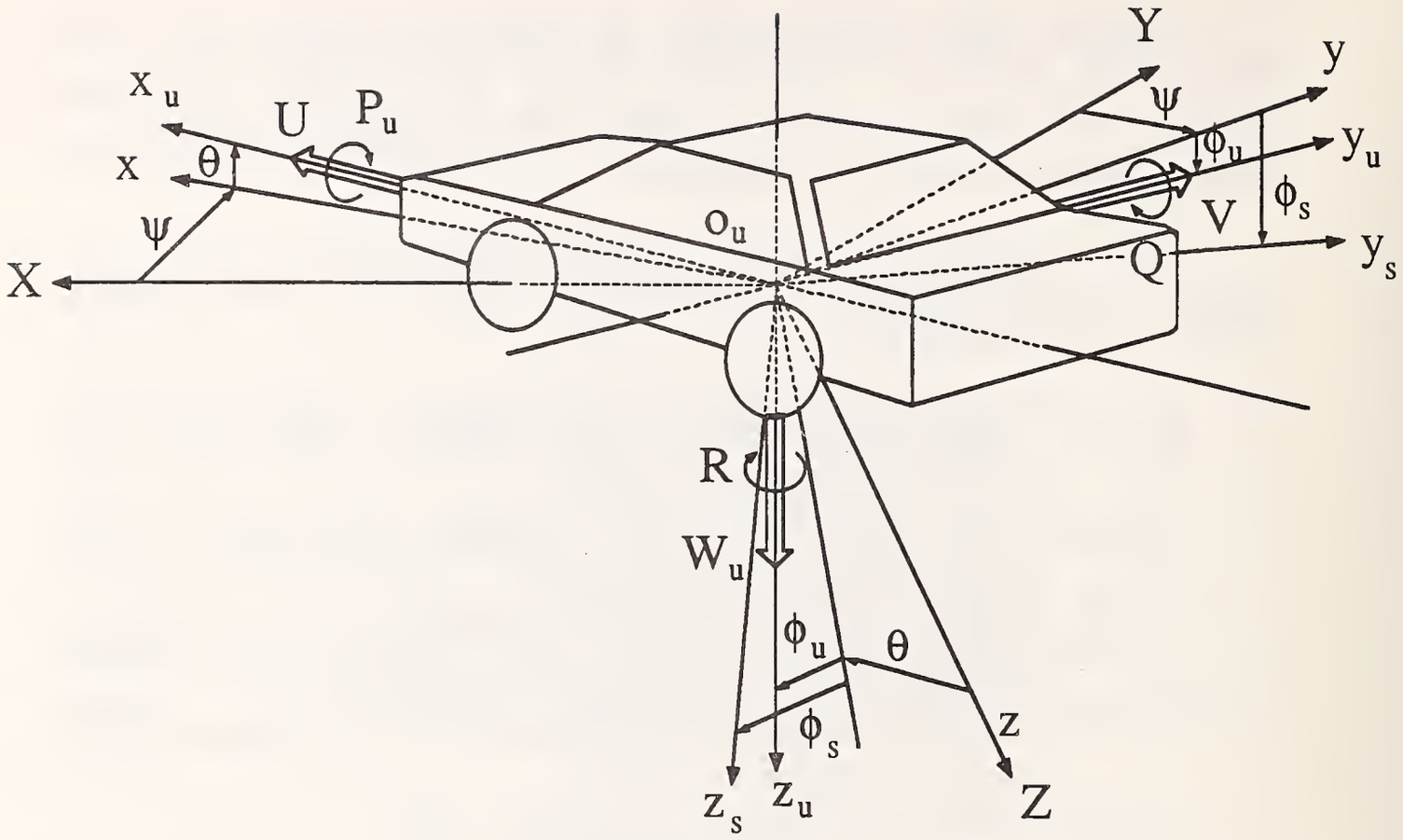

Figure 2. ITRS Reference Systems.

written in the form T_{ij}, where, this term represents the rotation transformation from the "i" axis to the "j" axis. All T_{ij} terms introduced are defined in Appendix A.

During development of the ITRS simulation, the following sequence of rotations were applied to the unsprung mass NIRS $o_u x_u y_u z_u$ (Figure 2):

1) rotation about z_u through yawing angle ψ
2) rotation about y_u through pitch angle θ
3) rotation about x_u through roll angle ϕ_u

The sprung mass NIRS $o_s x_s y_s z_s$ underwent a similar sequence of rotations which differed only by roll angle ϕ_s. The sprung mass sequence of rotation is given below:

$$\begin{bmatrix} \dot{x} \\ \dot{y} \\ \dot{z}_u \end{bmatrix} = [\,T\,] \begin{bmatrix} U \\ V \\ W_u \end{bmatrix} \tag{3}$$

$$\dot{z}_s = -(U - Qh)\sin\theta + (V + P_u h)\sin\phi_u\cos\theta + W_s\cos\phi_u\cos\theta$$

where,

$$[\,T\,] = \begin{bmatrix} \cos\theta\cos\psi & \sin\phi_u\sin\theta\cos\psi & \cos\phi_u\sin\theta\cos\psi \\ & -\cos\phi_u\sin\psi & +\sin\phi_u\sin\psi \\ \cos\theta\sin\psi & \sin\phi_u\sin\theta\sin\psi & \cos\phi_u\sin\theta\sin\psi \\ & +\cos\phi_u\cos\psi & -\sin\phi_u\cos\psi \\ -\sin\theta & \sin\phi_u\cos\theta & \cos\phi_u\cos\theta \end{bmatrix}$$

2.2 MATHEMATICAL MODEL

The equations of motion for the unsprung mass of the ITRS vehicle model were written using the Newton-Euler equations of motion for a rigid body. In order to derive the equations of motion for the sprung mass it was necessary to extend the Newton-Euler equations to allow motion of the sprung mass CG relative to the NIRS. By utilizing the Newton-Euler methodology to obtain the equations of motion, all dynamic couplings between the vehicle motions were included. The two masses were connected through the suspension system and by three pin forces, two acting laterally and one acting longitudinally in the unsprung mass reference system (Figures 1, 3

and 4). In order to determine each pin force it was necessary to write three additional equations of constraints and find their solutions. Thus, in order to obtain the eight final equations of motion it is necessary to derive a total of eleven equations for the sprung and unsprung masses. All of the equations of motions and equations of constraints were written in the unsprung NIRS $o_u x_u y_u z_u$.

2.2.1 Development of Unsprung Mass Equations of Motion

The free body diagram of unsprung mass, in its side, cross sectional and top view is shown in Figures 3, 4 and 5. The external forces acting on the unsprung mass include:

the gravitational force:	$M_u g$
combined spring and damping suspension forces:	$F_{slF}, F_{slR}, F_{srF}, F_{srR}$
connecting pin lateral and longitudinal reactions:	F_F, F_R, F_t
longitudinal tire frictional forces:	$F_{xlF}, F_{xlR}, F_{xrF}, F_{xrR}$
lateral tire frictional forces:	$F_{ylF}, F_{ylR}, F_{yrF}, F_{yrR},$
vehicle/curb impact forces:	$F_{dxF}, F_{dxR}, F_{dF}, F_{dR}$
tire/curb scrubbing forces:	F_{dsF}, F_{dsR}

The six equations of motion for the unsprung mass can be written as follows.

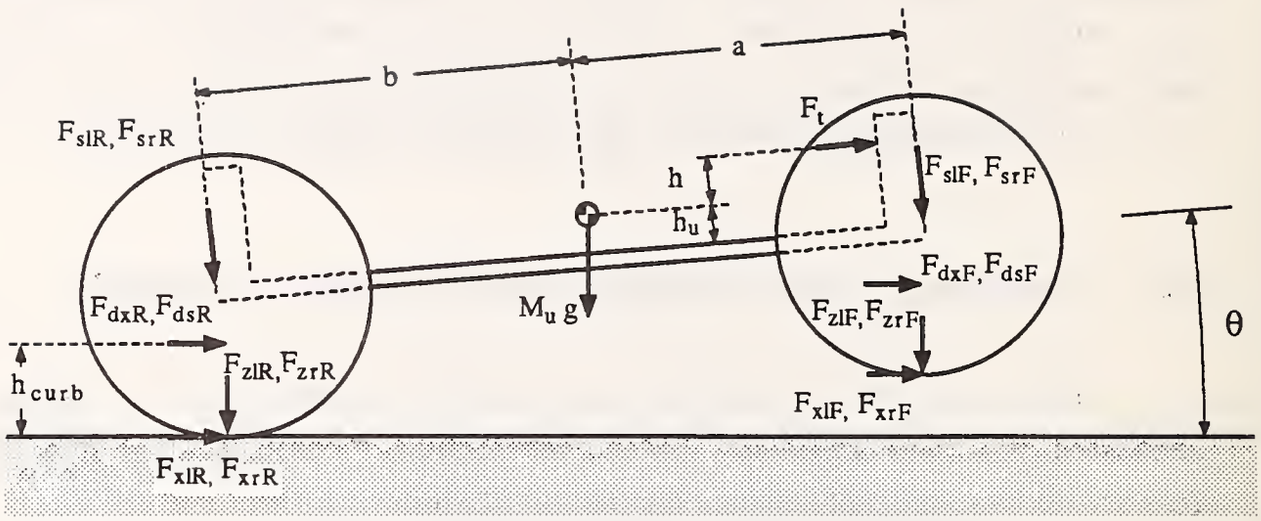

Figure 3. Side View of Free Body Diagram of Unsprung Mass.

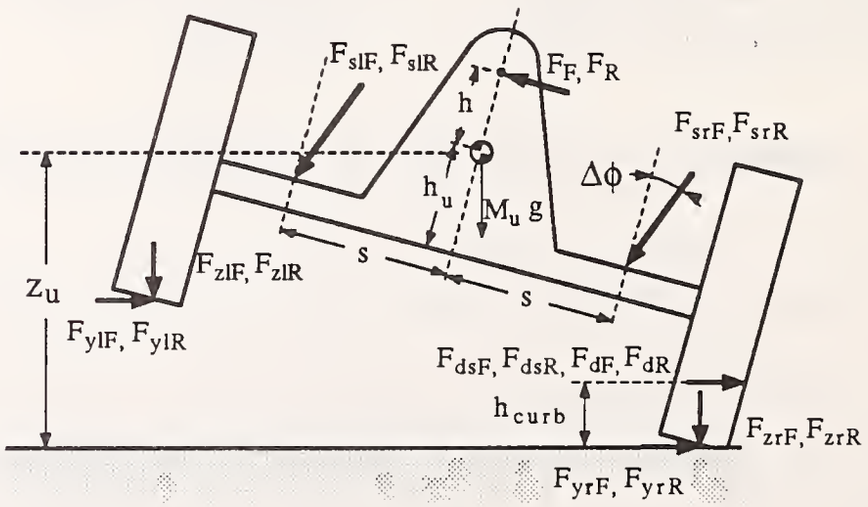

Figure 4. Cross Sectional View of Free Body Diagram of Unsprung Mass.

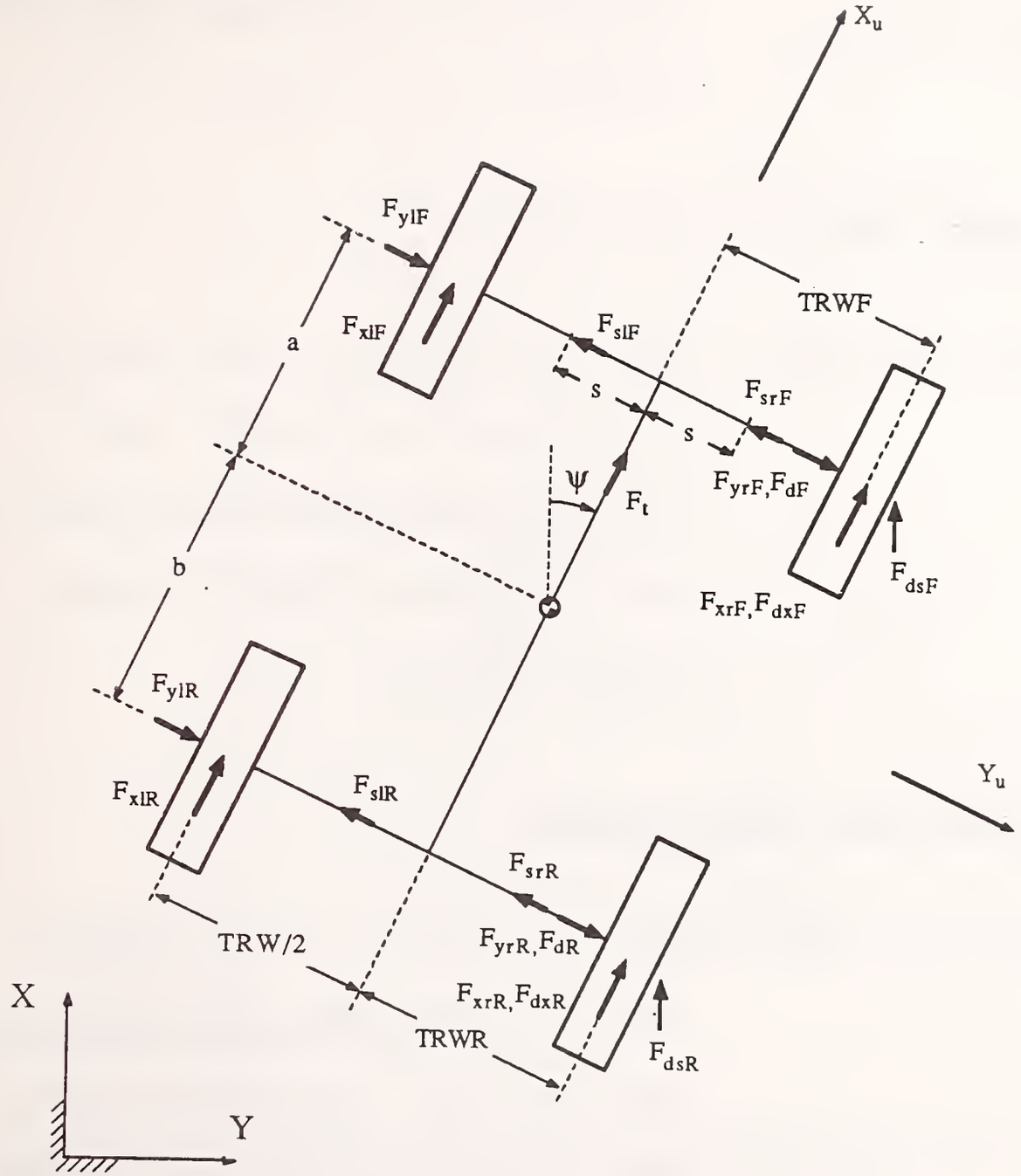

Figure 5. Top View of Free Body Diagram of Unsprung Mass.

Unsprung Mass Longitudinal Equation

$$M_u(\dot{U} - RV + WQ) = F_t + (F_{xlF} + F_{xlR} + F_{xrF} + F_{xrR} + F_{dxF} + F_{dxR})T_{xxu} + (F_{zlF} + F_{zlR} + F_{zrF} + F_{zrR})T_{zxu} + (F_{dsF} + F_{dsR})T_{xaxu} + M_u g T_{zxu} \quad (4)$$

Unsprung Mass Lateral Equation

$$M_u(\dot{V} - W_u P_u + UR) = -(F_F + F_R) - (F_{slF} + F_{slR} + F_{srF} + F_{srR})\sin(\Delta\phi) + (F_{ylF} + F_{ylR} + F_{yrF} + F_{yrR} + F_{dF} + F_{dR})T_{xxu} + (F_{xlF} + F_{xlR} + F_{xrF} + F_{xrR} + F_{dxF} + F_{dxR})T_{xyu} + (F_{zlF} + F_{zlR} + F_{zrF} + F_{zrR})T_{zyu} + M_u g T_{zyu} + (F_{dsF} + F_{dsR})T_{xayu} \quad (5)$$

Unsprung Mass Vertical Equation

$$M_u(\dot{W}_u - UQ + VP_u) = (F_{xlF} + F_{xlR} + F_{xrF} + F_{xrR} + F_{dxF} + F_{dxR})T_{xzu} + (F_{ylF} + F_{ylR} + F_{yrF} + F_{yrR} + F_{dF} + F_{dR})T_{xzu} + (F_{slF} + F_{slR} + F_{srF} + F_{srR})\sin(\Delta\phi) + M_u g T_{zzu} + (F_{dsF} + F_{dsR})T_{xazu} + (F_{zlF} + F_{zlR} + F_{zrF} + F_{zrR})T_{xzu} \quad (6)$$

Unsprung Mass Rolling Equation

$$I_{xxu}\dot{P}_u - I_{xyu}(\dot{Q} - P_uR) - I_{xzu}(\dot{R} + P_uQ) + (I_{zzu} - I_{yyu})QR - I_{yzu}(Q^2 - R^2)$$

$$= -(F_F + F_R)\,h + (F_{srF} + F_{srR} - F_{slF} - F_{slR})\cos(\Delta\phi)S$$

$$+ (F_{slF} + F_{slR} + F_{srF} + F_{srR})\sin(\Delta\phi)\,h_u$$

$$+ (F_{xrF} + F_{dxF})T_{xzu}\,TRWF + (F_{xrR} + F_{dxR})T_{xzu}\,TRWR$$

$$- (F_{xlF} + F_{xlR})T_{xzu}\frac{TRW}{2}$$

$$- (F_{xlF} + F_{xlR} + F_{xrF} + F_{xrR})T_{xyu}(h_u + T_r)$$

$$- (F_{ylF} + F_{ylR} + F_{yrF} + F_{yrR})T_{yyu}(h_u + T_r)$$

$$- (F_{zlF} + F_{zlR} + F_{zrF} + F_{zrR})T_{zyu}\,(h_u + T_r)$$

$$+ (F_{yrF} + F_{dF})T_{yzu}\,TRWF + (F_{yrR} + F_{dR})T_{yzu}\,TRWR$$

$$- (F_{ylF} + F_{ylR})T_{yzu}\frac{TRW}{2} - (F_{zlF} + F_{zlR})T_{zzu}\frac{TRW}{2}$$

$$+ (F_{zrF}T_{zzu} + F_{dsF}T_{xazu})\,TRWF + (F_{xrR}T_{zzu} + F_{dsR}T_{xazu})\,TRWR$$

$$- \{(F_{dsF} + F_{dsR})T_{xayu} + (F_{dxF} + F_{dxR})T_{xyu}$$

$$+ (F_{dF} + F_{dR})T_{yyu}\}\left(h + h_u + T_r - \frac{h_{curb}}{\cos\phi_u\cos\theta}\right) \qquad (7)$$

Unsprung Mass Yawing Equation

$$I_{zzu}\dot{R} - I_{xzu}(\dot{P}_u - QR) - I_{yzu}(\dot{Q} + P_uR) + (I_{yyu} - I_{xxu})\,P_uQ - I_{xyu}(P_u^2 - Q^2)$$

$$= \{F_R + (F_{srR} + F_{slR})\sin(\Delta\phi)\}b - \{F_F + (F_{srF} + F_{slF})\sin(\Delta\phi)\}a$$

$$- (F_{yrR} + F_{ylR} + F_{dR})T_{yyu}b + (F_{yrF} + F_{ylF} + F_{dF})T_{yyu}a$$

$$- (F_{xrR} + F_{xlR} + F_{dxR})T_{xyu}b + (F_{zrF} + F_{xlF} + F_{dxF})T_{xyu}a$$

$$- (F_{zrR} + F_{zlR})T_{zyu}b + (F_{zrF} + F_{zlF})T_{zyu}a$$

$$- F_{dsR}T_{xayu} + F_{dsF}T_{xayu}$$

$$- \{F_{zrF}T_{zxu} + (F_{xrF} + F_{dxF})T_{xxu} + F_{dsF}T_{xaxu}\}\ TRWF$$

$$- \{F_{zrR}T_{zxu} + (F_{xrR} + F_{dxR})T_{xxu} + F_{dsR}T_{xaxu}\}\ TRWR$$

$$+ \{(F_{xlF} + F_{xlR})T_{xxu} + (F_{zlF} + F_{zlR})T_{zxu}\}\ \frac{TRW}{2} \qquad (8)$$

Unsprung Mass Pitching Equation

$$I_{yyu}\dot{Q} - I_{xyu}(\dot{P}_u + QR) - I_{yzu}(\dot{R} - P_uQ) + (I_{xxu} - I_{zzu})P_uR + I_{xzu}(P_u^2 - R^2)$$

$$= \{(F_{xrR} + F_{xlR})T_{xzu} + F_{dxR}T_{xzu} + (F_{yrR} + F_{ylR} + F_{dR})T_{yzu}$$

$$+ (F_{zrR} + F_{zlR})T_{zzu} + (F_{srR} + F_{slR})\cos(\Delta\phi)\}b$$

$$- \{(F_{xrF} + F_{xlF})T_{xzu} + F_{dxF}T_{xzu} + (F_{yrF} + F_{ylF} + F_{dF})T_{yzu}$$

$$+ (F_{zrF} + F_{zlF})T_{zzu} + (F_{srF} + F_{slF})\cos(\Delta\phi)\}a$$

$$+ (F_{xlF} + F_{xlR} + F_{xrF} + F_{xrR})T_{xxu}(h_u + T_r)$$

$$+ (F_{zlF} + F_{zlR} + F_{zrF} + F_{zrR})T_{zxu}(h_u + T_r)$$

$$- (F_{dxF} + F_{dxR})T_{xxu}\left(h_u + T_r - \frac{h_{curb}}{\cos\phi_u \sin\phi_u}\right) - F_t h \qquad (9)$$

2.2.2 Development of Sprung Mass Equations of Motion

In order to derive dynamic equations of motion of sprung mass in the NIRS reference system $O_u x_u y_u z_u$ (sprung mass CG does not coincide with origin of $O_u x_u y_u z_u$ system), the Newton-Euler equations of motion were extended to allow for motion of sprung mass relative to this NIRS system.

Position of arbitrary point P' of sprung mass (Figure 6) in moving reference system $O_u x_u y_u z_u$ is given by vector $\bar{r}_{p'}$

$$\bar{r}_{p'} = \bar{r}_1 + \bar{r}_2 + \bar{r}_s \qquad (10)$$

where,

$\bar{r}_1$ - position vector of pivot point P ($\bar{h}$)

$\bar{r}_2$ - vector from the pivot point P to sprung mass CG ($\bar{h}_{ra}$)

$\bar{r}_s$ - position vector of components x_s, y_s, z_s of point P' in NIRS $O_s x_s y_s z_s$.

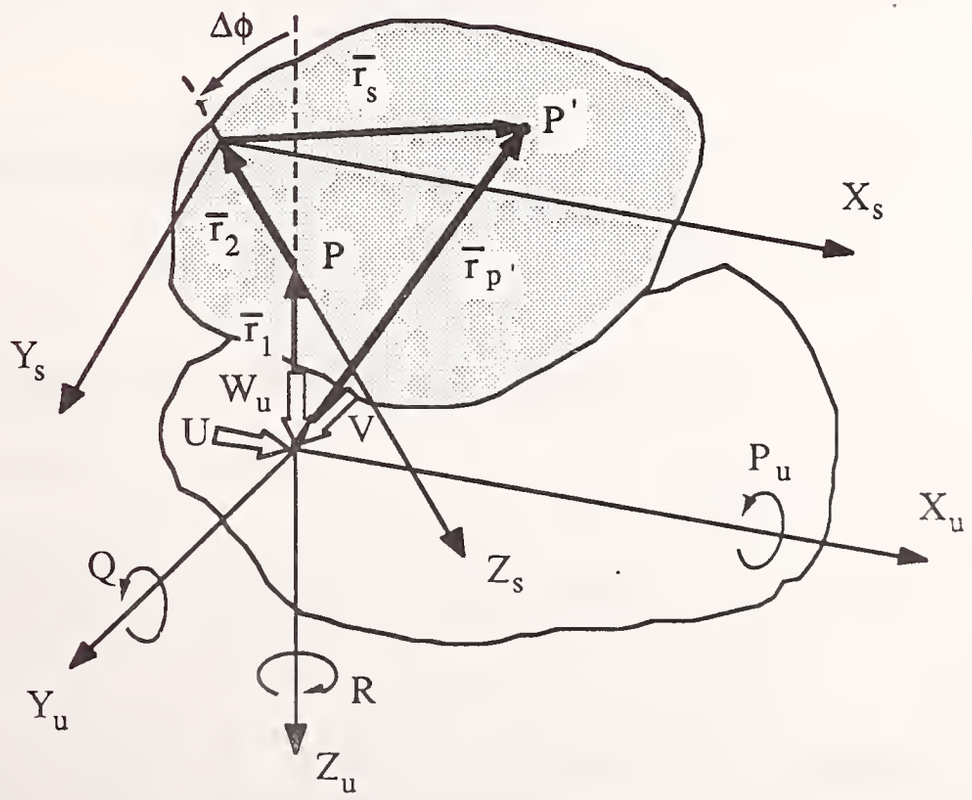

Figure 6. Position of Point P' of Sprung Mass In NIRS.

Based on kinematic relations between both sprung mass and unsprung mass NIRS reference systems, the position vector $\bar{r}_{p'}$ in $O_u x_u y_u z_u$ system can be written:

$$\bar{r}_{p'} = x_s\bar{i} + (y_s\cos(\Delta\phi) - z_s\sin(\Delta\phi) + h_{ra}\sin(\Delta\phi))\bar{j} + (-h + y_s\sin(\Delta\phi) + z_s\cos(\Delta\phi) - h_{ra}\cos(\Delta\phi))\bar{k} \quad (11)$$

The velocity of point P' is determined by:

$$\bar{V}_{p'} = u\bar{i} + v\bar{j} + w\bar{k} \quad (12)$$

where, u, v and w are velocity components parallel to x_u, y_u, z_u axes and are given by following expressions:

$$u = U - Ry_s\cos(\Delta\phi) + Rz_s\sin(\Delta\phi) + Qz_s\cos(\Delta\phi) + Qy_s\sin(\Delta\phi) - Rh_{ra}\sin(\Delta\phi) - Qh - Qh_{ra}\cos(\Delta\phi)$$

$$v = V - P_s y_s\sin(\Delta\phi) - P_s z_s\cos(\Delta\phi) + Rx_s - P_s h_{ra}\cos(\Delta\phi) + P_u h$$

$$w = W_u - \dot{h} + P_s y_s\cos(\Delta\phi) - P_s z_s\sin(\Delta\phi) - Qx_s + P_s h_{ra}\sin(\Delta\phi)$$

The sprung mass equations of motion in $O_u x_u y_u z_u$ reference system can be obtained by summing the forces and moments acting on individual particles which make up the sprung mass:

$$\Sigma X_s = \Sigma \dot{u}\, dM_s$$

$$\Sigma Y_s = \Sigma \dot{v}\, dM_s$$

$$\Sigma Z_s = \Sigma \dot{w}\, dM_s \qquad (13)$$

$$\Sigma L_s = \Sigma(y\dot{w} - z\dot{v})dM_s$$

$$\Sigma M_s = \Sigma(z\dot{u} - x\dot{w})dM_s$$

$$\Sigma N_s = \Sigma(x\dot{v} - y\dot{u})dM_s$$

It should be noted that only five equations of motion of sprung mass are needed for the development of ITRS vehicle model. Two of these equations should describe the sprung mass roll and heave motions and the remaining three should determine the unknown pin reactions.

First, the inertia forces and moments acting on sprung mass were determined and they are shown below.

Sprung Mass Longitudinal Inertia Force

$$\begin{aligned}\Sigma X_s &= \Sigma \dot{u}\, dM_s \\ &= M_s [\, \dot{U} - V(R\cos(\Delta\phi) - Q\sin(\Delta\phi)) + W_u(R\sin(\Delta\phi) + Q\cos(\Delta\phi)) \\ &\quad - h\{P_u(R\cos(\Delta\phi) - Q\sin(\Delta\phi)) + \dot{Q}\} - (\dot{W}_u - \dot{W}_s)(Q + R\sin(\Delta\phi) \\ &\quad + Q\cos(\Delta\phi)) - h_{ra}\cos(\Delta\phi)\{\dot{Q} + R\Delta\dot{\phi} + P_s(R\cos(\Delta\phi) - Q\sin(\Delta\phi)\} \\ &\quad + h_{ra}\sin(\Delta\phi)\{P_s(R\sin(\Delta\phi) + Q\cos(\Delta\phi)) - \dot{R} + Q\Delta\dot{\phi}\}] \qquad (14)\end{aligned}$$

Sprung Mass Lateral Inertia Force

$$\Sigma Y_s = \Sigma \dot{v}\, dM_s$$

$$= M_s[\dot{V} - P_s(W_u\cos(\Delta\phi) + V\sin(\Delta\phi)) + RU + h(\dot{P}_u - P_sP_u\sin(\Delta\phi) - QR) + (\dot{W}_u - \dot{W}_s)(P_u + P_s\cos(\Delta\phi)) + h_{ra}\cos(\Delta\phi)(\dot{P}_s - P_s^2\sin(\Delta\phi) - RQ) - h_{ra}\sin(\Delta\phi)(P_s^2\cos(\Delta\phi) + R^2 + P_s\Delta\dot{\phi})] \quad (15)$$

Sprung Mass Vertical Inertia Force

$$\Sigma Z_s = \Sigma \dot{w}\, dM_s$$

$$= M_s\{\dot{W}_s - QU + P_s(V\cos(\Delta\phi) - W_u\sin(\Delta\phi)) + h(Q^2 + P_sP_u\cos(\Delta\phi)) + h_{ra}\cos(\Delta\phi)(Q^2 + P_s^2\cos(\Delta\phi) + P_s\Delta\dot{\phi}) + h_{ra}\sin(\Delta\phi)(\dot{P}_s - P_s^2\sin(\Delta\phi) + QR)\} \quad (16)$$

Sprung Mass Rolling Inertia Moment

$$\Sigma L_s = \Sigma(y\dot{w} - z\dot{v})dM_s$$

$$= I_{xxs}(\dot{P}_s - P_s^2\sin(\Delta\phi)) + I_{xys}(P_sR - \dot{Q}\cos(\Delta\phi) - \dot{R}\sin(\Delta\phi)) + (I_{yys} - I_{zzs})\{(Q\sin(\Delta\phi) - R\cos(\Delta\phi))(R\sin(\Delta\phi) + Q\cos(\Delta\phi))\} + I_{yzs}\{(R\cos(\Delta\phi) - Q\sin(\Delta\phi))^2 - (R\sin(\Delta\phi) + Q\cos(\Delta\phi))^2\} + I_{xzs}(\dot{Q}\sin(\Delta\phi) - \dot{R}\cos(\Delta\phi) - P_sQ) + M_sh[\dot{V} - P_s(W\cos(\Delta\phi) + RU + V\sin(\Delta\phi)) + h\{\dot{P}_u - P_sP_u\sin(\Delta\phi) - QR\} + h_{ra}\cos(\Delta\phi)(\dot{P}_s - RQ - P_s^2\sin(\Delta\phi)) + (\dot{W}_u - \dot{W}_s)(P_u + P_s\cos(\Delta\phi)) - h_{ra}\sin(\Delta\phi)(P_s^2\cos(\Delta\phi) + R^2 + P_s\Delta\dot{\phi})]$$

$$+ M_s h_{ra}[\dot{V}\cos(\Delta\phi) + \dot{W}_s\sin(\Delta\phi) + U(R\cos(\Delta\phi) - Q\sin(\Delta\phi)) - P_s W_u$$

$$+ h\{\dot{P}_u\cos(\Delta\phi) + Q(Q\sin(\Delta\phi) - R\cos(\Delta\phi))\} + (W_u - W_s)(P_u\cos(\Delta\phi)$$

$$+ P_s) + h_{ra}\{\dot{P}_s - P_s^2\sin(\Delta\phi) + Q\sin(\Delta\phi)(Q\cos(\Delta\phi) + R\sin(\Delta\phi))$$

$$- R\cos(\Delta\phi)(Q\cos(\Delta\phi) + R\sin(\Delta\phi))\}] \qquad (17)$$

Sprung Mass Pitching Inertia Moment

$$\Sigma N_s = \Sigma(x\dot{v} - y\dot{u})dM_s$$

$$= - I_{xxs}(P_s Q\sin(\Delta\phi) + \frac{1}{2}Q\Delta\dot{\phi}) - I_{yys}\{P_s Q\cos(\Delta\phi)(1 - 2\sin^2(\Delta\phi))$$

$$+ \dot{R}\sin^2(\Delta\phi) - P_s R\sin(\Delta\phi)(1 - 2\cos^2(\Delta\phi)) + (\dot{V} + R\Delta\dot{\phi})\sin(\Delta\phi)\cos(\Delta\phi)$$

$$+ \frac{1}{2}Q\Delta\dot{\phi}(\cos^2(\Delta\phi) - \sin^2(\Delta\phi))\}$$

$$+ I_{zzs}\{2P_s(Q\sin(\Delta\phi) - R\cos(\Delta\phi))\sin(\Delta\phi)\cos(\Delta\phi) - R\Delta\dot{\phi}\sin(\Delta\phi)\cos(\Delta\phi)$$

$$+ (\dot{R}\cos(\Delta\phi) - \dot{Q}\sin(\Delta\phi))\cos(\Delta\phi) - \frac{1}{2}Q\Delta\dot{\phi}(\cos^2(\Delta\phi) - \sin^2(\Delta\phi))\}$$

$$+ I_{yzs}[P_s\{3(R\sin(\Delta\phi) - Q\cos(\Delta\phi))\sin(\Delta\phi)\cos(\Delta\phi) - (R\cos^3(\Delta\phi)$$

$$- Q\sin^3(\Delta\phi)\} + 2(Q\Delta\dot{\phi} - \dot{R})\sin(\Delta\phi)\cos(\Delta\phi)$$

$$- (R\Delta\dot{\phi} + \dot{Q})(\cos^2(\Delta\phi) - \sin^2(\Delta\phi))]$$

$$+ I_{xzs}\{2P_s^2\cos(\Delta\phi)\sin(\Delta\phi) - \dot{P}_s\cos(\Delta\phi) + R_s^2\sin(\Delta\phi)(1 - \cos(\Delta\phi))$$

$$+ P_s\Delta\dot{\phi}\sin(\Delta\phi) + Q\cos(\Delta\phi)(R - Q\sin(\Delta\phi))\}$$

$$+ I_{xys}\{(Q^2 + R^2)\cos^2(\Delta\phi) - \dot{P}_s\sin(\Delta\phi) - P_s^2(\cos^2(\Delta\phi) - \sin^2(\Delta\phi))$$

$$- P_s\Delta\dot{\phi}\cos(\Delta\phi) - R^2\cos(\Delta\phi) + QR\sin(\Delta\phi)\}$$

$$- M_s h_{ra}[\dot{U}\sin(\Delta\phi) - V(R\cos(\Delta\phi) - Q\sin(\Delta\phi))\sin(\Delta\phi) + W_u(R\sin(\Delta\phi)$$

$$+ Q\cos(\Delta\phi))\sin(\Delta\phi) - h\{P_u(R\cos(\Delta\phi) - Q\sin(\Delta\phi)) + \dot{Q}\}\sin(\Delta\phi)$$

$$- (W_u - W_s)\{Q(1 + \cos(\Delta\phi)) + R\sin(\Delta\phi)\}\sin(\Delta\phi)$$

$$+ h_{ra}\sin(\Delta\phi)\{P_s R(\sin^2(\Delta\phi) - \cos^2(\Delta\phi)) - (R\cos(\Delta\phi)$$

$$- Q\sin(\Delta\phi))\Delta\dot{\phi} + 2P_s R\sin(\Delta\phi)\cos(\Delta\phi) - \dot{R}\sin(\Delta\phi) - \dot{Q}\cos(\Delta\phi)\}] \quad (18)$$

The external forces acting on the sprung mass (Figure 7) include the gravitational force, the suspension forces (F_{slF}, F_{srF}, F_{slR}, F_{srR}), and longitudinal and lateral forces at the pivot points (F_t,F_F,F_R). The expressions for the external forces acting on the sprung mass are given below:

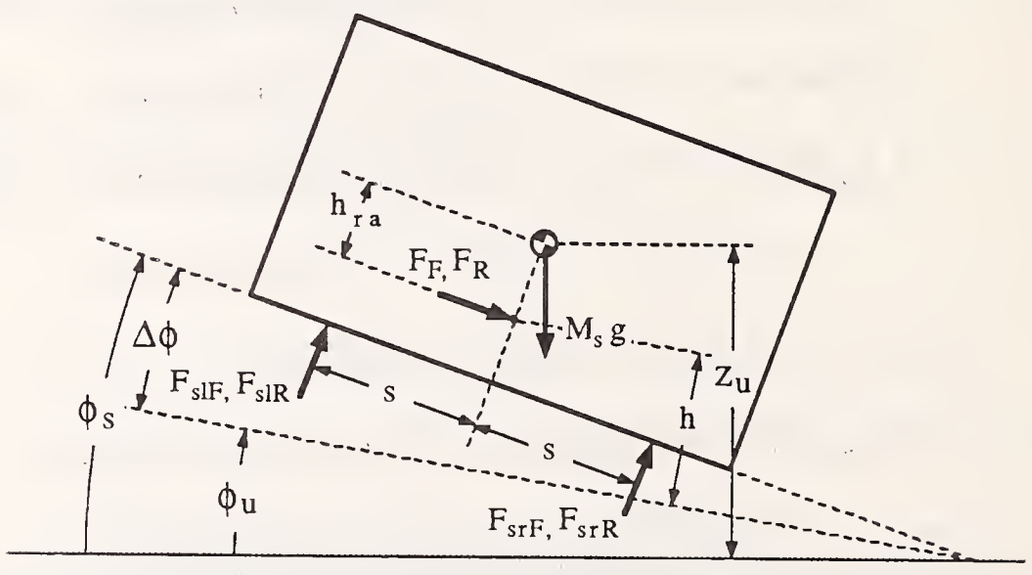

Figure 7. Free Body Diagram of Sprung Mass.

Sprung Mass Resultant Longitudinal Force

$$\Sigma X_s = - F_t + M_s g T_{zxu} \tag{19}$$

Sprung Mass Resultant Lateral Force

$$\Sigma Y_s = F_F + F_R + (F_{slF} + F_{slR} + F_{srF} + F_{srR})\sin(\Delta\phi) + M_s g T_{zyu} \tag{20}$$

Sprung Mass Resultant Vertical Force

$$\Sigma Z_s = - (F_{srF} + F_{srR} + F_{slF} + F_{slR})\cos(\Delta\phi) + M_s g T_{zzu} \tag{21}$$

Sprung Mass Resultant Rolling Moment

$$\Sigma L_s = (F_F + F_R)h + (F_{slF} + F_{slR})(s + h\sin(\Delta\phi)) - (F_{srF} + F_{srR})(s - h\sin(\Delta\phi)) + M_s g T_{zyu}(h_{ra}\cos(\Delta\phi) + h) + M_s g T_{zzu} h_{ra}\sin(\Delta\phi) \tag{22}$$

Sprung Mass Resultant Yawing Moment

$$\Sigma N_s = F_F a - F_R b + (F_{slF} + F_{slR})a \sin(\Delta\phi) - (F_{srF} + F_{srR})b \sin(\Delta\phi) + M_s g T_{zxu} h_{ra}\sin(\Delta\phi) \tag{23}$$

2.2.3 ITRS Equations of Motion

In the process of developing the ITRS vehicle model, six unsprung mass and five sprung mass equations of motion were derived to describe the eight generalized coordinates. The additional three equations derived were used to determine the pin reactions between the two masses. The equations of motion employed in the simulation are the following.

Vehicle Longitudinal Equation of Motion

$$
\begin{aligned}
&(M_s + M_u)\,\dot{U} - M_s\,(h + h_{ra}\cos(\Delta\phi))\,\dot{Q} - M_s h_{ra}\sin(\Delta\phi)\dot{R} \\
&\quad = \quad (F_{xlF} + F_{xlR} + F_{xrF} + F_{xrR} + F_{dxF} + F_{dxR})T_{xxu} \\
&\qquad + \{F_{zlF} + F_{zlR} + F_{zrF} + F_{zrR} + (M_s + M_u)g\}T_{zxu} - M_u(W_u Q - VR) \\
&\qquad - M_s[Q(V\sin(\Delta\phi) + W_u\cos(\Delta\phi)) - R(V\cos(\Delta\phi) - W_u\sin(\Delta\phi)) \\
&\qquad + hP_u(Q\sin(\Delta\phi) - R\cos(\Delta\phi)) - (W_u - W_s)(Q + Q\cos(\Delta\phi) + R\sin(\Delta\phi)) \\
&\qquad + h_{ra}\sin(\Delta\phi)\{Q\Delta\dot{\phi} + P_s(R\sin(\Delta\phi) + Q\cos(\Delta\phi)\} \\
&\qquad - h_{ra}\cos(\Delta\phi)\{R\Delta\dot{\phi} + P_s(R\cos(\Delta\phi) - Q\sin(\Delta\phi))\}] \\
&\qquad + (F_{dsF} + F_{dsR})T_{xaxu} \qquad (24)
\end{aligned}
$$

Vehicle Lateral Equation of Motion

$$
\begin{aligned}
&(M_s + M_u)\,\dot{V} + M_s\,h\dot{P}_u + M_s h_{ra}\dot{P}_s\cos(\Delta\phi) \\
&\quad = - M_s\{RU - P_s(V\sin(\Delta\phi) + W_u\cos(\Delta\phi)) - h(QR + P_s P_u\sin(\Delta\phi)) \\
&\qquad + (P_u + P_s\cos(\Delta\phi))(W_u - W_s) - h_{ra}\cos(\Delta\phi)(QR + P_s^2\sin(\Delta\phi)) \\
&\qquad - h_{ra}\sin(\Delta\phi)(R^2 + P_s^2\cos(\Delta\phi) + P_s\Delta\dot{\phi})\} - M_u(UR - W_u P_u) \\
&\qquad + (F_{xlF} + F_{xlR} + F_{xrF} + F_{xrR} + F_{dxF} + F_{dxR})T_{xyu}
\end{aligned}
$$

$$+ (F_{ylF} + F_{ylR} + F_{yrF} + F_{yrR} + F_{dF} + F_{dR})T_{yyu}$$

$$+ \{F_{zlF} + F_{zlR} + F_{zrF} + F_{zrR} + (M_u + M_s)g\}T_{zyu}$$

$$+ (F_{dsF} + F_{dsR})T_{xayu} \qquad (25)$$

Unsprung Mass Vertical Equation of Motion

$$M_u \dot{W}_u = - M_u(VP_u - UQ) + (F_{xlF} + F_{xlR} + F_{xrF} + F_{xrR} + F_{dxF} + F_{dxR})T_{xzu}$$

$$+ (F_{ylF} + F_{ylR} + F_{yrF} + F_{yrR} + F_{dF} + F_{dR})T_{yzu}$$

$$+ (F_{zlF} + F_{zlR} + F_{zrF} + F_{zrR} + M_u g)T_{zzu}$$

$$+ (F_{slF} + F_{slR} + F_{srF} + F_{srR})\cos(\Delta\phi) + (F_{dsF} + F_{dsR})T_{xazu} \qquad (26)$$

Sprung Mass Vertical Equation of Motion

$$M_s\dot{P}_s h_{ra}\sin(\Delta\phi) + M_s\dot{W}_s$$

$$= - M_s[P_s(V\cos(\Delta\phi) - W_u\sin(\Delta\phi)) - QU + h(Q^2 + P_sP_u\cos(\Delta\phi))$$

$$+ P_s\sin(\Delta\phi)(W_u - W_s) + h_{ra}\{(QR - P_s^2\sin(\Delta\phi))\sin(\Delta\phi)$$

$$+ (Q^2 + P_s^2\cos(\Delta\phi) + P_s\Delta\dot{\phi})\cos(\Delta\phi)\}]$$

$$- (F_{srF} + F_{srR} + F_{slF} + F_{slR})\cos(\Delta\phi) + M_s g T_{zzu} \qquad (27)$$

Unsprung Mass Roll Equation of Motion

$$I_{xxu}\dot{P} - I_{xyu}\dot{Q} - I_{xzu}\dot{R} - M_u h\dot{V}$$

$$= - I_{xyu}P_uR + I_{xzu}P_uQ + (I_{yyu} - I_{zzu})\,QR$$

$$
\begin{aligned}
&- I_{yzu}(R^2 - Q^2) + M_u h(UR - W_u P_u) - M_u g T_{zyu} h \\
&+ (F_{slF} + F_{slR} + F_{srF} + F_{srR})(h + h_u)\sin(\Delta\phi) \\
&- \{(F_{xlF} + F_{xlR})T_{xzu} + (F_{ylF} + F_{ylR})T_{yzu} + (F_{zlF} + F_{zlR})T_{zzu}\}\ \frac{TRW}{2} \\
&+ \{(F_{xrF} + F_{dxF})T_{xzu} + (F_{yrF} + F_{dF})T_{yzu} + F_{zrF}T_{zzu}\}TRWF \\
&+ \{(F_{xrR} + F_{dxR})T_{xzu} + (F_{yrR} + F_{dR})T_{yzu} + F_{zrR}T_{zzu}\}TRWR \\
&- \{(F_{xlF} + F_{xlR} + F_{xrF} + F_{xrR})T_{xyu} + (F_{ylF} + F_{ylR} + F_{yrF} + F_{yrR})T_{yyu} \\
&+ (F_{zlF} + F_{zlR} + F_{zrF} + F_{zrR})T_{zyu}\}(h + h_u + T_r) \\
&- \{(F_{dxF} + F_{dxR})T_{xyu} + (F_{dF} + F_{dR})T_{yyu}\}(h + h_u + T_r - \frac{h_{curb}}{\cos\phi_u \cos\theta}) \\
&- (F_{dsF} + F_{dsR})T_{xayu}(h + h_u + T_r - \frac{h_{curb}}{\cos\phi_u \cos\theta}) \\
&+ s(F_{srF} + F_{srR} - F_{slF} - F_{slR})\cos(\Delta\phi) \\
&+ F_{dsF}T_{xazu}TRWF + F_{dsR}T_{xazu}TRWR \qquad (28)
\end{aligned}
$$

Sprung Mass Roll Equation of Motion

$$
\begin{aligned}
&(I_{xxs} + M_s h_{ra}^2)\dot{P}_s - (I_{xys}\cos(\Delta\phi) - I_{xzs}\sin(\Delta\phi))\dot{Q} - (I_{xys}\sin(\Delta\phi) + I_{xzs}\cos(\Delta\phi))\dot{R} \\
&+ M_s h h_{ra}\cos(\Delta\phi)\dot{P}_u + M_s h_{ra}\cos(\Delta\phi)\dot{V} + M_s h_{ra}\sin(\Delta\phi)\dot{W}_s \\
&\quad = I_{xxs}P_s^2\sin(\Delta\phi) - I_{xys}P_s R + I_{xzs}P_s Q + (I_{yys} - I_{zzs})(Q\cos(\Delta\phi) \\
&\quad + R\sin(\Delta\phi))(R\cos(\Delta\phi) - Q\sin(\Delta\phi)) \\
&\quad - I_{yzs}\{(R\cos(\Delta\phi) - Q\sin(\Delta\phi))^2 - (R\sin(\Delta\phi) - Q\cos(\Delta\phi))^2\} \\
&\quad - M_s h_{ra}[U(R\cos(\Delta\phi) - Q\sin(\Delta\phi)) - Qh(R\cos(\Delta\phi) - Q\sin(\Delta\phi))
\end{aligned}
$$

$$+ (P_s + P_u\cos(\Delta\phi))(W_u - W_s) + h_{ra}\{(Q\sin(\Delta\phi) - R\cos(\Delta\phi))(Q\cos(\Delta\phi)$$

$$+ R\sin(\Delta\phi)) - P_s^2\sin(\Delta\phi) - P_sW_u\}] + (F_{slF} + F_{slR} - F_{srF} - F_{srR})s$$

$$+ M_sgh_{ra}(T_{zyu}\cos(\Delta\phi) + T_{zzu}\sin(\Delta\phi)) \qquad (29)$$

Vehicle Pitch Equation of Motion

$$M_uh\dot{U} + I_{yyu}\dot{Q} - I_{xyu}\dot{P}_u - I_{yzu}\dot{R}$$

$$= M_uh(RV - W_uQ) + I_{xyu}QR - I_{yzu}P_uQ - (I_{xxu} - I_{zzu})P_uR$$

$$- I_{xzu}(P_u^2 - R^2)$$

$$+ \{(F_{xrR} + F_{xlR} + F_{dxR})T_{xzu} + (F_{yrR} + F_{ylR} + F_{dR})T_{yzu}$$

$$+ (F_{zrR} + F_{zlR})T_{zzu} + (F_{srR} + F_{slR})\cos(\Delta\phi)\}b$$

$$- \{(F_{xrF} + F_{xlF} + F_{dxF})T_{xzu} + (F_{yrF} + F_{ylF} + F_{dF})T_{yzu}$$

$$+ (F_{zrF} + F_{zlF})T_{zzu} + (F_{srF} + F_{slF})\cos(\Delta\phi)\}a$$

$$+ (F_{xlF} + F_{xlR} + F_{xrF} + F_{xrR})T_{xxu}(h + h_u + T_r)$$

$$+ (F_{zlF} + F_{zlR} + F_{zrF} + F_{zrR})T_{zxu}(h + h_u + T_r)$$

$$- (F_{dsF} + F_{dsR})T_{xxu}\left(h_u + T_r - \frac{h_{curb}}{\cos\phi_u\sin\phi_u}\right)$$

$$+ (F_{dxF} + F_{dxR})T_{xxu}\left(h_u + T_r - \frac{h_{curb}}{\cos\phi_u\cos\theta}\right)$$

$$+ (F_{dsF} + F_{dsR})T_{xaxu}(h + h_u + T_r - \frac{h_{curb}}{\cos\phi_u\cos\theta})$$

$$+ (F_{dxF} + F_{dxR})T_{xxu}h + (F_{dsR}b - F_{dsF}a)T_{xazu} + M_u g T_{zxu}h \qquad (30)$$

Vehicle Yaw Equation of Motion

$$- M_s h_{ra}\sin(\Delta\phi)\dot{U}_s - I_{xzu}\dot{P}_u - (I_{xzs}\cos(\Delta\phi) + I_{xys}\sin(\Delta\phi))\dot{P}_s$$

$$+ \{I_{zzu} + I_{yys}\sin^2(\Delta\phi) + I_{zzs}\cos^2(\Delta\phi) - 2I_{yzs}\cos(\Delta\phi)\sin(\Delta\phi)$$

$$+ M_s h_{ra}^2\sin^2(\Delta\phi)\}\dot{R} + \{(I_{yys} - I_{zzs} + M_s h_{ra}^2)\sin(\Delta\phi)\cos(\Delta\phi)$$

$$- I_{yzu} + M_s h h_{ra}\sin(\Delta\phi) - I_{yzs}(\cos^2(\Delta\phi) - \sin^2(\Delta\phi))\}\dot{Q}$$

$$= I_{xxs}(P_s Q\cos(\Delta\phi) + \frac{1}{2}Q\Delta\dot{\phi}) - I_{yys}\{P_s Q\cos(\Delta\phi)(1 - 2\sin^2(\Delta\phi))$$

$$- P_s R\sin(\Delta\phi)(1 - 2\cos^2(\Delta\phi)) + R\Delta\dot{\phi}\sin(\Delta\phi)\cos(\Delta\phi)$$

$$+ \frac{1}{2}Q\Delta\dot{\phi}(\cos^2(\Delta\phi) - \sin^2(\Delta\phi))\}$$

$$+ I_{zzs}\{2P_s\cos(\Delta\phi)\sin(\Delta\phi)(R\cos(\Delta\phi) - Q\sin(\Delta\phi))$$

$$+ R\Delta\dot{\phi}\sin(\Delta\phi)\cos(\Delta\phi) + \frac{1}{2}Q\Delta\dot{\phi}(\cos^2(\Delta\phi) - \sin^2(\Delta\phi))\}$$

$$- I_{yzs}[P_s\{3\sin(\Delta\phi)\cos(\Delta\phi)(R\sin(\Delta\phi) - (R\cos^3(\Delta\phi) - Q\sin^3(\Delta\phi))$$

$$- Q\cos(\Delta\phi))\} + 2Q\Delta\dot{\phi}\sin(\Delta\phi)\cos(\Delta\phi)$$

$$- R\Delta\dot{\phi}(\cos^2(\Delta\phi) - \sin^2(\Delta\phi))]$$

$$- I_{xzs}\{2P_s^2\cos(\Delta\phi)\sin(\Delta\phi) + P_s\Delta\dot{\phi}\sin(\Delta\phi) + R_s^2\sin(\Delta\phi)(1 - \cos(\Delta\phi))$$

$$+ Q\cos(\Delta\phi)(R - Q\sin(\Delta\phi))\}$$

$$- I_{xys}\{(Q^2 + R^2)\cos^2(\Delta\phi) - P_s^2(\cos^2(\Delta\phi) - \sin^2(\Delta\phi)) - P_s\Delta\dot{\phi}\cos(\Delta\phi)$$

$$- R^2\cos(\Delta\phi)\}$$

$$
\begin{aligned}
&+ M_s h_{ra}[V\sin(\Delta\phi)(Q\sin(\Delta\phi) - R\cos(\Delta\phi)) + W_u\sin(\Delta\phi)(R\sin(\Delta\phi) \\
&\quad + Q\cos(\Delta\phi)) - hP_u\sin(\Delta\phi)(R\cos(\Delta\phi) - Q\sin(\Delta\phi)) \\
&\quad - (W_u - W_s)\{Q\sin(\Delta\phi)(1 + \cos(\Delta\phi) + R\sin^2(\Delta\phi)\} \\
&\quad + h_{ra}\sin(\Delta\phi)\{P_s R(\sin^2(\Delta\phi) - \cos^2(\Delta\phi)) - (R\cos(\Delta\phi) \\
&\quad - Q\sin(\Delta\phi))\dot{\Delta\phi} + 2P_s R\sin(\Delta\phi)\cos(\Delta\phi)\}] \\
&+ \{(F_{xrF} + F_{xlF} + F_{dxF})T_{xyu} + (F_{yrF} + F_{ylF} + F_{dF})T_{yyu} \\
&\quad + (F_{zrF} + F_{zlF})T_{zyu} + F_{dsF}T_{xayu}\}\, a \\
&- \{(F_{xrR} + F_{xlR} + F_{dxR})T_{xyu} + (F_{yrR} + F_{ylR} + F_{dR})T_{yyu} \\
&\quad + (F_{zrR} + F_{zlR})T_{zyu} + F_{dsR}T_{xayu}\}\, b \\
&- \{F_{zrF}T_{zxu} + (F_{xrF} + F_{dxF})T_{xxu} + F_{dsF}T_{xaxu}\}TRWF \\
&- \{F_{zrR}T_{zxu} + (F_{xrR} + F_{dxR})T_{xxu} + F_{dsR}T_{xaxu}\}TRWR \\
&- \{(F_{xlF} + F_{xlR})T_{xxu} + (F_{zlF} + F_{zlR})T_{zxu}\}\frac{TRW}{2} \\
&+ M_s g T_{zxu} h_{ra}\sin(\Delta\phi) \qquad (31)
\end{aligned}
$$

2.2.4 Suspension Forces

The vehicle suspension model consists of four springs, upper and lower bump stops, and four shock absorbers (Figure 1). Springs are assumed to have linear characteristics (Figure 8) and shock absorbers are modelled using viscous damping elements. In addition, each bump stop has its own damping element to simulate energy dissipation within the particular bump stop. The combined spring and damping suspension forces acting on each side of vehicle front and rear are:

$$
\begin{aligned}
F_{slF} &= K_1 d_{sl} + B_1 \dot{d}_{sl} + K_2 d_{bl} + B_2 \dot{d}_{bl} \\
F_{srF} &= K_1 d_{sr} + B_1 \dot{d}_{sr} + K_2 d_{br} + B_2 \dot{d}_{br} \\
F_{slR} &= K_1 d_{sl} + B_1 \dot{d}_{sl} + K_2 d_{bl} + B_2 \dot{d}_{bl} \\
F_{srR} &= K_1 d_{sr} + B_1 \dot{d}_{sr} + K_2 d_{br} + B_2 \dot{d}_{br}
\end{aligned} \tag{32}
$$

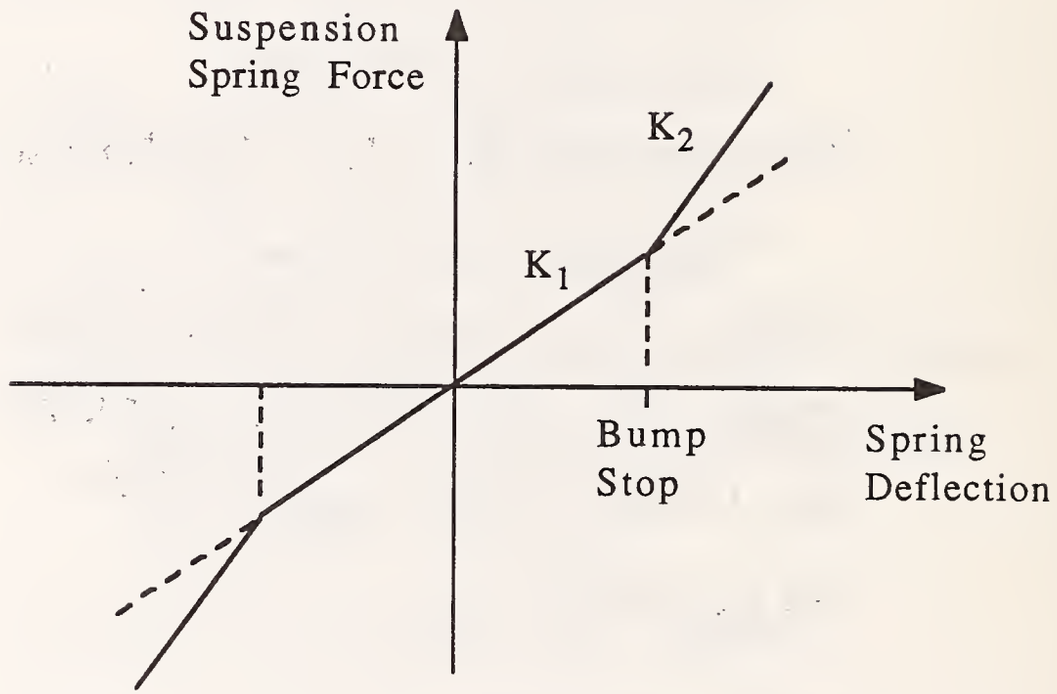

Figure 8. ITRS Spring Deflection Characteristic.

The spring deflections (d_{sl}, d_{sr}) can be found (Figure 9) by subtracting the length of the spring at any instant in time from the unloaded spring length (SPRLNG):

$$
\begin{aligned}
d_{sl} &= \text{SPRLNG} - \{(h + h_u)/\cos(\Delta\phi) - (h_s - h_{ra}) + s \tan(\Delta\phi)\} \\
d_{sr} &= \text{SPRLNG} - \{(h + h_u)/\cos(\Delta\phi) - (h_s - h_{ra}) - s \tan(\Delta\phi)\}
\end{aligned} \tag{33}
$$

If a bump stop is in contact with the axle, the bump stop deflection can be determined by subtracting the actual spring length from the the bump stop size (Figure 10). It should be noted that the bump stop size is not necessarily equal to the actual length of the bump stop. While the upper bump stop size represents the actual length of the bump stop, the lower bump stop size represents the distance from the sprung mass bottom to the point of contact of the lower bump stop.

Bump Stop Size Upper = Static Loaded Spring Length
- Static Allowable Bump Stop Distance (ABSDEF)

Bump Stop Size Lower = Static Loaded Spring Length
+ Static Allowable Bump Stop Distance (ABSDEF)

The bump stop deflections are found using the following algorithm. If the deflected spring length is less than Bump Stop Size Upper:

$$d_{bl} = \text{Bump Stop Size Upper} - \{(h + h_u)/\cos(\Delta\phi) - (h_s - h_{ra}) + s\tan(\Delta\phi)\}$$
$$d_{br} = \text{Bump Stop Size Upper} - \{(h + h_u)/\cos(\Delta\phi) - (h_s - h_{ra}) - s\tan(\Delta\phi)\} \quad (34)$$

If the deflected spring length is greater than Bump Stop Size Lower:

$$d_{bl} = \text{Bump Stop Size Lower} - \{(h + h_u)/\cos(\Delta\phi) - (h_s - h_{ra}) + s\tan(\Delta\phi)\}$$
$$d_{br} = \text{Bump Stop Size Lower} - \{(h + h_u)/\cos(\Delta\phi) - (h_s - h_{ra}) - s\tan(\Delta\phi)\} \quad (35)$$

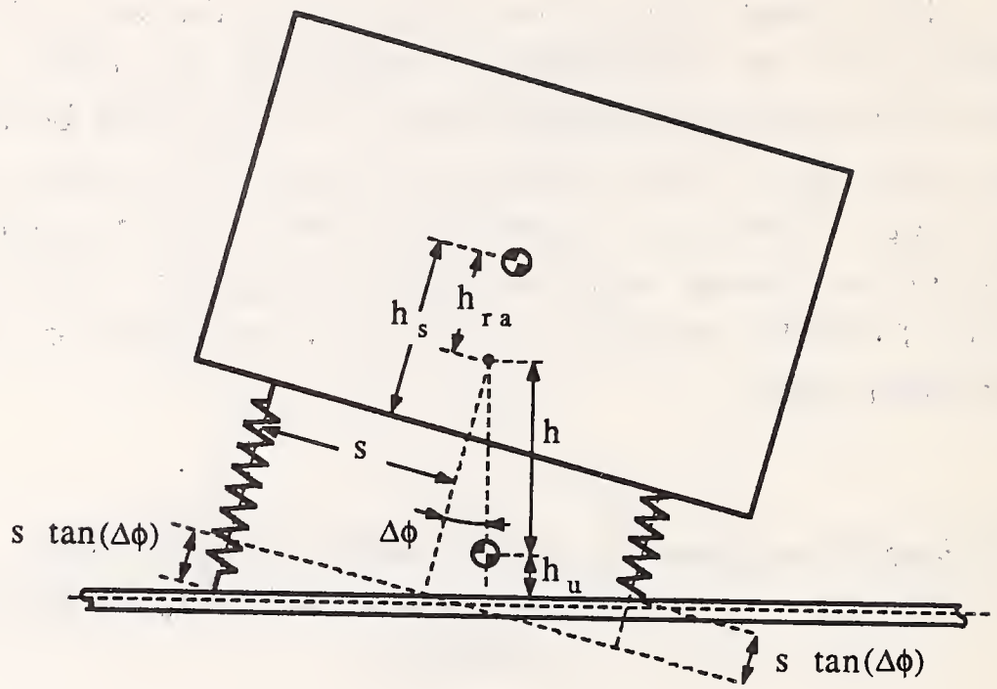

Figure 9. ITRS Spring Deflection Diagram.

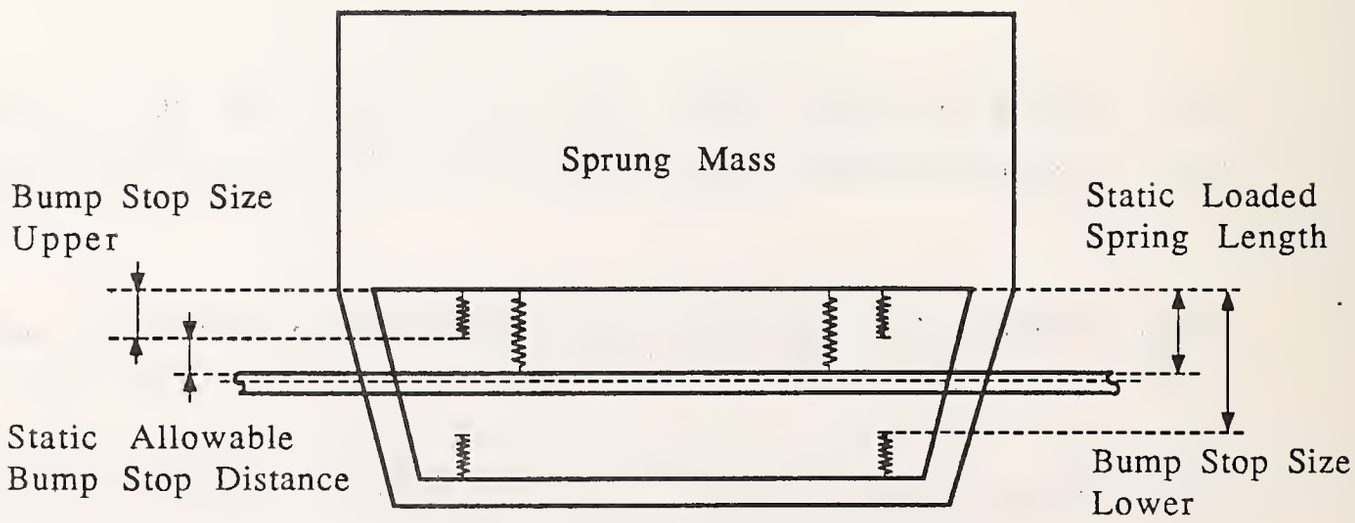

Figure 10. ITRS Bump Stop Model.

2.2.5 Tire Forces

The tire model utilized in the ITRS simulation calculates the normal and skidding forces which act on individual tires under locked conditions. Each of the vehicle's tires is modelled using a spring-damper system to calculate normal reaction as function of tire radial deformation and its time rate of change.

$$
\begin{aligned}
F_{zrF} &= -K_z(T_r - T_{rF}) - B_z\dot{T}_{rF} && T_{rF} \leq T_r \\
&= 0 && T_{rF} > T_r \\
F_{zlF} &= -K_z(T_r - T_{lF}) - B_z\dot{T}_{lF} && T_{lF} \leq T_r \\
&= 0 && T_{lF} > T_r \\
F_{zrR} &= -K_z(T_r - T_{rR}) - B_z\dot{T}_{rR} && T_{rR} \leq T_r \\
&= 0 && T_{rR} > T_r \\
F_{zlR} &= -K_z(T_r - T_{lR}) - B_z\dot{T}_{lR} && T_{lR} \leq T_r \\
&= 0 && T_{lR} > T_r
\end{aligned}
\qquad (36)
$$

The tire normal reactions change as the vehicle heaves, rolls, and pitches. The distance between the ground and the wheel center is dependent on the unsprung mass CG height, the deformed track width, angles ψ, θ and ϕ_u, and is calculated using the following equations (Figure 11):

$$
\begin{aligned}
T_{rF} &= -(Z_u + a\,T_{xuz} + TRWF\,T_{yuz} + h_u\,T_{zuz})/\cos\phi_u \\
T_{lF} &= -(Z_u + a\,T_{xuz} - \frac{TRW}{2}\,T_{yuz} + h_u\,T_{zuz})/\cos\phi_u \\
T_{rR} &= -(Z_u - b\,T_{xuz} + TRWR\,T_{yuz} + h_u\,T_{zuz})/\cos\phi_u \\
T_{lR} &= -(Z_u - b\,T_{xuz} - \frac{TRW}{2}\,T_{yuz} + h_u\,T_{zuz})/\cos\phi_u
\end{aligned}
\qquad (37)
$$

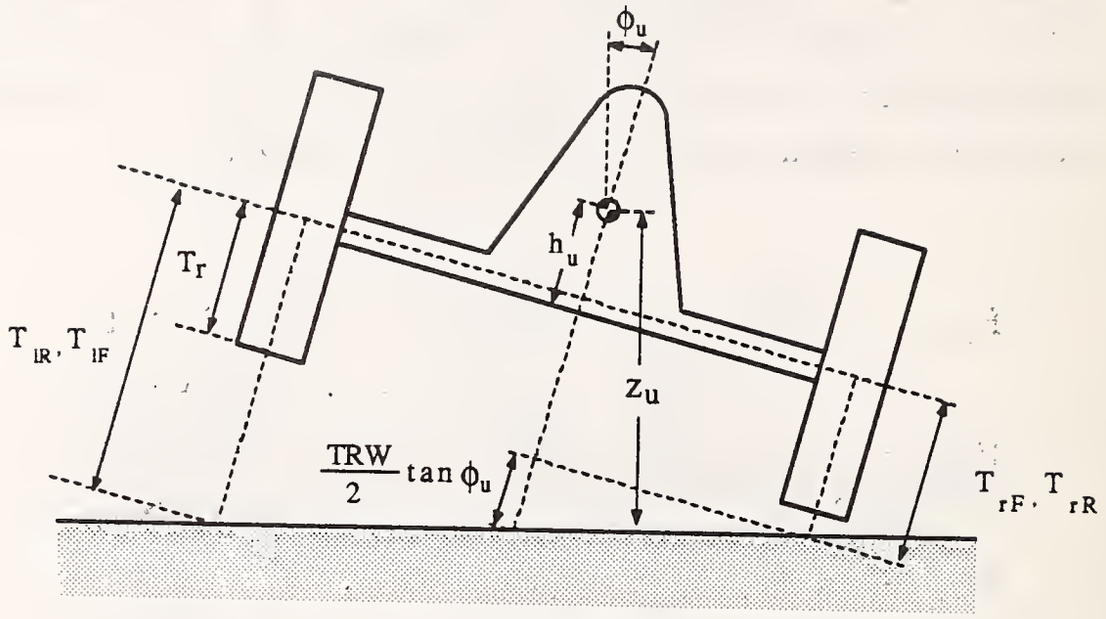

Figure 11. Tire Radial Deformations.

The tire deflection rates are determined as shown below:

$$\dot{T}_{rF} = - \dot{Z}_u/\cos\phi_u - \dot{\phi}_u(TRWF + Z_u\sin\phi_u)/\cos\phi_u/\cos\phi_u + a\dot{\theta}/\cos^2\theta$$

$$\dot{T}_{lF} = - \dot{Z}_u/\cos\phi_u + \dot{\phi}_u(\frac{TRW}{2} - Z_u\sin\phi_u)/\cos\phi_u/\cos\phi_u + a\dot{\theta}/\cos^2\theta \qquad (38)$$

$$\dot{T}_{rR} = - \dot{Z}_u/\cos\phi_u - \dot{\phi}_u(TRWR + Z_u\sin\phi_u)/\cos\phi_u/\cos\phi_u - b\dot{\theta}/\cos^2\theta$$

$$\dot{T}_{lR} = - \dot{Z}_u/\cos\phi_u + \dot{\phi}_u(\frac{TRW}{2} - Z_u\sin\phi_u)/\cos\phi_u/\cos\phi_u - b\dot{\theta}/\cos^2\theta$$

The longitudinal (F_{xlF}, F_{xrF}, F_{xlR}, F_{xrR}) and lateral tire skidding forces (F_{ylF}, F_{yrF}, F_{ylR}, F_{yrR}) depend on tire normal reactions, tire/ground frictional properties, and a non-linear skidding velocity function (Figure 12):

$$
\begin{aligned}
F_{xlF} &= \mu_x F_{zlF} f_x(\dot{x}_{lF}) \\
F_{xrF} &= \mu_x F_{zrF} f_x(\dot{x}_{rF}) \\
F_{xlR} &= \mu_x F_{zlR} f_x(\dot{x}_{lR}) \\
F_{xrR} &= \mu_x F_{zrR} f_x(\dot{x}_{rR})
\end{aligned}
\tag{39}
$$

$$
\begin{aligned}
F_{ylF} &= \mu_y F_{zlF} f_y(\dot{y}_{lF}) \\
F_{yrF} &= \mu_y F_{zrF} f_y(\dot{y}_{rF}) \\
F_{ylR} &= \mu_y F_{zlR} f_y(\dot{y}_{lR}) \\
F_{yrR} &= \mu_y F_{zrR} f_y(\dot{y}_{rR})
\end{aligned}
\tag{40}
$$

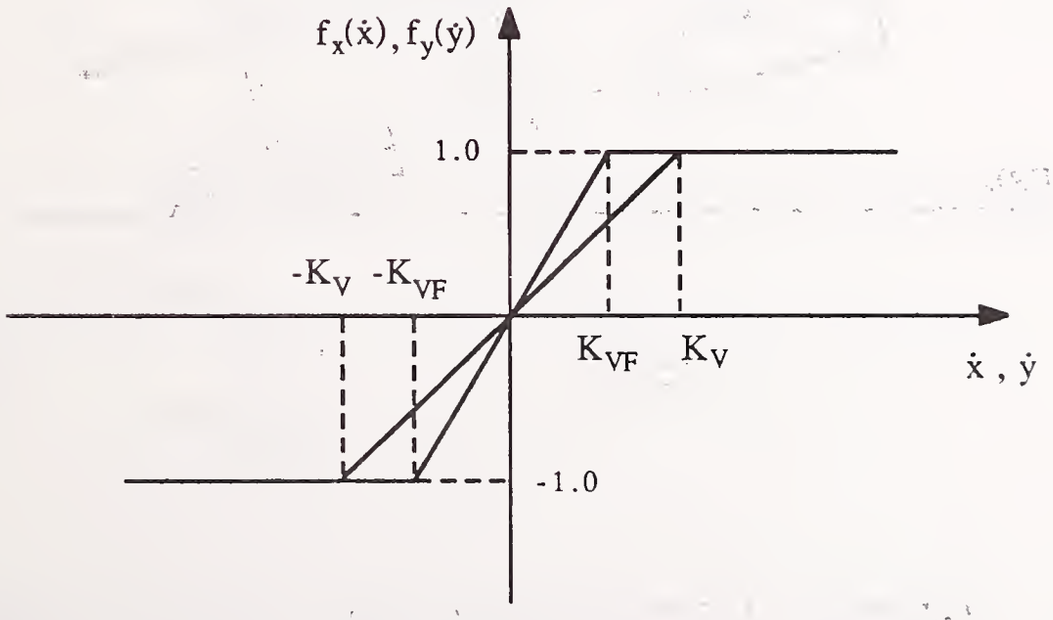

Figure 12. Non Linear Skidding Velocity Function.

2.2.6 Vehicle-Curb Impact Model

The forces which occur when one of the tires comes into contact with the curb include an impact force F_{IMP} which is perpendicular to the curb, and a scrub force F_{ds} which acts parallel to the curb. Figure 13 illustrates both component forces in case of a front right wheel impacting a curb. The impact force is dependent on the amount of structural deformation as well as the time rate of change of this deformation. The structural deformation is determined based on the location and orientation of the vehicle relative to the curb.

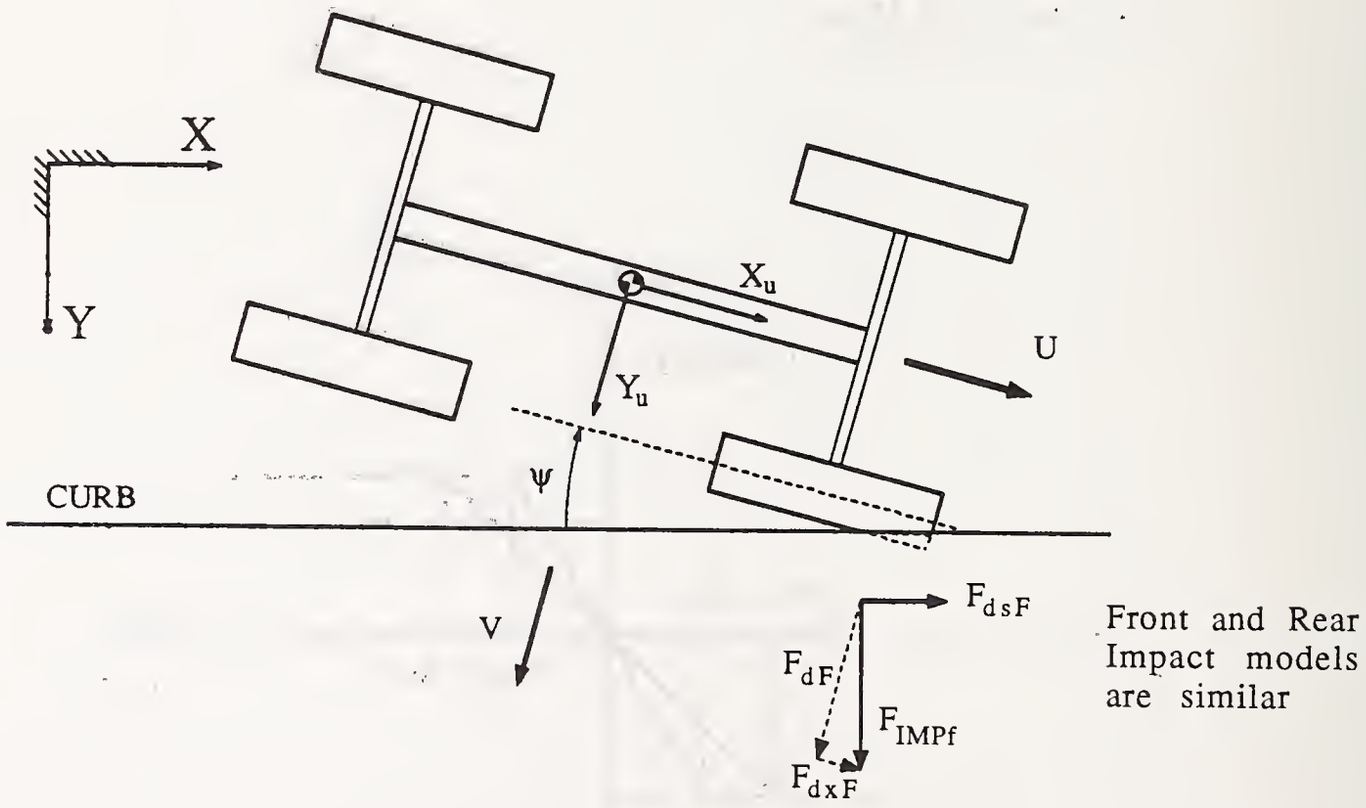

Figure 13. Forces Generated During Wheel-Curb Impact.

A nonlinear force displacement curve having different slopes in three regions is used to calculate the portion of the impact force due to structural deformation and is shown in Figure 14. The first region of the force displacement curve is totally elastic and is used to

represent wheel compliance. The second region represents a zone where plastic deformation occurs as the wheel and suspension elements undergo permanent crush. As the amount of deformation increases, more solid members of the vehicle such as the frame and powertrain are deformed and the third region is utilized. If the

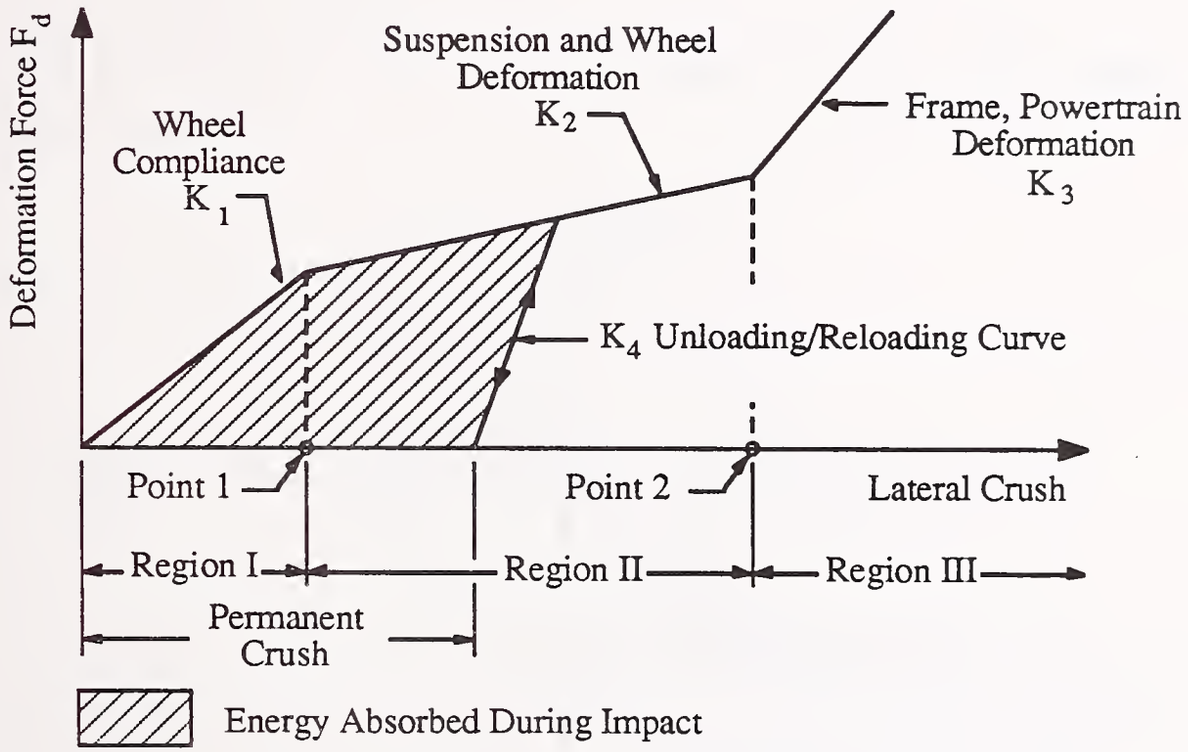

Figure 14. Force Deflection Characteristic Used For Curb Impact

vehicle rebounds after impact, the force displacement curve will unload using one of two slopes. If the deformation is totally elastic, i.e. in region I, then the force displacement curve will unload at slope K_1. If the deformation is plastic, i.e. in regions II and III, then the curve will unload at slope K_3. If plastic deformation does occur then the amount of permanent deformation is noted and the force

deformation curve will reload using slope K_3 on subsequent impacts. Thus in subsequent impacts the impact force is computed as a function of previous plastic deformation.

The portion of the impact force which is dependent on the time rate of change in the deformation is modelled using a viscous damping characteristic. The force component which depends on deformation and the force component dependent on the rate of deformation are added together to obtain the total impact force F_{IMP}.

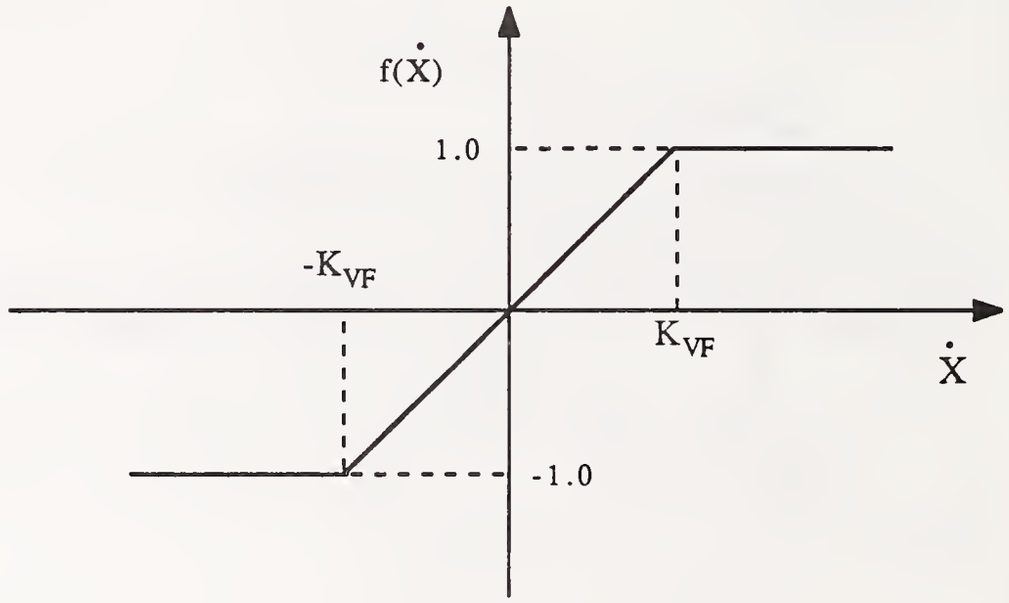

Figure 15. Velocity Dependent Tire Scrub Force Function.

In case of an oblique impact with the curb (vehicle heading angle relative to the curb is different from zero) the total impact force F_{IMP} is projected on longitudinal and lateral directions of unsprung mass NIRS, thus producing forces F_{dxF} and F_{dF} as shown in Figure 13.

The scrub forces generated during the curb impact to oppose the vehicle skidding along the curb, for both front and rear wheels, are determined using the following relations

$$F_{dsF} = \mu_s F_{IMPf} f(\dot{X}_{rF})$$
$$F_{dsR} = \mu_s F_{IMPr} f(\dot{X}_{rR}) \qquad (41)$$

where, μ_s denotes the tire friction coefficient along the curb, F_{IMPf} and F_{IMPr} are front and rear impact forces normal to the curb, and $f(\dot{X}_{rF})$, $f(\dot{X}_{rR})$, represent non-linear functions of tires' scrub velocities shown in Figure 15.

3. ENERGY ANALYSIS OF ITRS TRIPPED ROLLOVER MODEL

One method of checking a simulation's validity is to examine whether it obeys the basic conservation laws of mass, momentum and energy. The principal of work and energy was applied to the ITRS simulation to check its correctness.

$$T_1 + V_1 + \Sigma U_{1\text{-}2} = T_2 + V_2 \tag{42}$$

This principle states that a system's initial (state 1) kinetic and potential energy (T_1, V_1, respectively) plus the work done by external forces must equal the final (state 2) kinetic and potential energy (T_2, V_2, respectively). In the ITRS simulation, all acting external forces are either conservative or dissipative, and consequently, the vehicle's total energy must decrease throughout time:

$$T_1 + V_1 > T_2 + V_2 \tag{43}$$

The total energy (E) of the ITRS vehicle system equals the sum of kinetic energies (T_{TRAN}, T_{ROT}) and gravitational (V_G) and elastic (V_E) potential energies:

$$E = T + V = T_{TRAN} + T_{ROT} + V_G + V_E \tag{44}$$

While the sum of these energies must continually decrease, energy may be exchanged from one type to another. For example, a substantial amount of the vehicle's kinetic translational energy will change to kinetic rotational energy upon impact with an rigid obstacle. Rotational kinetic energy will then be converted to gravitational and elastic potential energies as the vehicle rolls to a higher position.

The scrub forces generated during the curb impact to oppose the vehicle skidding along the curb, for both front and rear wheels, are determined using the following relations

$$F_{dsF} = \mu_s F_{IMPf} f(\dot{X}_{rF})$$
$$F_{dsR} = \mu_s F_{IMPr} f(\dot{X}_{rR}) \qquad (41)$$

where, μ_s denotes the tire friction coefficient along the curb, F_{IMPf} and F_{IMPr} are front and rear impact forces normal to the curb, and $f(\dot{X}_{rF})$, $f(\dot{X}_{rR})$, represent non-linear functions of tires' scrub velocities shown in Figure 15.

3. ENERGY ANALYSIS OF ITRS TRIPPED ROLLOVER MODEL

One method of checking a simulation's validity is to examine whether it obeys the basic conservation laws of mass, momentum and energy. The principal of work and energy was applied to the ITRS simulation to check its correctness.

$$T_1 + V_1 + \Sigma U_{1\text{-}2} = T_2 + V_2 \tag{42}$$

This principle states that a system's initial (state 1) kinetic and potential energy (T_1, V_1, respectively) plus the work done by external forces must equal the final (state 2) kinetic and potential energy (T_2, V_2, respectively). In the ITRS simulation, all acting external forces are either conservative or dissipative, and consequently, the vehicle's total energy must decrease throughout time:

$$T_1 + V_1 > T_2 + V_2 \tag{43}$$

The total energy (E) of the ITRS vehicle system equals the sum of kinetic energies (T_{TRAN}, T_{ROT}) and gravitational (V_G) and elastic (V_E) potential energies:

$$E = T + V = T_{TRAN} + T_{ROT} + V_G + V_E \tag{44}$$

While the sum of these energies must continually decrease, energy may be exchanged from one type to another. For example, a substantial amount of the vehicle's kinetic translational energy will change to kinetic rotational energy upon impact with an rigid obstacle. Rotational kinetic energy will then be converted to gravitational and elastic potential energies as the vehicle rolls to a higher position.

If the vehicle attains sufficient energy to roll the vehicle past the static tip-over angle, gravitational potential energy then begins to transform back to rolling kinetic energy as the vehicle roll motion continues. Otherwise, when the maximum gravitational potential energy is reached and the vehicle has momentarily stopped rotating before reaching the tip-over position, the vehicle begins to roll back to a stable four wheel stance as the gravitational potential energy is exchanged to rolling kinetic energy.

3.1 ITRS VEHICLE ENERGY COMPONENTS

The total translational kinetic energy (T_{TRAN}) of the vehicle equals the sum of translational kinetic energies of sprung and unsprung masses:

$$T_{TRAN} = \frac{1}{2} M_u\{U^2 + V^2 + W_u^2\} + \frac{1}{2} M_s[\{U - h_{ra}R\sin(\Delta\phi) - (h + h_{ra}\cos(\Delta\phi))Q\}^2 + \{V + h_{ra}P_s\cos(\Delta\phi) + P_u h\}^2 + \{W_s + h_{ra}P_s\sin(\Delta\phi)\}^2] \quad (45)$$

Vehicle rotational kinetic energy (T_{ROT}) consists of kinetic energies of rolling, pitching and yawing of both sprung and unsprung masses.

$$\begin{aligned} T_{ROT} = {} & \frac{1}{2} I_{xxu}P_u^2 + \frac{1}{2} I_{yyu}Q^2 + \frac{1}{2} I_{zzu}R^2 \\ & + I_{xyu}P_uQ + I_{xzu}QR + I_{yzu}P_uR \\ & + \frac{1}{2} I_{xxs}P_s^2 + \frac{1}{2} I_{yys}(R\sin(\Delta\phi) + Q\cos(\Delta\phi))^2 + \frac{1}{2} I_{zzs}(R\cos(\Delta\phi) - Q\sin(\Delta\phi))^2 \\ & - I_{xys}P_s\{P_u\sin(\Delta\phi) + Q\cos(\Delta\phi)\} + I_{xzs}P_s\{Q\sin(\Delta\phi) - R\cos(\Delta\phi)\} \\ & - I_{yzs}(R\cos(\Delta\phi) - Q\sin(\Delta\phi))(R\sin(\Delta\phi) + Q\cos(\Delta\phi)) \end{aligned} \quad (46)$$

When finding the rotational energy of the vehicle system, both sprung and unsprung masses' moments of inertia (I_{xxu}, I_{yyu}, I_{zzu}, I_{xxs}, I_{yys}, I_{zzs}) and products of inertia (I_{xyu}, I_{yzu}, I_{yzu}, I_{xys}, I_{yzs}, I_{yzs}) were included. While the sprung mass's inertia properties were determined in the sprung mass NIRS $o_s x_s y_s z_s$, its quasi-velocities (P_s, Q, R) were determined in the unsprung mass NIRS $o_u x_u y_u z_u$. These quasi-velocities must be transformed to the sprung mass coordinate system in order to correctly determine the vehicle's rotational kinetic energy.

Gravitational potential energy of a vehicle depends on the mass centers' height of both sprung and unsprung masses and has been determined relative to the roadway surface:

$$V_G = M_u(- Z_u)\, g + M_s(- Z_s + h_{ra}\cos(\Delta\phi)T_{zuz} + h_{ra}\cos(\Delta\phi)T_{yuz})\, g \qquad (47)$$

For the vehicle data employed in this report (Appendix ..), the gravitational potential energy reaches a maximum value at a unsprung mass roll angle of approximately 42°. This maximum gravitational potential energy can vary slightly depending on the initial conditions employed in the simulation.

The elastic potential energy of the ITRS vehicle model includes energy stored in suspension springs and bump stops, the vehicle tires, and the recoverable portion of energy stored in the vehicle structure during impact with the curb:

$$\begin{aligned} V_E = {} & 2\{\tfrac{1}{2} K_1(sd_l^2 + sd_r^2) + \tfrac{1}{2} K_2(bd_l^2 + bd_r^2)\} \\ & + \tfrac{1}{2}\{K_z(T_r - T_{lF})^2 + K_z(T_r - T_{rF})^2 + K_z(T_r - T_{lR})^2 + K_z(T_r - T_{rR})^2\} \\ & + V_{IMPf} + V_{IMPr} \end{aligned} \qquad (48)$$

where, for the front axle

$$V_{IMPf} = \begin{cases} \frac{1}{2} k_{d1} d_F^2 & \text{when deflection} \leq \text{Point 1} \\ \frac{1}{2} k_{d3} \{(F_{dF} + B_d\, d_{Fd})/k_{d3}\}^2 & \text{when deflection} > \text{Point 1} \end{cases} \quad (49)$$

and for the rear axle

$$V_{IMPr} = \begin{cases} \frac{1}{2} k_{d1} d_R^2 & \text{when deflection} \leq \text{Point 1} \\ \frac{1}{2} k_{d3} \{(F_{dR} + B_d\, d_{FR})/k_{d3}\}^2 & \text{when deflection} > \text{Point 1} \end{cases} \quad (50)$$

3.2 RESULTS OF ENERGY ANALYSIS

The ITRS vehicle model was thoroughly checked for the energy exchange between vehicle components as well as for the energy dissipation during the entire vehicle motion, including the rollover phase. The energy analyses were conducted for the vehicle data listed in Appendix B. All vehicle energies (equations (45) - (50)) were examined individually and together in a number of different rollover and non-rollover situations. The initial conditions used in the simulation and listed in Appendix C represent a vehicle which is sliding sideways toward a curb with different speeds and various heading angles. In all cases, the front right wheel is initially located at a distance 7.5 Ft away from the curb.

Figures 16 - 24 represent the time histories of various energy components obtained for the initial heading angles of the vehicle equal to 0 (resulting in nearly simultaneous impact of front and rear

wheels), 15 and 25 degrees (oblique impacts). In each of the three cases, the sliding velocity of the vehicle was equal to 20 Ft/s (which did not produce rollover), critical rollover speed and 25 Ft/s. The critical rollover speeds for heading angles of 0, 15 and 25 degrees were 22.13, 22.93 and 23.73 Ft/s respectively. The results show that total vehicle energy is continually decreased in all cases of the side and oblique impacts and that appropriate amount of vehicle energy is dissipated upon the impact with the curb. In this the ITRS simulation corrects the shortcomings of the STI's Tripped Rollover Model [6] which exhibited an increase of vehicle energy caused by ignoring of number of dynamic couplings in equations of motion and neglecting a vehicle's forward dynamics [7].

The amount of total energy which vehicle possesses depends on the vehicle's velocities and position, and is related to the angle of impact with the curb. In vehicle rollovers which occurred at critical speeds, the total energy of the vehicle at its tip-over angle varies from 12,500 - 12,700 Slug Ft^2/s^2 depending upon the angle of impact (Figs. 17, 20 and 23). For sliding velocities of 25 Ft/s, in the same tip-over position, the total vehicle energies equal 16,000, 15,000 and 14,000 Slug Ft^2/s^2 for heading angles of 0, 15 and 25 degrees, respectively. A detailed investigation of the non-rollover cases (side velocity of 20 Ft/s, Figs. 16, 19 and 22) also indicates that just after the curb impact (approximately 0.55 seconds) the vehicle's total energy in the side impact remains higher than in the oblique impact, and then it gradually decreases to 10,000 Slug Ft^2/s^2, which is the same value for all three heading angles. The smaller total energy attained by the vehicle in the oblique impact, as compared to side impact with the same speed, is caused by increased amount of energy dissipated prior to and upon impact when the vehicle heading angle is greater.

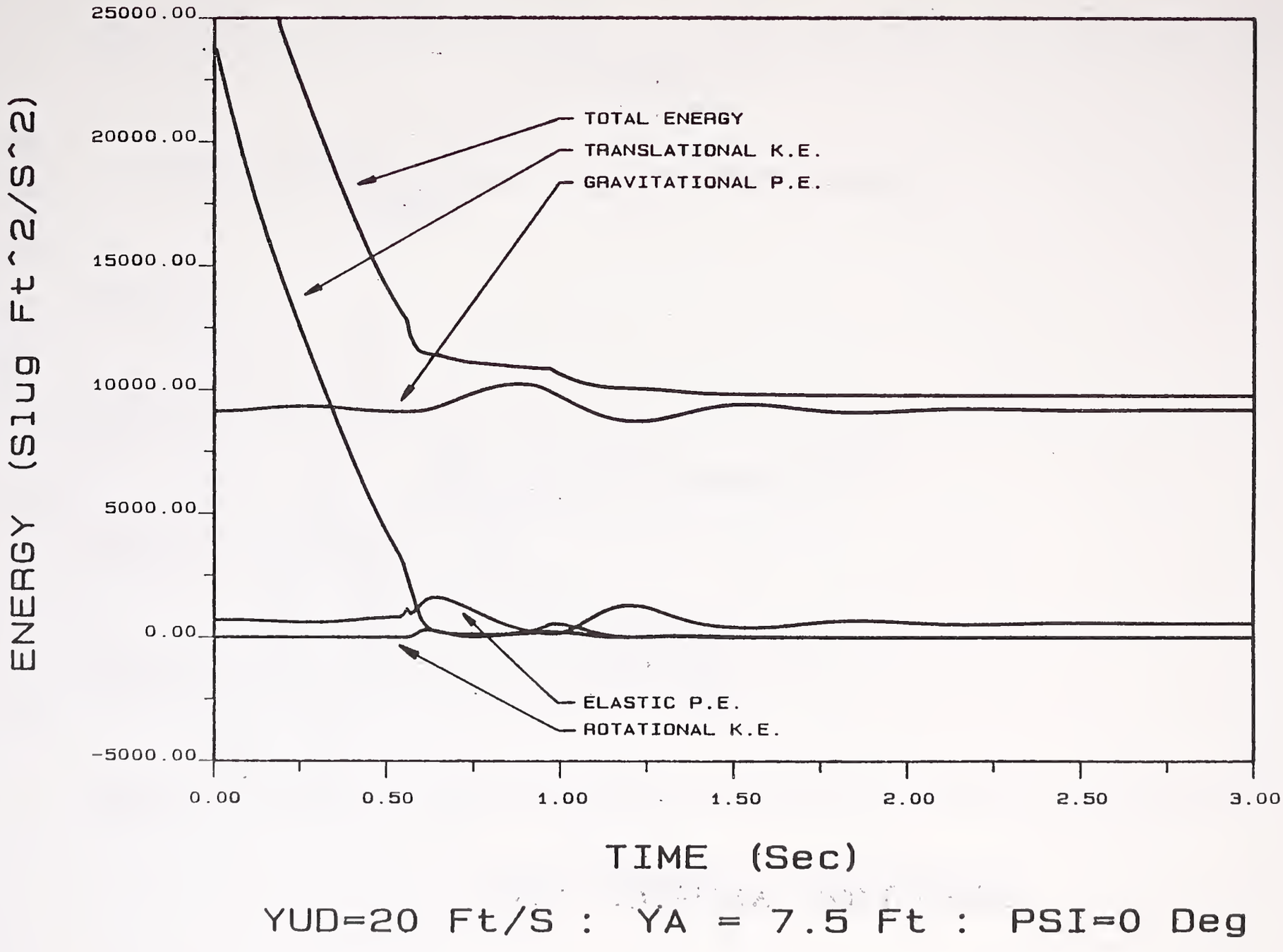
ITRS ENERGY ANALYSIS
ENERGY (Slug Ft^2/S^2)
25000.00
20000.00
15000.00
10000.00
5000.00
0.00
-5000.00
TOTAL ENERGY
TRANSLATIONAL K.E.
GRAVITATIONAL P.E.
ELASTIC P.E.
ROTATIONAL K.E.
0.00
0.50
1.00
1.50
2.00
2.50
3.00
TIME (Sec)
YUD=20 Ft/S : YA = 7.5 Ft : PSI=0 Deg

Figure 16.

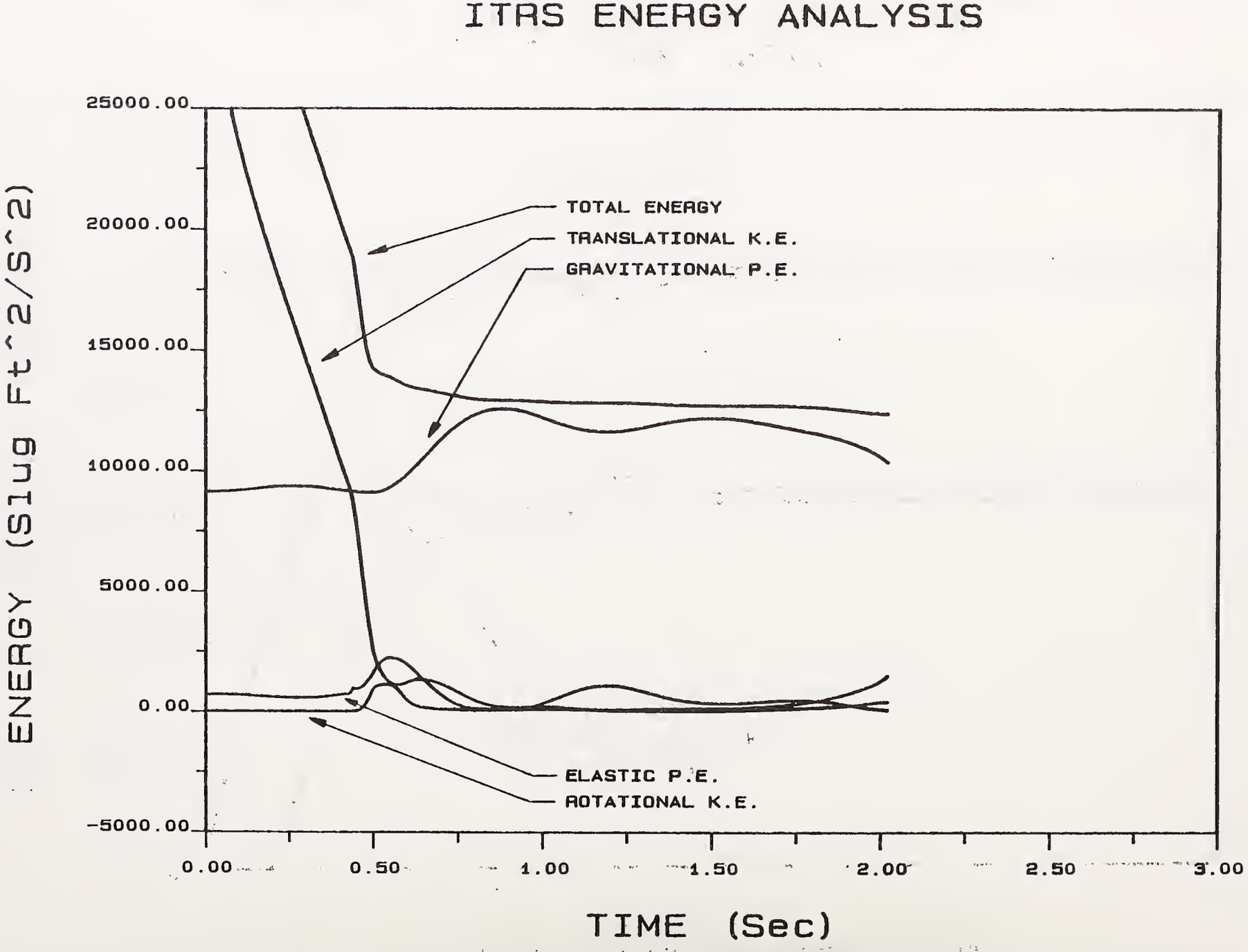
ITRS ENERGY ANALYSIS
25000.00
20000.00
15000.00
10000.00
5000.00
0.00
-5000.00
ENERGY (Slug Ft^2/S^2)
TOTAL ENERGY
TRANSLATIONAL K.E.
GRAVITATIONAL P.E.
ELASTIC P.E.
ROTATIONAL K.E.
0.00
0.50
1.00
1.50
2.00
2.50
3.00
TIME (Sec)
YUD=22.13 Ft/S : YA=7.5 Ft : PSI=0 Deg

Figure 17.

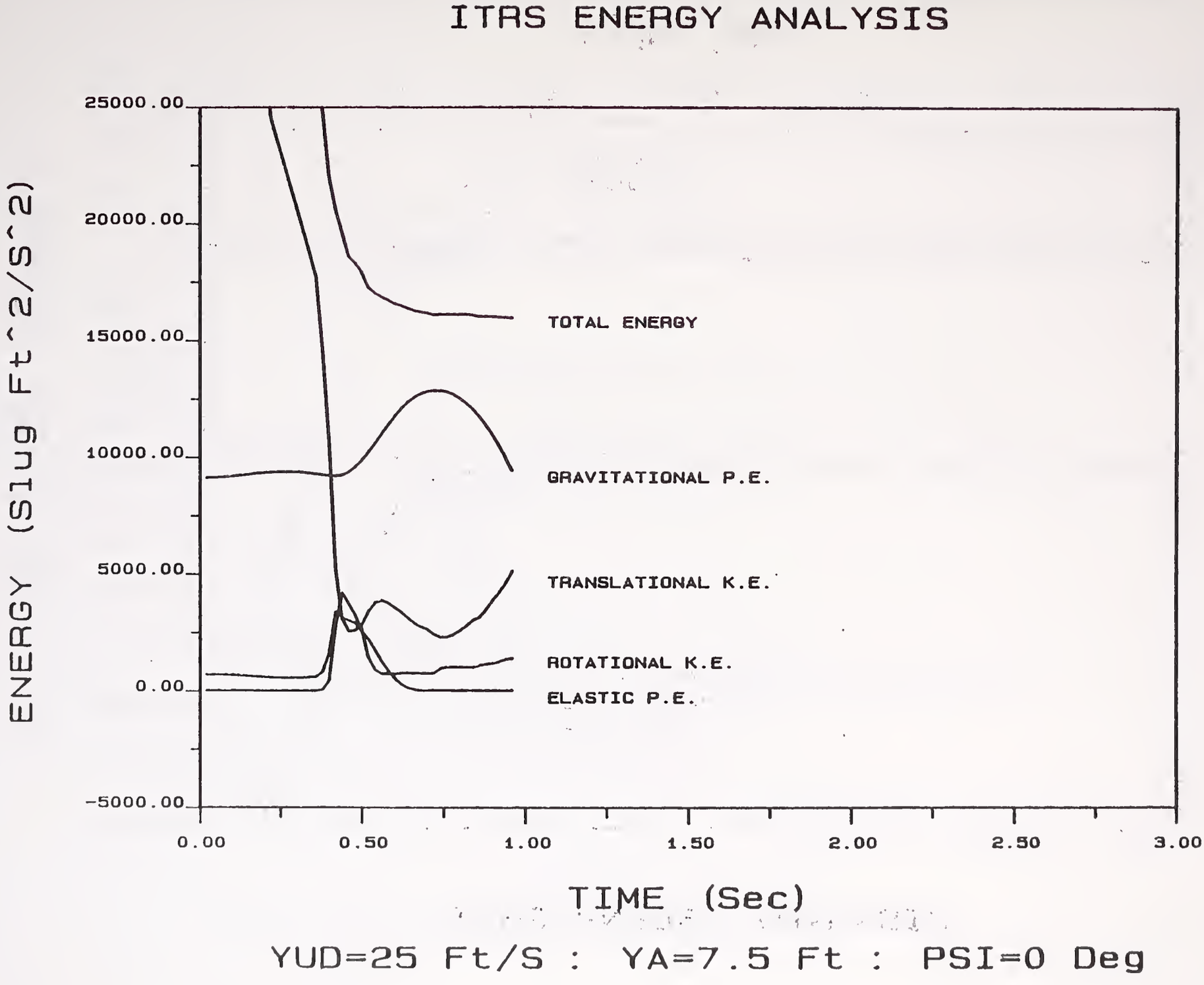
ITRS ENERGY ANALYSIS
ENERGY (Slug Ft^2/S^2)
25000.00
20000.00
15000.00
10000.00
5000.00
0.00
-5000.00
TOTAL ENERGY
GRAVITATIONAL P.E.
TRANSLATIONAL K.E.
ROTATIONAL K.E.
ELASTIC P.E.
0.00
0.50
1.00
1.50
2.00
2.50
3.00
TIME (Sec)
YUD=25 Ft/S : YA=7.5 Ft : PSI=0 Deg

Figure 18.

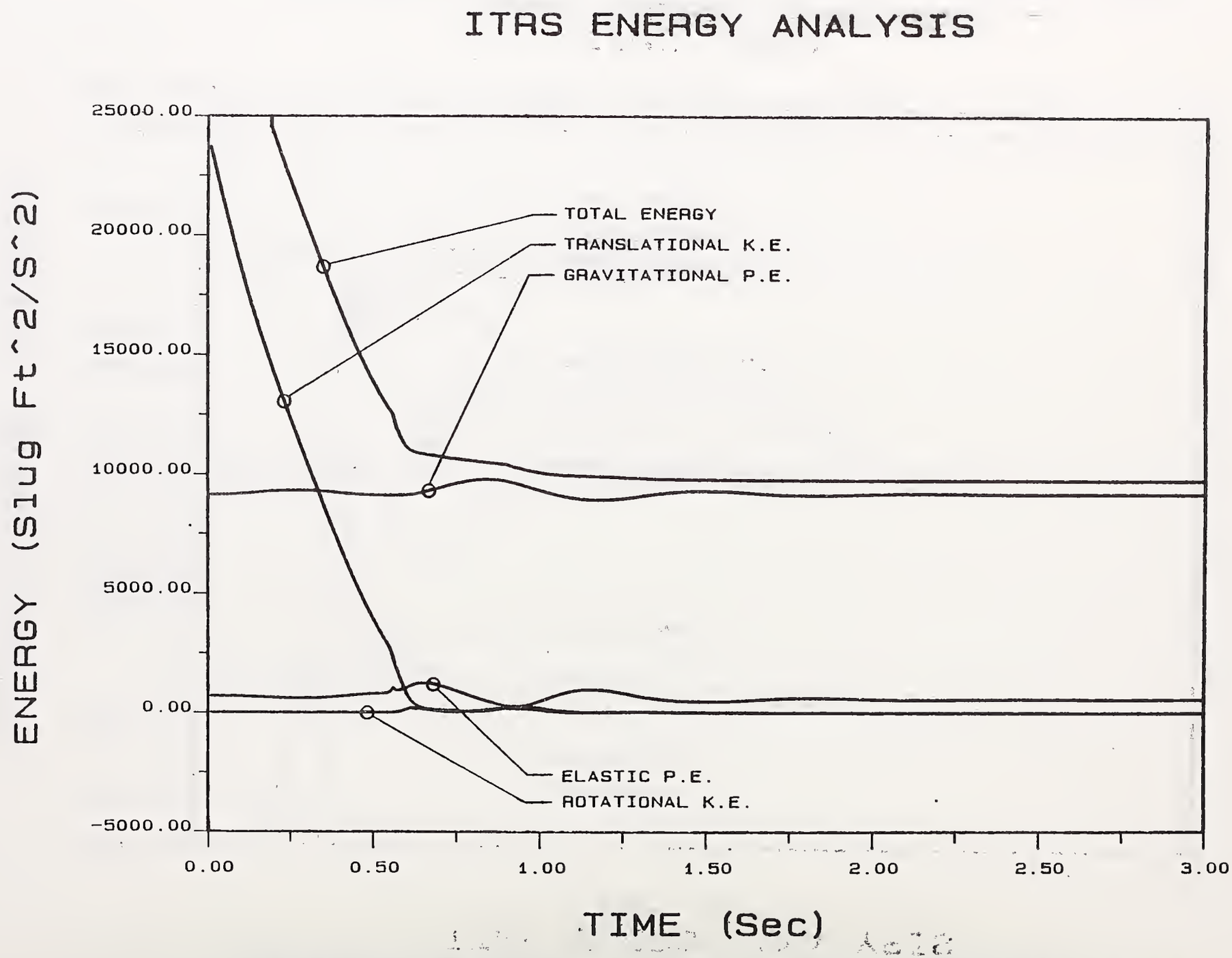
ITRS ENERGY ANALYSIS
25000.00
20000.00
15000.00
10000.00
5000.00
0.00
-5000.00
ENERGY (Slug Ft^2/S^2)
TOTAL ENERGY
TRANSLATIONAL K.E.
GRAVITATIONAL P.E.
ELASTIC P.E.
ROTATIONAL K.E.
0.00
0.50
1.00
1.50
2.00
2.50
3.00
TIME (Sec)
YUD=20 Ft/S : YA=7.5 Ft : PSI=15 Deg

Figure 19.

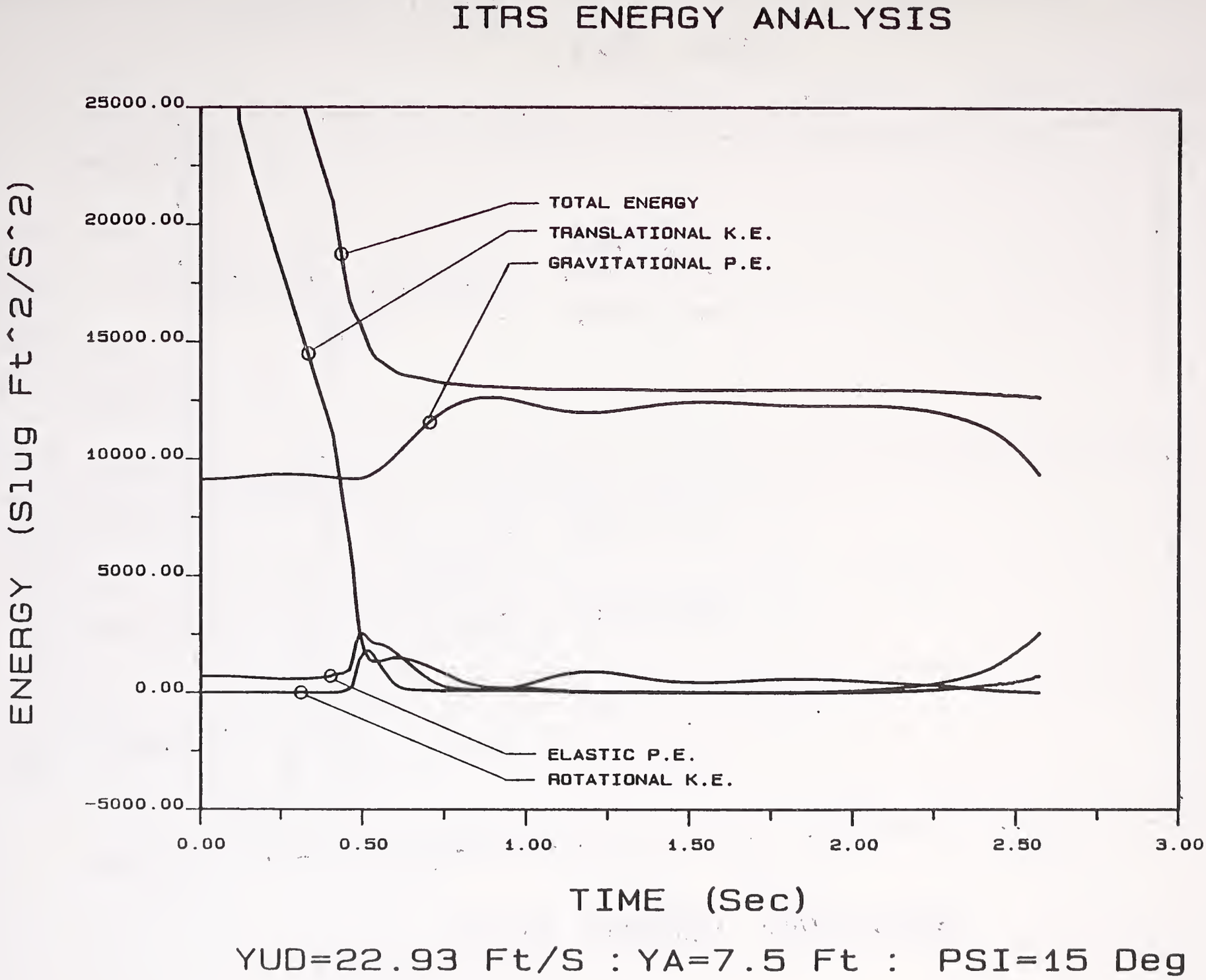
ITRS ENERGY ANALYSIS
25000.00
20000.00
15000.00
10000.00
5000.00
0.00
-5000.00
ENERGY (Slug Ft^2/S^2)
TOTAL ENERGY
TRANSLATIONAL K.E.
GRAVITATIONAL P.E.
ELASTIC P.E.
ROTATIONAL K.E.
0.00
0.50
1.00
1.50
2.00
2.50
3.00
TIME (Sec)
YUD=22.93 Ft/S : YA=7.5 Ft : PSI=15 Deg

Figure 20.

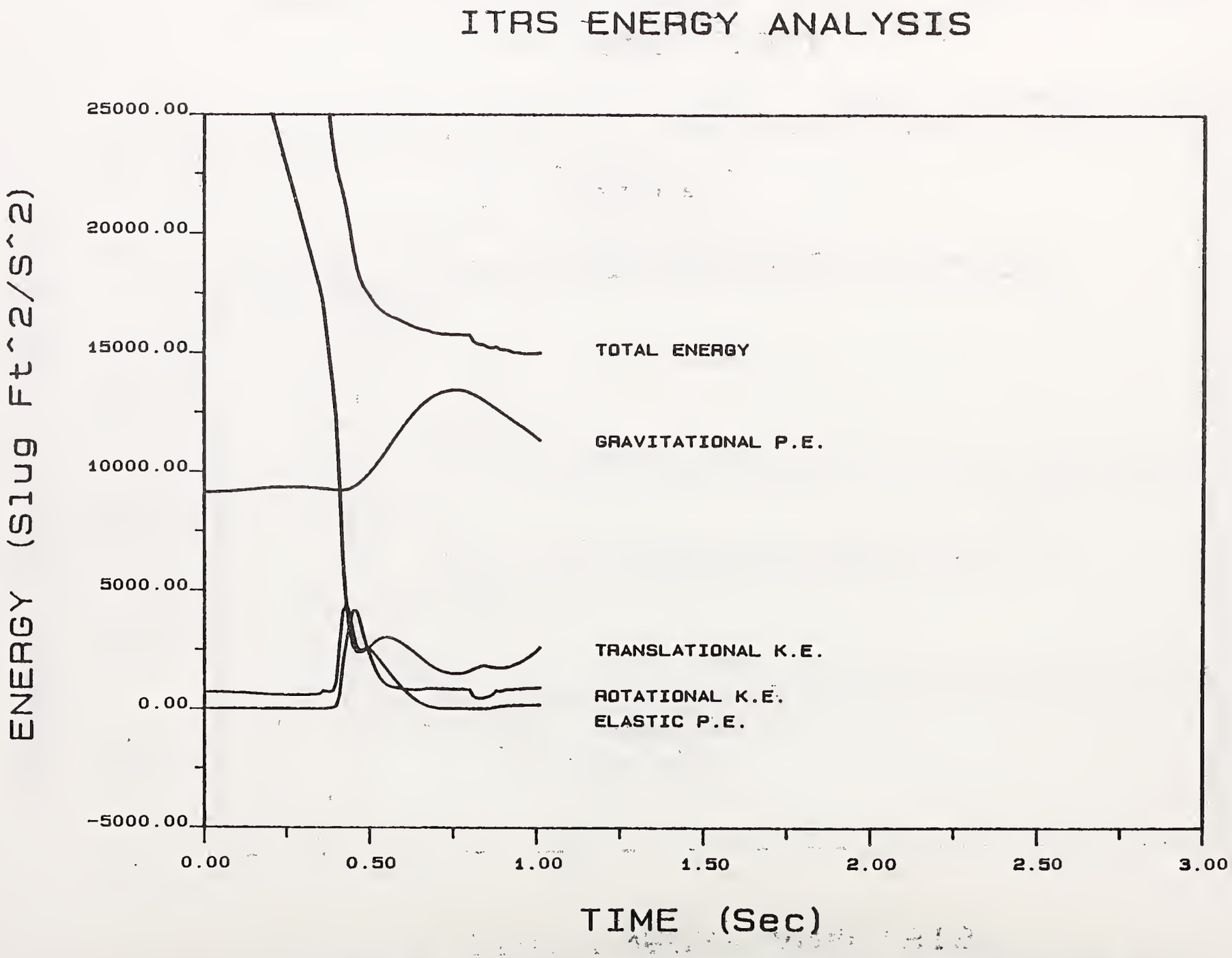
ITRS ENERGY ANALYSIS
ENERGY (Slug Ft^2/S^2)
25000.00
20000.00
15000.00
10000.00
5000.00
0.00
-5000.00
0.00
0.50
1.00
1.50
2.00
2.50
3.00
TIME (Sec)
TOTAL ENERGY
GRAVITATIONAL P.E.
TRANSLATIONAL K.E.
ROTATIONAL K.E.
ELASTIC P.E.
YUD=25 Ft/S : YA=7.5 Ft : PSI=15 Deg

Figure 21.

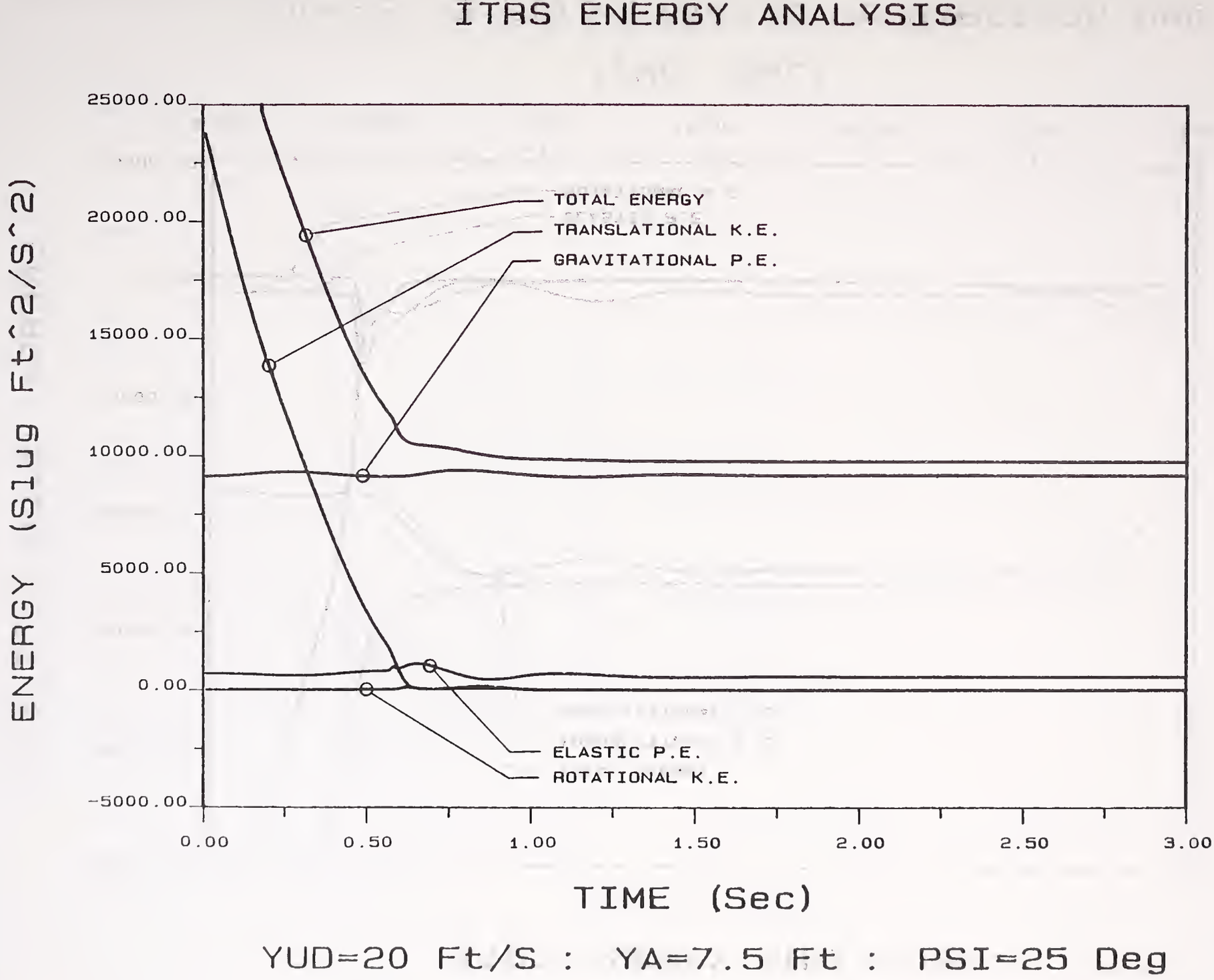
ITRS ENERGY ANALYSIS
25000.00
20000.00
15000.00
10000.00
5000.00
0.00
-5000.00
ENERGY (Slug Ft^2/S^2)
TOTAL ENERGY
TRANSLATIONAL K.E.
GRAVITATIONAL P.E.
ELASTIC P.E.
ROTATIONAL K.E.
0.00
0.50
1.00
1.50
2.00
2.50
3.00
TIME (Sec)
YUD=20 Ft/S : YA=7.5 Ft : PSI=25 Deg

Figure 22.

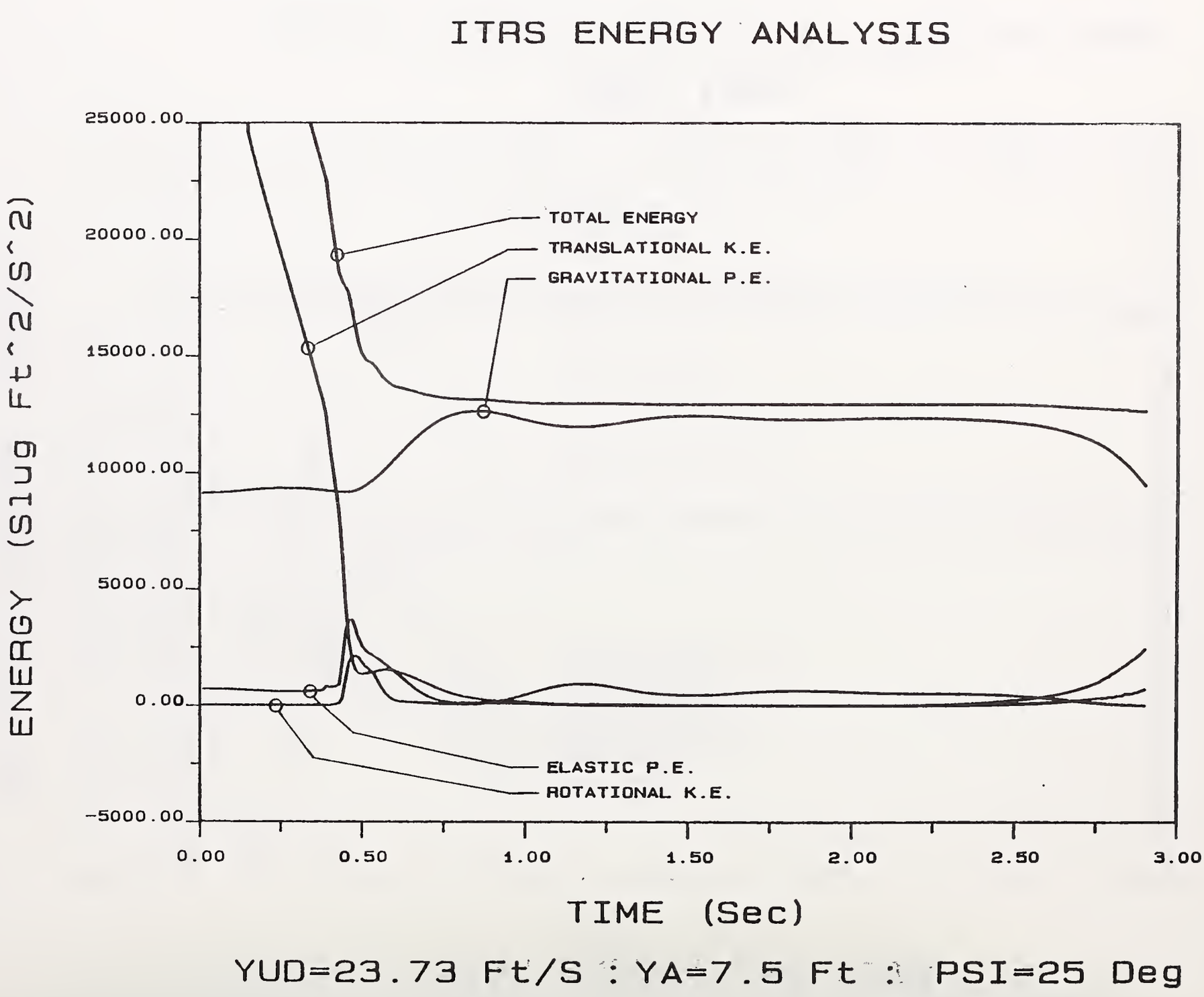
ITRS ENERGY ANALYSIS
25000.00
20000.00
15000.00
10000.00
5000.00
0.00
-5000.00
ENERGY (Slug Ft^2/S^2)
TOTAL ENERGY
TRANSLATIONAL K.E.
GRAVITATIONAL P.E.
ELASTIC P.E.
ROTATIONAL K.E.
0.00
0.50
1.00
1.50
2.00
2.50
3.00
TIME (Sec)
YUD=23.73 Ft/S : YA=7.5 Ft : PSI=25 Deg

Figure 23.

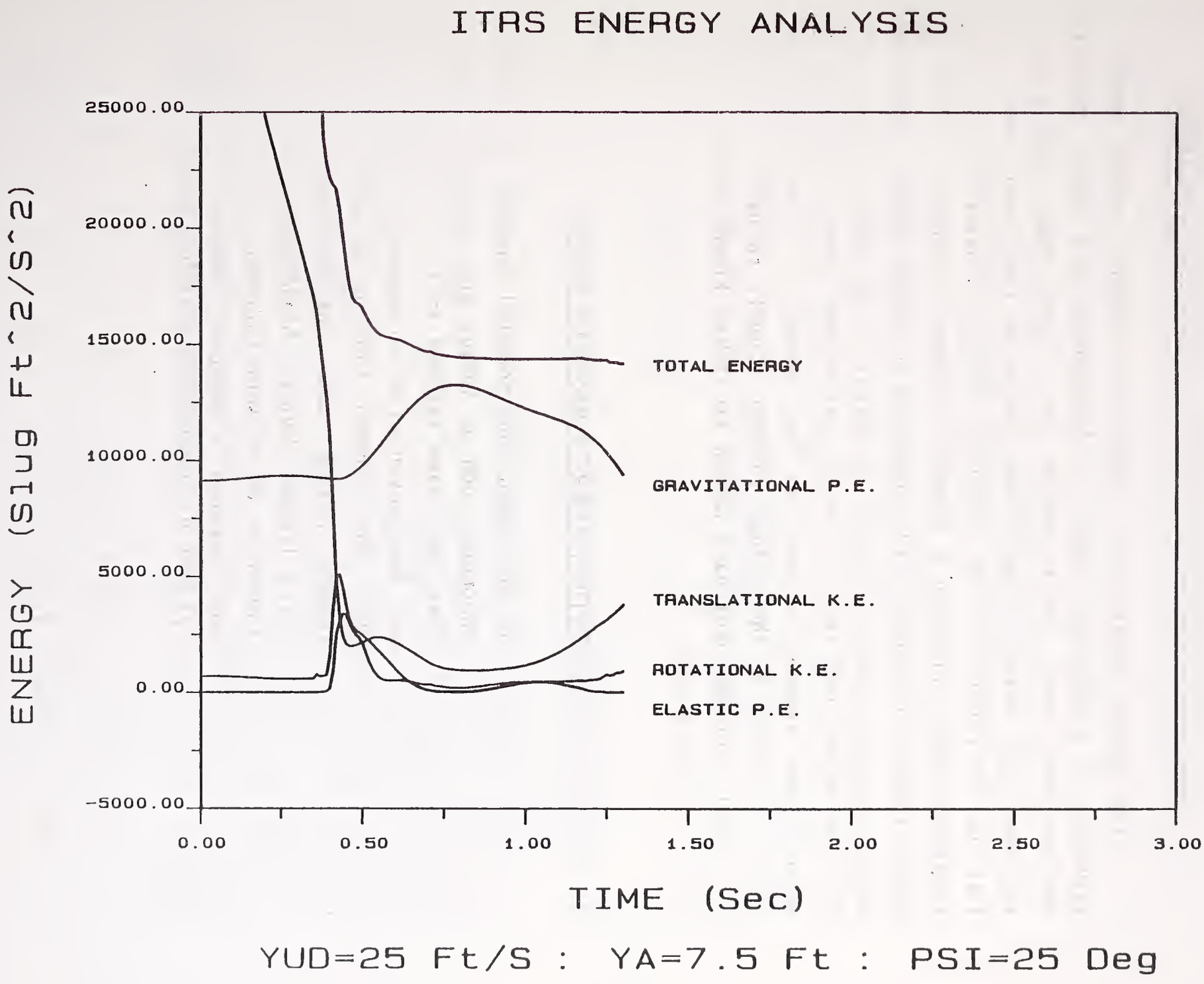
ITRS ENERGY ANALYSIS
ENERGY (Slug Ft^2/S^2)
25000.00
20000.00
15000.00
10000.00
5000.00
0.00
-5000.00
0.00
0.50
1.00
1.50
2.00
2.50
3.00
TIME (Sec)
TOTAL ENERGY
GRAVITATIONAL P.E.
TRANSLATIONAL K.E.
ROTATIONAL K.E.
ELASTIC P.E.
YUD=25 Ft/S : YA=7.5 Ft : PSI=25 Deg

Figure 24.

4. ROLLOVER PREVENTION ENERGY RESERVE FUNCTIONS

The kinetic energy of a vehicle in skidding motion consists primarily of translational energy of longitudinal and lateral motions and rotational energy due to vehicle yaw. Upon impact with a curb or other rigid obstacle, a significant portion of this kinetic energy is lost and the majority of the remaining energy is converted to rolling rotational energy, initiating a potential rollover situation. A vehicle which strikes an obstacle will rollover if it attains enough rotational kinetic energy to raise its center of gravity to the static tip-over angle (the largest roll angle at which gravitational forces would return a motionless vehicle to stand on four wheels). A vehicle which impacts the curb at the critical rollover velocity (minimum velocity for vehicle rollover) will have almost no rolling kinetic energy at the static tip-over angle.

4.1 ROLLOVER PREVENTION ENERGY RESERVE (RPER)

Investigations into the kinetic and potential energies of a vehicle system and its components such as sprung and unsprung masses, suspension elements, tires, ect., have resulted in the development of a dynamic function which has proven to be an accurate indicator of a vehicle's rollover stability. This dynamic function is called Rollover Prevention Energy Reserve (RPER) and was first used in the sensitivity analysis of STI's Tripped Rollover Model performed by Dr. A. G. Nalecz at the University of Missouri-Columbia [7]. RPER is defined as the difference between a vehicle's critical gravitational potential energy (V_{CRIT}) and its non-centroidal rolling kinetic energy (T_{NR}):

$$RPER = V_{CRIT} - T_{NR} \tag{51}$$

The critical gravitational potential energy (V_{CRIT}) of a vehicle is defined as the potential energy necessary to raise the vehicle from its four wheel stance to static tip-over position (see Figure 25):

$$V_{CRIT} = (M_u + M_s)\, g \left[\sqrt{h_{CG}^2 + \left(\frac{TRW}{2}\right)^2} - h_{CG}\right]$$

$$= (M_u + M_s)\, g\, h_{CG} \left[\sqrt{1 + SRSF^2} - 1\right] \qquad (52)$$

where,

h_{CG} = static vehicle CG height

$$SRSF = \frac{TRW}{2\, h_{CG}}$$

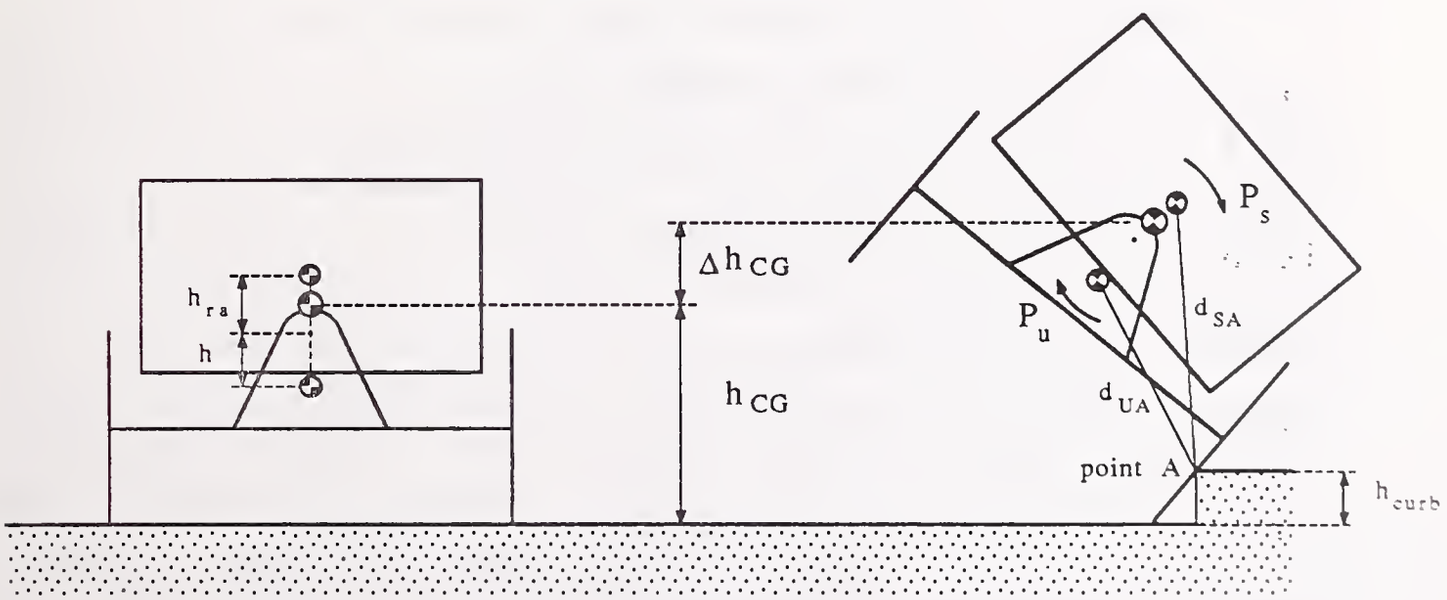

h_{CG} = Static vehicle CG height

Δh_{CG} = CG height change

Figure 25. Vehicle CG Height.

The non-centroidal rolling kinetic energy (T_{NR}) is defined as the kinetic energy of a vehicle's rolling motion about the edge of the curb:

$$T_{NR} = \frac{1}{2} I_{xxsA} P_s^2 + \frac{1}{2} I_{xxuA} P_u^2 \qquad (53)$$

Using the parallel-axis theorem, the non-centroidal moments of inertia of the vehicle's sprung and unsprung masses (Figure 25) can be found using the following relations:

$$I_{xxsA} = I_{xxs} + M_s d_{SA}^2 \qquad (54)$$

$$I_{xxuA} = I_{xxu} + M_u d_{UA}^2$$

Although the static rollover stability factor (SRSF) can be used to assess vehicle's rollover propensity under static conditions, the RPER has been found to be a much better measure since it includes both static and dynamic factors influencing the dynamic rollover behavior. Analysis of the RPER function provides a reliable method of assessing a vehicle's rollover stability. During tripped rollover situations involving simultaneous curb impact of both side tires (side impact), RPER must drop to a value less than zero if vehicle rollover is to occur, however, if the vehicle's RPER remains positive, the vehicle will not rollover. If a vehicle's RPER remains positive at all times this indicates that the vehicle failed to achieve sufficient rolling kinetic energy to initiate a rollover.

Figures 26 - 30 show the time histories of RPER obtained for several different test speeds during vehicle side impacts with the curb (vehicle heading angle upon impact equals 0). The vehicle data and the initial conditions utilized in these tests are the same which were used in the energy analysis (listed in Appendices B and C).

With a skidding lateral velocity of 17 Ft/s, the vehicle, which initially was 7.5 Ft from the curb, comes to a complete stop before reaching the curb (Figure 26). A small reduction of the vehicle's RPER, which occurs between 0.7 and 1.0 seconds, is caused by the change of the vehicle's roll angle when coming to rest.

At a lateral velocity of 20 Ft/s, the vehicle impacts the curb but does not rollover (Figure 27). In this case, the vehicle impacts the curb, rolls to a maximum roll angle which is smaller than the static tip-over angle, and then returns to a stable position on four wheels. The chassis continues to roll after returning to a four wheel stance, causing roll oscillations which are damped out by the shock absorbers and tires. Figure 27 shows that RPER drops by about 1,300 units just after the impact but still remains positive throughout the entire motion.

Figure 28 represents the time history of RPER obtained for the vehicle skidding with critical rollover velocity of 22.13 Ft/s. The vehicle impacted the curb at approximately 0.44 seconds. Immediately after curb impact, the vehicle's RPER dropped sharply to a value of approximately -220 Slug Ft^2/s^2 and then increased when the vehicle's roll angle approached the static tip-over value (second RPER's peak at about 1.37 seconds). At the static tip-over position, the roll angular velocities of the sprung and unsprung masses were nearly zero and RPER assumed a value equal to that just before the impact. The RPER then drops again once the vehicle passes through the static tip-over position and rolls over.

The instant of rollover initiation can be determined from Figure 28 as the instant when dynamic criteria for vehicle rollover is satisfied, which occurs when RPER drops to zero (approximately 0.50 seconds). Also, from the same figure it can be found that the vehicle rolls to the static tip-over position within 0.87 seconds from the instant of rollover initiation.

It should be noted that a velocity of 22.13 Ft/s, which has been designated throughout this report as critical rollover velocity in side impact, is the smallest initial skidding velocity of the vehicle (being 7.5 Ft away from the curb) for which the vehicle rolls over. The critical rollover velocity is not a velocity with which the vehicle impacts the curb. The velocity with which the vehicle impacted the curb can be found from the system response to be approximately 12 Ft/s (Figure D-10 in Appendix D).

The time histories of RPER obtained for the lateral skidding velocities higher than the critical rollover speed are presented in Figures 29 and 30. For the initial velocity equal to 25 Ft/s (Figure 29) the vehicle impacts the curb at about 0.38 seconds and the dynamic criteria for rollover are satisfied (RPER = 0) at approximately 0.41 seconds. After vehicle rollover is initiated, the vehicle's RPER continues to drop to a negative value of 7,500 Slug Ft^2/s^2 and then increases to 2,720 Slug Ft^2/s^2 when vehicle reaches the static tip over position (at approximately 0.65 seconds). At the initial speed of 27 Ft/s (Figure 30) the vehicle's RPER drops to -15,000 Slug Ft^2/s^2 immediately after curb impact, thus illustrating that a higher initial speed (and also impact speed) results in a larger drop of vehicle RPER. It is also interesting to notice that at an initial speed of 27 Ft/s it takes only 0.17 seconds for the vehicle to roll to its static tip-over position once rollover has been initiated. At an initial speed of 25 Ft/s, the equivalent rollover time was 0.24 seconds.

Figure 31 represents vehicle RPER at each of the five initial speeds. This figure clearly illustrates that vehicle RPER remains positive in all non-rollover cases (speeds smaller than critical rollover speed) and becomes negative when vehicle rollover occurs (critical speed and higher). The instant when the vehicle impacts the curb and when rollover is initiated, as well as the duration of vehicle rollover, can easily be determined from this figure. Since RPER is an energy function, it is very sensitive to changes in vehicle skidding velocities. This is demonstrated by a wide range of RPER values exhibited upon impacts with a curb.

The time histories of vehicle RPER obtained for various speeds during oblique impacts with curb and for two initial heading angles equal to 15 and 25 degrees are shown in Figures 32 and 33. In both cases the initial distance from vehicle's front wheel to the curb was 7.5 Ft and vehicle's skidding velocity was perpendicular to curb, which resulted in the front wheel impacting the curb first. Figures 32 and 33 were obtained for the same velocities as Figure 31 (side impact) with the exception of the critical speeds. The initial skidding velocities of 22.93 and 23.73 Ft/s were designated as critical rollover speeds for oblique impacts at angles of 15 and 25 degrees, respectively.

Figures 32 and 33 show that the minimum value of RPER is positive for speeds which did not result in rollover (17 and 20 Ft/s) and negative for speeds equal to and greater than critical rollover speeds. This confirms that RPER is also very useful indicator of vehicle rollover propensity in oblique impacts with the curb.

From comparing Figures 32 and 33 it can be seen that the minimum values of RPER in the case of an oblique impact at an angle of 15 degrees are smaller than those at an angle of 25 degrees for the same skidding velocities. This clearly demonstrates that less rolling kinetic energy is created (and more energy is dissipated) upon impact at larger angle than smaller angle, and that a greater skidding velocity is needed to roll the vehicle over in first case. The critical rollover velocities in both of these cases are another good examples, the speed of 22.93 Ft/s for 15 degree impact and 23.73 Ft/s for 25 degree impact. Close examinations of both figures also confirm that vehicle rollover lasts longer in case of larger than smaller impact angle for the same speeds, including critical rollover speeds.

For rollovers from oblique impacts with the curb, the RPER must drop below zero by the amount of energy which will be dissipated between the instant when the minimum RPER is achieved

and the moment when the static tip over angle is reached. The amount of energy to be dissipated is obviously greater for larger angles of impact. In particular, this can be seen in Figures 32 and 33 for critical speeds.

4.2 ROLLOVER PREVENTION ENERGY RESERVE #3 (RPER3)

In order to investigate rollover behavior in further detail, additional research was performed to construct a refined rollover propensity measure. To more adequately describe the stabilizing effect of a vehicle's gravitational potential energy, the vehicle's critical gravitational potential energy was modified to include changes caused by impact with the curb, such as reduction of track width, and CG height variation due to spring deformations. Research was conducted into the vehicle's kinetic energy to determine which energy components were capable of influencing rollover behavior. The influence of elastic potential energy stored in the tires, suspension systems and elastic impact on RPER was also examined. The more complex version of rollover prevention energy reserve (RPER3) includes a modified critical gravitational potential energy term, and additional elastic potential and kinetic energy terms. RPER3 was constructed to use the same criteria for rollover prediction as the original RPER. The formulation of RPER3 contains five potential and three kinetic energy terms and is shown below.

$$RPER3 = V_{CRITc} + \Delta V_{SUS} + \Delta V_T - V_{IMPf} - V_{IMPr} - T_{NR} - T_{ROTy} - T_{TRANh} \quad (55)$$

The individual terms of equation (55) are explained in detail in the sections below.

4.2.1 Instantaneous Critical Gravitational Potential Energy (V_{CRITc})

The V_{CRITc} represents the gravitational potential energy needed to raise the vehicle from a rest to the static tip-over position based upon the instantaneous suspension geometry.

$$V_{CRITc} = (M_u + M_s)\, g \left[\sqrt{\left(h_{CGc}^2 + TRW_c^2 \right)} - h_{CGc} \right]$$

$$= (M_u + M_s)\, g\, h_{CGc} \left[\sqrt{1 + IRSF^2} - 1 \right] \qquad (56)$$

where,

h_{CGc} = instantaneous vehicle CG height

TRW_c = instantaneous vehicle half track width

$$IRSF = \frac{TRW_c}{h_{CGc}}$$

The instantaneous vehicle half track width (TRW_c) includes vehicle lateral elastic and plastic deformations and is determined using a weighted average of the vehicle front and rear half track widths (TRWF, TRWR). The instantaneous rollover stability factor (IRSF) is an analogous term to SRSF, but IRSF is calculated based on the instantaneous values of track width and includes changes in the static CG height of the vehicle caused by relative motions of sprung and unsprung masses.

It was determined that the potential energy V_{CRITc} used in RPER3 is a superior representation of a vehicle's stabilizing gravitational potential energy when compared with the term V_{CRIT} used in the previous formulation of RPER. Lateral deformation of the wheel and axle can significantly alter the amount of energy necessary to bring a vehicle to the static tip-over position, which in turn affects the amount of stabilizing potential energy V_{CRITc} within the vehicle.

4.2.2 Suspension Elastic Potential Energy (ΔV_{SUS})

ΔV_{SUS} represents the change in elastic potential energy stored in suspension springs and bump stops.

$$\Delta V_{SUS} = V_{SUS} - V_{SUSi} = 2\{\frac{1}{2} K_1(d_{sl}^2 + d_{sr}^2) + \frac{1}{2} K_2(d_{bl}^2 + d_{br}^2)\} - V_{SUSi} \quad (57)$$

where,

V_{SUSi} = initial suspension elastic energy

The springs and bump stops of the suspension systems restrain relative motions between sprung and unsprung masses by storing potential energy. At the instant of rollover initiation, just after impact with the curb, the rolling kinetic energy of relative motion of sprung and unsprung masses contributes to vehicle rollover. A portion of this energy is stored in elastic elements of the suspension system. For this reason, ΔV_{SUS} was added to the RPER3 function. If the vehicle fails to rollover, this energy is released after the instant which under other circumstances vehicle rollover would have been initiated. If the vehicle does rollover, this energy will be released after the instant of rollover initiation when rollover is inevitable.

4.2.3 Tire Elastic Potential Energy (ΔV_T)

The term ΔV_T represents the change of potential elastic energy of all four tires from their static position.

$$\Delta V_T = V_T - V_{Ti} = \frac{1}{2}\{K_z(T_r - T_{lF})^2 + K_z(T_r - T_{rF})^2 + K_z(T_r - T_{lR})^2 + K_z(T_r - T_{rR})^2\} - V_{Ti} \quad (58)$$

where,

V_{Ti} = initial tire elastic energy

The change in the elastic potential energy associated with the tires is treated in a manner similar to that used for the change in elastic potential energy stored in the suspension elements. A vehicle's tires store a portion of the unsprung mass's rolling kinetic energy. Like suspension elastic energy, the stored elastic tire energy is released after the instant when the vehicle either begins to return to its four wheel stance or the vehicle has reached a position where the energy release would be unable to stop vehicle rollover. This term is also added to the modified rollover prevention energy reserve RPER3 .

4.2.4 Impact Elastic Potential Energies (V_{IMPf}, V_{IMPr})

The elastic potential energies stored within the front and rear wheel/axle/structure (V_{IMPf}, V_{IMPr}) are non-linear functions dependant upon the first region loading slope (K_{d1}), the unloading/reloading slope (K_{d3}), lateral crush (d_F, d_R) and the impact force (F_{dF}, F_{dR}).

For the front axle:

$$V_{IMPf} = \begin{cases} \frac{1}{2} K_{d1} d_F^2 & \text{when deflection} \leq \text{Point 1} \\ \frac{1}{2} K_{d3} \{(F_{dF} + B_d \dot{d}_{Fd})/K_{d3}\}^2 & \text{when deflection} > \text{Point 1} \end{cases} \quad (59)$$

For the rear axle:

$$V_{IMPr} = \begin{cases} \frac{1}{2} K_{d1} d_R^2 & \text{when deflection} \leq \text{Point 1} \\ \frac{1}{2} K_{d3} \{ (F_{dR} + B_d \dot{d}_{Fd})/K_{d3} \}^2 & \text{when deflection} > \text{Point 1} \end{cases} \quad (60)$$

The energy components V_{IMPf} and V_{IMPr} store translational energy of the vehicle and release it in a manner which will increase the vehicle's rollover motion. Thus, the impact elastic energy is subtracted from RPER3.

4.2.5 Relative Translational Kinetic Energy (T_{TRANh})

The amount of relative heave and roll of both sprung and unsprung masses depends on the amount of elastic energy stored within the suspension system. The rollover propensity of a vehicle is not directly influenced by relative heave of both masses. In order to eliminate the elastic energy which influences relative heave motion, the vehicle's translational kinetic energy (T_{TRANh}) was subtracted from RPER3 energy function.

$$T_{TRANh} = \frac{1}{2} M_s \dot{h}^2 \quad (61)$$

where,

$\dot{h}$ = relative vertical velocity of the two masses

4.2.6 Yawing Kinetic Energy (T_{ROTy})

The yawing kinetic energy (T_{ROTy}) of ITRS vehicle system is represented by the following expression:

$$T_{ROTy} = \frac{1}{2} I_{zzu} R^2 + \frac{1}{2} I_{zzs} (R\cos(\Delta\phi) - Q\sin(\Delta\phi))^2 \qquad (62)$$

A vehicle which strikes a curb at an oblique angle will convert a portion of translational kinetic energy to yawing kinetic energy. This yawing kinetic energy tends to accelerate the vehicle's rollover motion when, upon the second wheel/axle impact, a significant amount of this energy is converted to rolling kinetic energy. T_{ROTy} is included in RPER3 to account for the amount of energy of vehicle yaw motion until it is changed to rolling kinetic energy. Accordingly, the yawing rotational kinetic energy was subtracted from the modified rollover prevention energy reserve RPER3.

4.2.7 RPER3 Results in Side and Oblique Impacts

The Rollover Prevention Energy Reserve #3 (RPER3) defined by equations (55) - (62) has been investigated in an identical way as RPER. The vehicle data and initial conditions used were the same as before, and, to ease the comparison between RPER3 and RPER, all plots were made in the same scales.

The time histories of RPER3 obtained for the five initial skidding velocities during vehicle side impact with the curb are shown in Figures 34 - 41. In non-rollover cases (Figures 34 and 35 for skidding velocities of 17 and 20 Ft/s), the RPER3 remains positive for all times during the simulation run indicating that the vehicle did not gain enough energy which would bring it to a tip-over position. With a skidding lateral velocity of 17 Ft/s, the vehicle (which

initially was 7.5 Ft from the curb) stops completely before reaching the curb. In this case, the changes of RPER3 are caused by roll oscillations of sprung mass when the vehicle comes to a stop (at about 1.0 second). At the skidding velocity of 20 Ft/s the vehicle impacts the curb, rolls to an angle smaller than tip-over angle and then returns to a rest. As a result of curb impact the suspension springs, bump stops, axles and tires store the potential energy which soon after is exchanged into kinetic energy when vehicle rolls, and then is dissipated when vehicle comes to a stable position on four wheels. The non-uniform changes of the RPER3 value, which occur between 0.5 and 2 seconds, are caused by the fact that various vehicle sub-systems release and/or exchange their energies in different ways and at various instants.

From comparison of Figures 34 and 35 with 26 and 27 it can be seen that RPER3 exhibits greater initial oscillations than RPER does (over the time interval 0 - 0.4 seconds). This is because RPER3 is more sensitive than RPER to the accuracy with which ITRS initial conditions were determined.

In all rollover cases (Figures 36, 37 and 38) RPER3 drops to a negative value just after the curb impact, then increases when vehicle rolls to a tip-over position and drops again when the vehicle rolls over. After the instant of rollover initiation, minimum values of RPER3 are approximately the same as they were in the case of RPER (Figures 28, 29 and 30); however, when the vehicle approaches the tip-over position, the characteristics of changes in RPER3 are different from that in RPER. At the critical rollover speed of 22.13 Ft/s, RPER3 does not attain the value it had before impact (as it was for RPER) because the vehicle track width is shorten as a result of crash, and the tires and suspension springs are not deformed as much at the tip-over angle as they were when the vehicle was skidding. In addition to this, at the speeds greater than critical rollover velocity (Figures 37 and 38), values of RPER3 at tip-over angle are further reduced by the increased amount of energy lost when plastic deformation of the wheel/axle structure occurs.

Figure 39 represents the vehicle's RPER3 obtained for the five initial skidding velocities during side impacts with curb. This figure clearly demonstrates that RPER3, similarly to RPER, is a reliable dynamic function governing the rollover behavior and a valuable indicator of vehicle rollover stability. If vehicle rollover occurs, the value of RPER3 becomes negative. If rollover does not take place, RPER3 remains positive. From a comparison of Figures 39 and 31 it can be seen that RPER3 is more sensitive to initial conditions than RPER is and that minimum values of both functions RPER3 and RPER are almost identical when the vehicle approaches the tip-over position.

The time histories of the vehicle's RPER3 obtained during oblique impacts with the curb at the two angles of 15 and 25 degrees are shown in Figures 40 and 41, respectively. Each figure represents RPER3 for five skidding velocities, which include 17, 20 Ft/s,. critical rollover speed, 25, and 27 Ft/s. The critical rollover speeds are the same as in the case of RPER during oblique impacts, and they are 22.93 and 23.73 Ft/s for heading angles of 15 and 25 degrees, respectively.

Figures 40 and 41 demonstrate that values of RPER3 remain positive for skidding velocities of 17 and 20 Ft/s (which did not result in rollover). At the critical rollover and higher speeds, the RPER3 drops below zero immediately after the impact, then increases when vehicle rolls, and drops again when vehicle rolls over. The character of changes of RPER3 during the oblique impact is similar to the side impact (Figure 39) with the exception that now, for vehicle rollover to occur, RPER3 must drop more than in case of side impact. The amount of energy by which RPER3 must drop below zero at the critical rollover speed equals the energy which will be dissipated after the impact and before the vehicle reaches the static tip-over angle. As it is seen from Figures 40 and 41, at critical rollover speeds the minimum values of RPER3, just after the impact, are -1,250 and -2,500 Slug Ft^2/s^2 for impact angles of 15 and 25

degrees, respectively. This confirms that amount of energy by which RPER3 must drop below zero increases as impact angle increases.

From the comparison of corresponding plots obtained for RPER3 and RPER during oblique impacts (Figures 40 and 32, 41 and 33), it can be seen that minimum values of both functions are similar and the same qualitative criteria for the occurrence of vehicle rollover may be applied to both RPER3 and RPER. However, RPER3 displays greater sensitivity to initial conditions than does RPER.

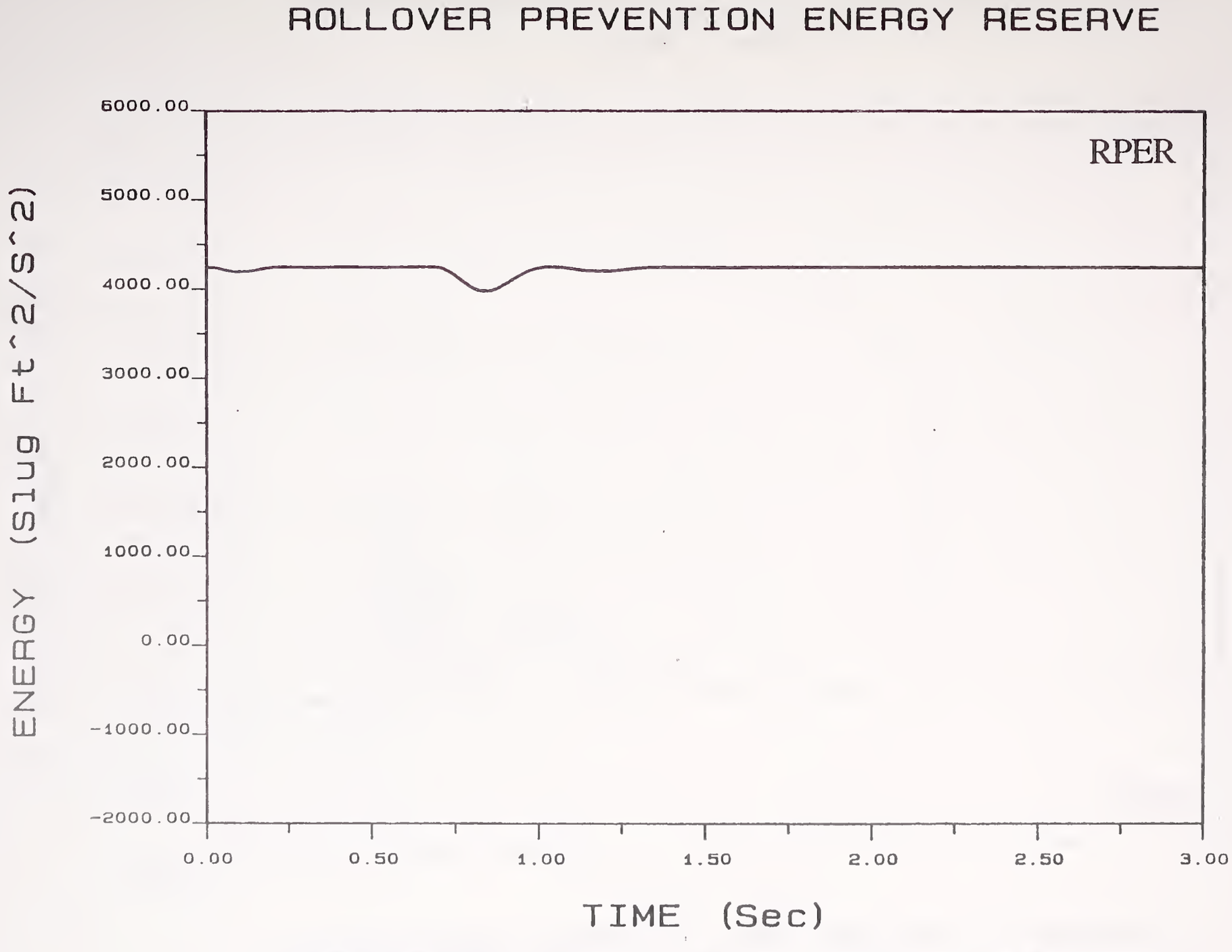
ROLLOVER PREVENTION ENERGY RESERVE
RPER
ENERGY (Slug Ft^2/S^2)
6000.00
5000.00
4000.00
3000.00
2000.00
1000.00
0.00
-1000.00
-2000.00
0.00
0.50
1.00
1.50
2.00
2.50
3.00
TIME (Sec)
YUD=17 Ft/S : YA=7.5 Ft : PSI=0 Deg

Figure 26.

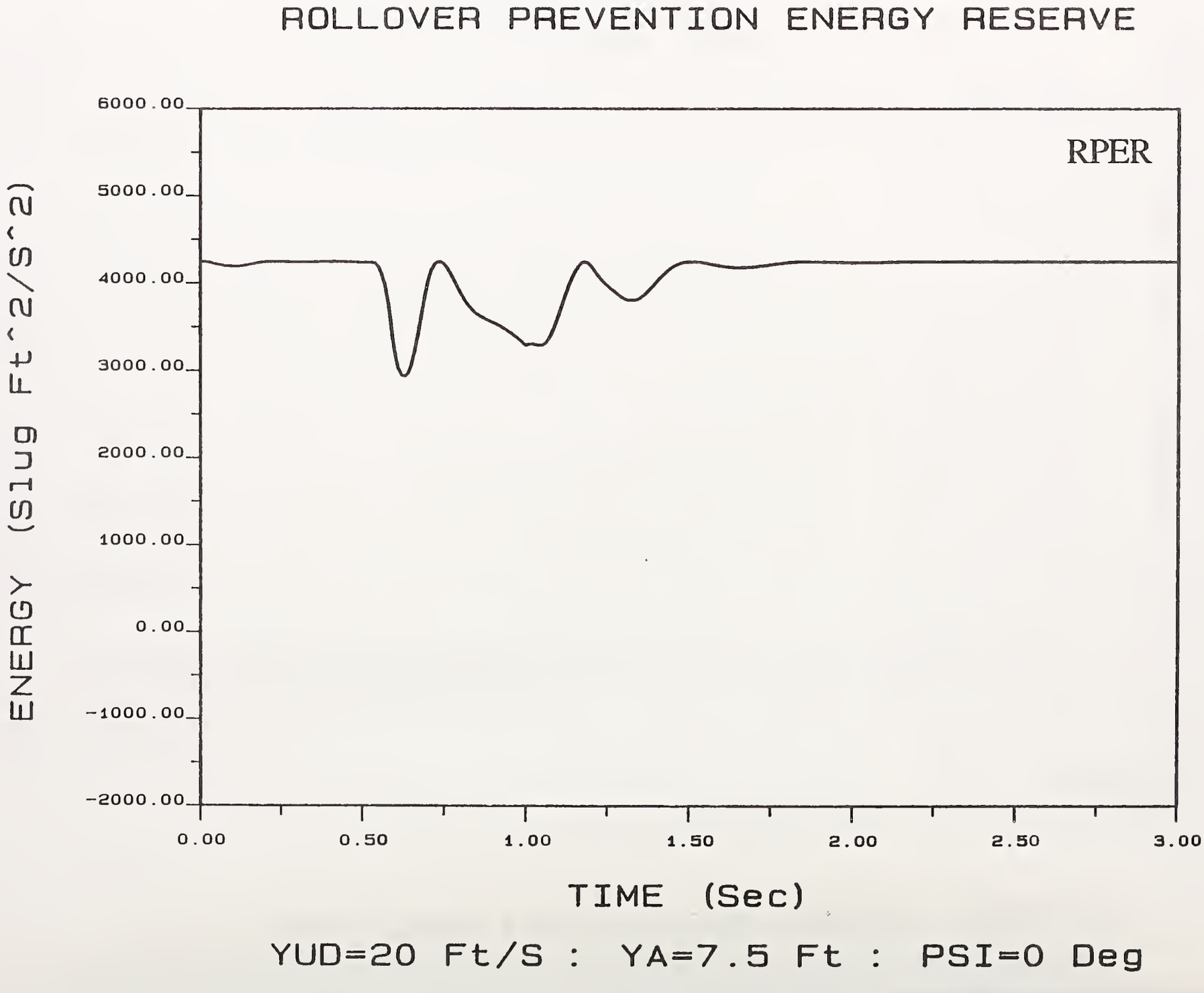
ROLLOVER PREVENTION ENERGY RESERVE
RPER
6000.00
5000.00
4000.00
3000.00
2000.00
1000.00
0.00
-1000.00
-2000.00
ENERGY (Slug Ft^2/S^2)
0.00
0.50
1.00
1.50
2.00
2.50
3.00
TIME (Sec)
YUD=20 Ft/S : YA=7.5 Ft : PSI=0 Deg

Figure 27.

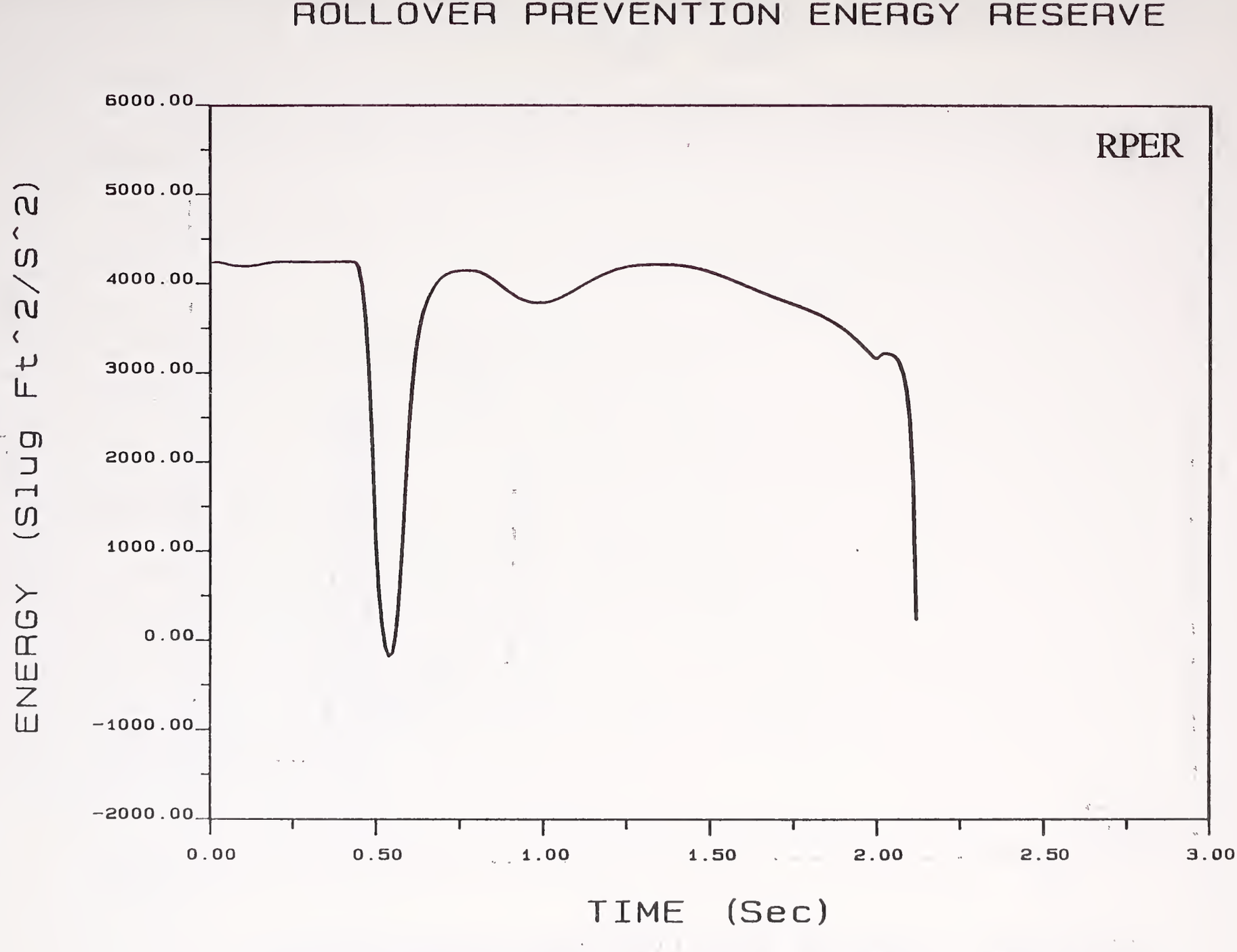
ROLLOVER PREVENTION ENERGY RESERVE
RPER
ENERGY (Slug Ft^2/S^2)
6000.00
5000.00
4000.00
3000.00
2000.00
1000.00
0.00
-1000.00
-2000.00
0.00
0.50
1.00
1.50
2.00
2.50
3.00
TIME (Sec)
YUD=22.13 Ft/S : YA=7.5 Ft : PSI=0 Deg

Figure 28.

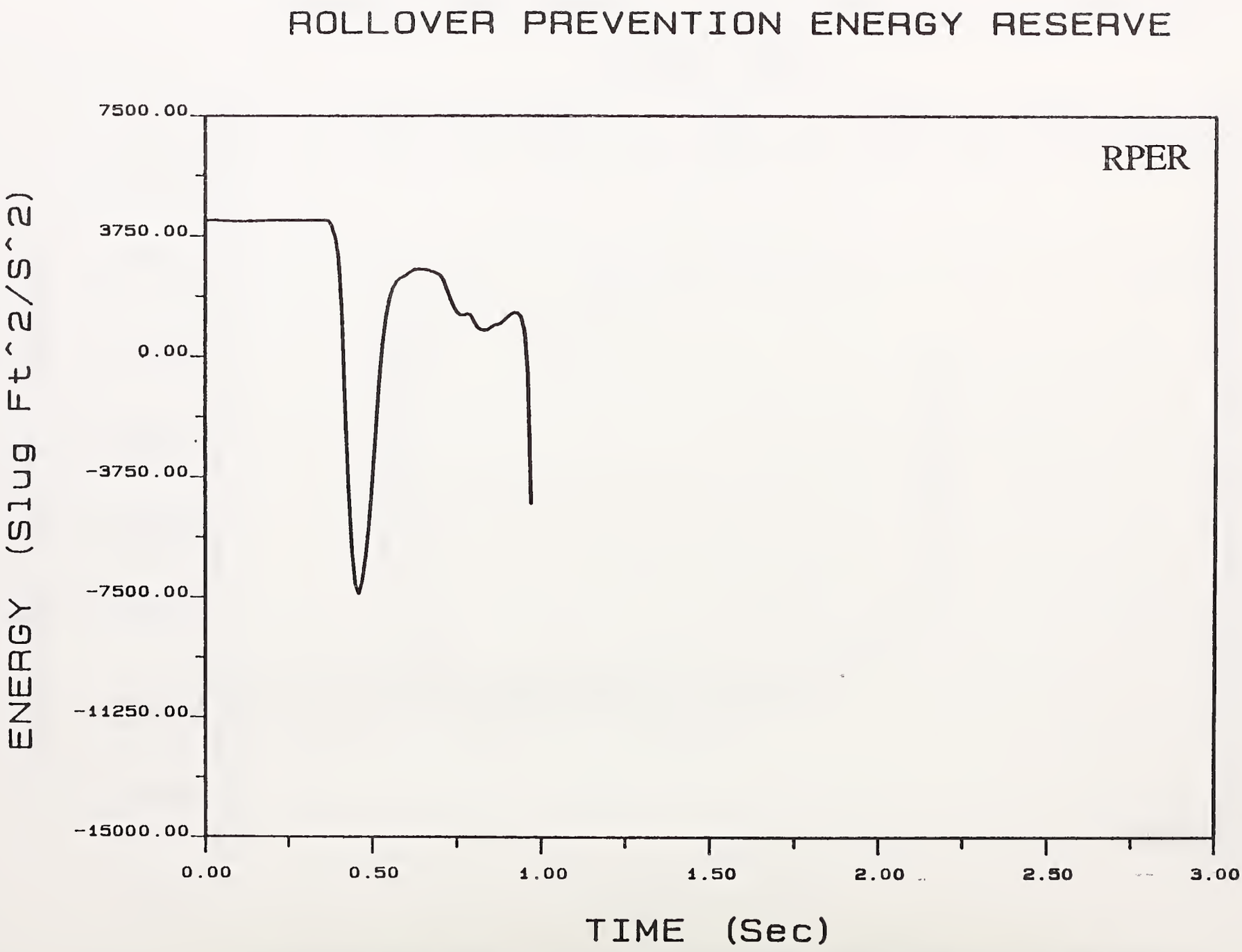
ROLLOVER PREVENTION ENERGY RESERVE
RPER
7500.00
3750.00
0.00
-3750.00
-7500.00
-11250.00
-15000.00
ENERGY (Slug Ft^2/S^2)
0.00
0.50
1.00
1.50
2.00
2.50
3.00
TIME (Sec)
YUD=25 Ft/S : YA = 7.5 Ft : PSI = 0 Deg

Figure 29.

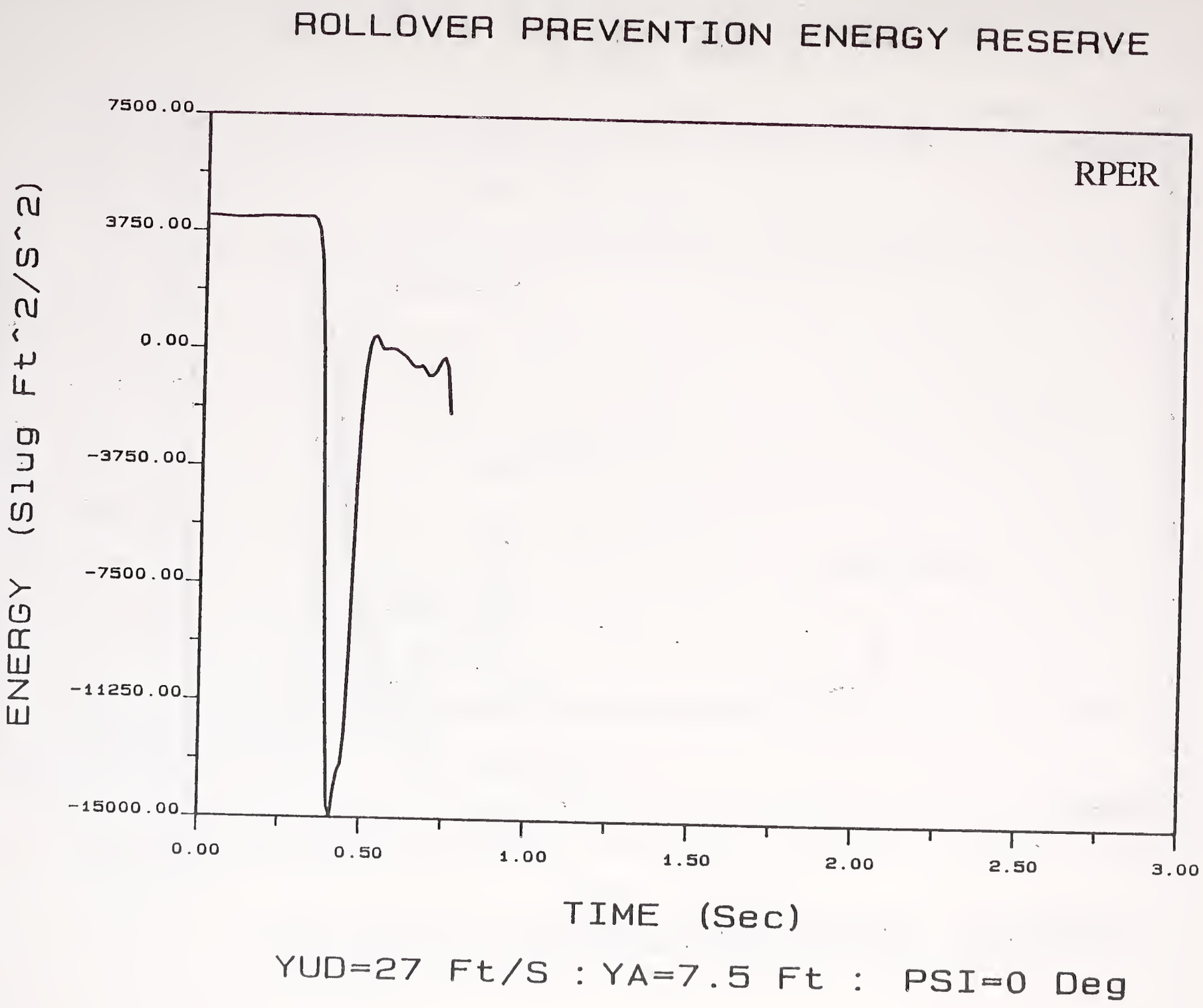
ROLLOVER PREVENTION ENERGY RESERVE
RPER
7500.00
3750.00
0.00
-3750.00
-7500.00
-11250.00
-15000.00
ENERGY (Slug Ft^2/S^2)
0.00
0.50
1.00
1.50
2.00
2.50
3.00
TIME (Sec)
YUD=27 Ft/S : YA=7.5 Ft : PSI=0 Deg

Figure 30.

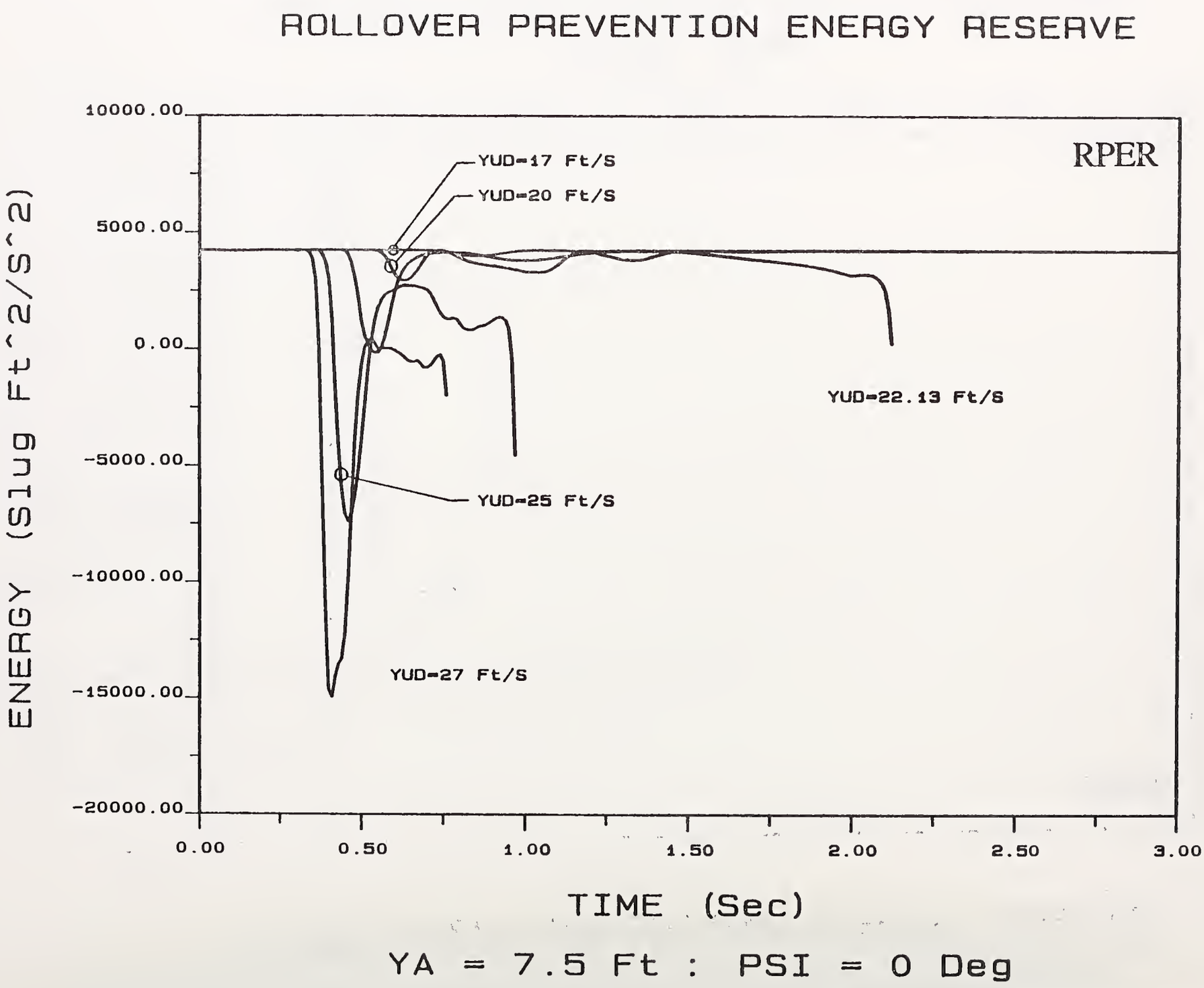
ROLLOVER PREVENTION ENERGY RESERVE
RPER
YUD=17 Ft/S
YUD=20 Ft/S
YUD=22.13 Ft/S
YUD=25 Ft/S
YUD=27 Ft/S
ENERGY (Slug Ft^2/S^2)
10000.00
5000.00
0.00
-5000.00
-10000.00
-15000.00
-20000.00
0.00
0.50
1.00
1.50
2.00
2.50
3.00
TIME (Sec)
YA = 7.5 Ft : PSI = 0 Deg

Figure 31.

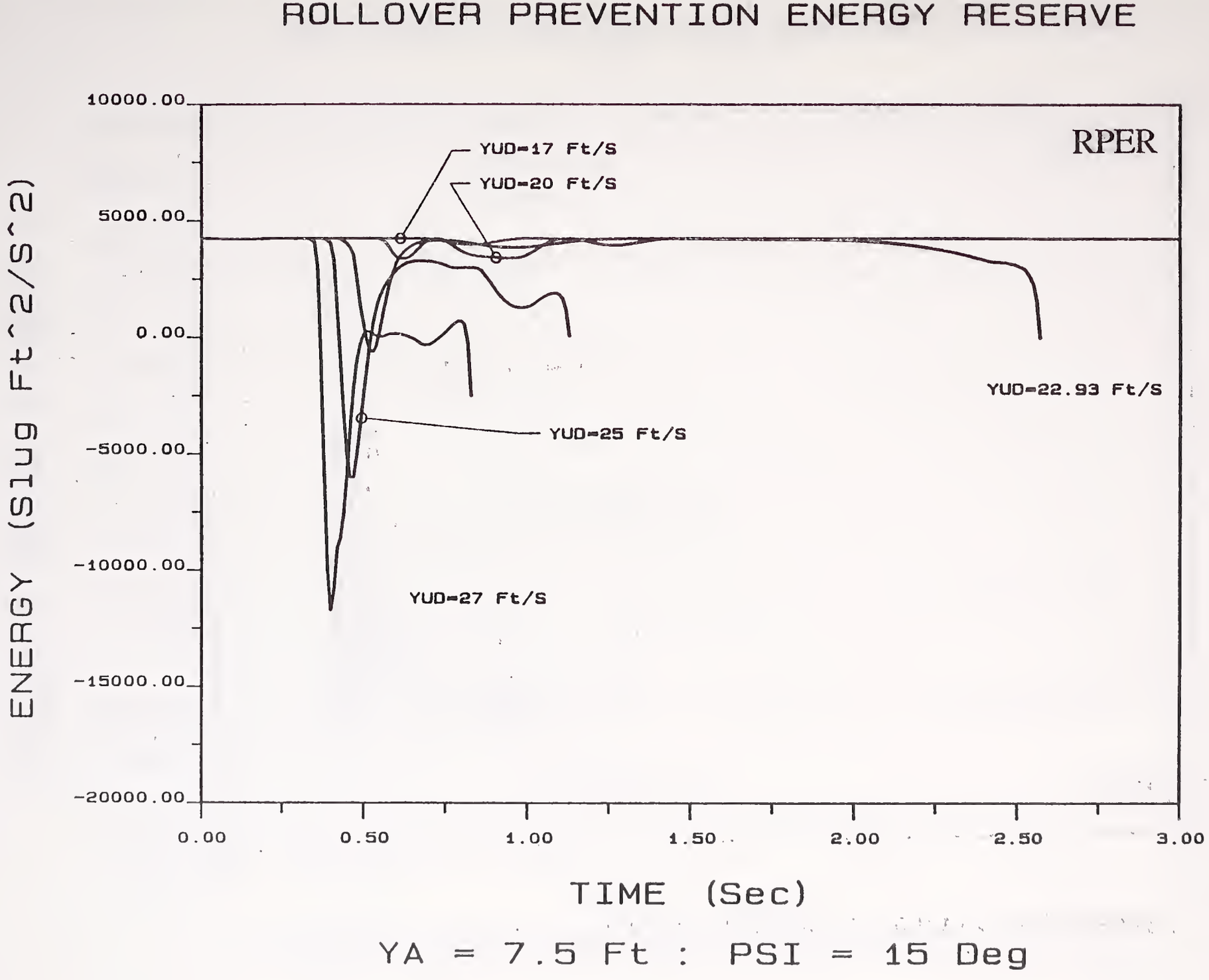
ROLLOVER PREVENTION ENERGY RESERVE
RPER
YUD=17 Ft/S
YUD=20 Ft/S
YUD=22.93 Ft/S
YUD=25 Ft/S
YUD=27 Ft/S
ENERGY (Slug Ft^2/S^2)
10000.00
5000.00
0.00
-5000.00
-10000.00
-15000.00
-20000.00
0.00
0.50
1.00
1.50
2.00
2.50
3.00
TIME (Sec)
YA = 7.5 Ft : PSI = 15 Deg

Figure 32.

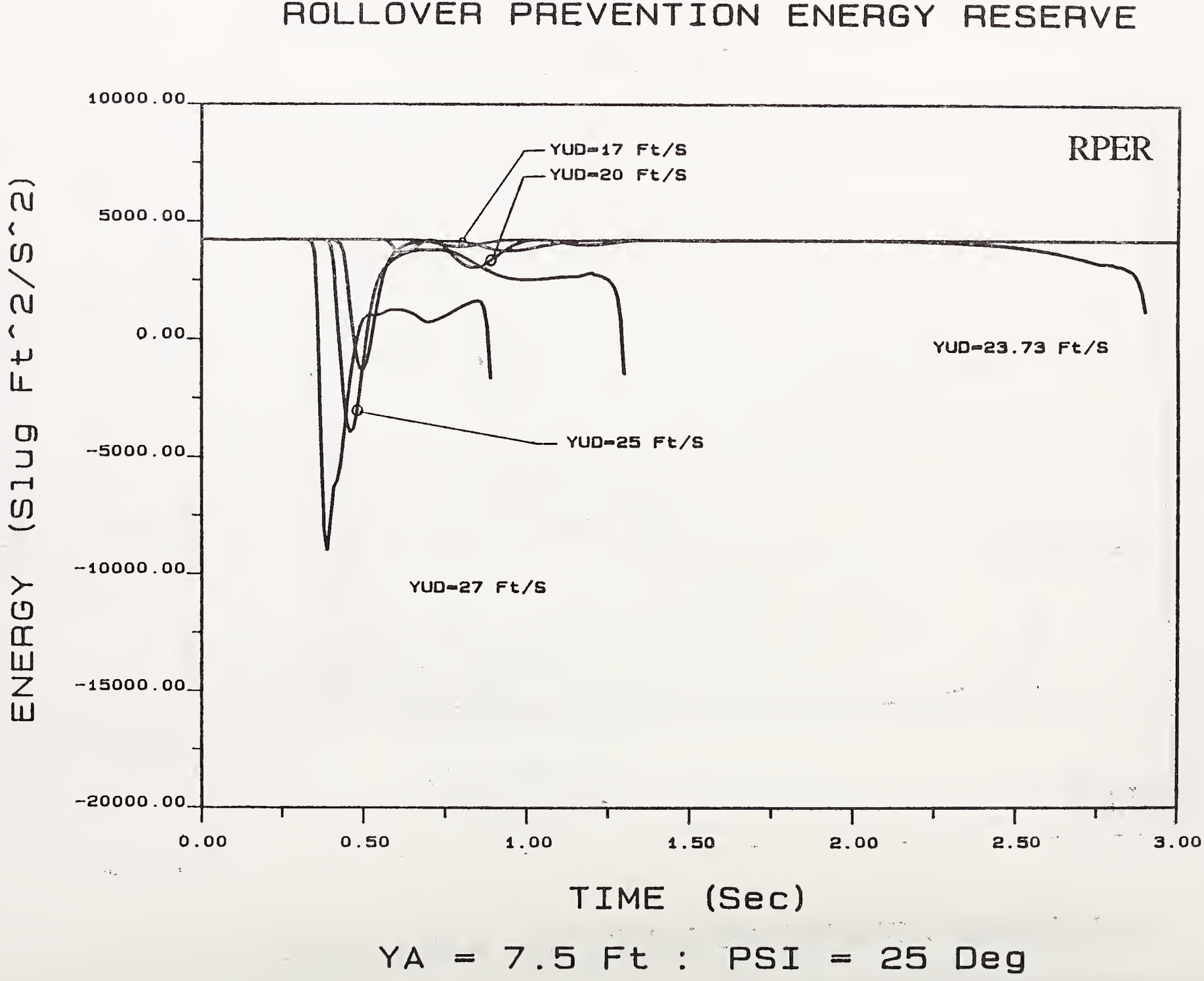
ROLLOVER PREVENTION ENERGY RESERVE
RPER
YUD=17 Ft/S
YUD=20 Ft/S
YUD=23.73 Ft/S
YUD=25 Ft/S
YUD=27 Ft/S
ENERGY (Slug Ft^2/S^2)
10000.00
5000.00
0.00
-5000.00
-10000.00
-15000.00
-20000.00
0.00
0.50
1.00
1.50
2.00
2.50
3.00
TIME (Sec)
YA = 7.5 Ft : PSI = 25 Deg

Figure 33.

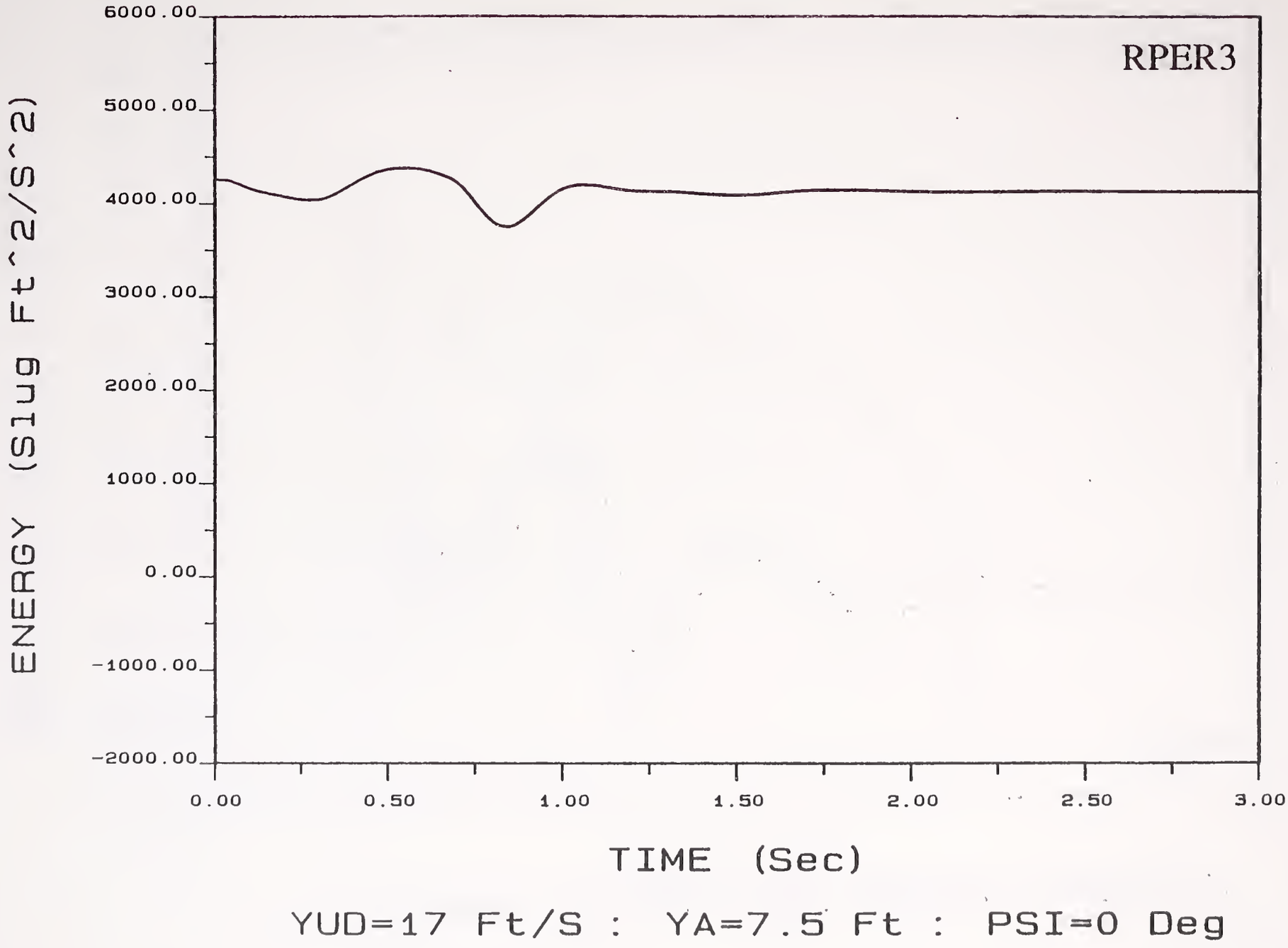
ROLLOVER PREVENTION ENERGY RESERVE
RPER3
ENERGY (Slug Ft^2/S^2)
6000.00
5000.00
4000.00
3000.00
2000.00
1000.00
0.00
-1000.00
-2000.00
0.00
0.50
1.00
1.50
2.00
2.50
3.00
TIME (Sec)
YUD=17 Ft/S : YA=7.5 Ft : PSI=0 Deg

Figure 34.

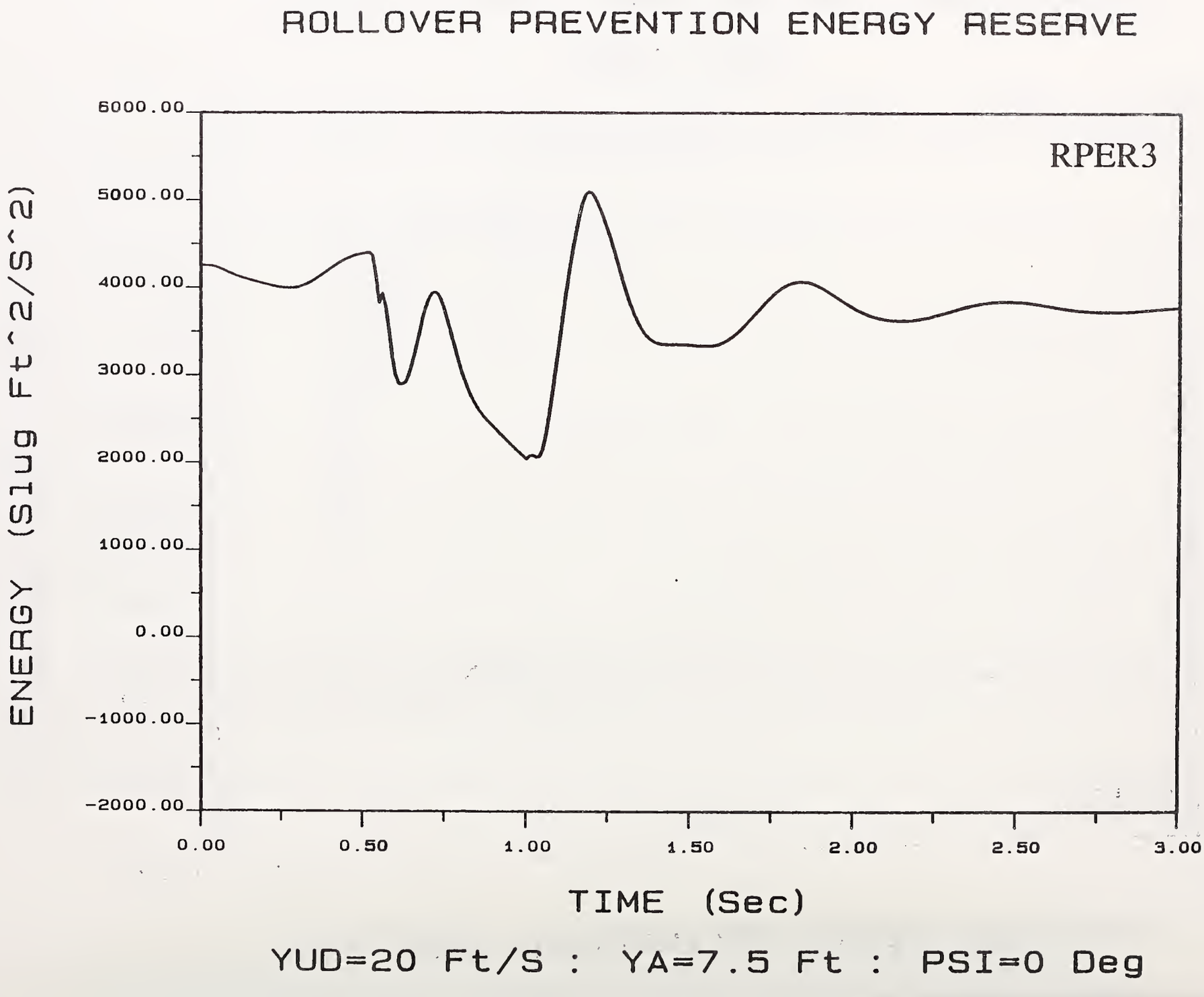
ROLLOVER PREVENTION ENERGY RESERVE
RPER3
ENERGY (Slug Ft^2/S^2)
6000.00
5000.00
4000.00
3000.00
2000.00
1000.00
0.00
-1000.00
-2000.00
0.00
0.50
1.00
1.50
2.00
2.50
3.00
TIME (Sec)
YUD=20 Ft/S : YA=7.5 Ft : PSI=0 Deg

Figure 35.

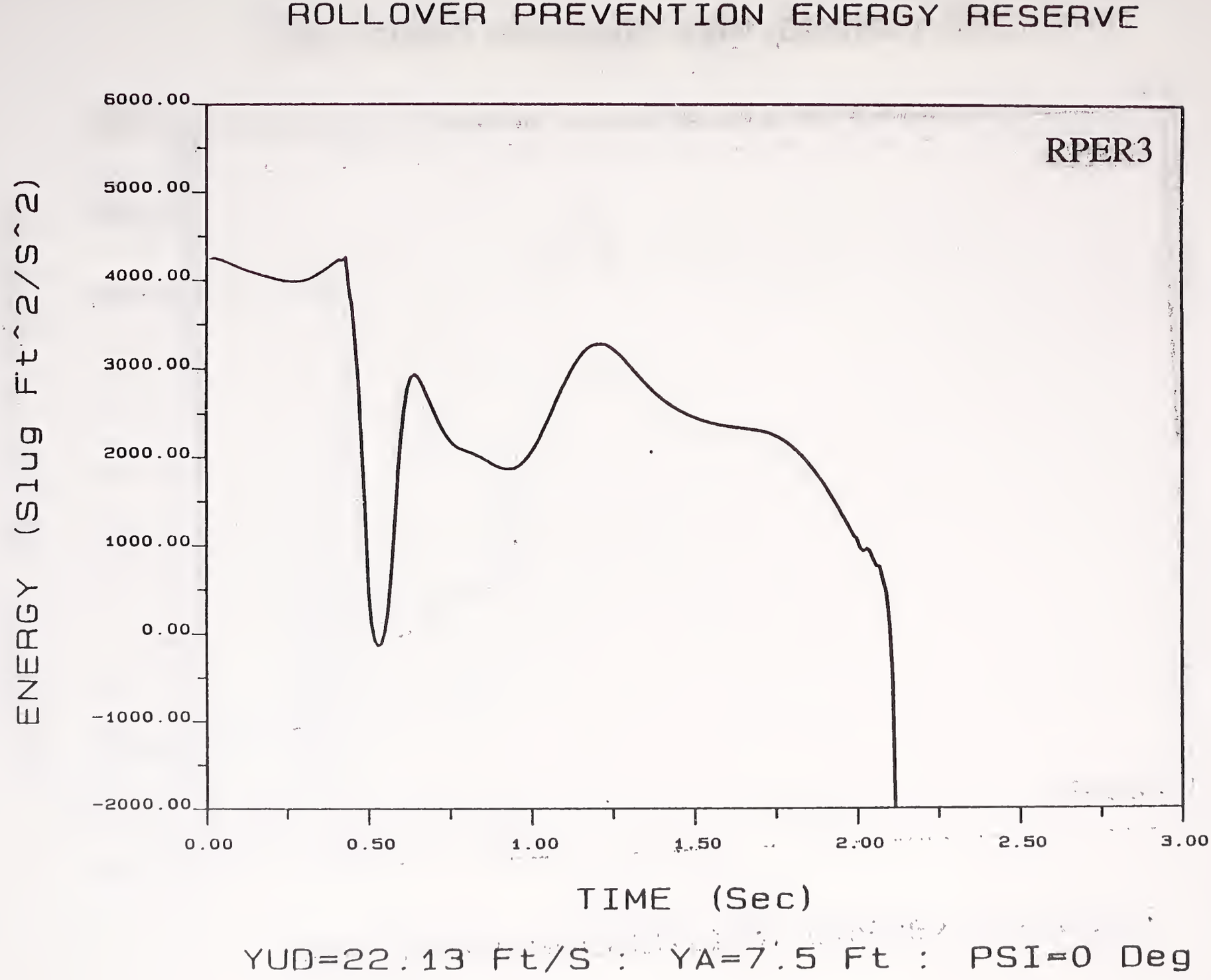
ROLLOVER PREVENTION ENERGY RESERVE
RPER3
ENERGY (Slug Ft^2/S^2)
6000.00
5000.00
4000.00
3000.00
2000.00
1000.00
0.00
-1000.00
-2000.00
0.00
0.50
1.00
1.50
2.00
2.50
3.00
TIME (Sec)
YUD=22.13 Ft/S : YA=7.5 Ft : PSI=0 Deg

Figure 36.

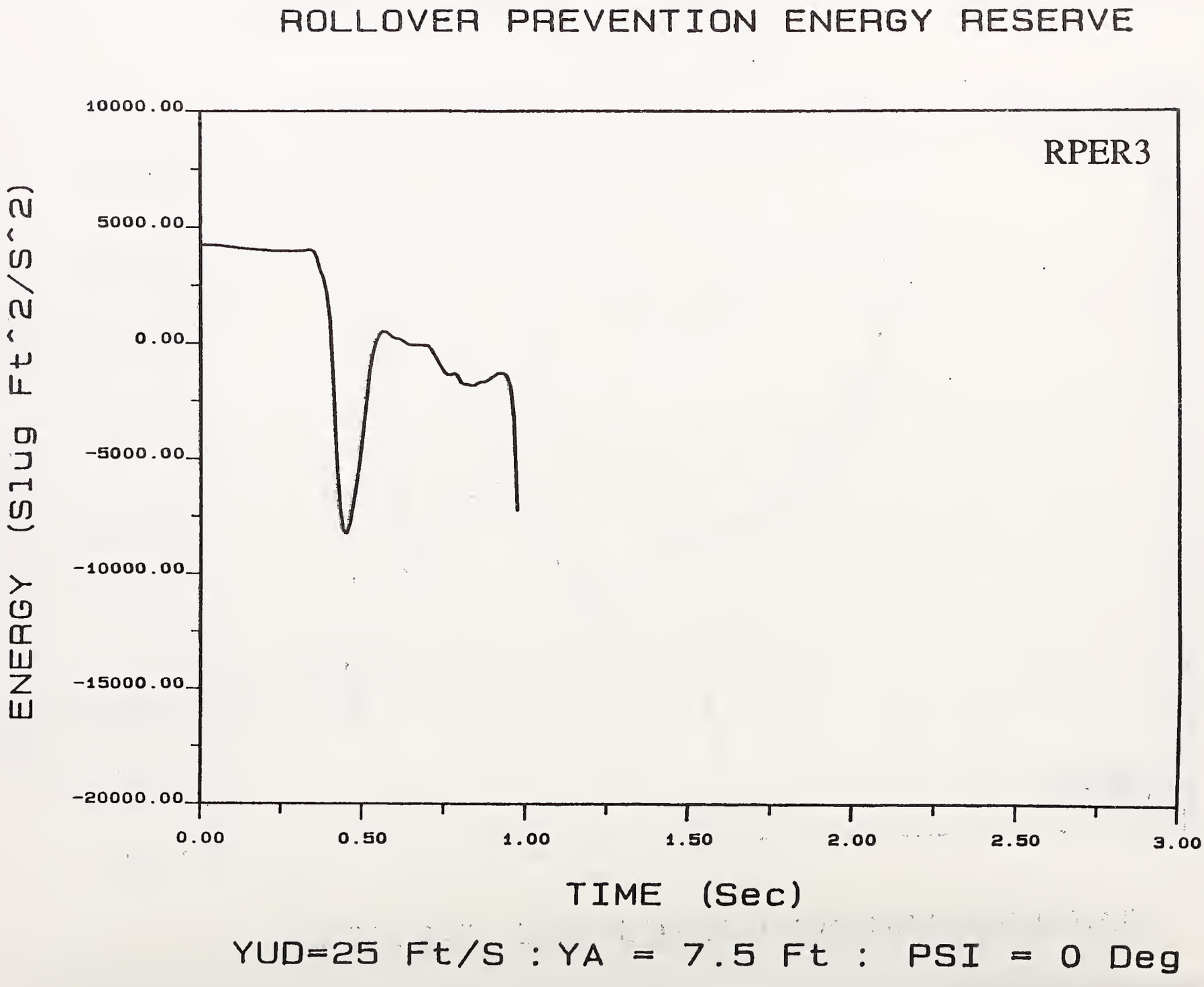
ROLLOVER PREVENTION ENERGY RESERVE
RPER3
10000.00
5000.00
0.00
-5000.00
-10000.00
-15000.00
-20000.00
ENERGY (Slug Ft^2/S^2)
0.00
0.50
1.00
1.50
2.00
2.50
3.00
TIME (Sec)
YUD=25 Ft/S : YA = 7.5 Ft : PSI = 0 Deg

Figure 37.

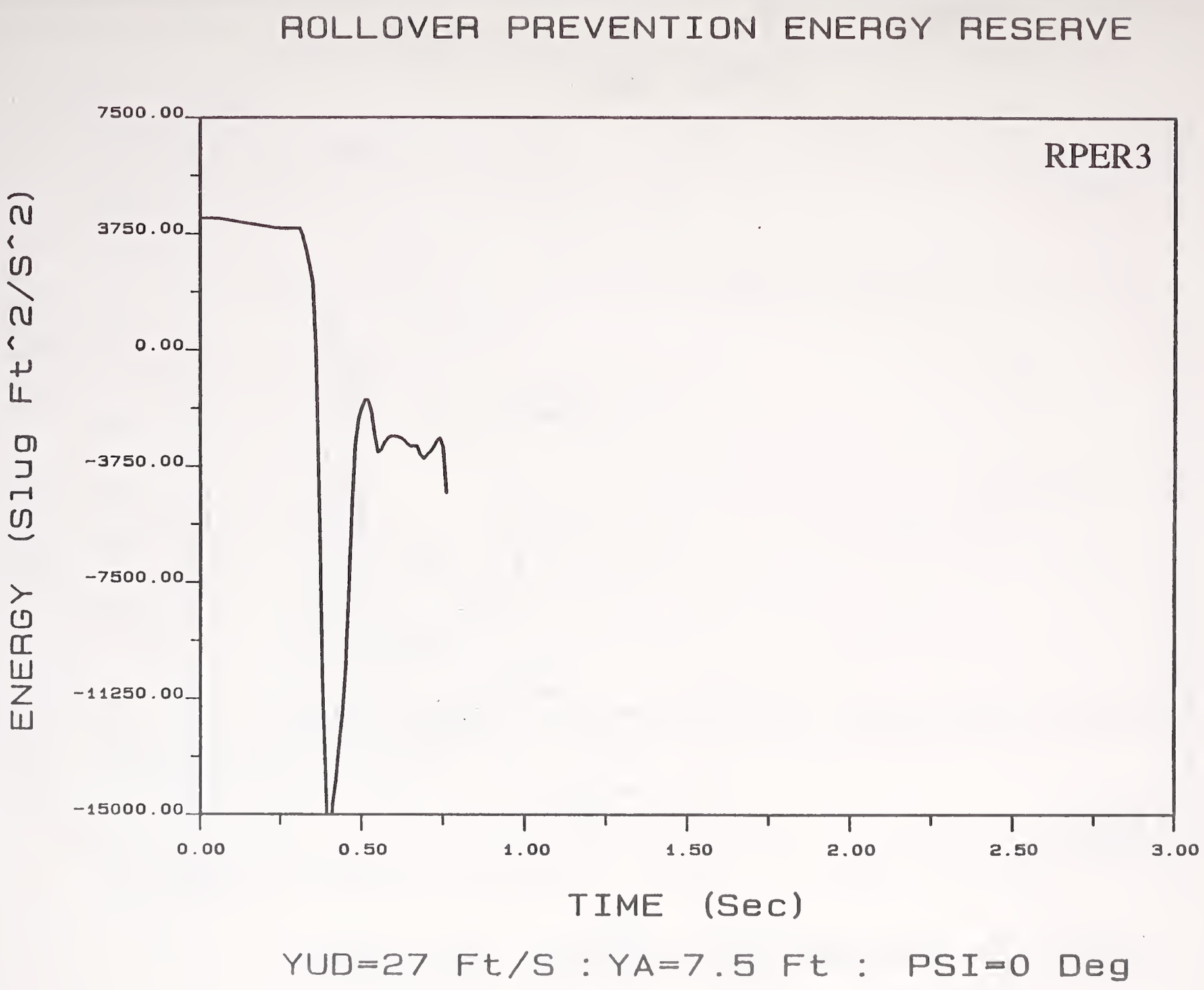
ROLLOVER PREVENTION ENERGY RESERVE
RPER3
7500.00
3750.00
0.00
-3750.00
-7500.00
-11250.00
-15000.00
ENERGY (Slug Ft^2/S^2)
0.00
0.50
1.00
1.50
2.00
2.50
3.00
TIME (Sec)
YUD=27 Ft/S : YA=7.5 Ft : PSI=0 Deg

Figure 38.

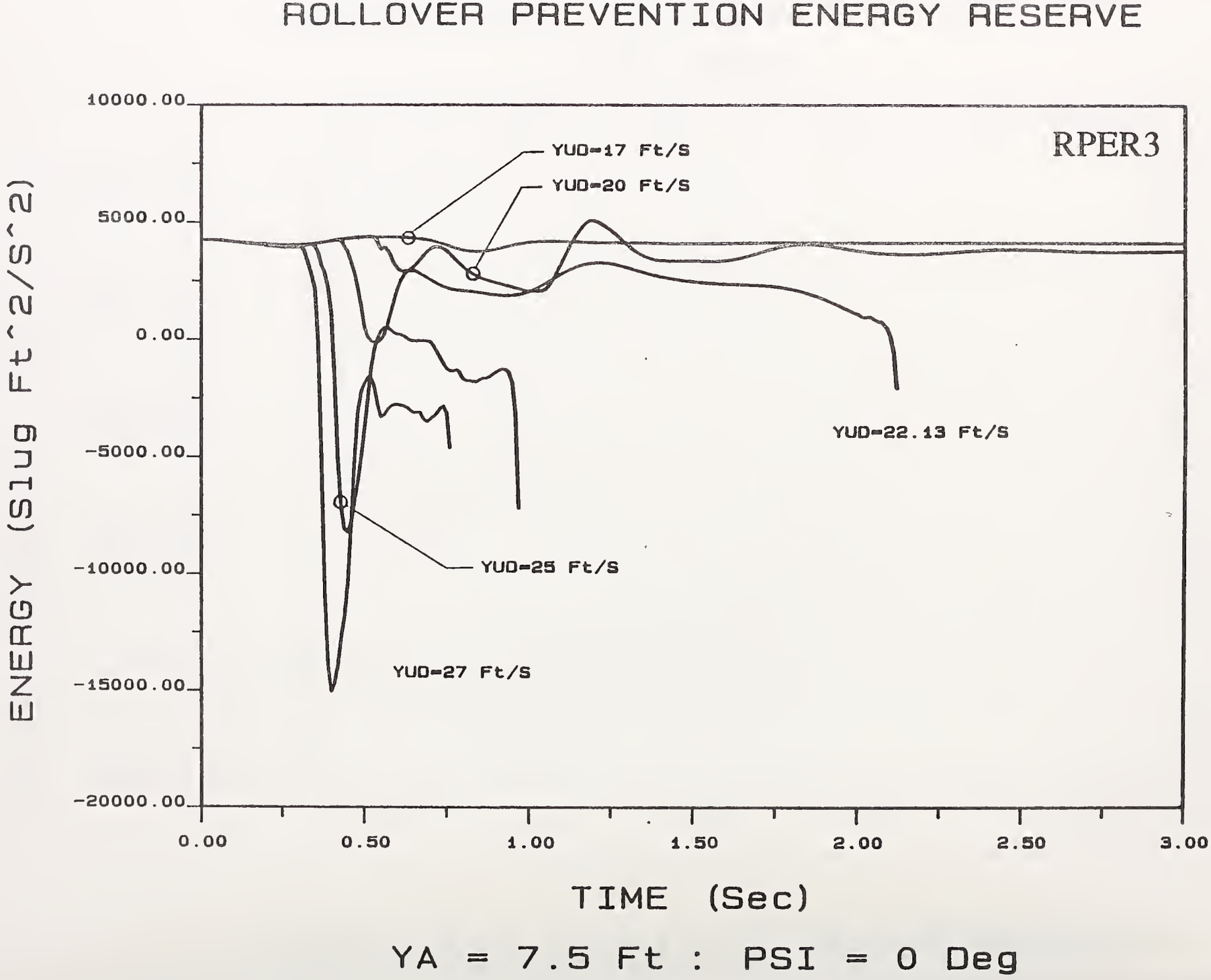
ROLLOVER PREVENTION ENERGY RESERVE
RPER3
YUD=17 Ft/S
YUD=20 Ft/S
YUD=22.13 Ft/S
YUD=25 Ft/S
YUD=27 Ft/S
ENERGY (Slug Ft^2/S^2)
10000.00
5000.00
0.00
-5000.00
-10000.00
-15000.00
-20000.00
0.00
0.50
1.00
1.50
2.00
2.50
3.00
TIME (Sec)
YA = 7.5 Ft : PSI = 0 Deg

Figure 39.

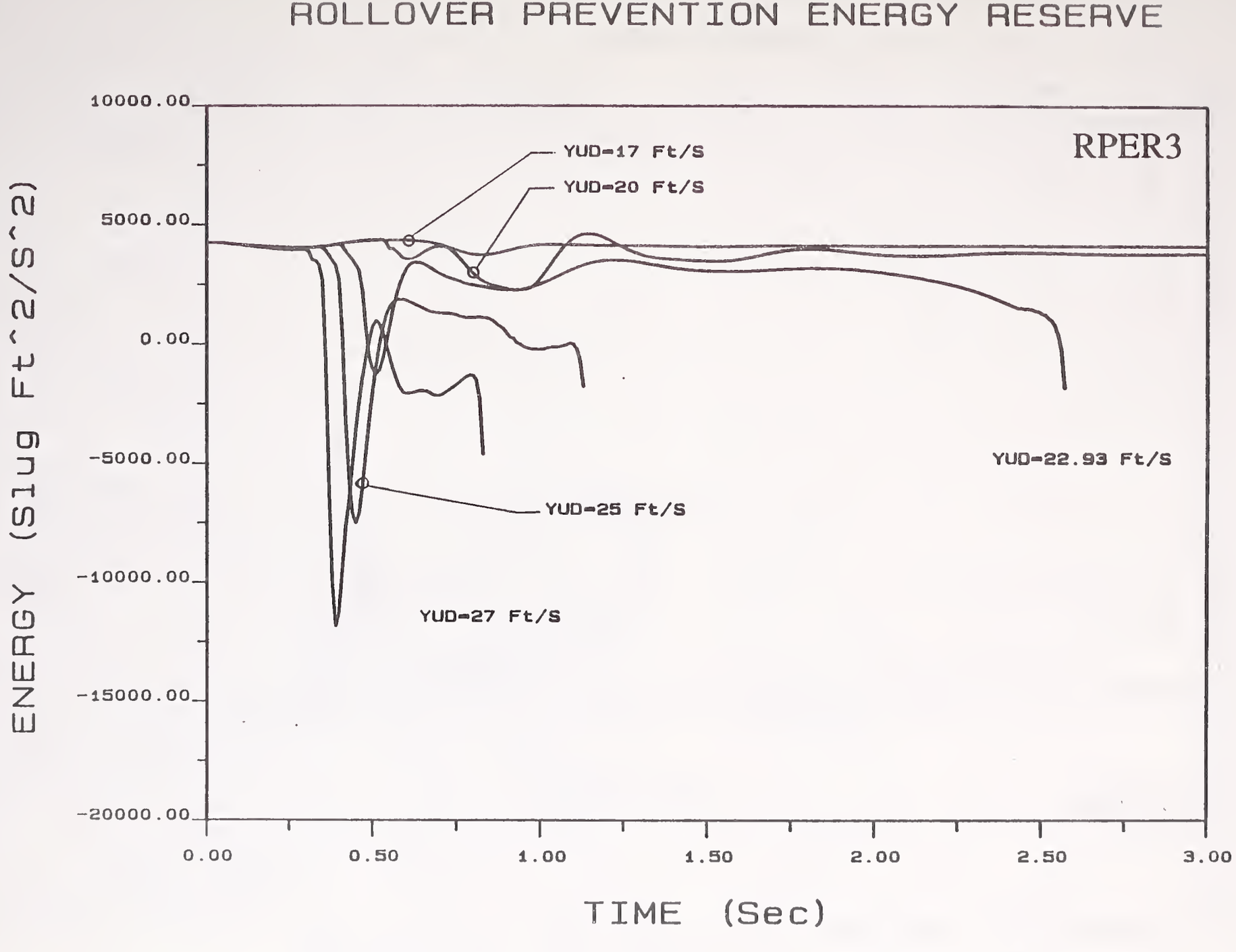
ROLLOVER PREVENTION ENERGY RESERVE
RPER3
YUD=17 Ft/S
YUD=20 Ft/S
YUD=22.93 Ft/S
YUD=25 Ft/S
YUD=27 Ft/S
ENERGY (Slug Ft^2/S^2)
10000.00
5000.00
0.00
-5000.00
-10000.00
-15000.00
-20000.00
0.00
0.50
1.00
1.50
2.00
2.50
3.00
TIME (Sec)
YA = 7.5 Ft : PSI = 15 Deg

Figure 40.

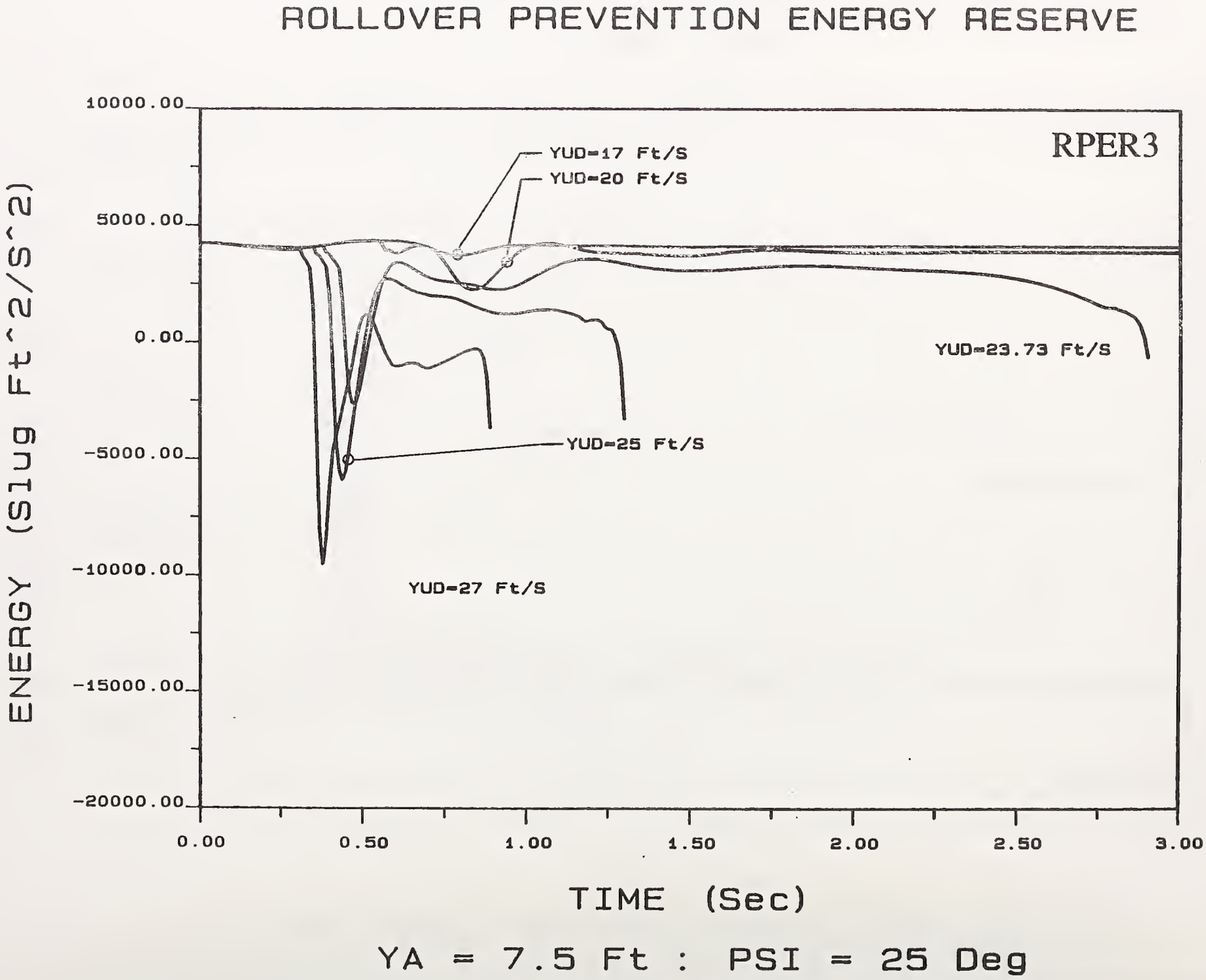
ROLLOVER PREVENTION ENERGY RESERVE
RPER3
YUD=17 Ft/S
YUD=20 Ft/S
YUD=23.73 Ft/S
YUD=25 Ft/S
YUD=27 Ft/S
10000.00
5000.00
0.00
-5000.00
-10000.00
-15000.00
-20000.00
ENERGY (Slug Ft^2/S^2)
0.00
0.50
1.00
1.50
2.00
2.50
3.00
TIME (Sec)
YA = 7.5 Ft : PSI = 25 Deg

Figure 41.

5. SENSITIVITY ANALYSIS OF ITRS TRIPPED ROLLOVER MODEL

5.1 GENERAL INFORMATION

The process of designing and analyzing a complex vehicle system requires information describing the influence of individual design characteristics upon the system's dynamic response. The properties of individual elements in the vehicle system, through direct or indirect means, can significantly influence this response. Previously, detailed information on parametric influence was difficult to obtain in cases involving complex systems, and such analyses were costly and time consuming. By utilizing sensitivity methods, the influence of the complete set of design characteristics on vehicle system response can be quickly and efficiently determined.

Sensitivity analysis can be carried out in both time and frequency domains. When the dynamic characteristics of a mechanical system are given in the form of amplitude/phase frequency characteristics or equivalent frequency transfer functions then sensitivity functions in the frequency domain are the most useful. If a system is given by differential equations of motion and the transient response is of interest then sensitivity analysis in the time domain is the most appropriate.

As part of the research sponsored by NHTSA the University of Missouri-Columbia has developed several general purpose programs which can be used to calculate the sensitivity functions of mechanical systems. Complete descriptions of these sensitivity algorithms and the methods developed by UMC are given in references [8] to [13]. The algorithms are capable of analyzing virtually any system, regardless of its complexity and permit analysis of nonlinear mechanical models in the time domain, nonlinear steady state models, as well as linear mechanical models in the frequency domain. The latest version of these algorithms allow investigation of six different types of sensitivity functions which are first order standard, first

order percentage, first order logarithmic, second order standard, the logarithmic general sensitivity measure, and the percentage general sensitivity measure. Deciding which type of sensitivity functions should be used depends on the objectives of the user. A brief description of each type of sensitivity function is given below.

First Order Standard Sensitivity Function

The first order standard sensitivity function represents the partial derivative of a system variable taken with respect to a particular system parameter. This type of sensitivity function is useful for determining the influence of a particular parameter on a particular system variable. For example, if a designer wished to investigate the influence of wheelbase on vehicle yaw velocity then first order standard sensitivity functions could be used.

First Order Percentage Sensitivity Function

First order percentage sensitivity function represents the variable change caused by a parameter change of some user specified percentage. Percentage sensitivity functions are useful for comparing the influence of various parameters on a particular system variable. For example, if a designer wanted to know whether a 2 percent change in wheelbase affected yaw angular velocity more than a 2 percent change in track width, the percentage sensitivity function would show the change in yaw velocity associated with each parameter change. Because percentage sensitivity functions have units which are identical to that of the system variable, they can be used to compare the effect of various parameters on a particular variable.

First Order Logarithmic Sensitivity Function

The first order logarithmic sensitivity function is the only dimensionless sensitivity function available, making it useful to compare and rank the influence of various parameters on several system

variables. Users should be aware that if the variable value approaches zero then the logarithmic sensitivity functions can become very large. It should also be noted that logarithmic sensitivity is dependent on both system sensitivity and system response, which can sometimes make interpretation of the time behavior of a logarithmic sensitivity function difficult. However, logarithmic sensitivity functions are useful in comparing the order of influence of various system parameters at a particular time.

Second Order Standard Sensitivity Function

Second order sensitivity functions represent the second partial derivative of a system variable taken with respect to a system parameter. The second order sensitivity function can be used to gain additional insight into results obtained using first order standard sensitivity functions. When the system exhibits similar sensitivity to a number of parameters then second order sensitivity functions are particularly useful.

Logarithmic and Percentage General Sensitivity Measures

The general sensitivity measure determines the global effect of all selected parameters on a particular variable. This is useful for analyzing the combined effects of related parameters. For example, one could compare the combined effects of parameters describing the system's stiffness with parameters describing the system's mass properties. The general sensitivity measure can be based on either percentage sensitivity or logarithmic sensitivity functions since these types possess compatible dimensions.

The different types of sensitivity functions can be used when carrying out sensitivity analysis. For certain situations, however, the most recommended sensitivity functions are given below.

Type of Sensitivity Function	Application
First order standard	- one parameter on one variable
Percentage and logarithmic	- many parameters on one variable
First order logarithmic	- one parameter on several variables
General sens. measure (perc.)	- various groups of parameters (geom., mass, stiff., etc.) on one variable
General sens. measure (log.)	- global effect of many parameters (in groups) on several variables
Second order standard and logarithmic	- when system exhibits similar sensitivity to a number of parameters

5.2 NUMERICAL METHODS USED IN SENSITIVITY ANALYSIS

Time domain sensitivity functions are computed by integrating the system's differential equations of motion using different sets of parameter values. The equations of motion are first integrated using nominal parameter values. The parameter of interest is then increased by some user specified percentage (usually 1 %) and the equations of motion are integrated again to obtain a varied system response. The nominal parameter value is then reduced by the user specified percentage and the equations of motion are integrated again to obtain a second varied system response. Once the system response has been determined using the different sets of parameter values then the first order standard sensitivity and second order standard sensitivity functions can be computed by taking the first and second partial derivatives of the variable of interest with respect to the parameter. A 3, 5 or 7 point central difference method can be used to compute the partial derivatives. First order logarithmic sensitivity is computed by multiplying the first order standard sensitivity function by the nominal parameter value and then dividing it by the variable value obtained using the nominal parameter set. Percentage sensitivity is computed by finding the difference in the

variable caused by the user specified parameter change. Table 1 summarizes the differences between the various sensitivity functions.

Table 1

Sensitivity Type	Analytical Expression	Numerical Expression	Unit
1st Order Standard	$\frac{\partial V}{\partial P}$	$\frac{\Delta V}{\Delta P}$	$\frac{V}{P}$
1st Order Percentage	$\frac{\delta V}{\delta P}\ \delta P$	ΔV	V
1st Order Logarithmic	$\frac{\partial V}{\partial P}\ \frac{P}{V}$	$\frac{\Delta V}{\Delta P}\ \frac{P}{V}$	None
2nd Order Standard	$\frac{\partial^2 V}{\partial P^2}$	$\frac{\Delta(\frac{\Delta V}{\Delta P})}{\Delta P}$	$\frac{V}{P^2}$
General Sensitivity Measure	$GS_v = [\sum_{i=1}^{n} S_{iv}^2]^{\frac{1}{2}}$	(where S_{iv} is any of the sensitivity functions shown above)	

In the case of secondary parameters (parameters whose values do not remain constant, i.e. tire forces) the central difference expressions cannot be used since they assume that the distance between varied parameter values is constant. Therefore, in case of secondary parameters, the sensitivity algorithms use a polynomial fit to determine the first and second order standard sensitivity functions. The program utilizes a 2nd order polynomiall when using the three point method, a 4th order polynomial for the five point method and a 6th order polynomial for seven point method. A more complete description of the methods used in the sensitivity algorithms is given in references [8] and [9].

5.3 SENSITIVITY ANALYSIS OF ITRS VEHICLE MODEL

It has been demonstrated in the previous chapter that Rollover Prevention Energy Reserve can successfully be used to assess the occurrence of vehicle rollover. Both RPER and RPER3 proved to be reliable dynamic functions which govern the rollover behavior and, at the same time, can be used as a measure of a vehicle's rollover stability. Any change in a parameter's value (reduction or increase) which results in the increase of RPER (or RPER3) can be considered to have positive influence. The increase of RPER has a stabilizing effect since vehicles of larger RPER will be less prone to rollover. For this reason RPER and RPER3, and not the vehicle's system response, are chosen as a basis for sensitivity analysis of ITRS vehicle model.

The influence of all significant vehicle and terrain characteristics on vehicle rollover stability during both side and oblique impacts was determined for the vehicle data shown in Appendix B. The initial conditions used (Appendix C) represent the vehicle whose front wheel is located at a distance 7.5 Ft from the curb and is skidding sideways with different lateral velocities and with zero initial yaw velocity. The vehicle's initial roll angle was determined as a function of skidding deceleration and the initial heading angle was varied to cause required side and oblique impacts. The time responses of the ITRS model (vehicle position, orientation and velocities) for various initial conditions utilized in sensitivity analysis are enclosed in Appendix D.

The percentage sensitivity functions were utilized to determine the change in vehicle RPER (and RPER3) caused by a one percent change in parameter values. The vehicle and terrain parameters were divided into following seven groups.

Geometric Parameter Set #1:	a, L, TRW, SRSF, h_s, h_u h_{ra}
Geometric Parameter Set #2:	s, h_{curb}, T_r, Y_u, SPRLNG, ABSDEF
Mass Parameter Set:	M_s, M_u, I_{xxs}, I_{yys}, I_{zzs}, I_{xxu}, I_{yyu}, I_{zzu}
Products of Inertia Par. Set:	I_{xys}, I_{xzs}, I_{yzs}, I_{xyu}, I_{xzu}, I_{yzu}
Stiffness Parameter Set:	K_1, K_2, K_z, K_{d1}, K_{d2}, K_{d3}, K_{d4}
Damping Parameter Set:	B_1, B_2, B_d, B_z
Force Parameter Set:	μ_s, μ_x, μ_y, K_V, K_{VF}, POINT1, POINT2

In order to ease analysis of results, all percentage sensitivity functions of RPER and RPER3, during both side and oblique impacts, were plotted in the same scale. Although they were plotted within time interval 0 - 2 seconds, the most significant information they carry is contained in between the initial instant and the moment when static tip-over position of vehicle is reached.

It should also be noted that, based on the definition, the percentage sensitivity functions of RPER (and RPER3) represent the absolute changes in the vehicle's RPER (and RPER3) caused by user-specified percentage change in parameter values (1% in this analysis).

5.3.1 Parametric Sensitivity of RPER in Side Impact

The influences of the various parameter groups on RPER during vehicle side impact with the curb (zero heading angle) obtained at two different initial lateral velocities, 20 Ft/s (which did not result in rollover) and critical rollover speed (equal to 22.13 Ft/s) are presented in Figures 42 - 55.

The influence of geometric parameter set #1 on RPER is shown in Figures 42 and 43. In both rollover and non-rollover cases the vehicle track width (TRW) and static rollover stability factor (SRSF)

are the most influential among all elements of the geometric parameter set #1. The sensitivity functions of these parameters remain positive and this indicates that increase of SRSF and TRW results in increase of RPER, which makes the vehicle less prone to rollover. A negative sensitivity function of the distance from roll axis to sprung mass c.g. (h_{ra}) indicates that increasing h_{ra} decreases vehicle RPER. This finding is also significant because an increase in h_{ra} increases the c.g. height of the vehicle.

In both rollover and non-rollover situations, the vehicle wheelbase (L) has positive sensitivity indicating that increase of L increases RPER. Also, a negative value of the sensitivity function of parameter a, for both skidding velocities, indicates that the vehicle's RPER can be increased by reducing the distance from sprung mass c.g. to front axle.

The distance from the sprung mass c.g. to the bottom of the sprung mass (h_s) displays qualitatively different sensitivity in rollover and non-rollover cases. Its sensitivity function is positive just after the curb impact with the initial speed of 20 Ft/s (Figure 42), and negative at the instant of rollover initiation (Figure 43). The distance from axle centerline to the unsprung mass c.g. (h_u), whose sensitivity function is nearly zero in both rollover and non-rollover cases, appears to have the smallest influence on RPER.

Since the initial skidding velocity of 20 Ft/s did not result in rollover, the vehicle rocks back and forth after impact. These roll oscillations cause the sensitivity functions to oscillate as well and change signs several times until vehicle comes to rest.

Figures 44 - 45 show the percentage sensitivity functions of RPER obtained for geometric parameter set #2. These figures illustrate that the vehicle's initial distance from the curb (Y_u) is by far the most influential among all parameters considered in this group. Its large positive sensitivity function, in both rollover and non-rollover situations, clearly demonstrates that vehicle's RPER can

be increased by increasing initial distance Y_u. This is because increasing the initial distance from the curb reduces the speed of impact, thus makes the situation less dangerous. It should be remembered, however, that the initial distance from the curb is neither a vehicle design parameter nor a roadside feature but rather a parameter dependent on circumstances.

The percentage sensitivity of tire radius (T_r) and undeflected suspension spring length (SPRLNG) depends on the vehicle's initial speed and roll angle. In the non-rollover case, the sensitivity functions of T_r and SPRLNG are positive just after the curb impact and then become negative when vehicle roll angle increases. However, at critical rollover velocity, when rollover is unavoidable, the sensitivity functions of T_r and SPRLNG are negative soon after the impact.

The distance between left and right suspension springs (springs track width s) exhibits relatively smaller sensitivity. Its sensitivity function is positive at both speeds which means that increasing s has a positive influence of vehicle RPER. Figure 45 also reveals that vehicle RPER can be increased by increasing the height of the curb height. The curb height does not appear to be important parameter in non-rollover situation (Figure 44).

The influence of the mass/inertia parameter set on vehicle RPER is shown in Figures 46 and 47. In both non-rollover and rollover situations (skidding velocities equal to 20 Ft/s and the critical rollover speed of 22.13 Ft/s, respectively), the sensitivity functions of sprung mass have similar positive values until the vehicle impacts the curb. After the curb impact, the sensitivity function drops to almost zero in Figure 46 and to - 38 in Figure 47. This means that the sprung mass exhibits negative influence on RPER (increase of M_s reduces RPER) at the instant when vehicle rollover is about to initiate. This is obviously a reasonable result because an increase of sprung mass increases the vehicle inertia force which tends to roll the vehicle over (inertia force has an opposite direction

to the deceleration caused by impact). However, the roll moments of inertia of both sprung and unsprung masses have a positive effect on vehicle RPER. The sensitivity functions of I_{xxs} and I_{xxu}, which remained zero during vehicle skidding (because there were no roll oscillations), become positive just after the curb impact. This suggests that an increase in roll moments of inertia increases vehicle RPER (thus making vehicle less prone to rollover). This is logical since the inertia couple, which is proportional to roll moment of inertia and acts in the direction opposite to that of angular acceleration, resists the vehicle roll motion. The sensitivity of vehicle RPER to changes of unsprung mass (M_u) as well as pitch (I_{yys}, I_{yyu}) and yaw (I_{zzs}, I_{zzu}) moments of inertia is relatively smaller during the side impact with the curb.

The sensitivity of vehicle RPER taken with respect to products of inertia at the initial lateral velocity of 20 Ft/s (Figure 48) is almost negligible. At the critical rollover speed (Figure 49), the I_{xzu} product of inertia has a negative sensitivity function immediately after the impact and then turns positive when the vehicle rolls over. The I_{xys} and I_{xyu} products of inertia display smaller and qualitatively different sensitivity than that of I_{xzu}. Their sensitivity functions are first positive and then negative when vehicle rolls over. Other products of inertia, such as I_{yzs} and I_{yzu}, appear to be relatively unimportant.

Figures 50 - 51 illustrate the influence of the stiffness parameter set on vehicle RPER during side impact. These figures show that suspension spring stiffness (K_1) is the most influential among all stiffness parameters at the initial speed of 20 Ft/s and that its sensitivity is positive. At the critical rollover speed, the impact force deformation rate (K_{d1}), which has negative sensitivity just after the impact and positive when vehicle rolls over, becomes a dominant parameter. The sensitivity function for tire radial stiffness (K_z) is positive at both speeds which indicates that increase of K_z increases RPER. The influence of bump stop stiffness (K_2) and impact force

deformation rates (K_{d2}, K_{d3}, K_{d4}) on RPER is almost negligible for skidding velocities tested.

The effects of variation of damping parameters on vehicle RPER is shown in Figures 52 and 53. Both figures reveal that, overall, damping parameters have much less influence on vehicle's stability in tripped rollover situations than geometrical, mass and stiffness parameters. The damping coefficient of shock absorbers (B_1) exhibited the largest influence among all damping parameters examined.

The percentage sensitivity functions of the force parameter set are shown in Figures 54 and 55. The lateral sliding coefficient of friction between tire and pavement (μ_y), which has a positive sensitivity function, is the most influential parameter of the set at both speeds. A higher friction coefficient μ_y delays the time of impact and reduces the impact velocity, thus increases vehicle RPER as expected. The lateral deformation parameter POINT1 has a negative sensitivity function in both rollover and non-rollover situations. This means that increasing POINT1 decreases RPER. Figure 55 also reveals that vehicle RPER can be increased by increasing frictional saturation speed (K_V). Other elements of the force parameter set, such as longitudinal (μ_x) and scrubbing tire/curb (μ_s) friction coefficients as well as deformation parameter (POINT2) have practically no influence on vehicle rollover stability at the initial speeds tested.

5.3.2 Parametric Sensitivity of RPER in Oblique Impact

The effects of the various parameter groups on RPER during vehicle oblique impact with the curb was investigated for two angles of impact, 15 and 25 degrees. In both cases of oblique impact, the initial skidding velocities were equal to critical rollover speeds (minimum skidding velocities which result in vehicle rollover). It has been determined that for the initial conditions utilized in the

analysis (Appendix C) critical rollover speeds were 22.93 and 23.73 Ft/s for impact angles of 15 and 25 degrees, respectively.

The percentage sensitivity functions of vehicle RPER obtained for geometric parameter set #1 are presented in Figures 56 and 57. These figures show that vehicle track width (TRW) and static rollover stability factor (SRSF) have positive sensitivities that indicate that increasing both TRW and SRSF increases RPER and improves vehicle rollover stability. Also, at impact angles of 15 and 25 degrees, the distance from roll axis to sprung mass c.g. (h_{ra}) has a negative sensitivity function at the instant of rollover initiation. This confirms that increasing h_{ra} (which results in an increase of vehicle c.g. height) decreases vehicle RPER, thus makes vehicle more prone to rollover. Results identical to these were obtained in both rollover and non-rollover cases during vehicle side impact with the curb (Figures 42 - 43).

During vehicle oblique impact with the curb, the distance from vehicle c.g. to front axle (a) displays qualitatively different sensitivity than does vehicle wheelbase (L). At the instant of rollover initiation, at heading angles of both 15 and 25 degrees, the distance a has a positive sensitivity which indicates that increasing a increases RPER. This seems logical because increasing distance a requires more rolling kinetic energy to be created in order to rollover the vehicle impacting the curb under some heading angle. The sensitivity function of vehicle wheelbase L is negative at the instant of rollover initiation, and it suggests that an increase of L decreases vehicle RPER. Although, this result is also correct it may not be so readily evident without explanation, particularly when accident statistics show that vehicles of longer wheelbase are overall less prone to rollover.

In the ITRS vehicle model wheelbase L and distance a are primary (input) parameters and the distance from the vehicle c.g. to rear axle (b) is calculated as b = L - a. Due to arrangements made in the sensitivity programs ([8], [9] and [13]) the requested variation of

parameter L actually results in the variation of parameter b since distance a remains constant when L is being changed. According to sensitivity codes, the sensitivity function of parameter L describes the influence of parameter b instead of true effect of L. In order to determine the actual effect of wheelbase L both a and b need to be varied when computing the sensitivity functions of L.

Figures 56 and 57 also show that the distance from sprung mass c.g. to bottom of sprung mass (h_s) has a positive sensitivity function at the instant of rollover initiation, which soon after becomes negative when the vehicle rolls. The distance from the axle centerline to the unsprung mass c.g. (h_u), whose sensitivity function is almost zero, exhibits the smallest influence on RPER among all of the parameters in geometric set #1 for both psi equal to 15 and 25 degrees. Results similar to these were obtained in the case of vehicle side impact with the curb (Figure 43).

The influence of geometric parameter set #2 on vehicle RPER in oblique impacts with the curb is shown in Figures 58 - 59. As it was during side impact, the vehicle initial distance from the curb (Y_u) is now also the most influential among all parameters in this group. Its sensitivity function attains a very large positive value just after the impact and then immediately drops to a negative value when vehicle rolls. Increasing the distance Y_u reduces the speed of impact and increases RPER value. However, as it was stated before, the initial distance from the curb is not a vehicle design characteristics but rather is a random parameter. The percentage sensitivity function of the spring track width (s) and the height of the curb (h_{curb}) exhibit positive sensitivities at both angles of impact, which means that increase of these parameters results in increase of RPER.

From Figures 58 - 59 it can also be seen that sensitivity functions of tire radius (T_r) and undeflected suspension spring length (SPRLNG) have similar influences on RPER. Their values become negative soon after the impact and then oscillate once rollover is initiated. This makes difficult to draw any firm conclusion regarding

the influence of T_r and SPRLNG on RPER during oblique impacts. The distance from the axle to the bump stop (ABSDEF) displays negative sensitivity after the curb impact, which means that increase of ABSDEF decreases vehicle RPER. This is because increase of ABSDEF allows to develop a larger roll acceleration of sprung mass, which in turn generates a larger inertia couple rolling the vehicle over when the bump stop rests on the axle. From Figures 58 and 59 it can be seen that sensitivity function of ABSDEF is zero at the instant of impact, simply because the bump stops are not deformed yet. The sensitivity function of ABSDEF becomes negative at approximately 0.15 seconds after the curb impact and attains a zero value again when the bump stop comes into contact with the axle.

The percentage sensitivity functions of RPER to variation of the mass-inertia parameter set are presented in Figures 60 and 61. From these figures it can be seen that the sensitivity function of sprung mass (M_s), which was positive when vehicle was skidding, becomes negative after the vehicle impacts the curb and attains a positive value again when the vehicle rolls over. This means that an increase in vehicle sprung mass M_s reduces RPER at the instant of rollover initiation. A similar result was observed during rollover in side impact (Figure 47). During oblique impact the sensitivity function of M_s is smaller than in side impact and its value decreases as the angle of impact increases. For example, the sensitivity function of M_s equals - 56 and - 72 for impact angles 15 and 25 degrees, respectively. The influence of unsprung mass (M_u) is smaller than that of sprung mass; however, at both heading angles the sensitivity function remains positive and does not change much after the curb impact . The roll moments of inertia of both sprung (I_{xxs}) and unsprung (I_{xxu}) masses have positive sensitivity functions after the impact, which indicates that increases in I_{xxs} and I_{xxu} increase RPER. Figures 60 and 61 also show that other moments of inertia, such as yawing (I_{zzs}) and pitching (I_{yyu}), which were of negligible importance during side impact, become more influential in oblique impact, particularly with larger angles.

The effect of the product of inertia parameter set on vehicle RPER is demonstrated in Figures 62 and 63. These figures reveal that sensitivity functions of all mass products of inertia of both sprung and unsprung masses are very small and oscillate between positive and negative values after the curb impact. The mass products of inertia have a much smaller influence on RPER during oblique impact as compared to side impact.

Figures 64 and 65 illustrate the influence of stiffness parameters on RPER. For both impact angles the impact force deformation rate (K_{d1}) is the most dominant of all stiffness parameters. Its sensitivity function is first negative (just after the impact), then positive, and negative again when the vehicle rolls over. The absolute value of the sensitivity function of K_{d1} just after the impact is smaller now than during the side impact. This reveals that K_{d1} is less influential in oblique impacts than in side impacts. Also, tire radial stiffness (K_z) shows decreased influence on RPER during oblique impact as compared to side impact (Figure 51). The sensitivity of suspension stiffness (K_1) exhibits a qualitatively different influence on RPER during impact at larger angles. At a 25 degree impact angle, the sensitivity function of K_1 first becomes positive (at instant of rollover initiation) and then becomes negative. During impact under the 15 degree angle, and also during side impact, K_1 displayed negative sensitivity. The bump stop stiffness (K_2) and impact force deformation rates (K_{d2}, K_{d4}) have practically no influence on vehicle rollover stability during oblique impact situations.

The influence of the damping parameter set on RPER remains small during oblique impact (Figures 66 - 67), although the sensitivity functions of the damping parameters are larger now than in side impact (Figures 52, 53). This is because in oblique impact more energy needs to be dissipated before the vehicle rolls over than in side impact.

Figures 68 and 69 illustrate the effect of the force parameter set on vehicle RPER (rollover stability measure). The lateral tire/roadway friction coefficient (μ_y) is the most influential parameter among those considered in this group. Its sensitivity function sharply rises to a large value just after the impact (the maximum is greater for a larger angle of impact) and then falls to a negative value and oscillates when the vehicle rolls. This verifies that rollover stability reserve of the vehicle can be enlarged (or RPER increased) by an increase of μ_y, which slows down the speed of impact. From comparison of sensitivity values in both figures it can be seen that a change in μ_y affects RPER more in the case of a large angle of impact.

The lateral deformation parameter (POINT2) is the second influential parameter of the group. The sensitivity function of POINT2 reaches the positive values of 85 and 100 for impact angles 15 and 25 degrees, respectively, which indicates that increasing POINT2 increases RPER. The relatively large sensitivity of RPER to variations of POINT2 can be explained by the fact that the total impact force is now exerted on a single front wheel instead of both front and rear wheels as it was during side impact. This impact force is large enough (approximately twice larger than a force acting on a single wheel during side impact) to cause permanent (plastic) deformation of front axle even if the rollover occurs at the critical rollover speed. A larger plastic deformation of the front axle obviously means more energy is dissipated during the impact and therefore less rolling kinetic energy is created.

Figures 68 and 69 also show that the sensitivity function of the deformation parameter (POINT1) is negative immediately after the impact and soon afterward becomes positive. The influence of POINT1 on RPER decreases (sensitivity function has smaller absolute value) as the angle of impact increases. The influence of longitudinal (μ_x) and scrubbing tire/curb (μ_s) friction characteristics on RPER is small and the oscillatory character of their sensitivity functions makes it difficult to draw any firm conclusions about them. The

parameters K_V and K_{VF} have practically no influence on vehicle rollover stability during oblique impacts at critical rollover speeds.

5.3.3 Parametric Sensitivity of RPER3 in Side Impact

The influence of seven parameter groups (described in chapter 5.3) on vehicle RPER3 during side impact with the curb is illustrated in Figures 70 - 76. These figures show percentage sensitivity functions of RPER3 obtained at the critical rollover speed of 22.13 Ft/s and at the same initial conditions as those used to investigate the sensitivity of RPER.

From the comparison of Figures 70 - 76 with the corresponding sensitivity plots obtained for RPER at the critical rollover speed of 22.13 Ft/s (Figures 43, 45, 47, 49, 51, 53 and 55), it can be seen that both functions RPER3 and RPER exhibit very similar sensitivities to changes in the parameters investigated in this report. The qualitative and quantitative influences of vehicle and terrain characteristics on both RPER3 and RPER is virtually the same at the instant of impact and when rollover is initiated. Some differences between the values of the sensitivity functions of RPER3 and RPER exist during vehicle skidding motion prior to the curb impact. The sensitivity functions of RPER3 tend to oscillate more than those of RPER. This is because RPER3 is more sensitive to the accuracy with which initial conditions were determined. In this study, the initial conditions for the simulation were determined based upon kineto-static equilibrium of the vehicle and not using a classical dynamic analysis. This fact, however, does not affect sensitivity results because the vehicle is allowed to skid 7.5 Ft before impacting the curb which, in case of RPER3 and the skidding velocities used, is sufficient to achieve almost steady skidding conditions.

Figures 70 - 76 reveal that the most influential parameters, for which increases in values result in increases of vehicle RPER3, are, in order of decreasing influence: vehicle initial distance from the curb

(Y_u), tire/pavement lateral sliding coefficient of friction (μ_y), track width (TRW) and static rollover stability factor (SRSF), sprung mass roll moment of inertia (I_{xxs}) and suspension springs' track width (s). Among the parameters, whose increases reduce the vehicle rollover stability (decreases RPER3) at critical rollover speed, there are: distance from roll axis to sprung mass c.g. (h_{ra}), tire radius (T_r), distance from vehicle c.g. to front axle (a), sprung mass (M_s), mass product of inertia (I_{xzu}), impact force deformation rate (K_{d1}) and deformation parameter (POINT1).

5.3.4 Parametric Sensitivity of RPER3 in Oblique Impact

The percentage sensitivity functions of RPER3 taken with respect to the seven parameter sets during vehicle oblique impact with the curb are presented in Figures 77 - 90. These figures alternately contain results obtained at two angles of impact equal to 15 and 25 degrees. In both cases the initial skidding velocities were equal to critical rollover speeds (22.93 and 23.77 Ft/s for the angles of 15 and 25 degrees, respectively) and the initial position of vehicle front wheel from the curb was 7.5 Ft.

A comparison of Figures 77 - 90, with corresponding Figures 56 - 69, acquired to investigate sensitivity of RPER during oblique impacts, reveals that both functions RPER3 and RPER demonstrate very similar sensitivities to parameter variations. For both angles of impact, the values of sensitivity functions of RPER3 are very close to those of RPER at the instant of rollover initiation, which occurs when the rollover prevention energy reserve of vehicle falls to zero. The values of sensitivity functions at the instant when rollover is initiated are important, particularly because they carry information regarding the parameters' effect on vehicle rollover stability. The oscillations in sensitivity functions of RPER3 during vehicle skidding motion are an effect of the increased sensitivity of RPER3 to initial conditions prior to the curb impact.

Overall, the results of sensitivity analysis of RPER3 are practically the same as those obtained from investigating the RPER and for this reason they are not repeated here. For a detailed analysis of parametric sensitivity results during vehicle oblique impact with the curb a reader is referred to chapter 5.3.2.

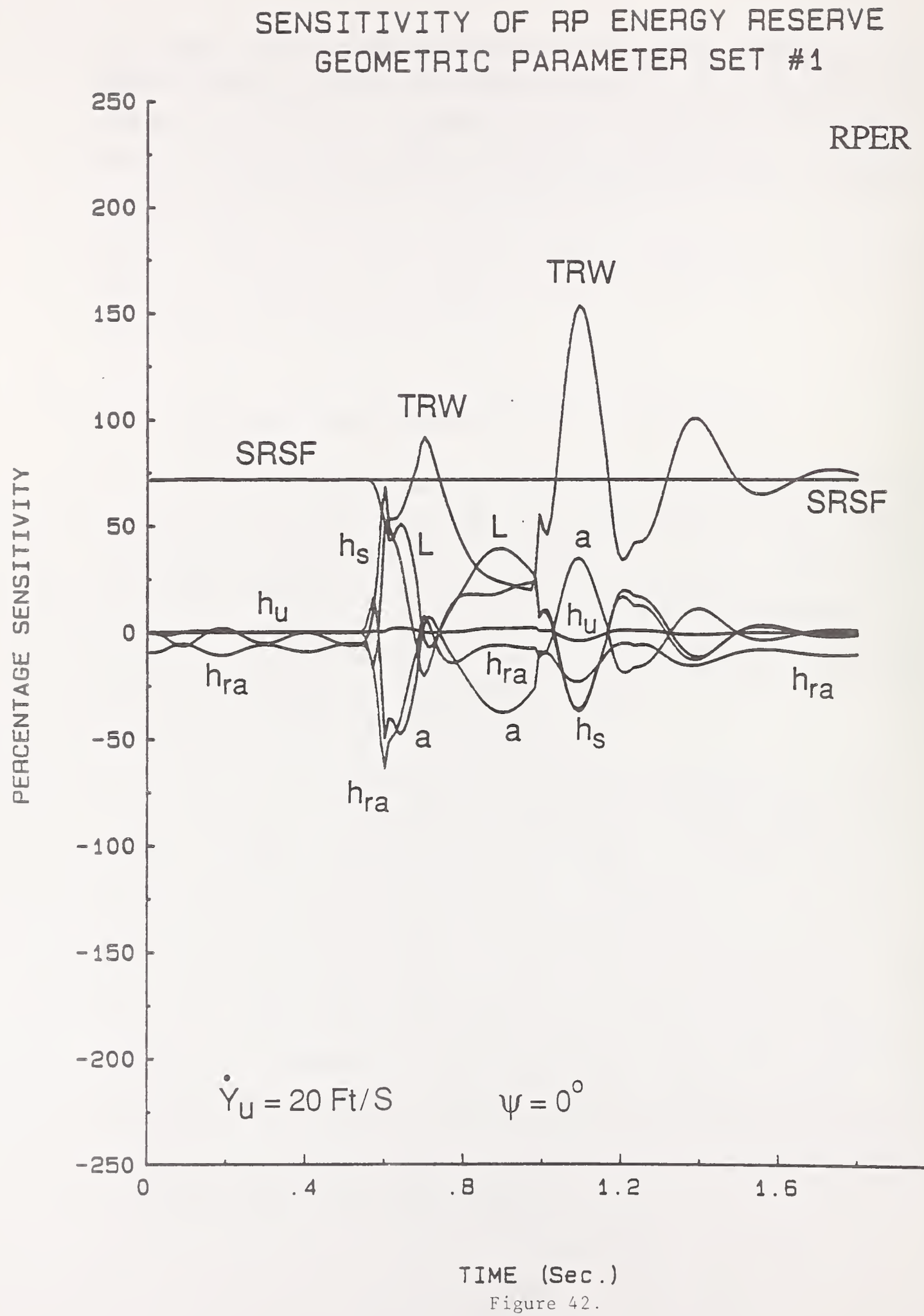
SENSITIVITY OF RP ENERGY RESERVE
GEOMETRIC PARAMETER SET #1
RPER
PERCENTAGE SENSITIVITY
TIME (Sec.)
250
200
150
100
50
0
-50
-100
-150
-200
-250
0
.4
.8
1.2
1.6
2
TRW
TRW
SRSF
SRSF
h_s
L
L
a
h_u
h_u
h_{ra}
h_{ra}
h_{ra}
a
a
h_s
h_{ra}
$\dot{Y}_u = 20$ Ft/S
$\psi = 0^\circ$

Figure 42.

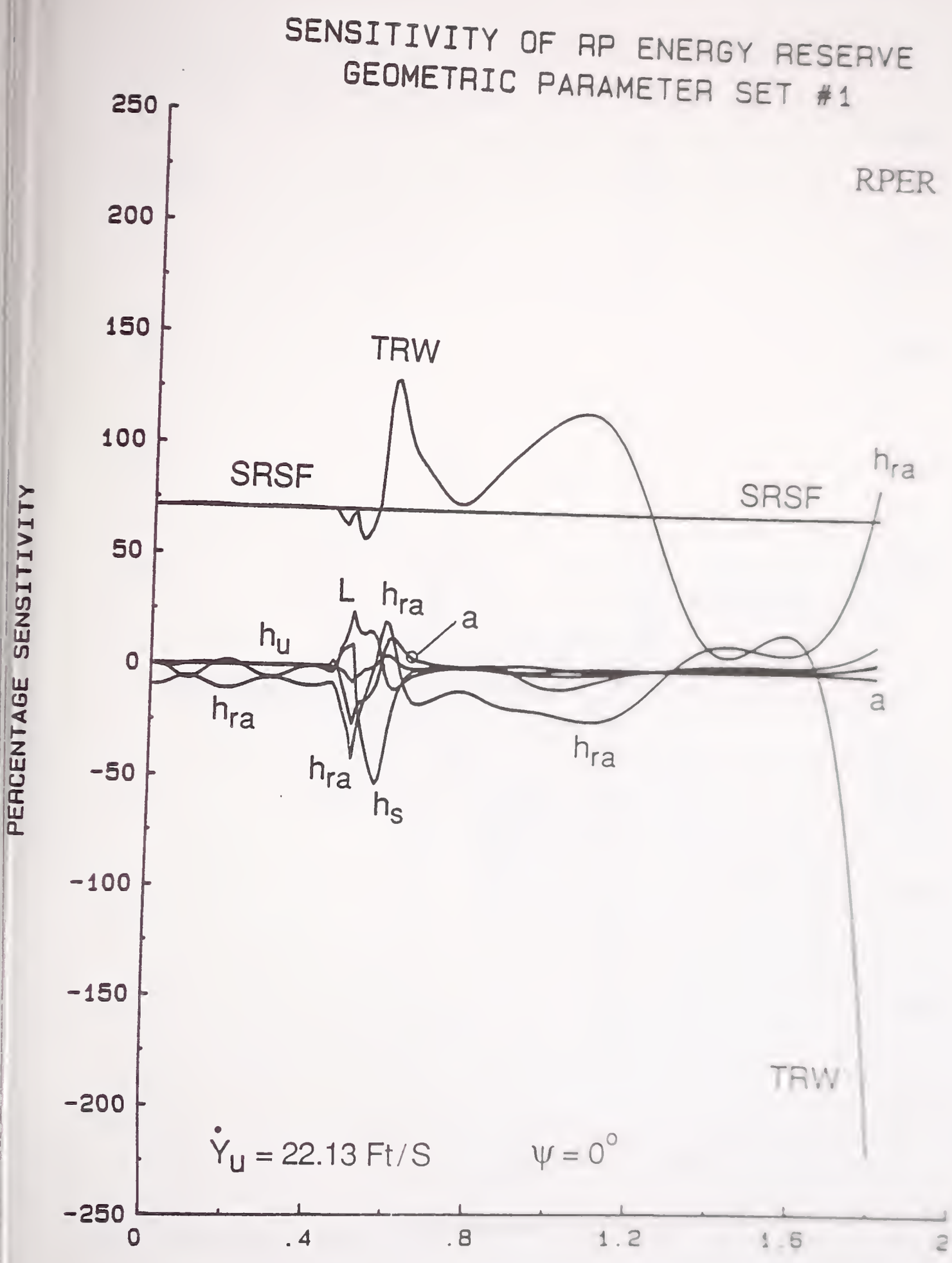
SENSITIVITY OF RP ENERGY RESERVE
GEOMETRIC PARAMETER SET #1
RPER
PERCENTAGE SENSITIVITY
TIME (Sec.)
250
200
150
100
50
0
-50
-100
-150
-200
-250
0
.4
.8
1.2
1.6
2
TRW
SRSF
SRSF
h_{ra}
L
h_{ra}
a
h_u
h_{ra}
h_{ra}
h_s
h_{ra}
a
TRW
$\dot{Y}_u$ = 22.13 Ft/S
$\psi = 0^\circ$

Figure 43.

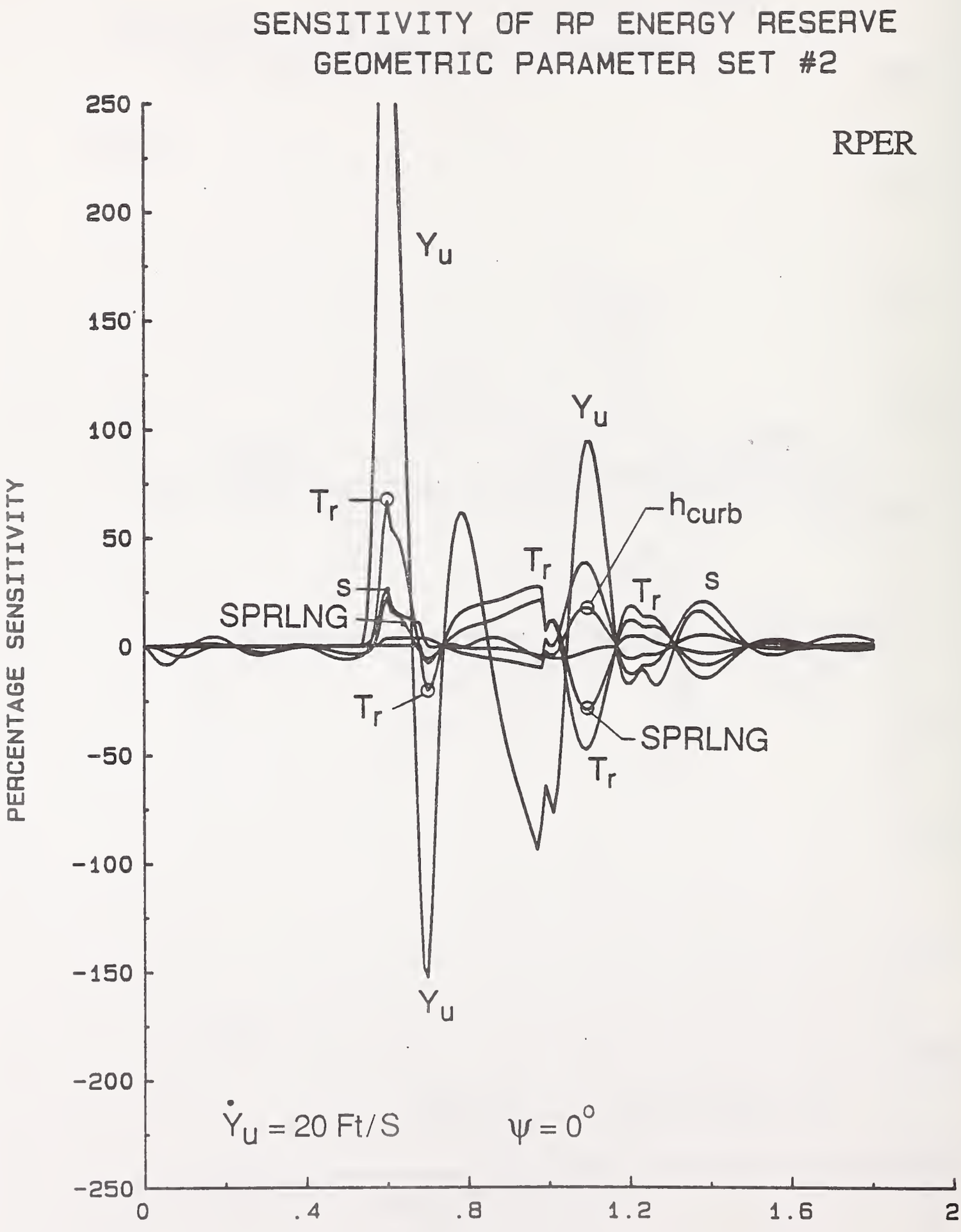
SENSITIVITY OF RP ENERGY RESERVE
GEOMETRIC PARAMETER SET #2
RPER
PERCENTAGE SENSITIVITY
TIME (Sec.)
250
200
150
100
50
0
-50
-100
-150
-200
-250
0
.4
.8
1.2
1.6
2
Y_u
Y_u
T_r
h_{curb}
T_r
T_r
s
s
SPRLNG
T_r
SPRLNG
T_r
Y_u
$\dot{Y}_u = 20$ Ft/S
$\psi = 0^\circ$

Figure 44.

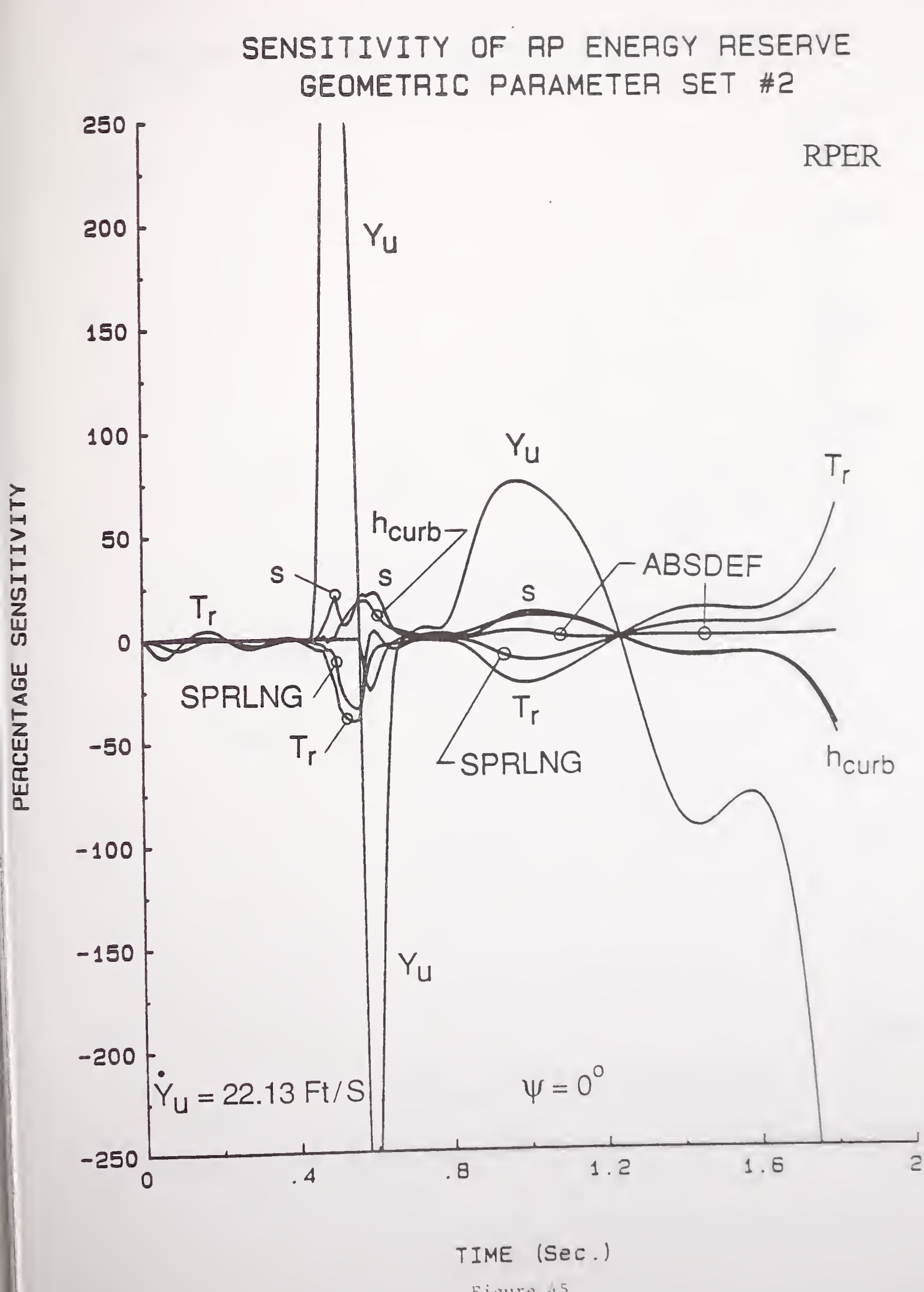
SENSITIVITY OF RP ENERGY RESERVE
GEOMETRIC PARAMETER SET #2
RPER
PERCENTAGE SENSITIVITY
TIME (Sec.)
250
200
150
100
50
0
-50
-100
-150
-200
-250
0
.4
.8
1.2
1.6
2
Y_u
Y_u
Y_u
T_r
T_r
T_r
T_r
h_{curb}
h_{curb}
s
s
s
ABSDEF
SPRLNG
SPRLNG
$\dot{Y}_u = 22.13$ Ft/S
$\psi = 0^\circ$

Figure 45.

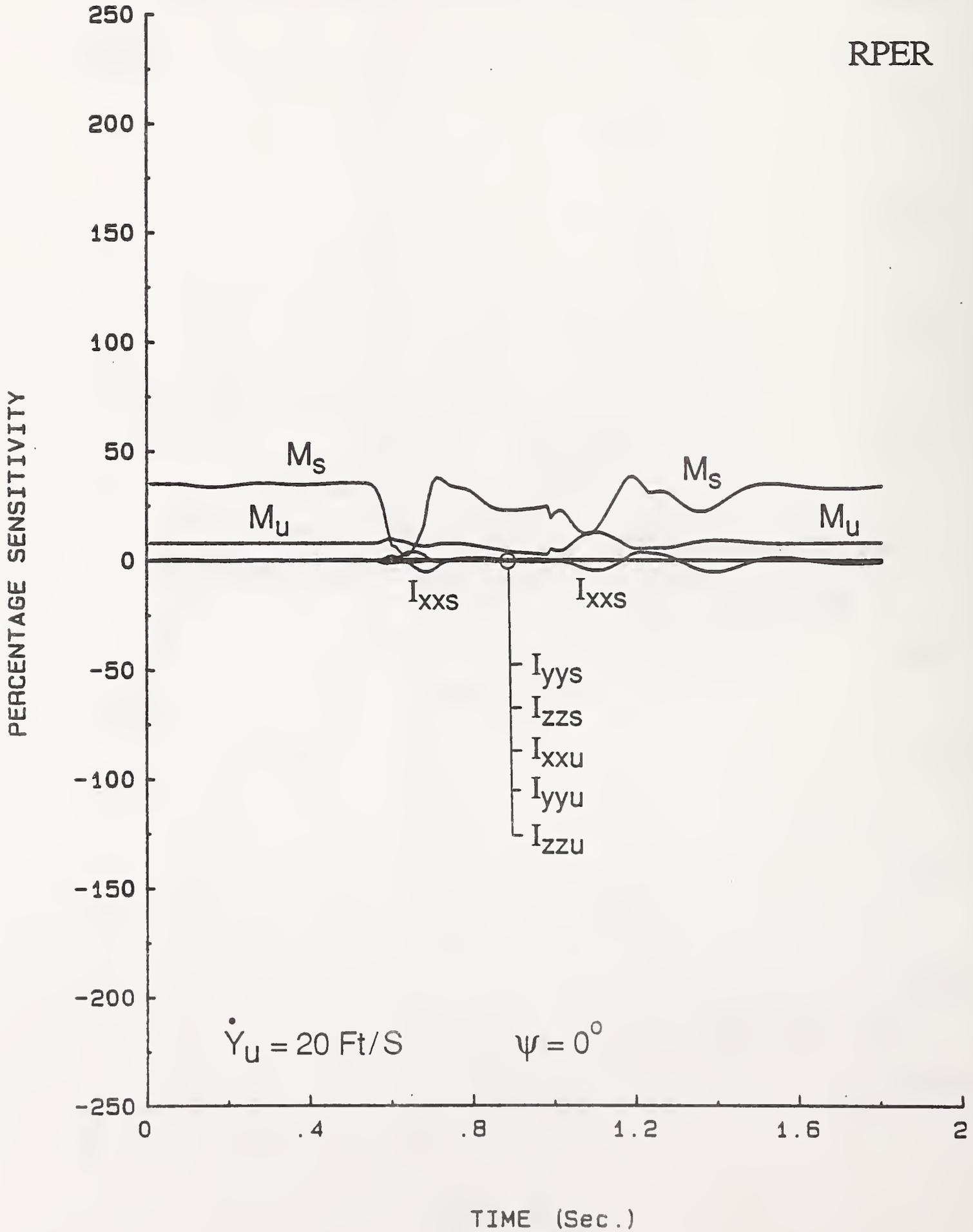
SENSITIVITY OF RP ENERGY RESERVE
MASS PARAMETER SET
RPER
250
200
150
100
50
0
-50
-100
-150
-200
-250
PERCENTAGE SENSITIVITY
M_s
M_u
M_s
M_u
I_{xxs}
I_{xxs}
I_{yys}
I_{zzs}
I_{xxu}
I_{yyu}
I_{zzu}
$\dot{Y}_u = 20$ Ft/S
$\psi = 0^\circ$
0
.4
.8
1.2
1.6
2
TIME (Sec.)

Figure 46.

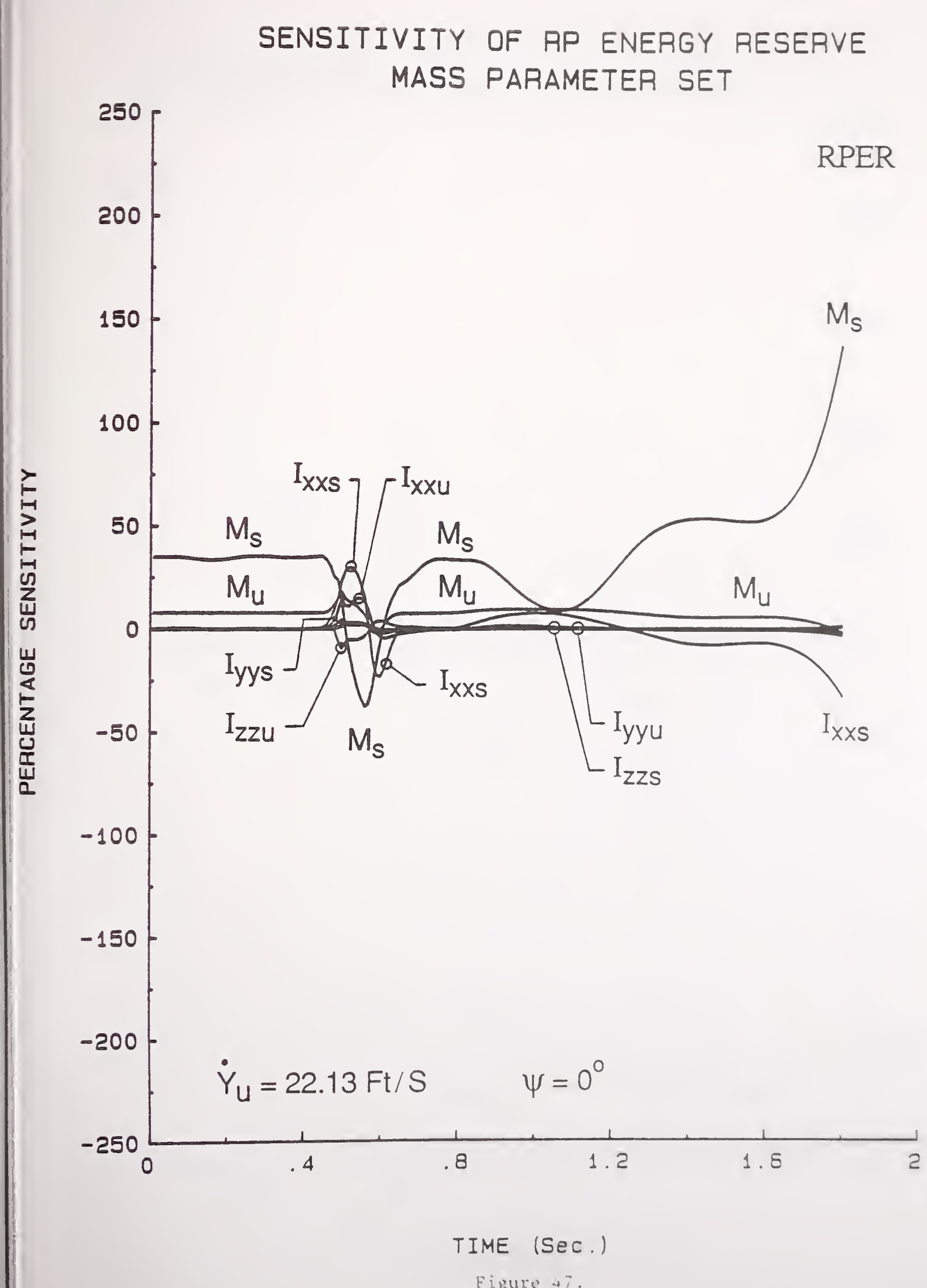
SENSITIVITY OF RP ENERGY RESERVE
MASS PARAMETER SET
RPER
PERCENTAGE SENSITIVITY
250
200
150
100
50
0
-50
-100
-150
-200
-250
0
.4
.8
1.2
1.6
2
TIME (Sec.)
M_s
I_{xxs}
I_{xxu}
M_s
M_u
M_s
M_u
M_u
I_{yys}
I_{xxs}
I_{zzu}
M_s
I_{yyu}
I_{zzs}
I_{xxs}
$\dot{Y}_u = 22.13$ Ft/S
$\psi = 0^\circ$

Figure 47.

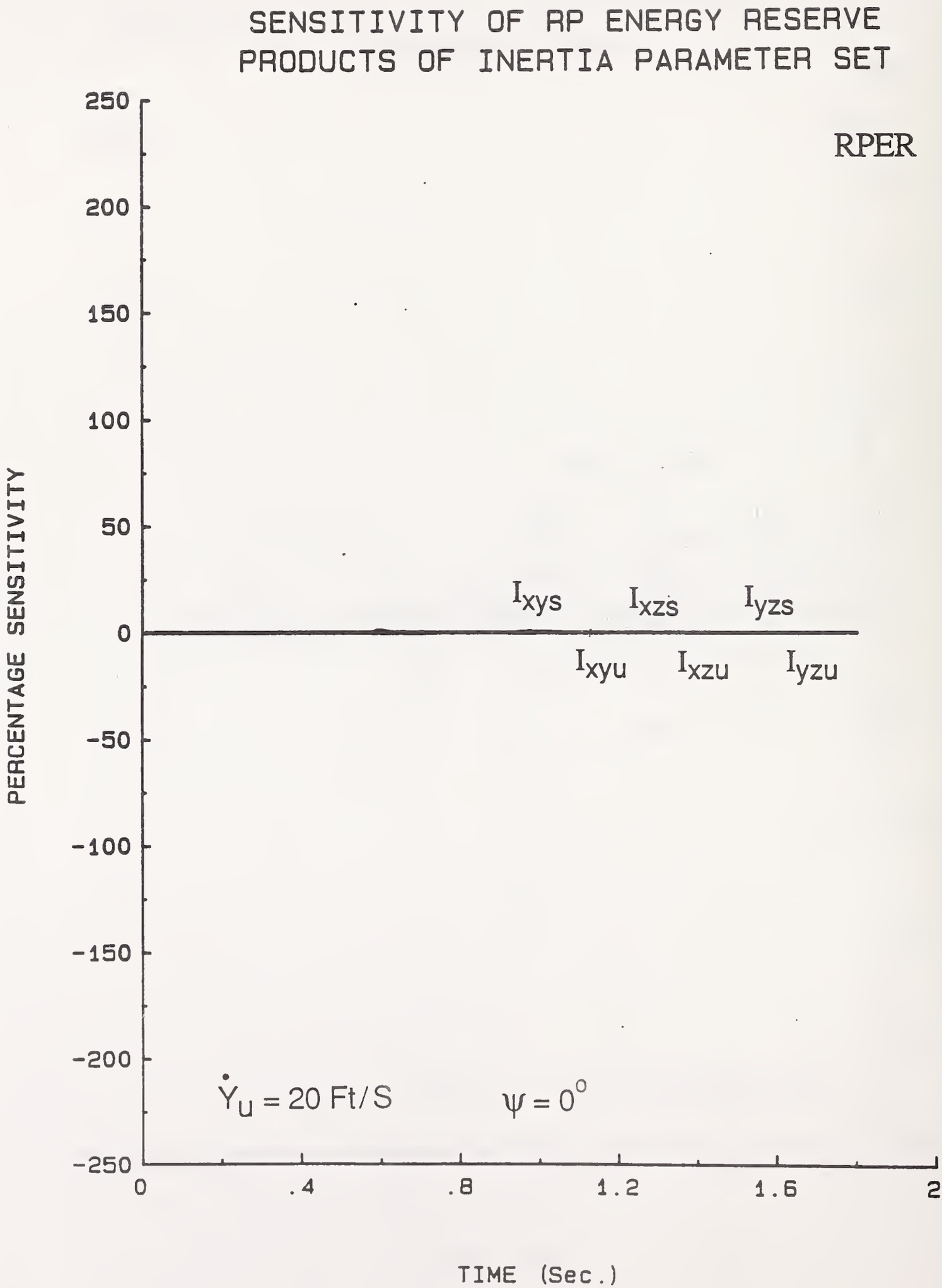
SENSITIVITY OF RP ENERGY RESERVE
PRODUCTS OF INERTIA PARAMETER SET
RPER
250
200
150
100
50
0
-50
-100
-150
-200
-250
PERCENTAGE SENSITIVITY
I_{xys}
I_{xzs}
I_{yzs}
I_{xyu}
I_{xzu}
I_{yzu}
$\dot{Y}_u = 20$ Ft/S
$\psi = 0^\circ$
0
.4
.8
1.2
1.6
2
TIME (Sec.)

Figure 48.

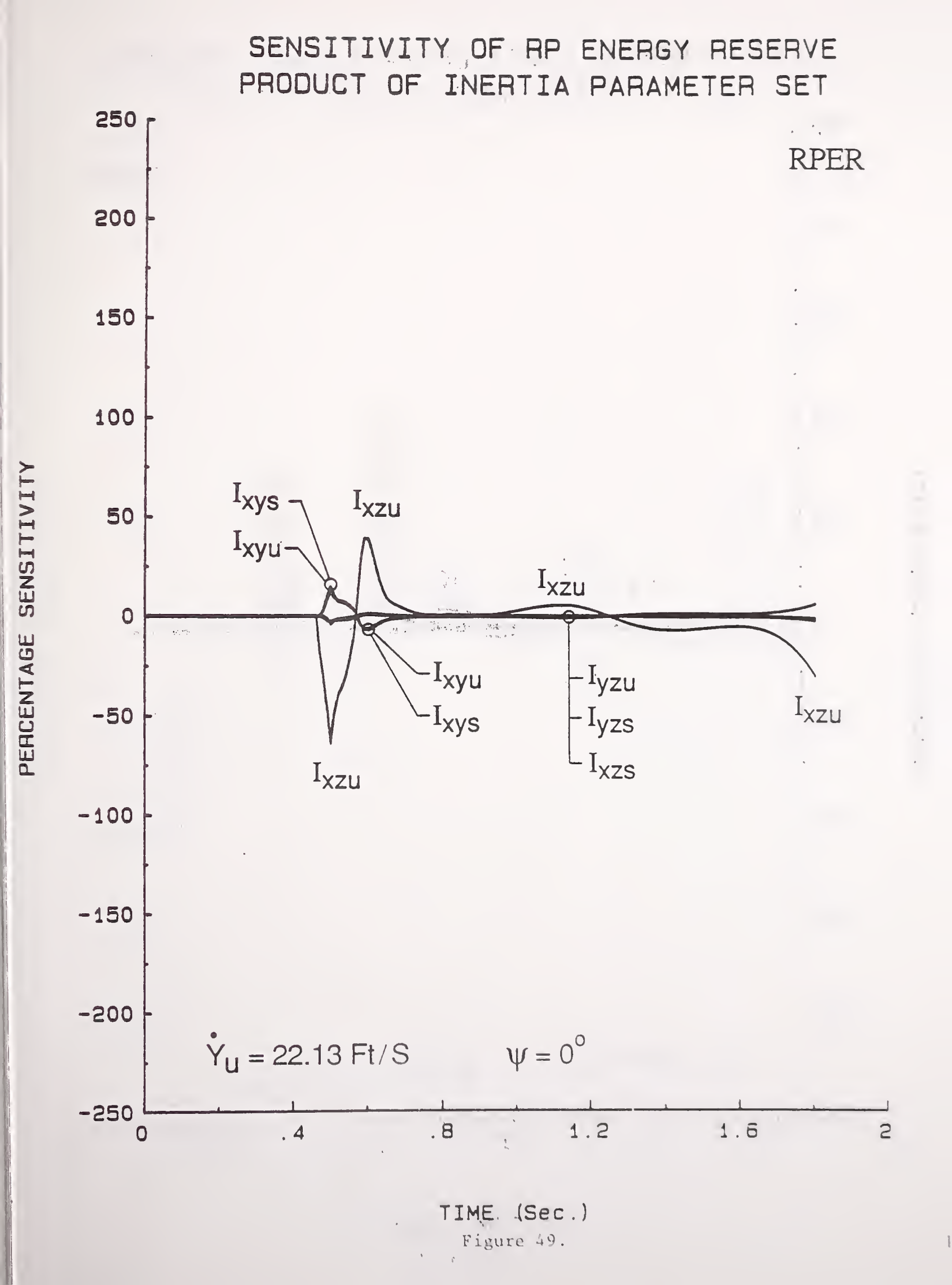
SENSITIVITY OF RP ENERGY RESERVE
PRODUCT OF INERTIA PARAMETER SET
RPER
250
200
150
100
50
0
-50
-100
-150
-200
-250
PERCENTAGE SENSITIVITY
I_{xys}
I_{xyu}
I_{xzu}
I_{xzu}
I_{xyu}
I_{xys}
I_{xzu}
I_{yzu}
I_{yzs}
I_{xzs}
I_{xzu}
$\dot{Y}_u = 22.13$ Ft/S
$\psi = 0^\circ$
0
.4
.8
1.2
1.6
2
TIME (Sec.)

Figure 49.

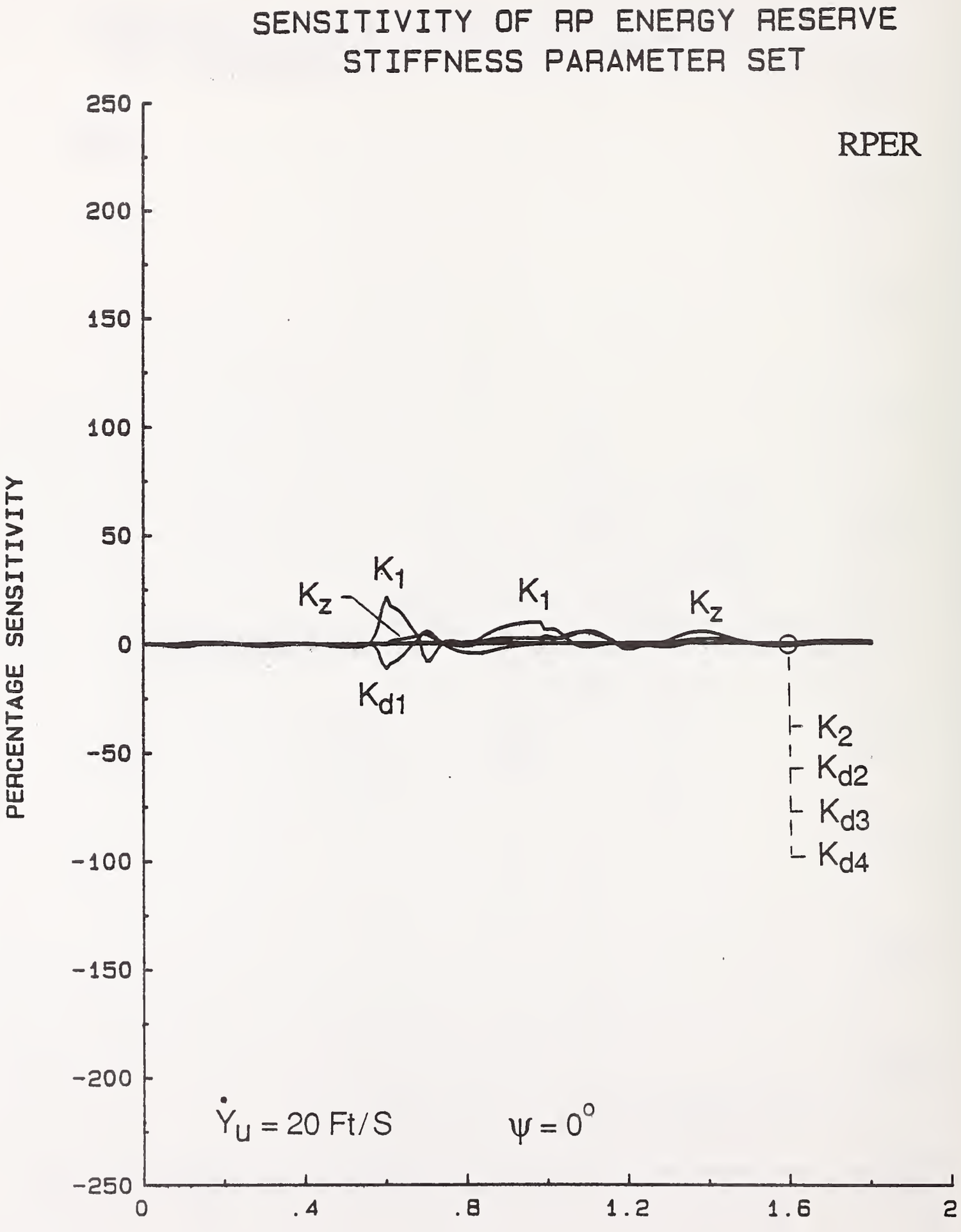
SENSITIVITY OF RP ENERGY RESERVE
STIFFNESS PARAMETER SET
RPER
250
200
150
100
50
0
-50
-100
-150
-200
-250
PERCENTAGE SENSITIVITY
K_z
K_1
K_{d1}
K_1
K_z
K_2
K_{d2}
K_{d3}
K_{d4}
$\dot{Y}_u = 20$ Ft/S
$\psi = 0^\circ$
0
.4
.8
1.2
1.6
2
TIME (Sec.)

Figure 50.

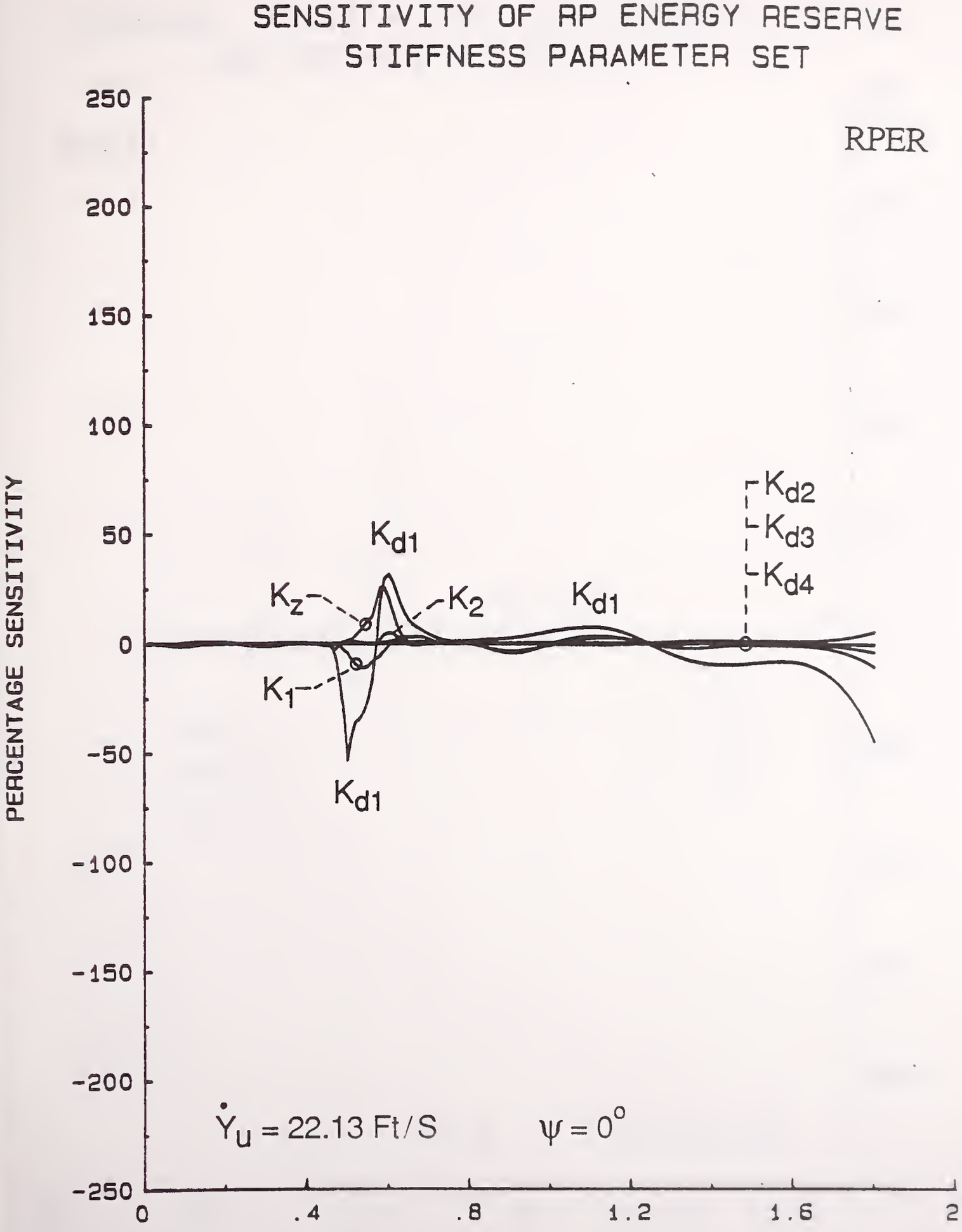
SENSITIVITY OF RP ENERGY RESERVE
STIFFNESS PARAMETER SET
RPER
250
200
150
100
50
0
-50
-100
-150
-200
-250
PERCENTAGE SENSITIVITY
K_{d1}
K_z
K_2
K_{d1}
K_{d2}
K_{d3}
K_{d4}
K_1
K_{d1}
$\dot{Y}_u = 22.13$ Ft/S
$\psi = 0^\circ$
0
.4
.8
1.2
1.6
2
TIME (Sec.)

Figure 51.

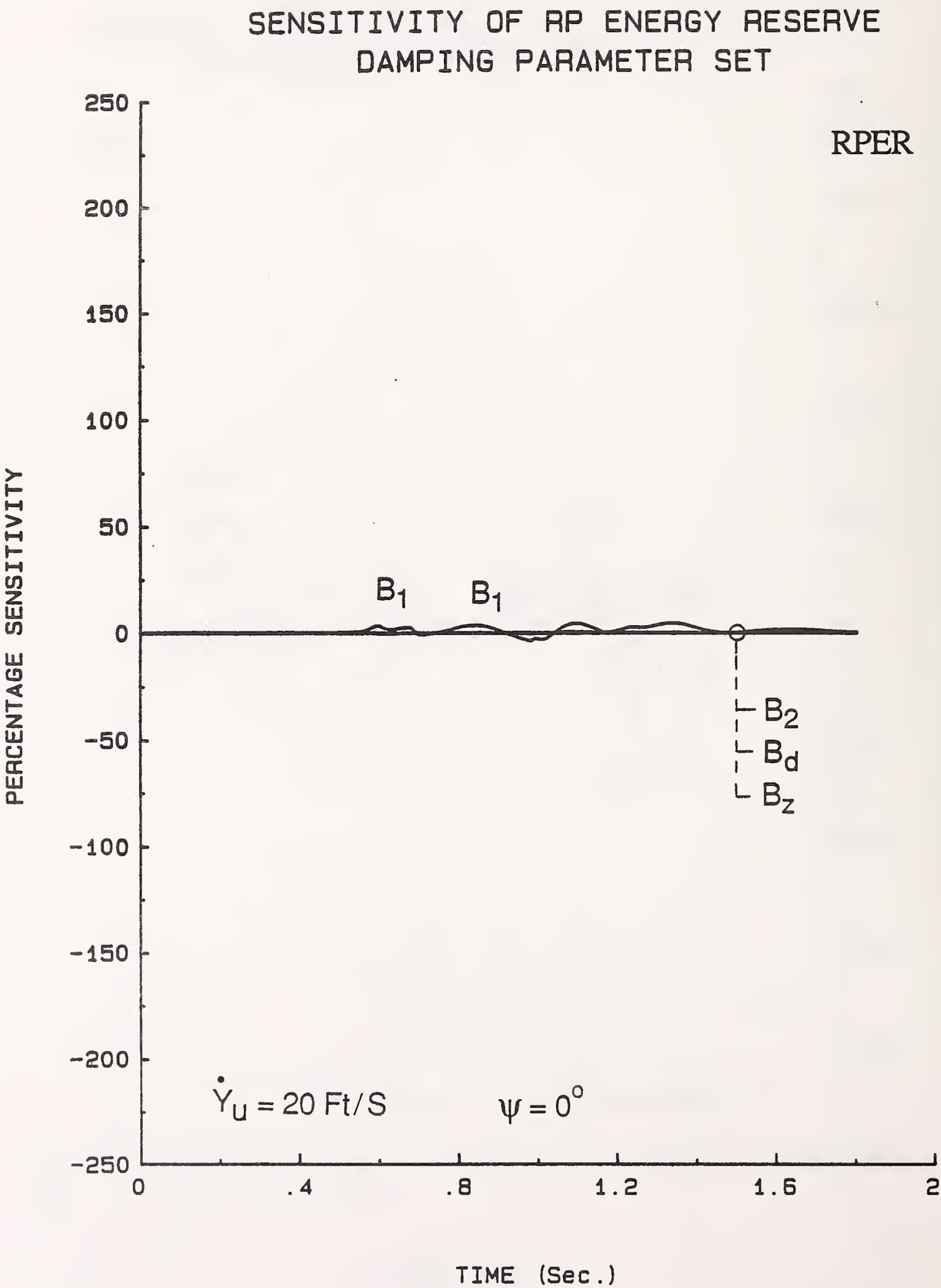
SENSITIVITY OF RP ENERGY RESERVE
DAMPING PARAMETER SET
RPER
250
200
150
100
50
0
-50
-100
-150
-200
-250
PERCENTAGE SENSITIVITY
B1
B1
B2
Bd
Bz
$\dot{Y}_u$ = 20 Ft/S
ψ = 0°
0
.4
.8
1.2
1.6
2
TIME (Sec.)

Figure 52.

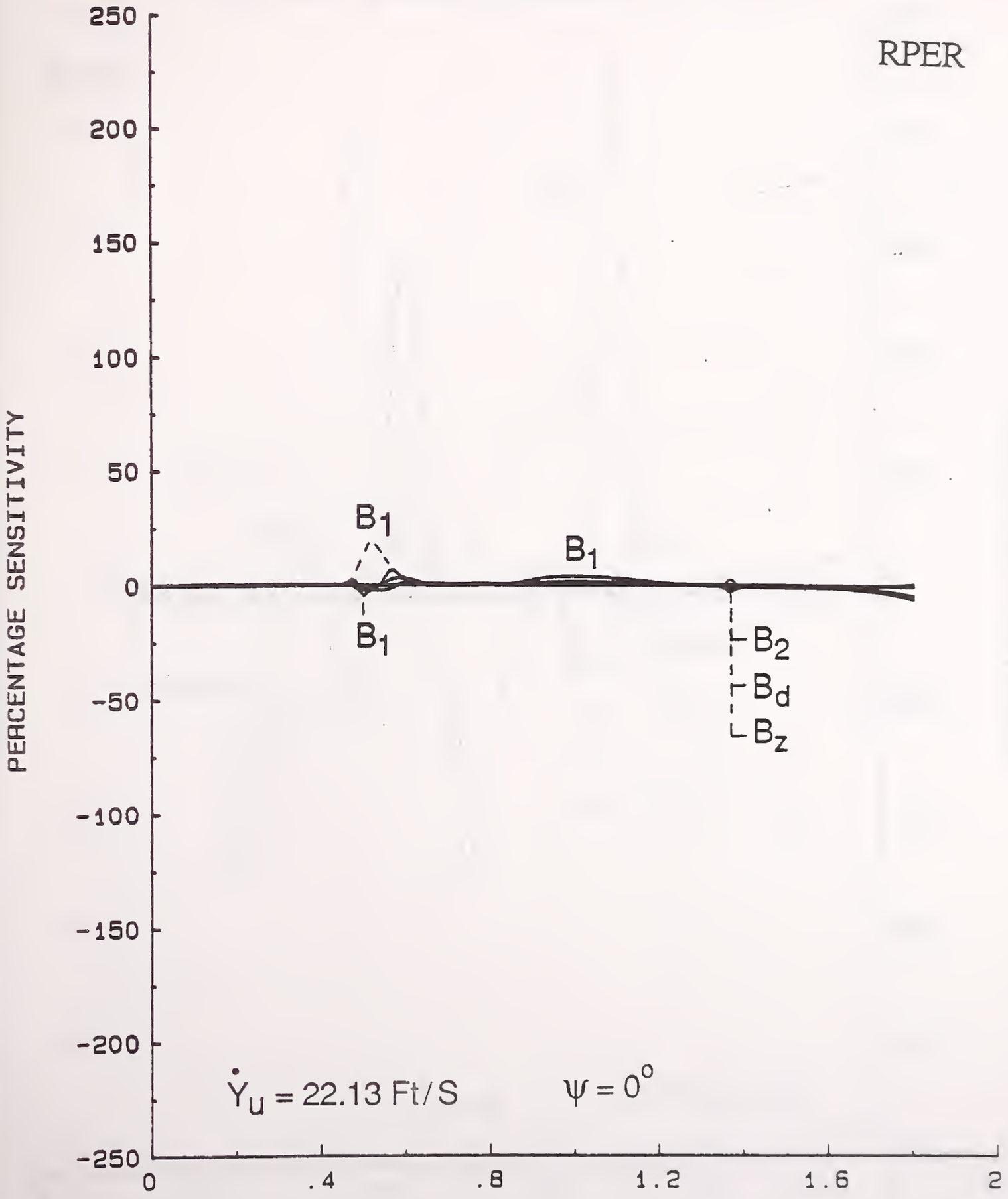
SENSITIVITY OF RP ENERGY RESERVE
DAMPING PARAMETER SET
RPER
250
200
150
100
50
0
-50
-100
-150
-200
-250
PERCENTAGE SENSITIVITY
B1
B1
B1
B2
Bd
Bz
$\dot{Y}_u$ = 22.13 Ft/S
ψ = 0°
0
.4
.8
1.2
1.6
2
TIME (Sec.)

Figure 53.

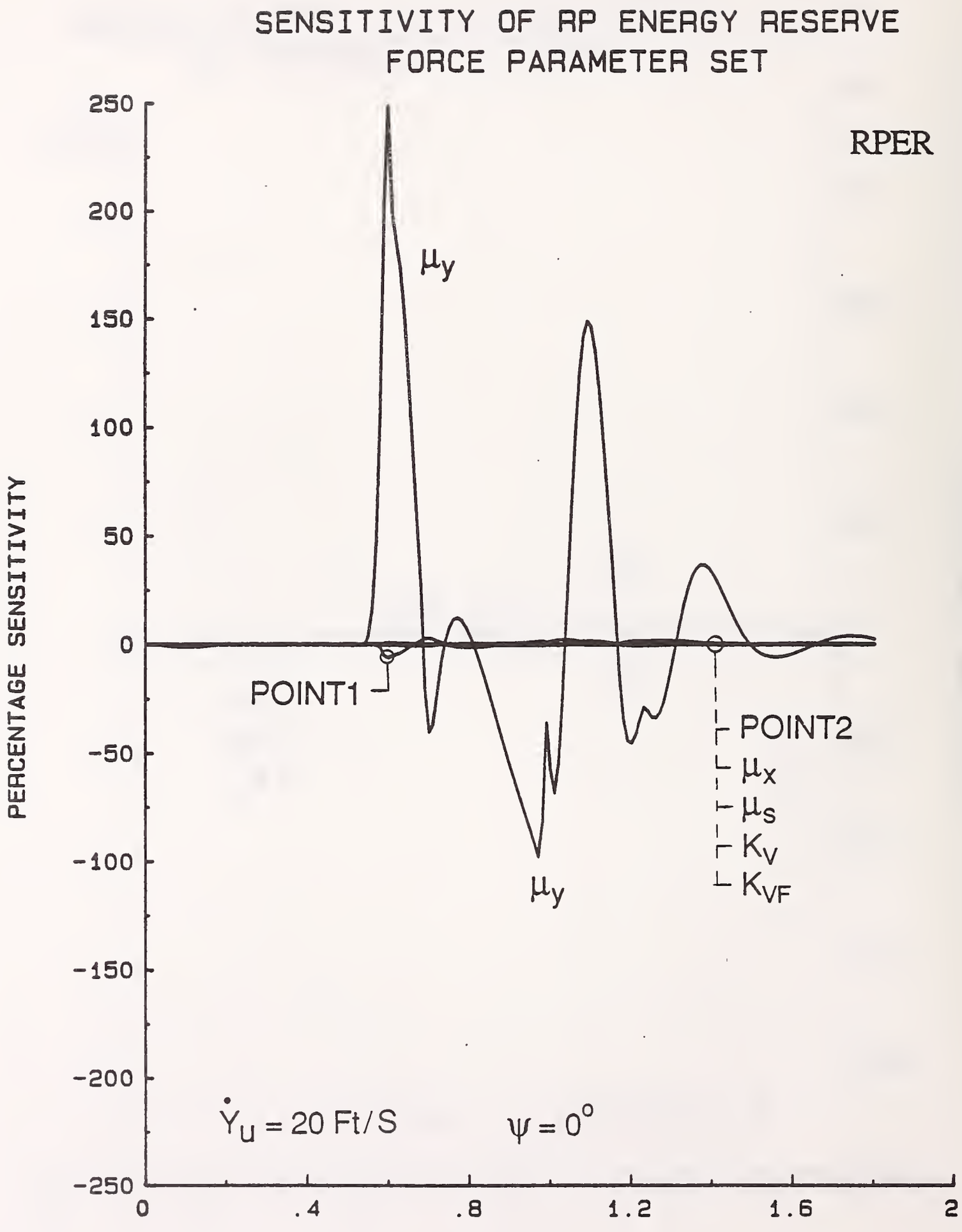
SENSITIVITY OF RP ENERGY RESERVE
FORCE PARAMETER SET
RPER
250
200
150
100
50
0
-50
-100
-150
-200
-250
PERCENTAGE SENSITIVITY
μ_y
POINT1
POINT2
μ_x
μ_s
K_V
K_{VF}
μ_y
$\dot{Y}_u = 20$ Ft/S
$\psi = 0^\circ$
0
.4
.8
1.2
1.6
2
TIME (Sec.)

Figure 54.

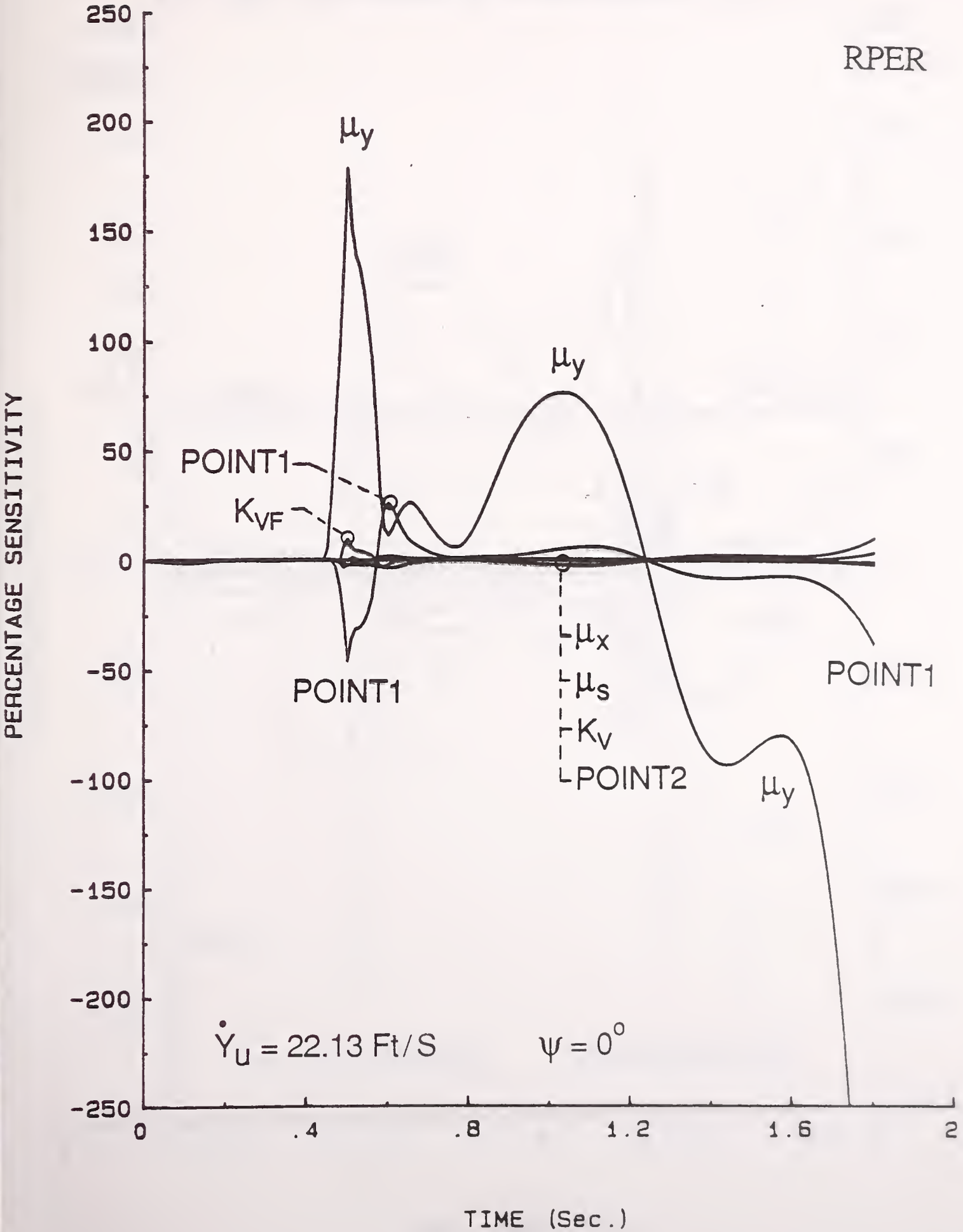
SENSITIVITY OF RP ENERGY RESERVE
FORCE PARAMETER SET
RPER
PERCENTAGE SENSITIVITY
250
200
150
100
50
0
-50
-100
-150
-200
-250
0
.4
.8
1.2
1.6
2
TIME (Sec.)
μ_y
μ_y
μ_y
POINT1
K_{VF}
POINT1
POINT1
μ_x
μ_s
K_v
POINT2
$\dot{Y}_u = 22.13$ Ft/S
$\psi = 0^\circ$

Figure 55.

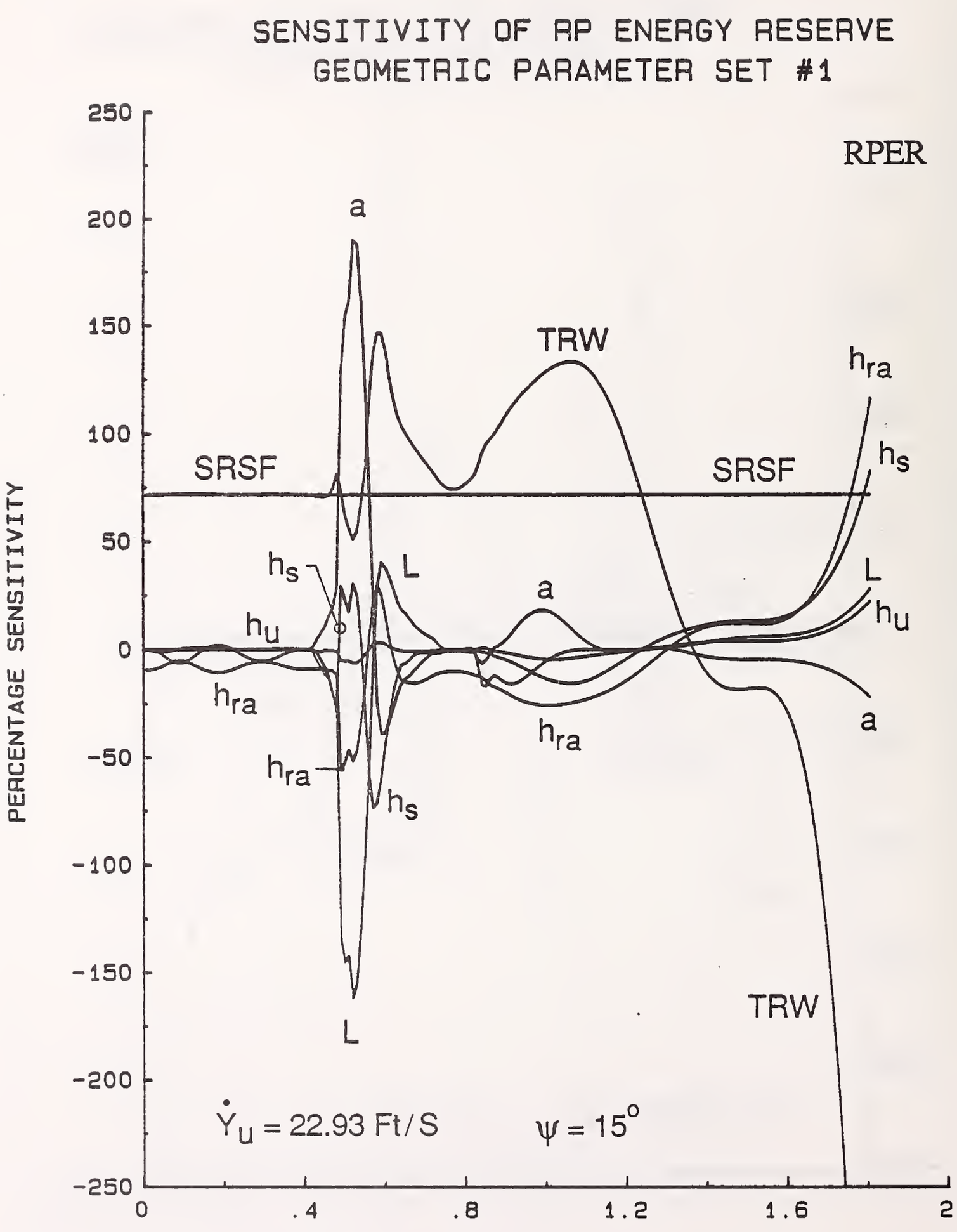
SENSITIVITY OF RP ENERGY RESERVE
GEOMETRIC PARAMETER SET #1
RPER
PERCENTAGE SENSITIVITY
TIME (Sec.)
250
200
150
100
50
0
-50
-100
-150
-200
-250
0
.4
.8
1.2
1.6
2
a
TRW
h_{ra}
h_s
SRSF
SRSF
L
h_s
h_u
h_{ra}
a
L
h_u
a
h_{ra}
h_{ra}
h_s
L
TRW
$\dot{Y}_u$ = 22.93 Ft/S
$\psi = 15^\circ$

Figure 56.

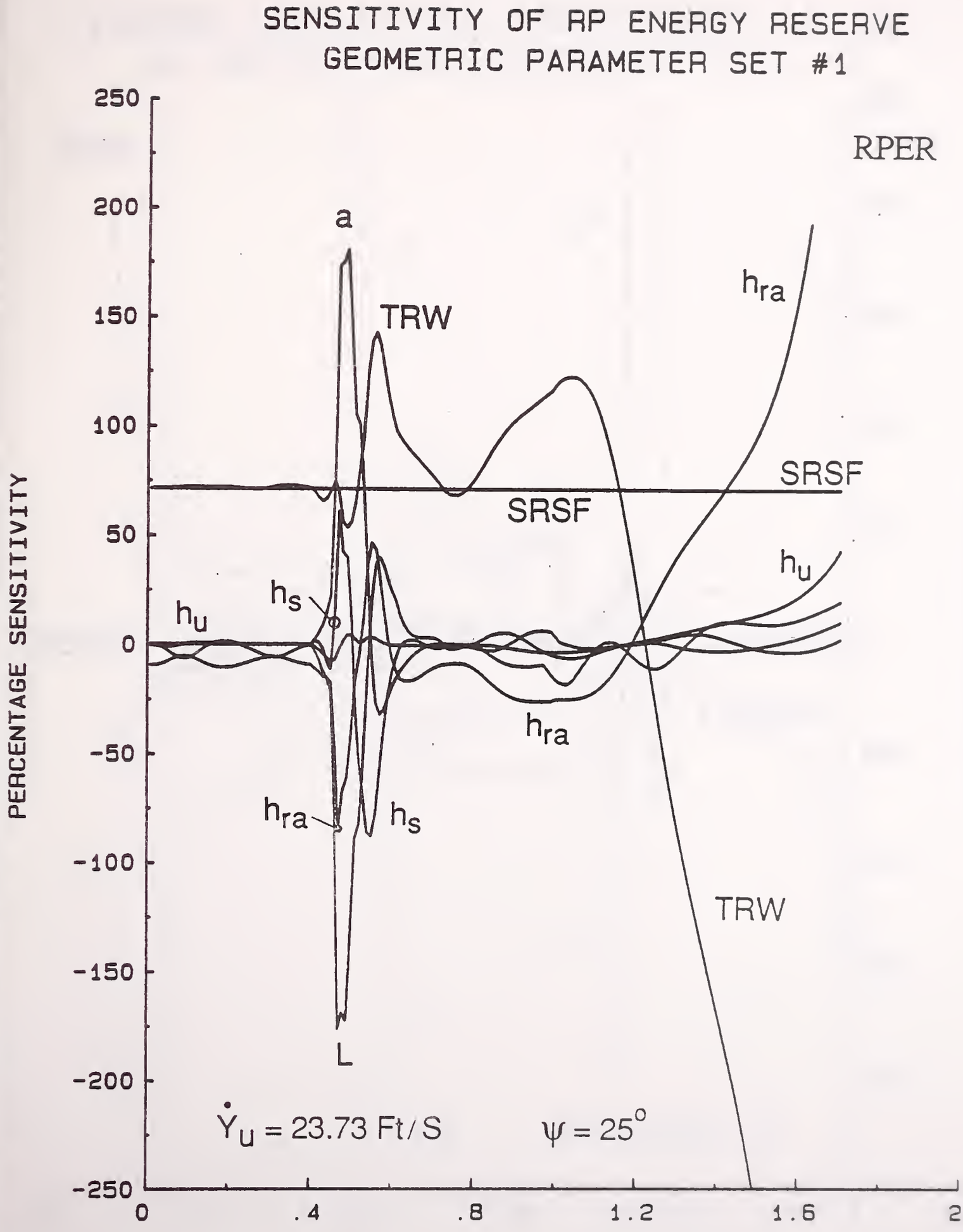
SENSITIVITY OF RP ENERGY RESERVE
GEOMETRIC PARAMETER SET #1
RPER
PERCENTAGE SENSITIVITY
TIME (Sec.)
250
200
150
100
50
0
-50
-100
-150
-200
-250
0
.4
.8
1.2
1.6
2
a
TRW
SRSF
SRSF
h_{ra}
h_u
h_s
h_u
h_{ra}
h_{ra}
h_s
TRW
L
$\dot{Y}_u = 23.73$ Ft/S
$\psi = 25^\circ$

Figure 57.

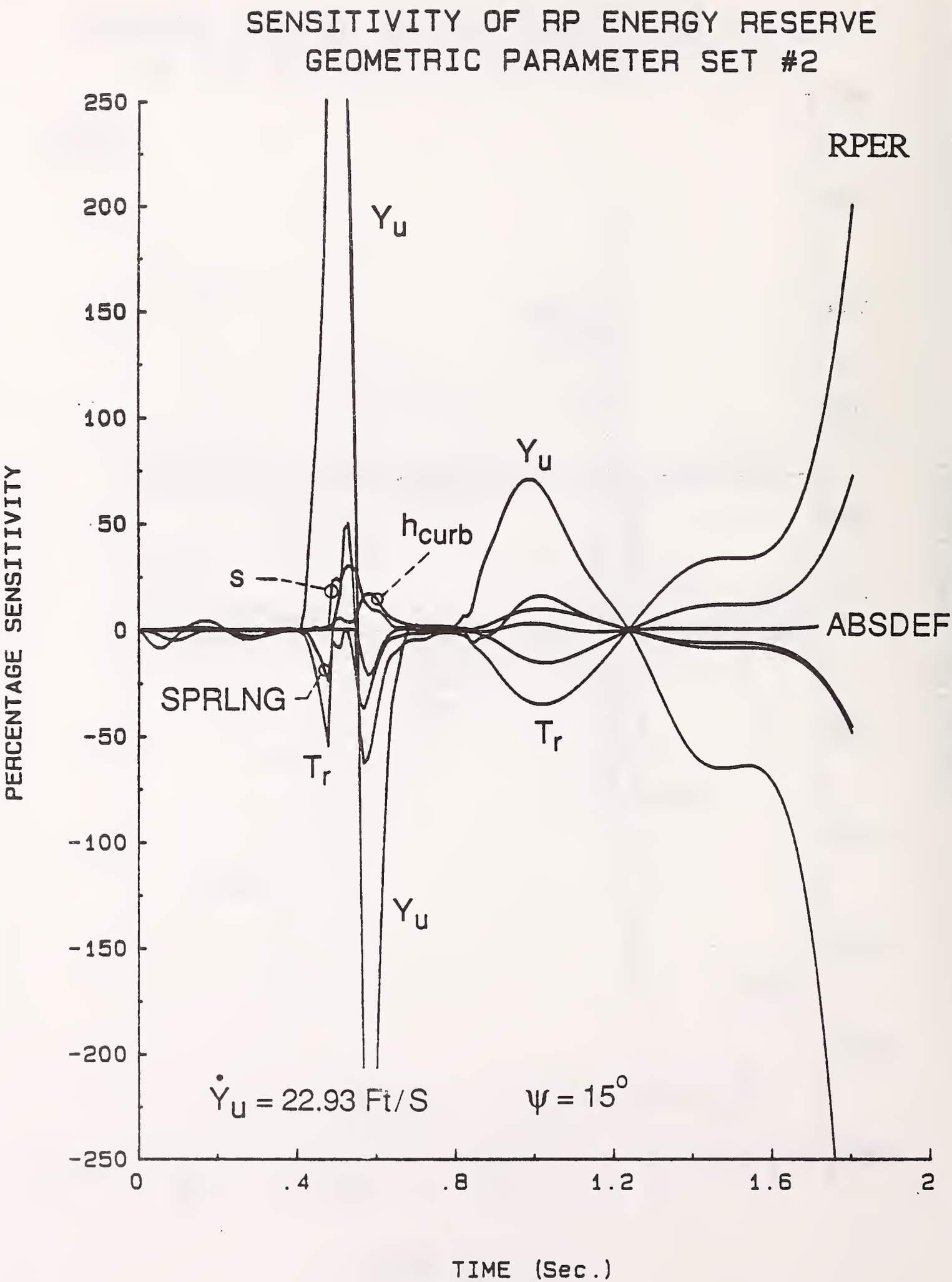
SENSITIVITY OF RP ENERGY RESERVE
GEOMETRIC PARAMETER SET #2
RPER
ABSDEF
Y_u
Y_u
h_{curb}
s
SPRLNG
T_r
T_r
Y_u
$\dot{Y}_u = 22.93$ Ft/S
$\psi = 15^\circ$
PERCENTAGE SENSITIVITY
250
200
150
100
50
0
-50
-100
-150
-200
-250
0
.4
.8
1.2
1.6
2
TIME (Sec.)

Figure 58.

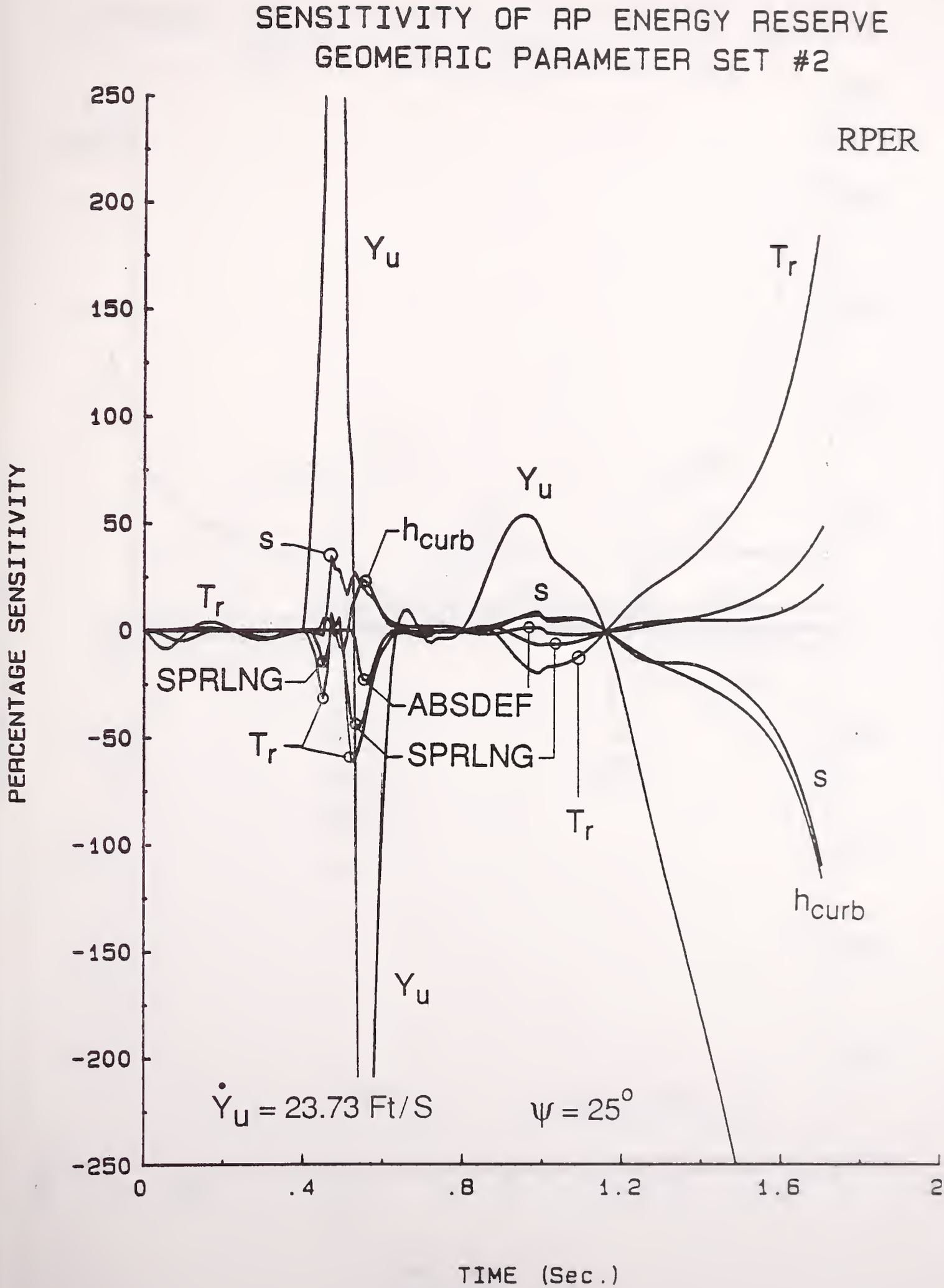
SENSITIVITY OF RP ENERGY RESERVE
GEOMETRIC PARAMETER SET #2
RPER
PERCENTAGE SENSITIVITY
TIME (Sec.)
250
200
150
100
50
0
-50
-100
-150
-200
-250
0
.4
.8
1.2
1.6
2
Yu
Tr
s
hcurb
SPRLNG
ABSDEF
Ẏu = 23.73 Ft/S
ψ = 25°

Figure 59.

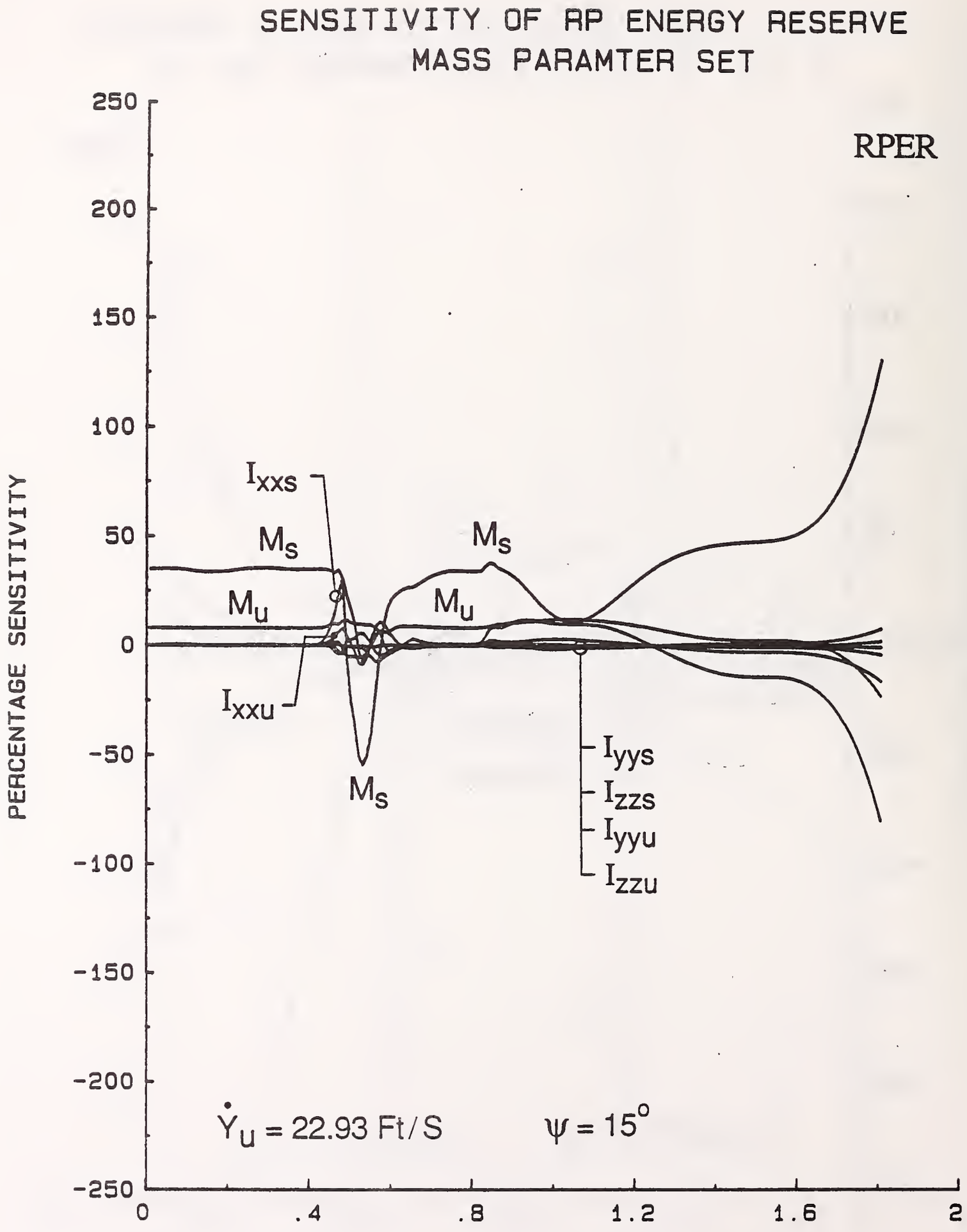
SENSITIVITY OF RP ENERGY RESERVE
MASS PARAMTER SET
RPER
PERCENTAGE SENSITIVITY
250
200
150
100
50
0
-50
-100
-150
-200
-250
0
.4
.8
1.2
1.6
2
I_{xxs}
M_s
M_u
I_{xxu}
M_s
M_s
M_u
I_{yys}
I_{zzs}
I_{yyu}
I_{zzu}
$\dot{Y}_u = 22.93$ Ft/S
$\psi = 15^o$
TIME (Sec.)

Figure 60.

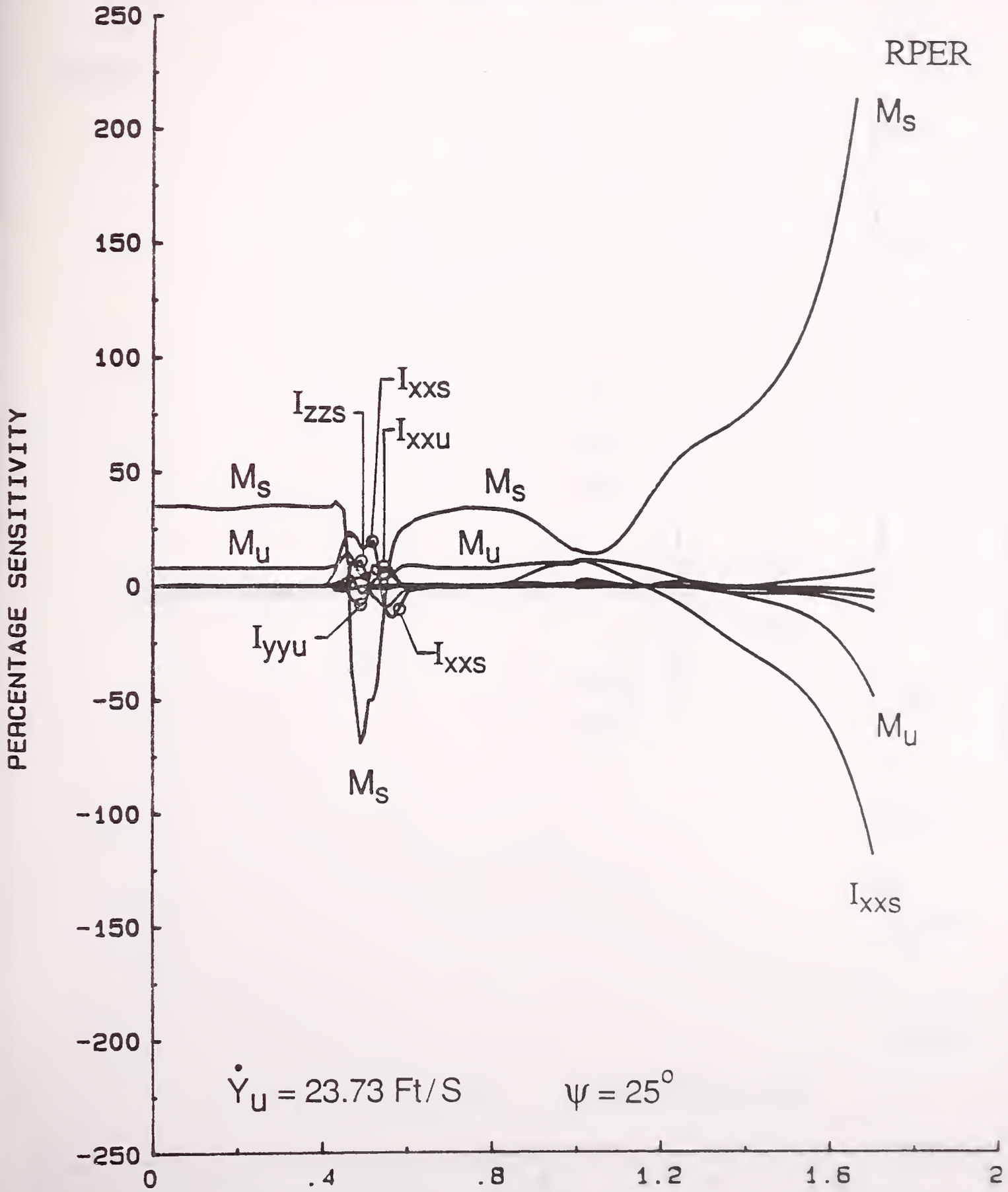
SENSITIVITY OF RP ENERGY RESERVE
MASS PARAMETER SET
RPER
M_s
I_{xxs}
I_{zzs}
I_{xxu}
M_s
M_s
M_u
M_u
I_{yyu}
I_{xxs}
M_s
M_u
I_{xxs}
$\dot{Y}_u = 23.73$ Ft/S
$\psi = 25^\circ$
PERCENTAGE SENSITIVITY
250
200
150
100
50
0
-50
-100
-150
-200
-250
0
.4
.8
1.2
1.6
2
TIME (Sec.)

Figure 61.

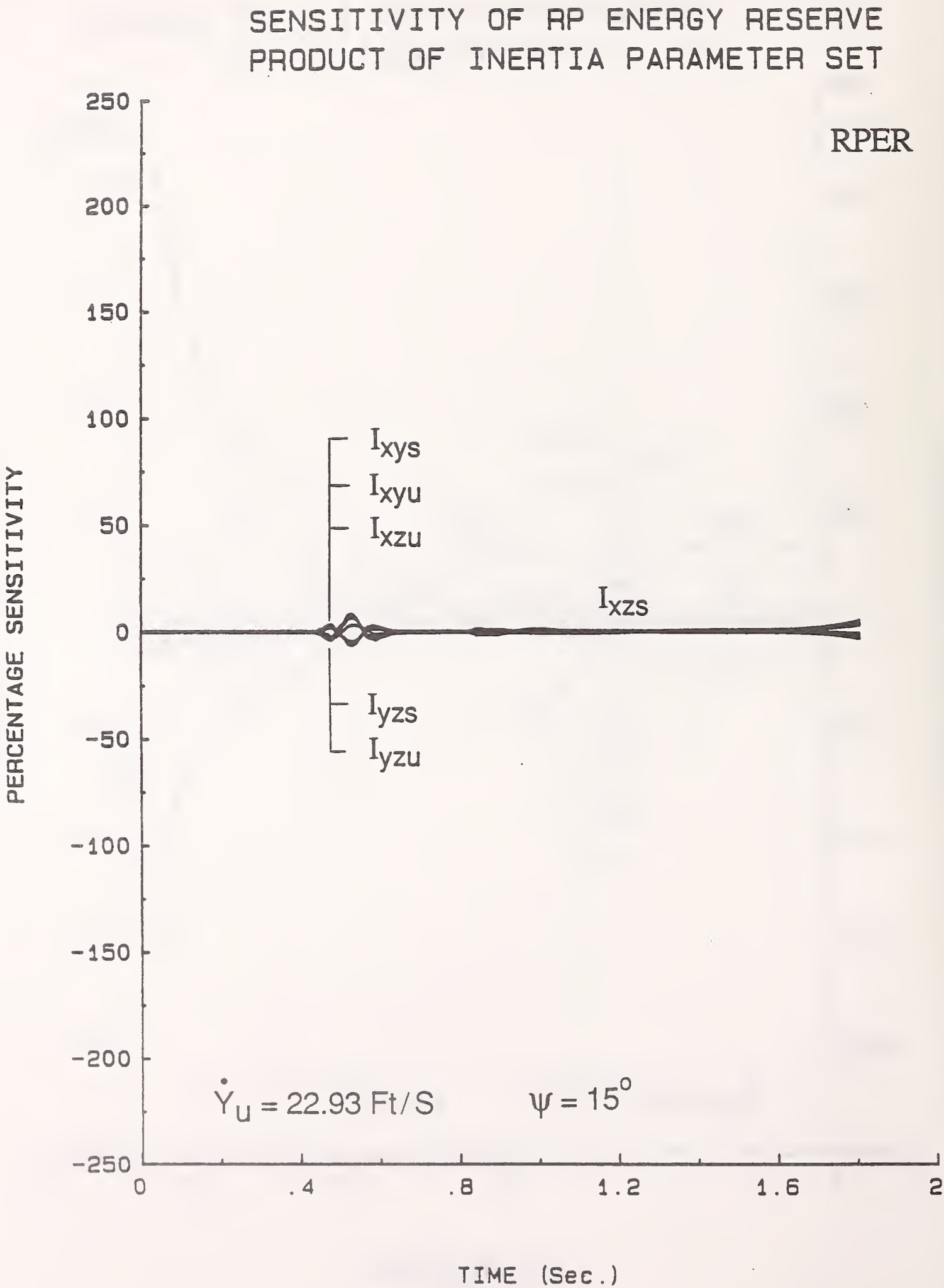
SENSITIVITY OF RP ENERGY RESERVE
PRODUCT OF INERTIA PARAMETER SET
RPER
250
200
150
100
50
0
-50
-100
-150
-200
-250
PERCENTAGE SENSITIVITY
I_{xys}
I_{xyu}
I_{xzu}
I_{xzs}
I_{yzs}
I_{yzu}
$\dot{Y}_u = 22.93$ Ft/S
$\psi = 15^\circ$
0
.4
.8
1.2
1.6
2
TIME (Sec.)

Figure 62.

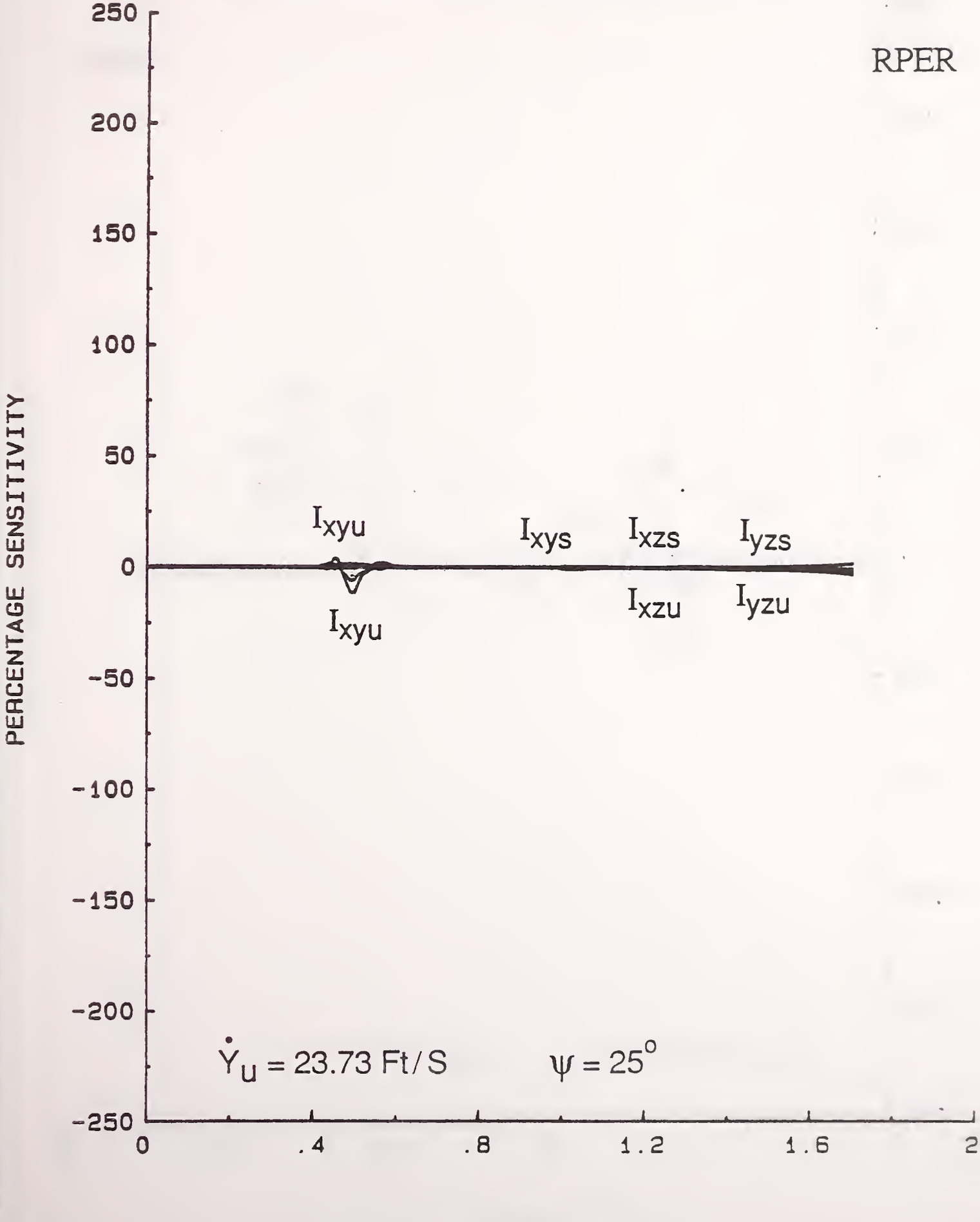
SENSITIVITY OF RP ENERGY RESERVE
PRODUCT OF INERTIA PARAMETER SET
RPER
250
200
150
100
50
0
-50
-100
-150
-200
-250
PERCENTAGE SENSITIVITY
I_{xyu}
I_{xys}
I_{xzs}
I_{yzs}
I_{xzu}
I_{yzu}
I_{xyu}
$\dot{Y}_u = 23.73$ Ft/S
$\psi = 25^\circ$
0
.4
.8
1.2
1.6
2
TIME (Sec.)

Figure 63.

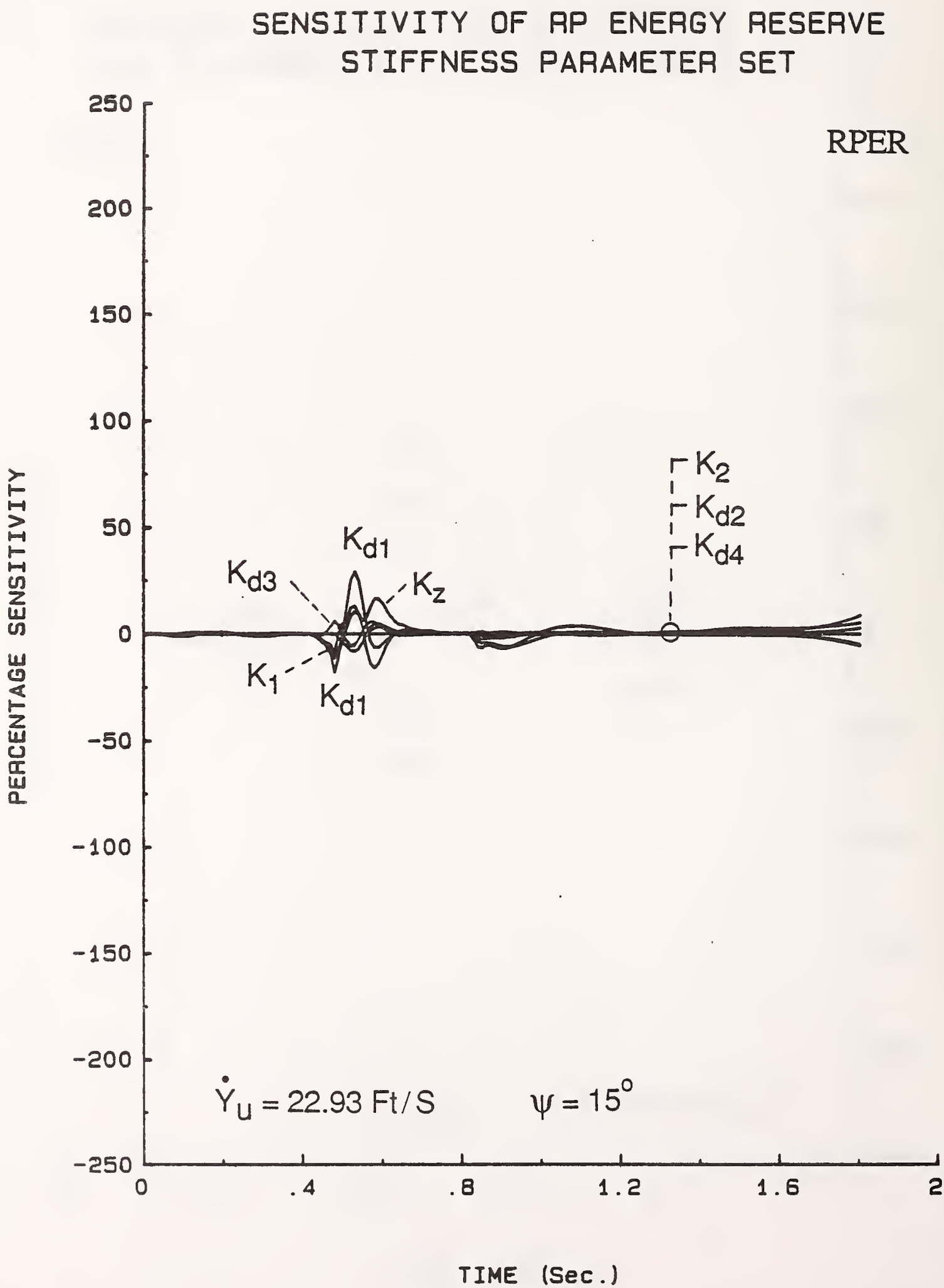
SENSITIVITY OF RP ENERGY RESERVE
STIFFNESS PARAMETER SET
RPER
250
200
150
100
50
0
-50
-100
-150
-200
-250
PERCENTAGE SENSITIVITY
K_2
K_{d2}
K_{d4}
K_{d1}
K_{d3}
K_z
K_1
K_{d1}
$\dot{Y}_u = 22.93$ Ft/S
$\psi = 15^\circ$
0
.4
.8
1.2
1.6
2
TIME (Sec.)

Figure 64.

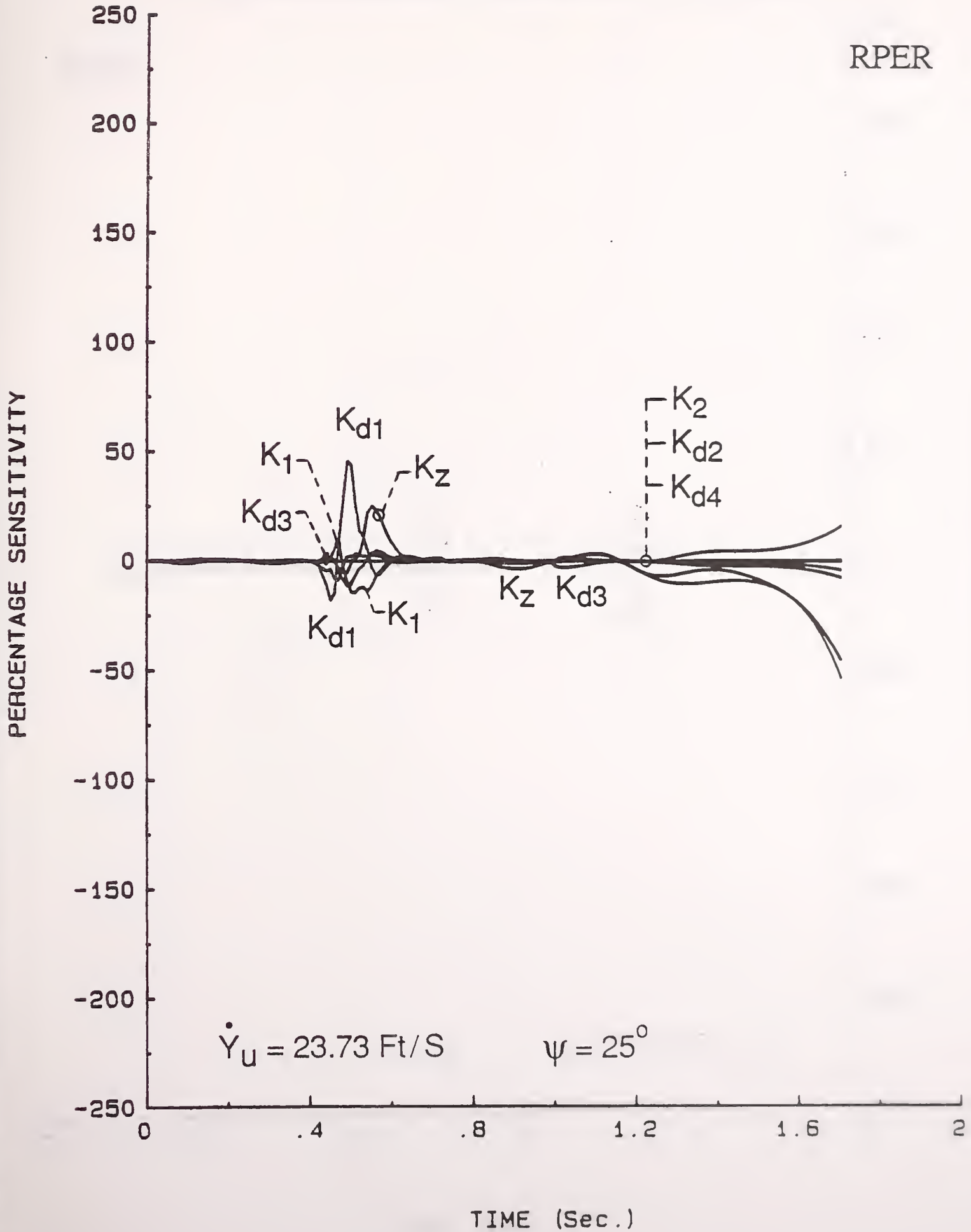
SENSITIVITY OF RP ENERGY RESERVE
STIFFNESS PARAMETER SET
RPER
250
200
150
100
50
0
-50
-100
-150
-200
-250
PERCENTAGE SENSITIVITY
K_{d1}
K_1
K_z
K_{d3}
K_2
K_{d2}
K_{d4}
K_z K_{d3}
K_{d1}
K_1
$\dot{Y}_u = 23.73$ Ft/S
$\psi = 25^o$
0
.4
.8
1.2
1.6
2
TIME (Sec.)

Figure 65.

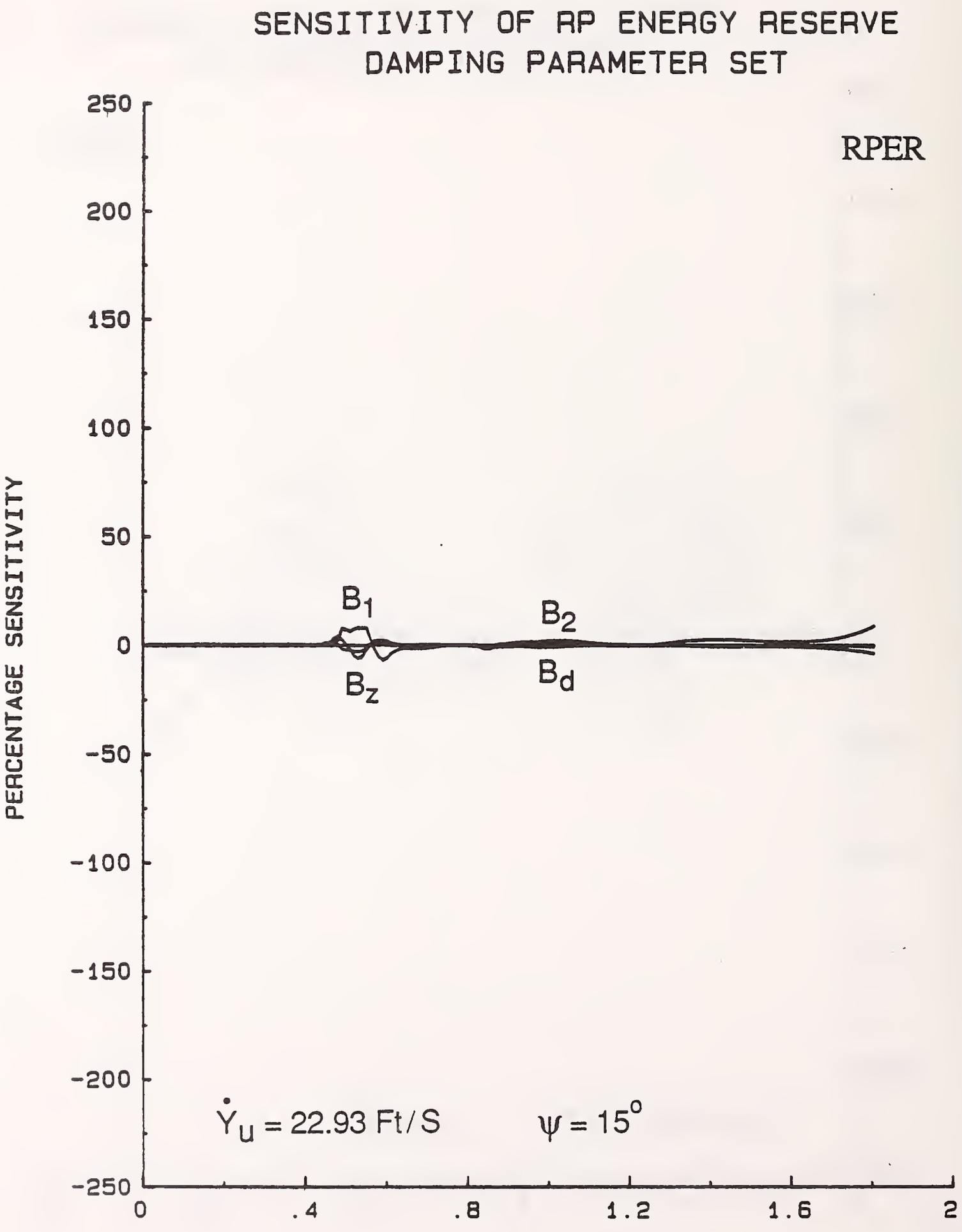
SENSITIVITY OF RP ENERGY RESERVE
DAMPING PARAMETER SET
RPER
250
200
150
100
50
0
-50
-100
-150
-200
-250
PERCENTAGE SENSITIVITY
B1
B2
Bz
Bd
Ẏu = 22.93 Ft/S
ψ = 15°
0
.4
.8
1.2
1.6
2
TIME (Sec.)

Figure 66.

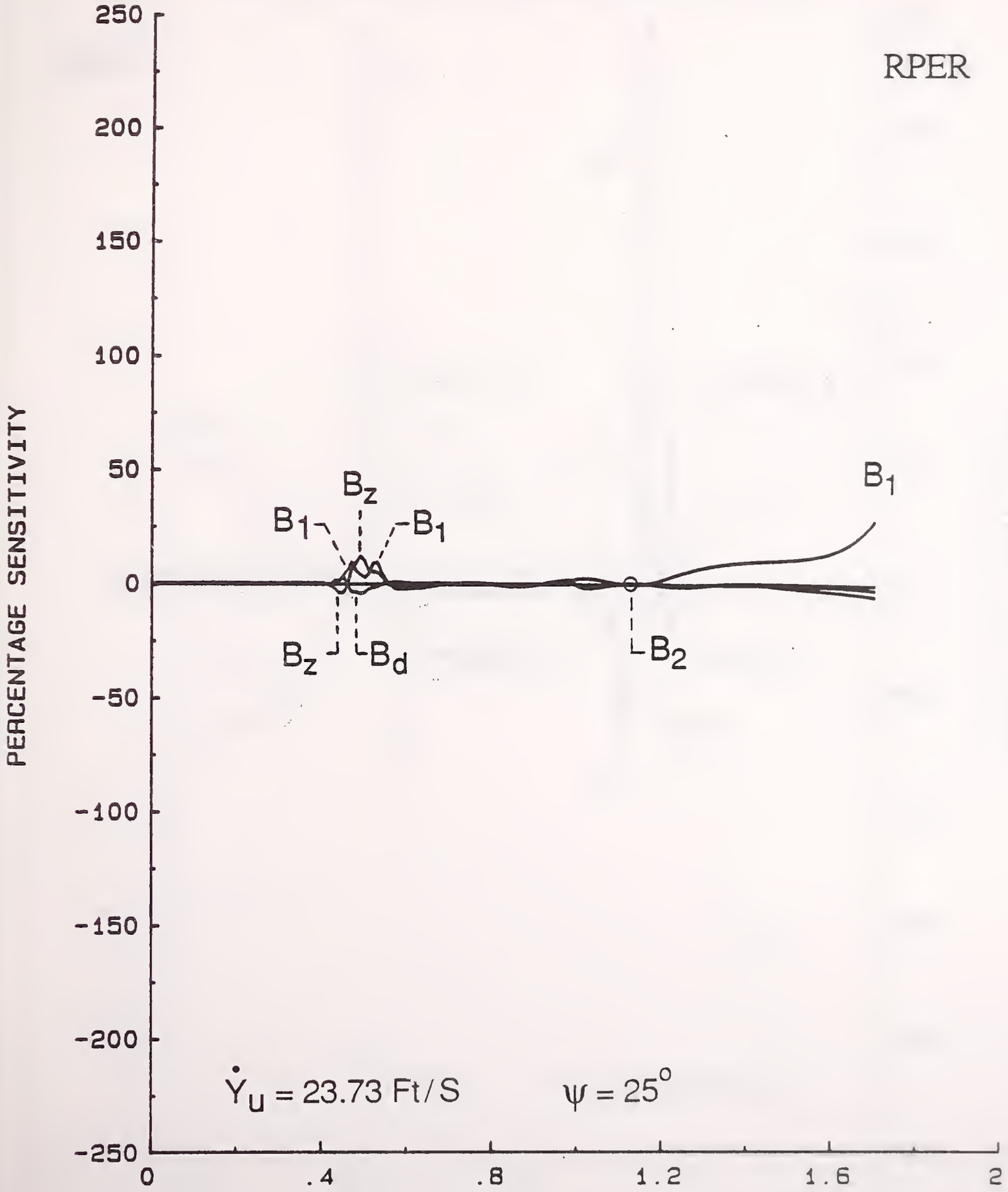
SENSITIVITY OF RP ENERGY RESERVE
DAMPING PARAMETER SET
RPER
250
200
150
100
50
0
-50
-100
-150
-200
-250
PERCENTAGE SENSITIVITY
B_z
B_1
B_1
B_1
B_z
B_d
B_2
$\dot{Y}_u = 23.73$ Ft/S
$\psi = 25^\circ$
0
.4
.8
1.2
1.6
2
TIME (Sec.)

Figure 67.

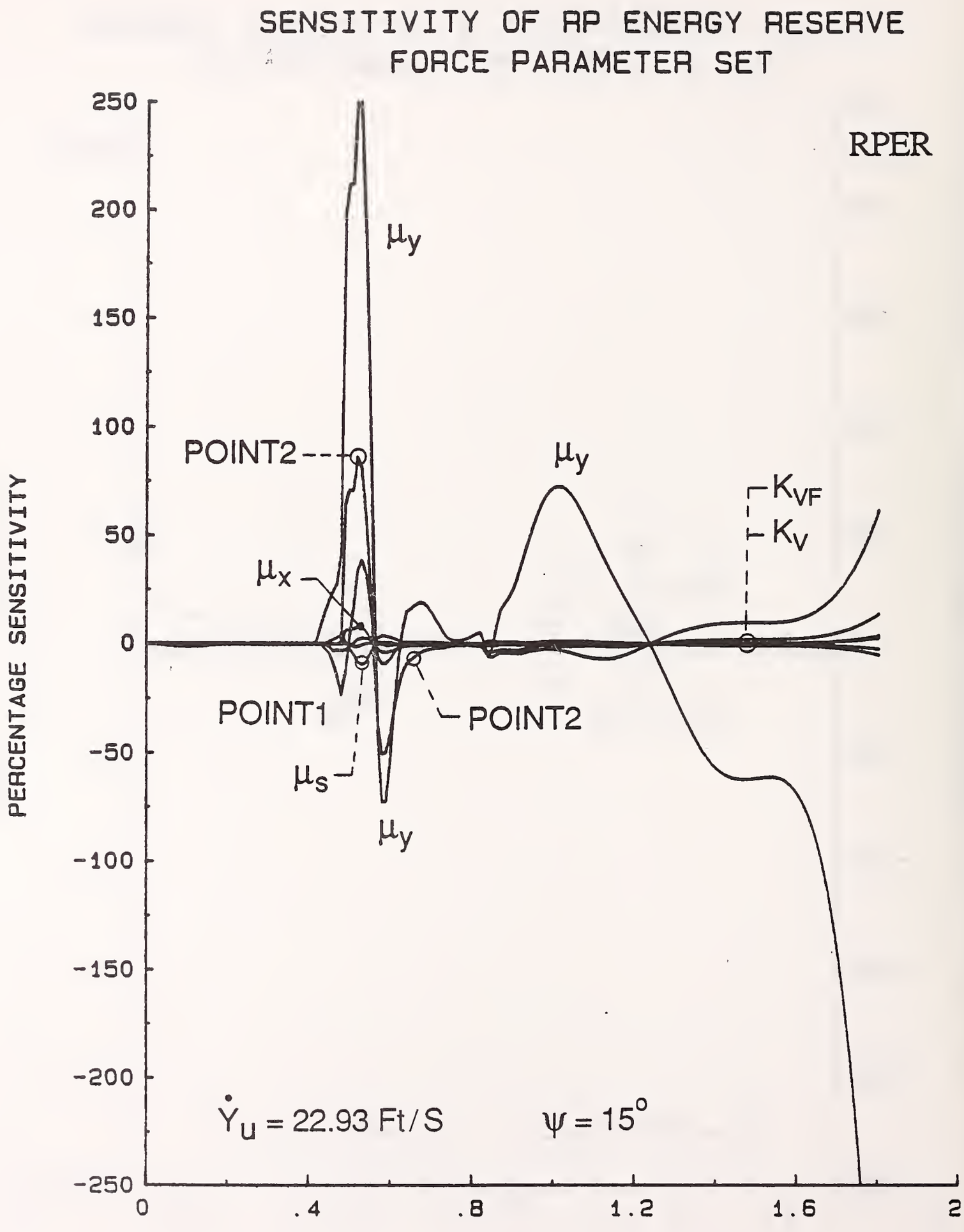
SENSITIVITY OF RP ENERGY RESERVE
FORCE PARAMETER SET
RPER
250
200
150
100
50
0
-50
-100
-150
-200
-250
PERCENTAGE SENSITIVITY
μ_y
POINT2
μ_y
K_{VF}
K_V
μ_x
POINT1
POINT2
μ_s
μ_y
$\dot{Y}_u = 22.93$ Ft/S
$\psi = 15^\circ$
0
.4
.8
1.2
1.6
2
TIME (Sec.)

Figure 68.

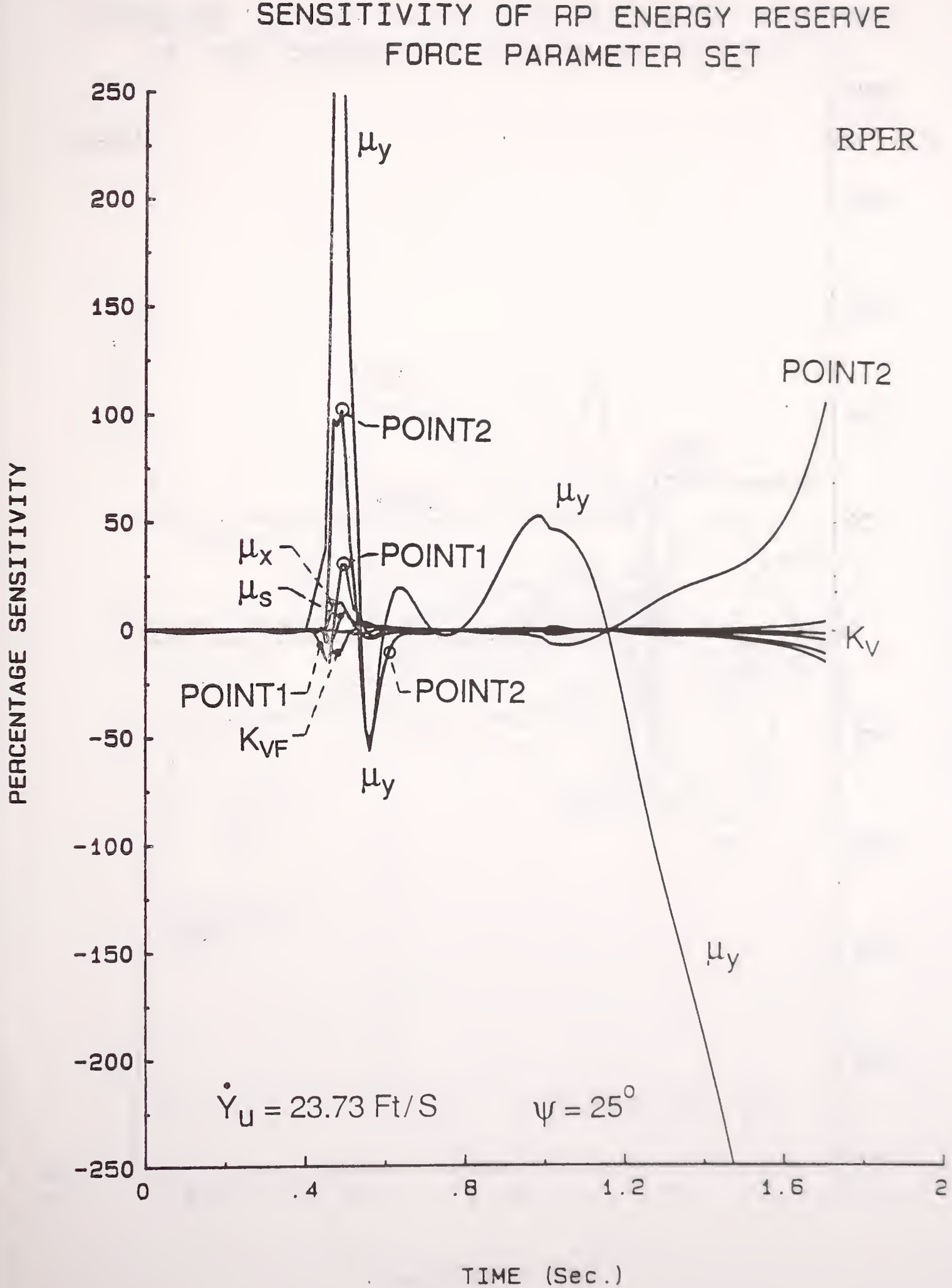
SENSITIVITY OF RP ENERGY RESERVE
FORCE PARAMETER SET
RPER
PERCENTAGE SENSITIVITY
TIME (Sec.)
250
200
150
100
50
0
-50
-100
-150
-200
-250
0
.4
.8
1.2
1.6
2
μ_y
POINT2
μ_y
POINT2
μ_x
μ_s
POINT1
K_V
POINT1
POINT2
K_{VF}
μ_y
μ_y
$\dot{Y}_u = 23.73$ Ft/S
$\psi = 25^\circ$

Figure 69.

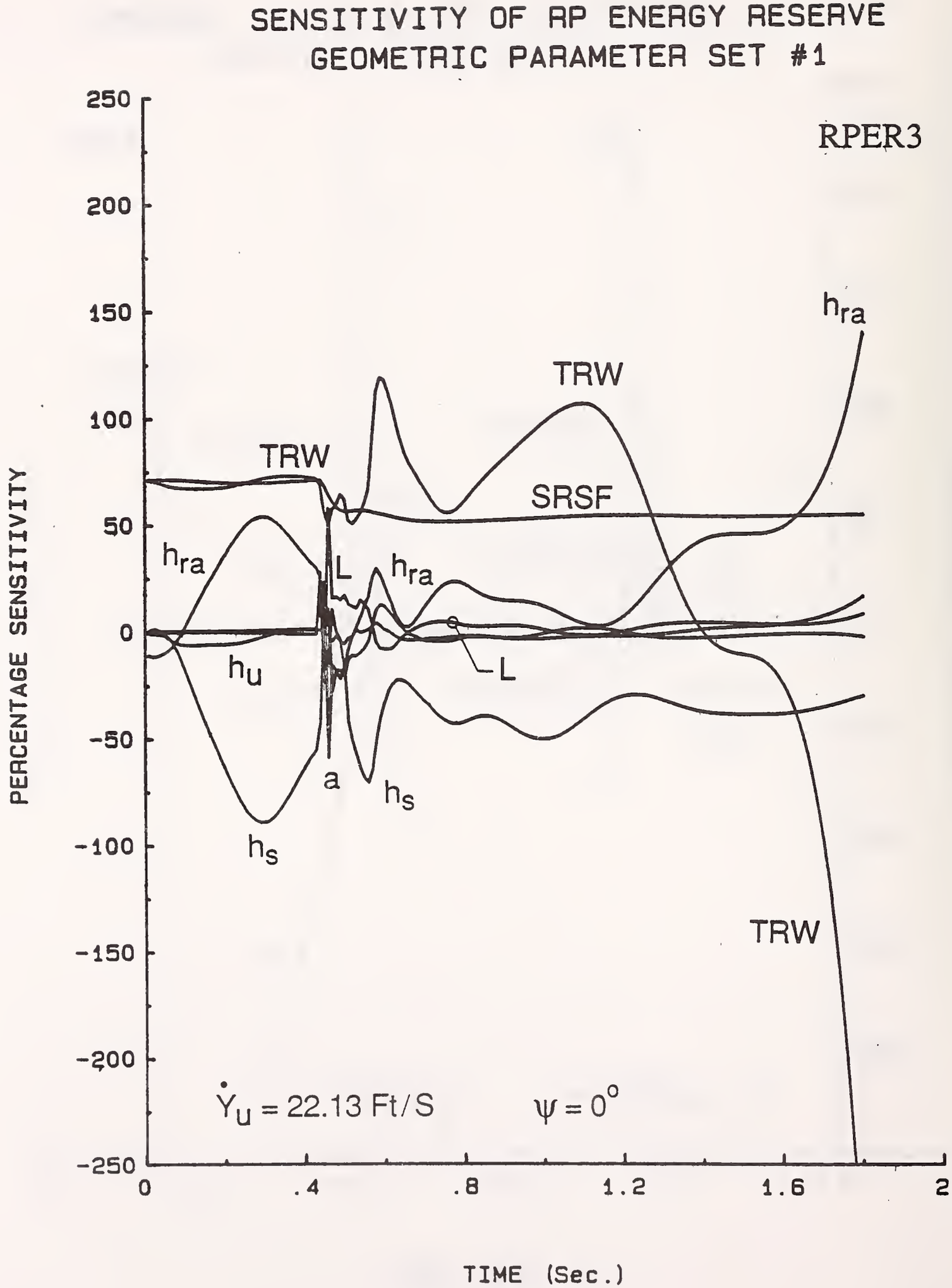
SENSITIVITY OF RP ENERGY RESERVE
GEOMETRIC PARAMETER SET #1
RPER3
PERCENTAGE SENSITIVITY
TIME (Sec.)
250
200
150
100
50
0
-50
-100
-150
-200
-250
0
.4
.8
1.2
1.6
2
TRW
TRW
TRW
SRSF
h_{ra}
h_{ra}
h_{ra}
L
L
h_u
a
h_s
h_s
$\dot{Y}_u = 22.13$ Ft/S
$\psi = 0^\circ$

Figure 70.

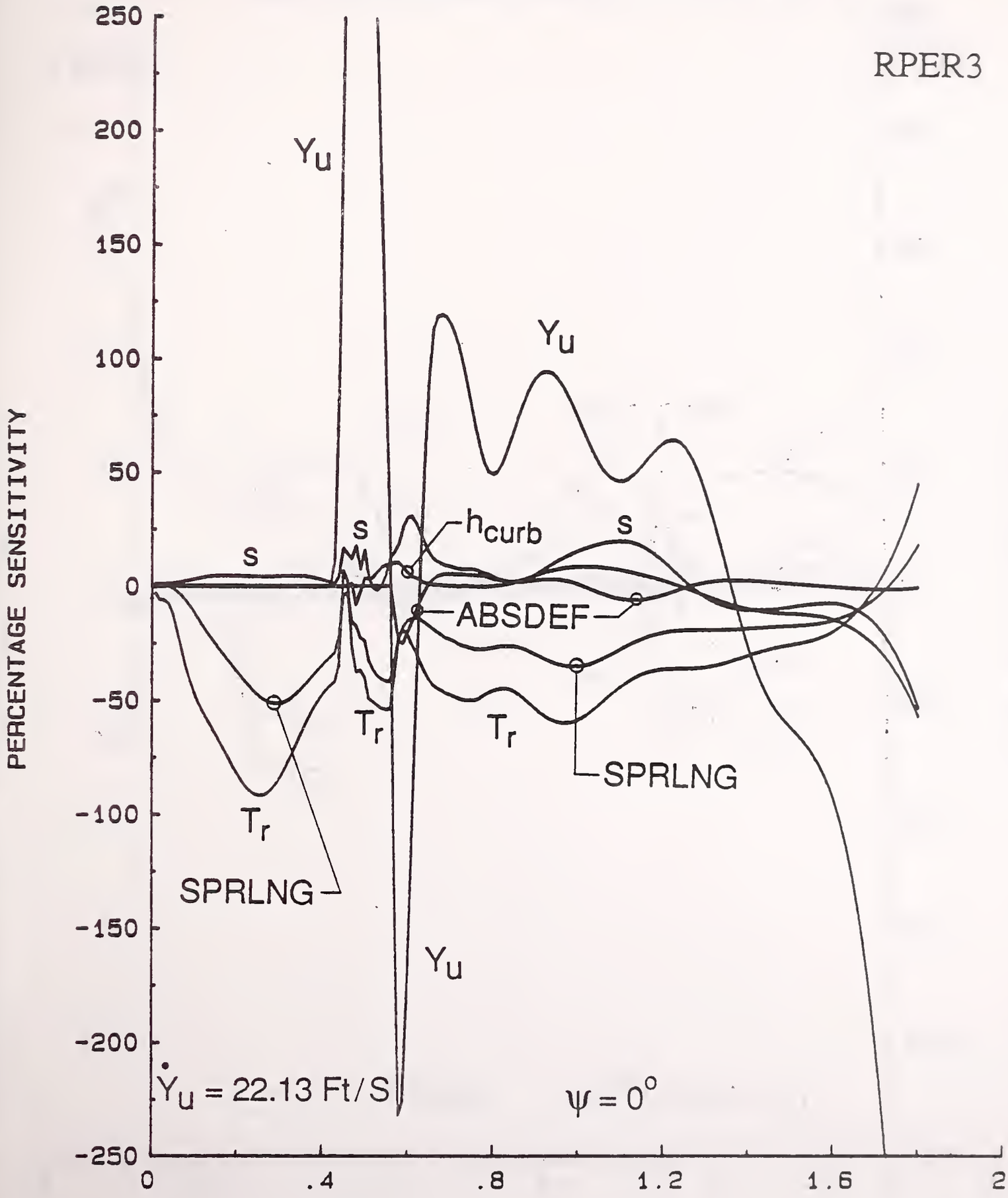
SENSITIVITY OF RP ENERGY RESERVE
GEOMETRIC PARAMETER SET #2
RPER3
PERCENTAGE SENSITIVITY
TIME (Sec.)
250
200
150
100
50
0
-50
-100
-150
-200
-250
0
.4
.8
1.2
1.6
2
Yu
Yu
Yu
Yu
s
s
s
hcurb
ABSDEF
Tr
Tr
Tr
SPRLNG
SPRLNG
Yu = 22.13 Ft/S
ψ = 0°

Figure 71.

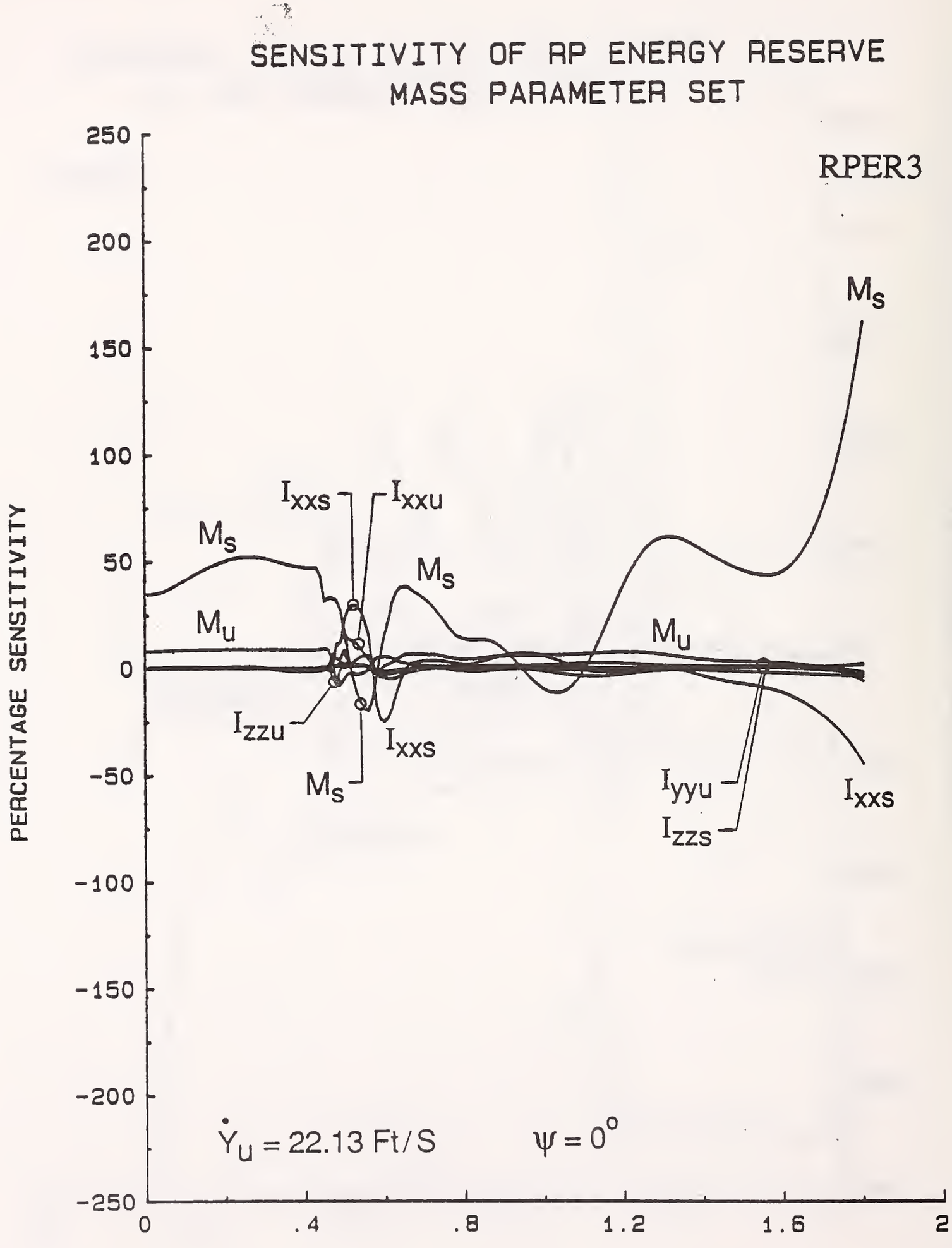
SENSITIVITY OF RP ENERGY RESERVE
MASS PARAMETER SET
RPER3
PERCENTAGE SENSITIVITY
TIME (Sec.)
250
200
150
100
50
0
-50
-100
-150
-200
-250
0
.4
.8
1.2
1.6
2
M_s
I_{xxs}
I_{xxu}
M_s
M_s
M_u
M_u
I_{zzu}
I_{xxs}
M_s
I_{yyu}
I_{zzs}
I_{xxs}
$\dot{Y}_u = 22.13$ Ft/S
$\psi = 0^\circ$

Figure 72.

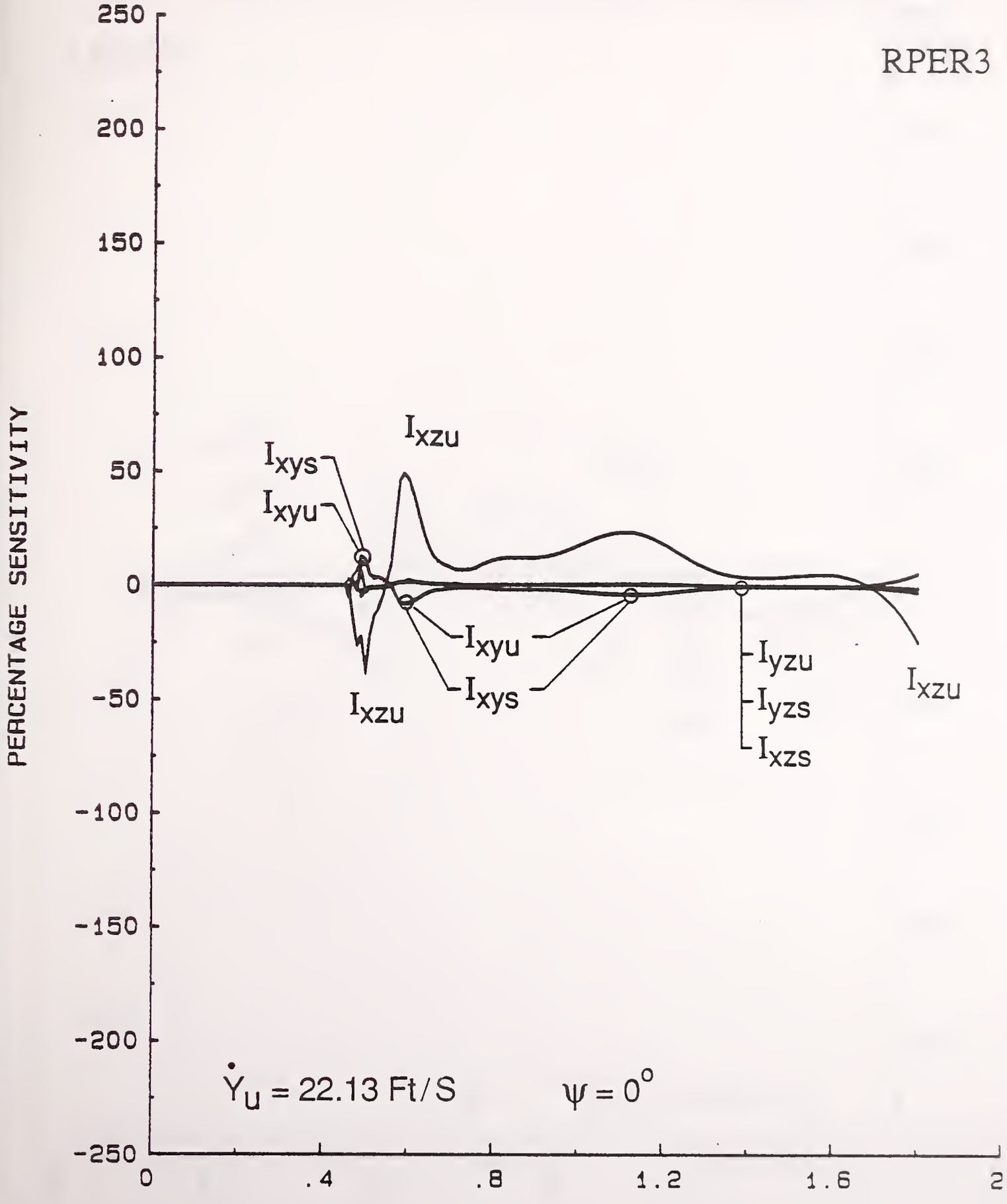
SENSITIVITY OF RP ENERGY RESERVE
PRODUCT OF INERTIA PARAMETER SET
RPER3
250
200
150
100
50
0
-50
-100
-150
-200
-250
PERCENTAGE SENSITIVITY
I_{xzu}
I_{xys}
I_{xyu}
I_{xyu}
I_{xzu}
I_{xys}
I_{yzu}
I_{yzs}
I_{xzs}
I_{xzu}
$\dot{Y}_u = 22.13$ Ft/S
$\psi = 0^\circ$
0
.4
.8
1.2
1.6
2
TIME (Sec.)

Figure 73.

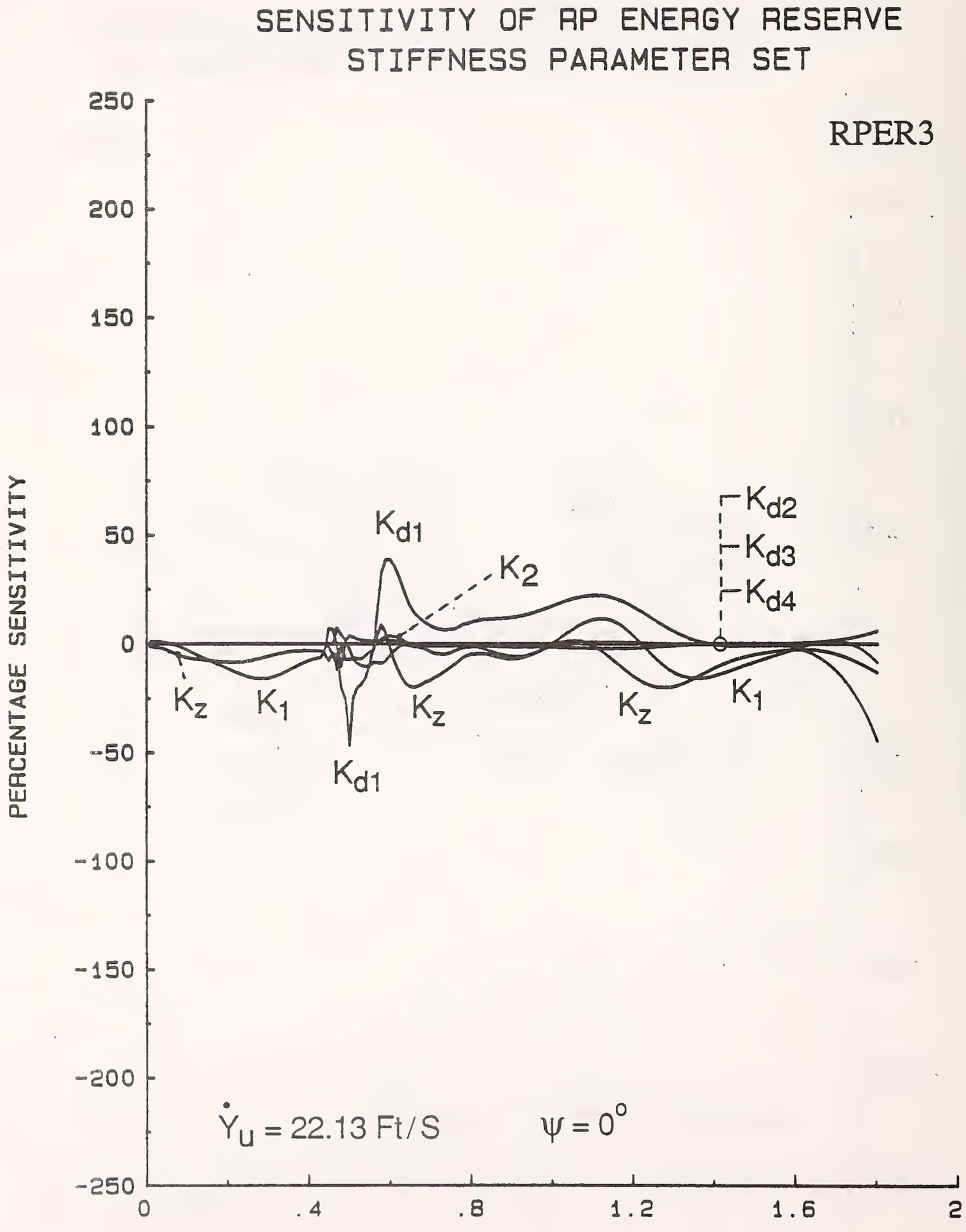
SENSITIVITY OF RP ENERGY RESERVE
STIFFNESS PARAMETER SET
RPER3
PERCENTAGE SENSITIVITY
250
200
150
100
50
0
-50
-100
-150
-200
-250
0
.4
.8
1.2
1.6
2
TIME (Sec.)
K_{d1}
K_2
K_{d2}
K_{d3}
K_{d4}
K_z
K_1
K_z
K_{d1}
K_z
K_1
$\dot{Y}_u = 22.13$ Ft/S
$\psi = 0^\circ$

Figure 74.

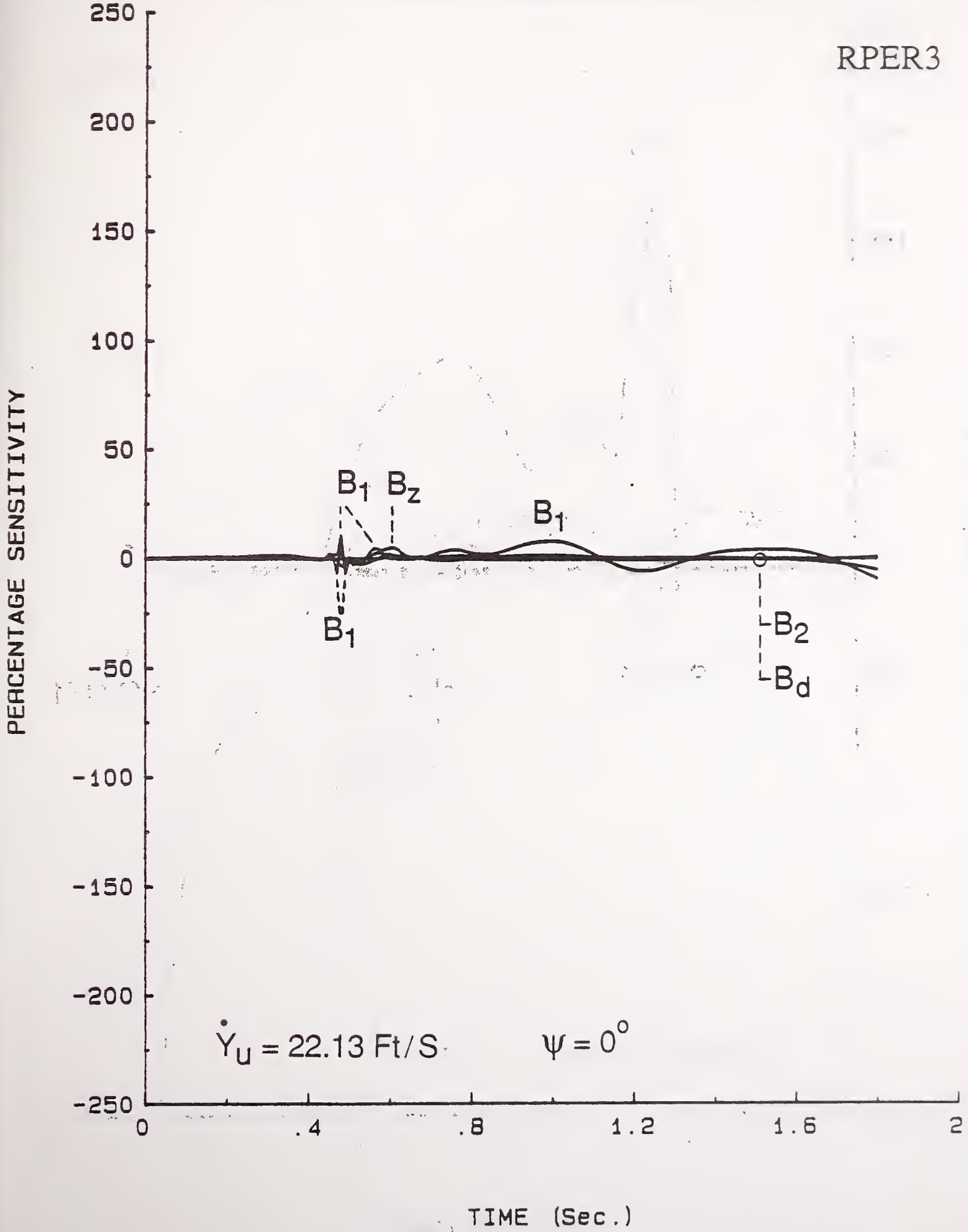
SENSITIVITY OF RP ENERGY RESERVE
DAMPING PARAMETER SET
RPER3
PERCENTAGE SENSITIVITY
250
200
150
100
50
0
-50
-100
-150
-200
-250
B1
Bz
B1
B1
B2
Bd
Ẏu = 22.13 Ft/S
ψ = 0°
0
.4
.8
1.2
1.6
2
TIME (Sec.)

Figure 75.

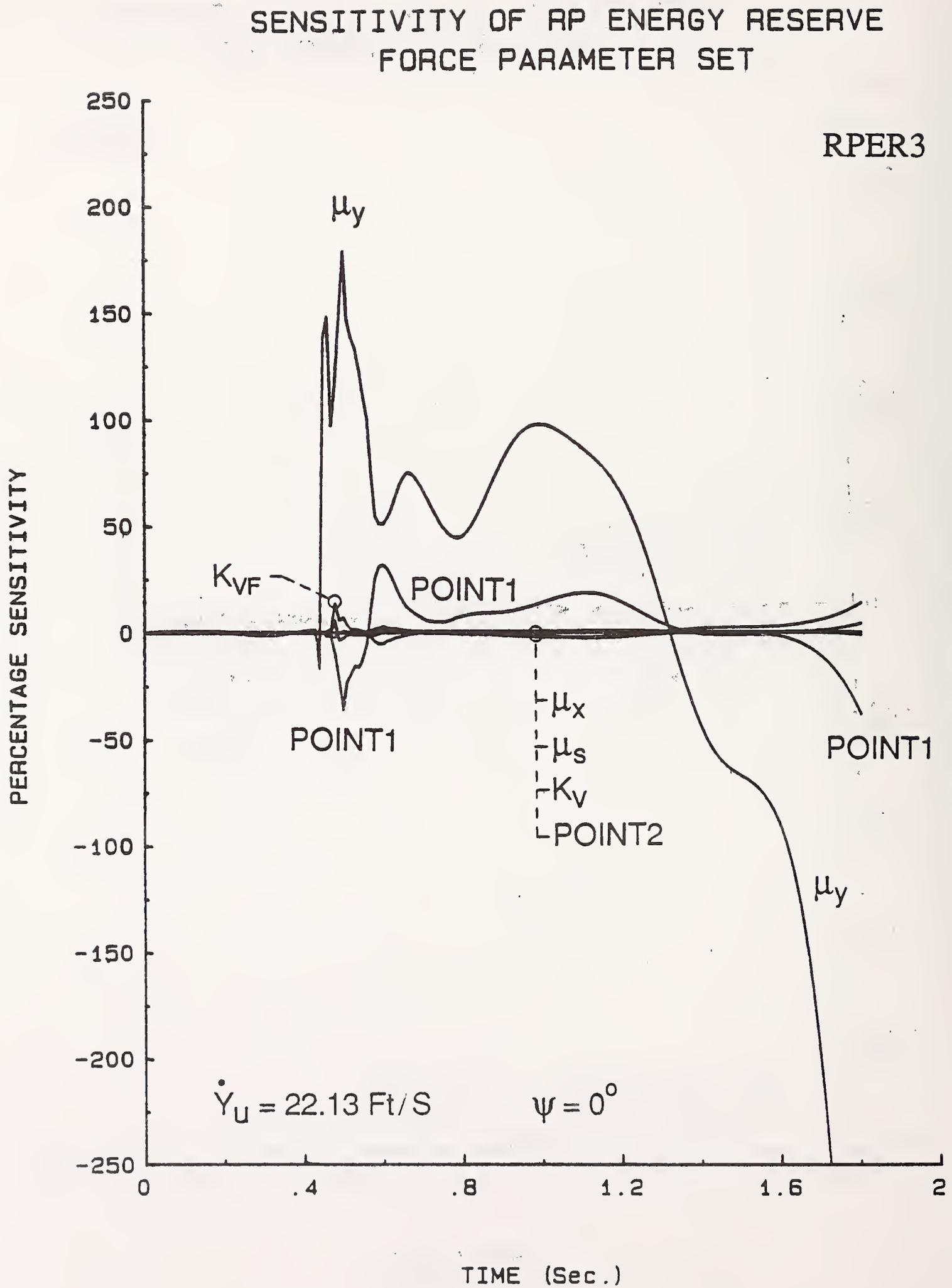
SENSITIVITY OF RP ENERGY RESERVE
FORCE PARAMETER SET
RPER3
PERCENTAGE SENSITIVITY
250
200
150
100
50
0
-50
-100
-150
-200
-250
μ_y
K_{VF}
POINT1
POINT1
POINT1
μ_x
μ_s
K_V
POINT2
μ_y
$\dot{Y}_u = 22.13$ Ft/S
$\psi = 0^\circ$
0
.4
.8
1.2
1.6
2
TIME (Sec.)

Figure 76.

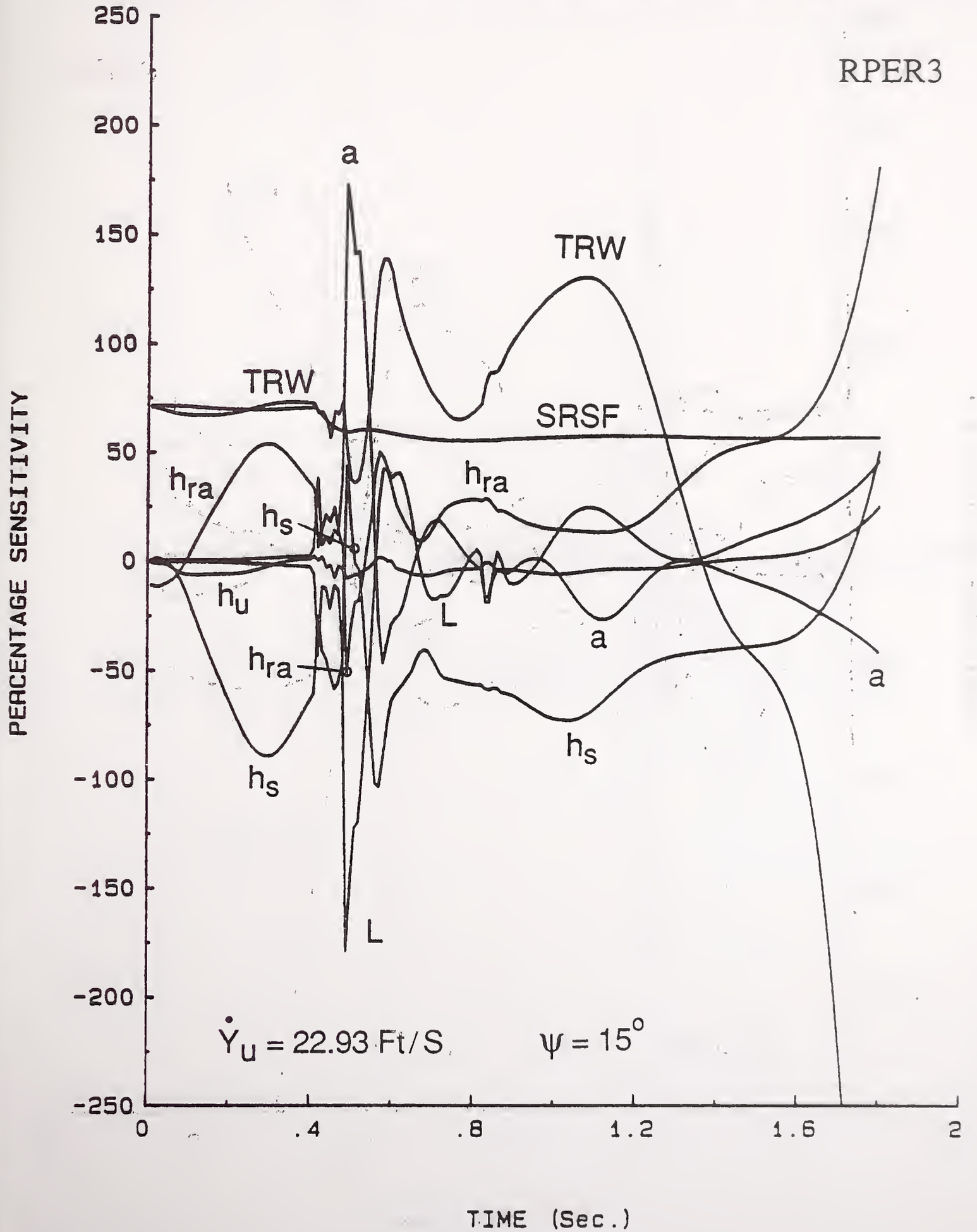
SENSITIVITY OF RP ENERGY RESERVE
GEOMETRIC PARAMETER SET #1
RPER3
PERCENTAGE SENSITIVITY
TIME (Sec.)
250
200
150
100
50
0
-50
-100
-150
-200
-250
0
.4
.8
1.2
1.6
2
a
TRW
TRW
SRSF
h_{ra}
h_s
h_u
L
h_{ra}
a
h_{ra}
h_s
h_s
a
L
$\dot{Y}_u = 22.93$ Ft/S
$\psi = 15^\circ$

Figure 77.

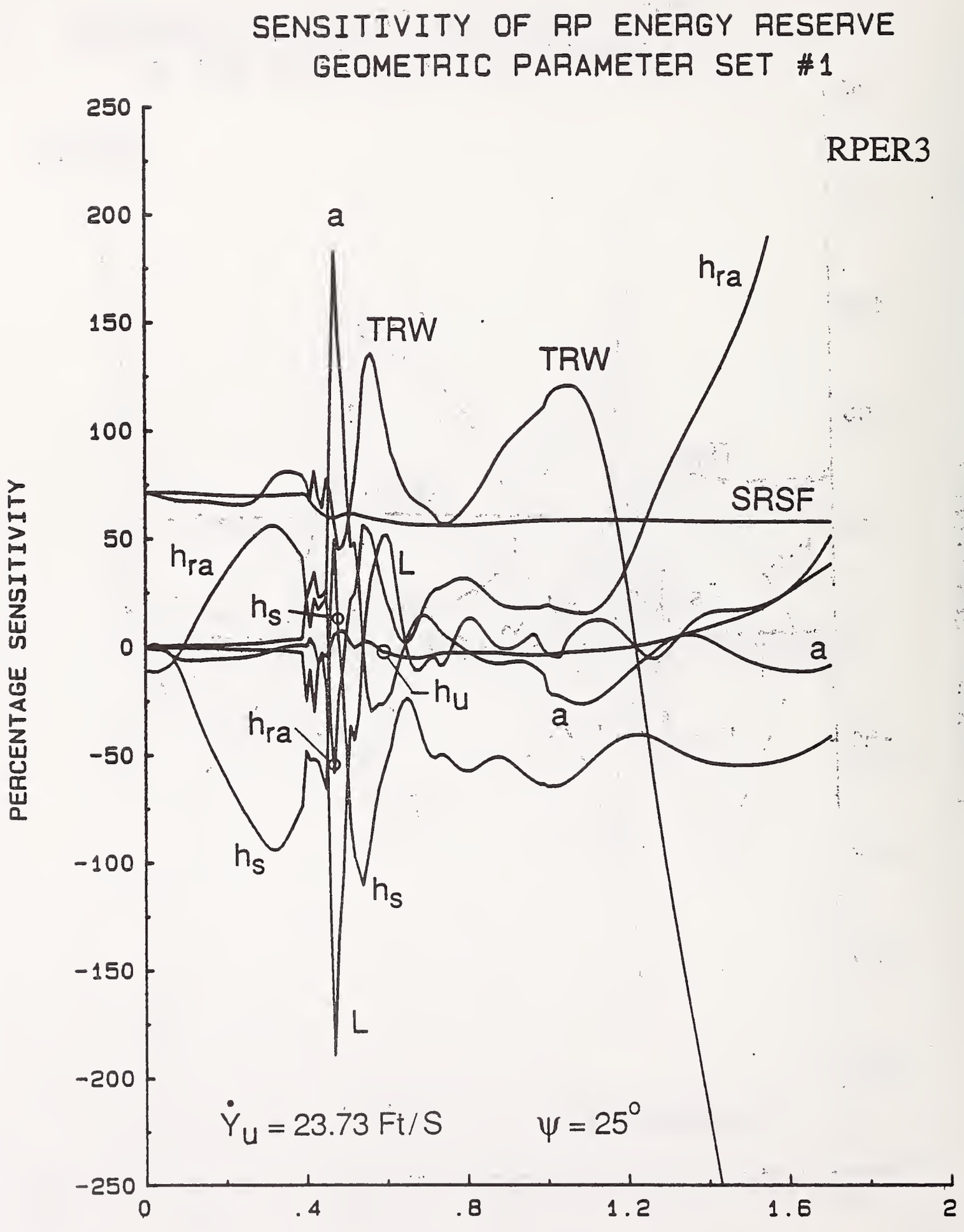
SENSITIVITY OF RP ENERGY RESERVE
GEOMETRIC PARAMETER SET #1
RPER3
PERCENTAGE SENSITIVITY
TIME (Sec.)
250
200
150
100
50
0
-50
-100
-150
-200
-250
0
.4
.8
1.2
1.6
2
a
TRW
TRW
h_{ra}
SRSF
h_{ra}
L
h_s
a
h_u
a
h_{ra}
h_s
h_s
L
$\dot{Y}_u$ = 23.73 Ft/S
ψ = 25°

Figure 78.

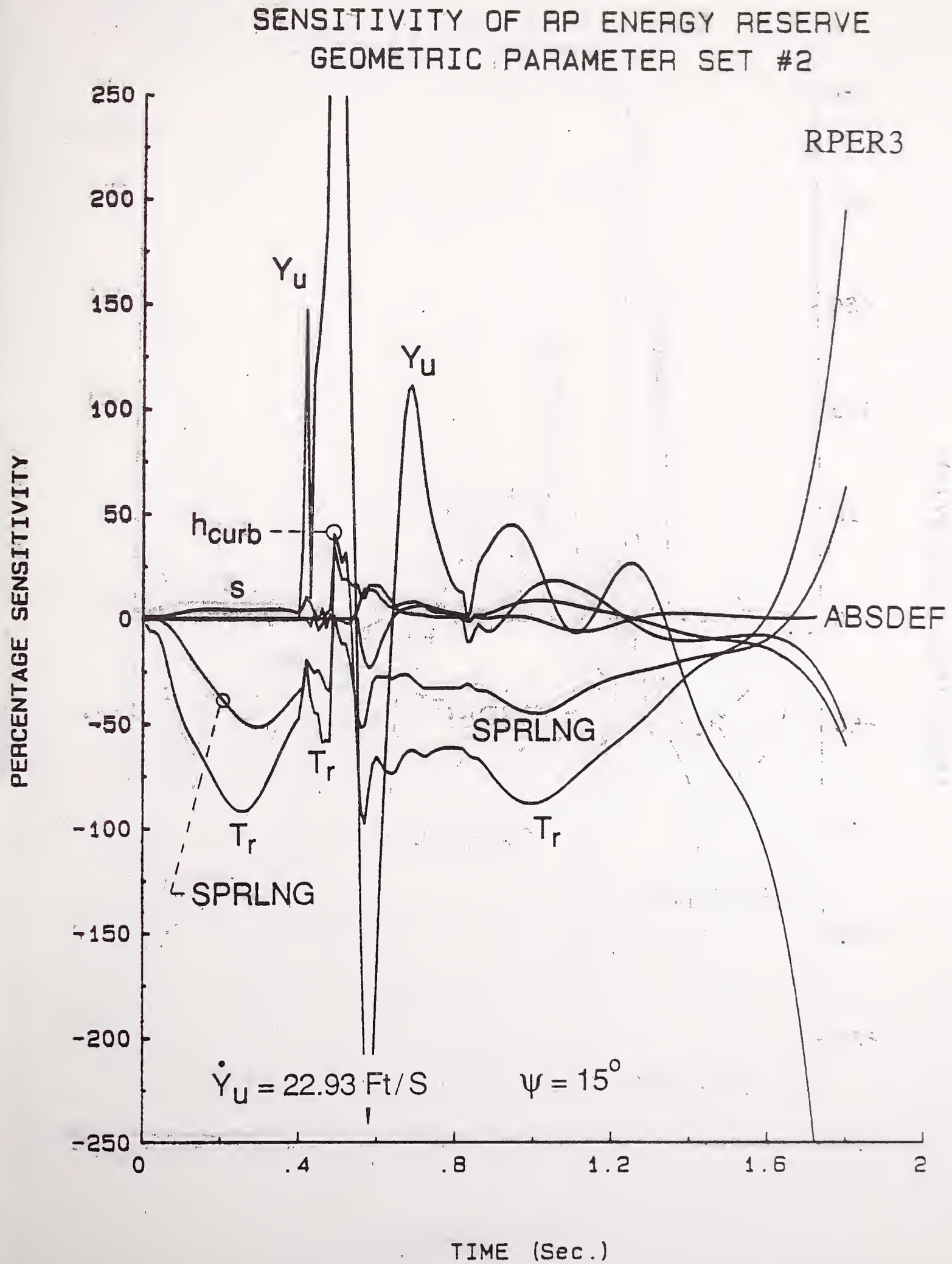
SENSITIVITY OF RP ENERGY RESERVE
GEOMETRIC PARAMETER SET #2
RPER3
PERCENTAGE SENSITIVITY
TIME (Sec.)
250
200
150
100
50
0
-50
-100
-150
-200
-250
0
.4
.8
1.2
1.6
2
Y_u
Y_u
h_{curb}
s
ABSDEF
SPRLNG
T_r
T_r
T_r
SPRLNG
$\dot{Y}_u = 22.93$ Ft/S
$\psi = 15^o$

Figure 79.

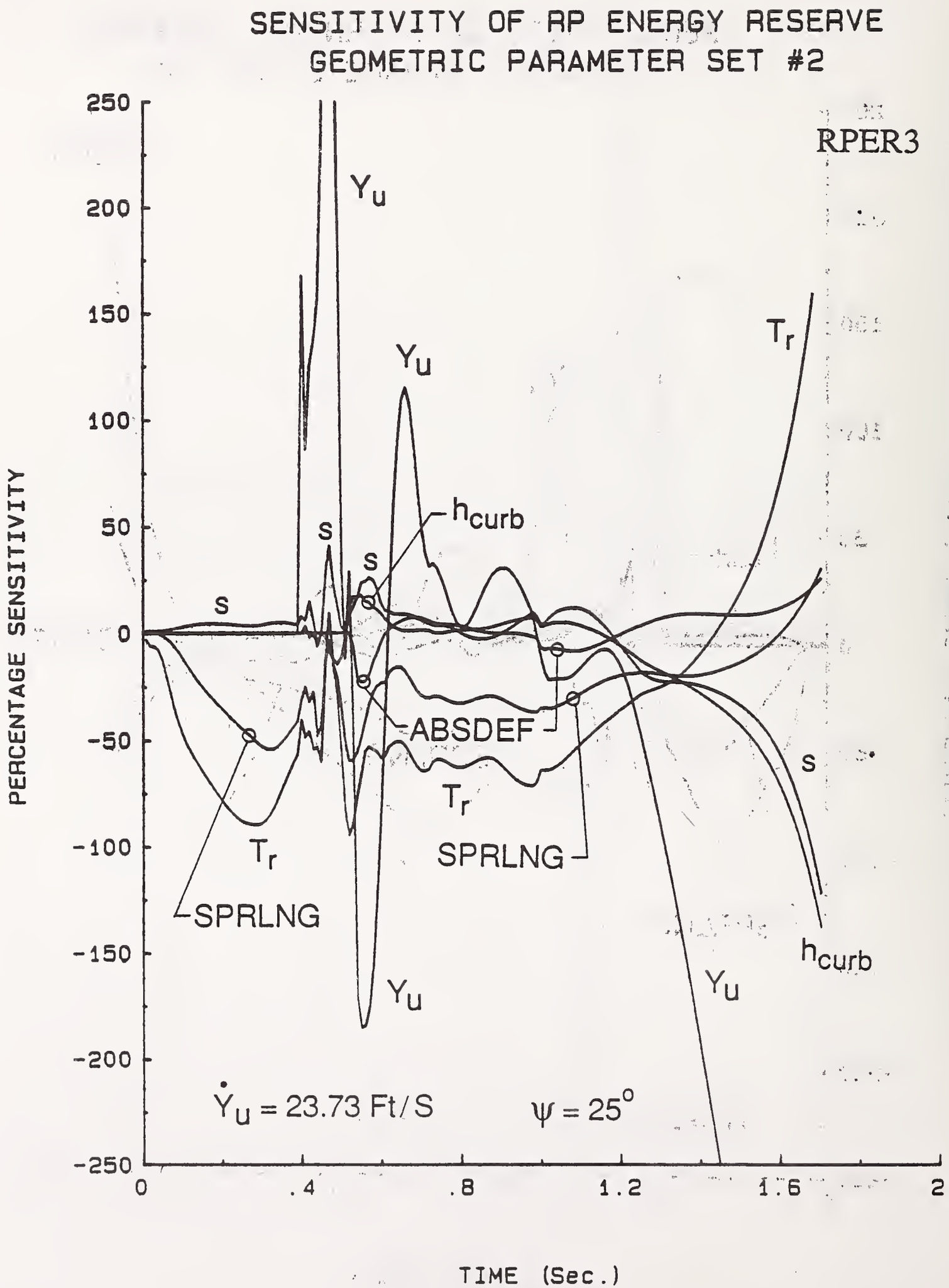
SENSITIVITY OF RP ENERGY RESERVE
GEOMETRIC PARAMETER SET #2
RPER3
PERCENTAGE SENSITIVITY
TIME (Sec.)
250
200
150
100
50
0
-50
-100
-150
-200
-250
0
.4
.8
1.2
1.6
2
Yu
Tr
hcurb
ABSDEF
SPRLNG
s
Ẏu = 23.73 Ft/S
ψ = 25°

Figure 80.

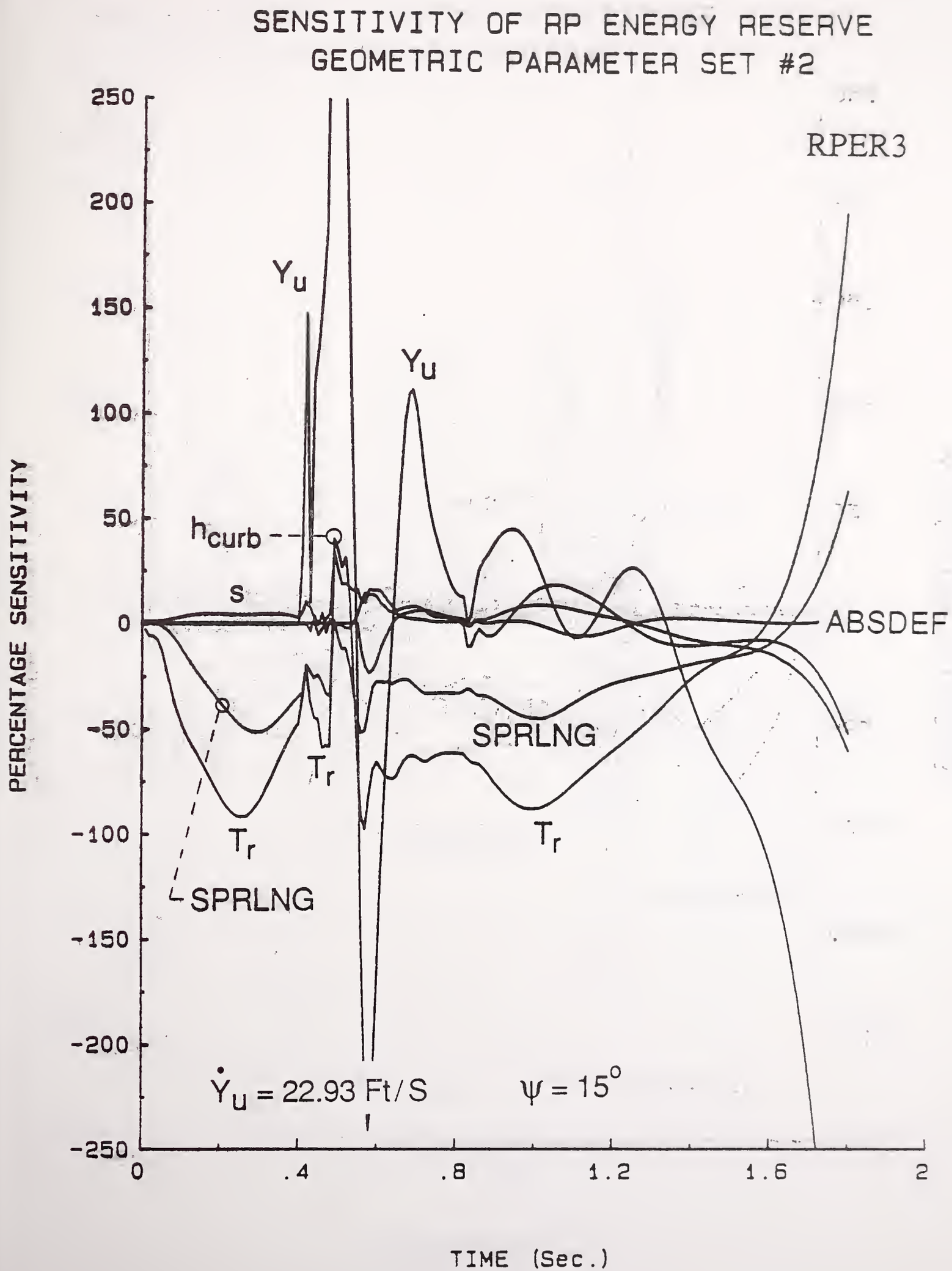
SENSITIVITY OF RP ENERGY RESERVE
GEOMETRIC PARAMETER SET #2
RPER3
PERCENTAGE SENSITIVITY
TIME (Sec.)
250
200
150
100
50
0
-50
-100
-150
-200
-250
0
.4
.8
1.2
1.6
2
Y_u
Y_u
h_{curb}
s
ABSDEF
SPRLNG
T_r
T_r
T_r
SPRLNG
$\dot{Y}_u = 22.93$ Ft/S
$\psi = 15^\circ$

Figure 79.

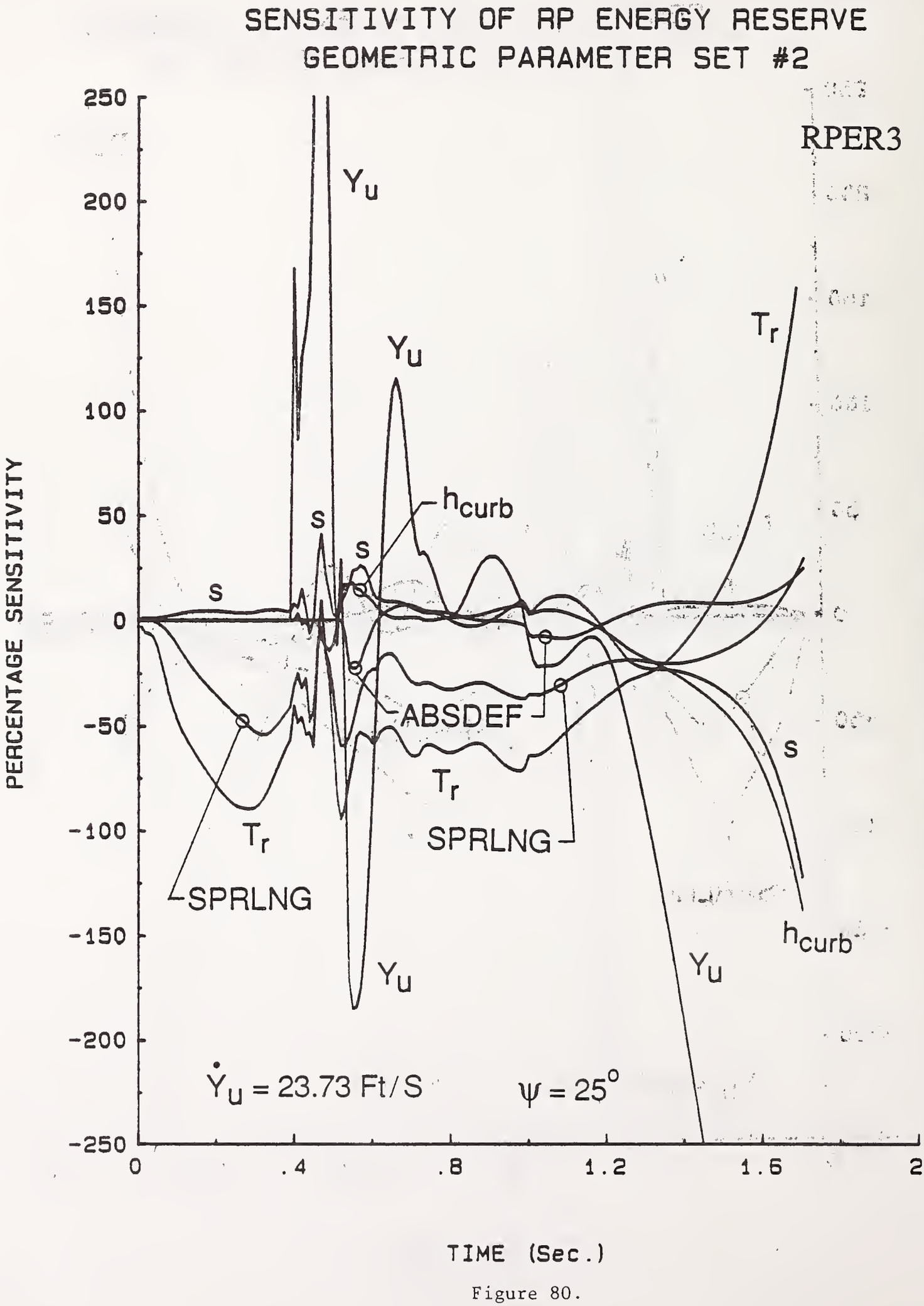
SENSITIVITY OF RP ENERGY RESERVE
GEOMETRIC PARAMETER SET #2
RPER3
PERCENTAGE SENSITIVITY
TIME (Sec.)
250
200
150
100
50
0
-50
-100
-150
-200
-250
0
.4
.8
1.2
1.6
2
Y_u
T_r
h_{curb}
s
ABSDEF
SPRLNG
$\dot{Y}_u = 23.73$ Ft/S
$\psi = 25^\circ$

Figure 80.

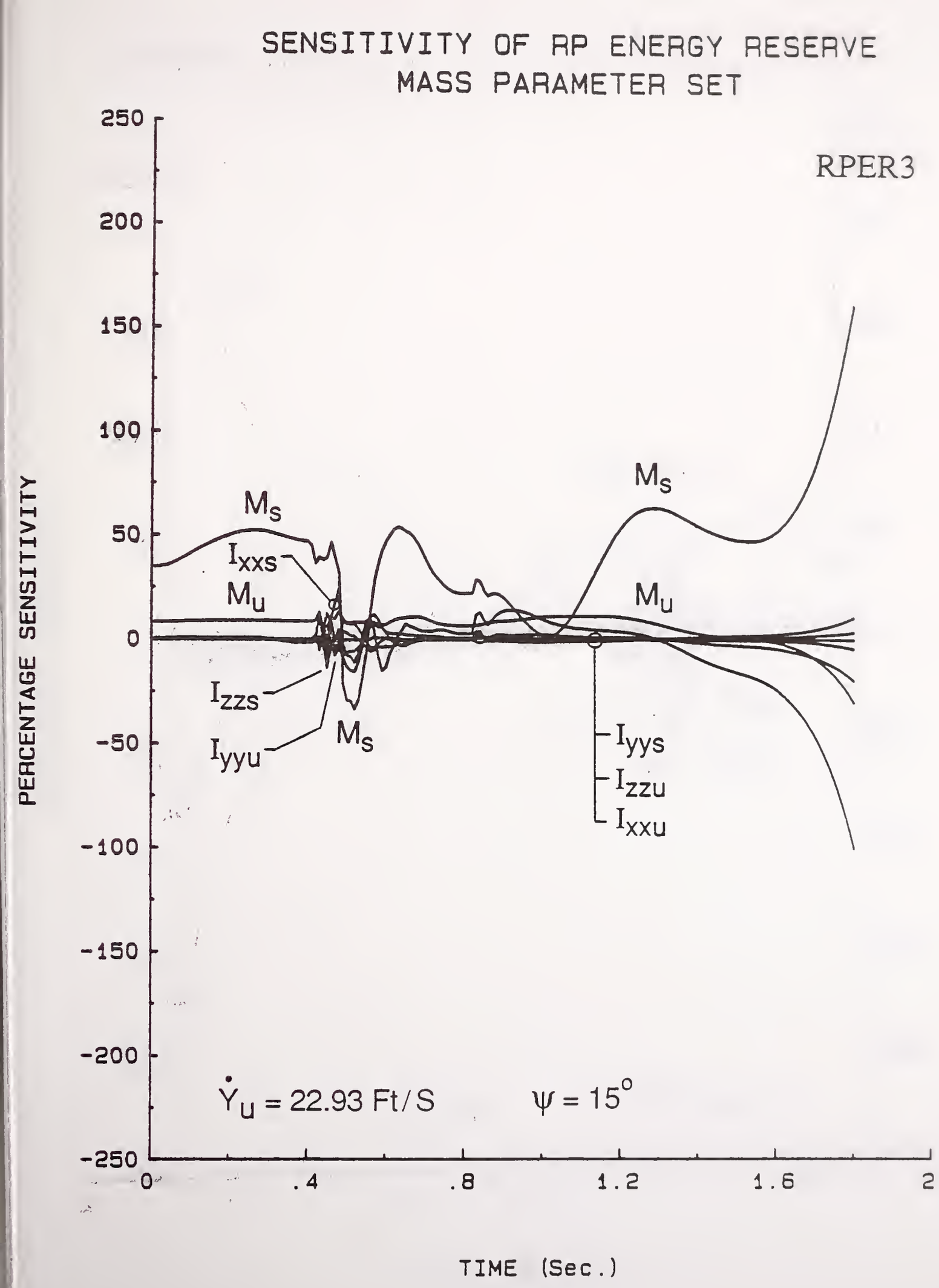
SENSITIVITY OF RP ENERGY RESERVE
MASS PARAMETER SET
RPER3
PERCENTAGE SENSITIVITY
250
200
150
100
50
0
-50
-100
-150
-200
-250
0
.4
.8
1.2
1.6
2
TIME (Sec.)
M_s
I_{xxs}
M_u
I_{zzs}
I_{yyu}
M_s
M_s
M_u
I_{yys}
I_{zzu}
I_{xxu}
$\dot{Y}_u = 22.93$ Ft/S
$\psi = 15^\circ$

Figure 81.

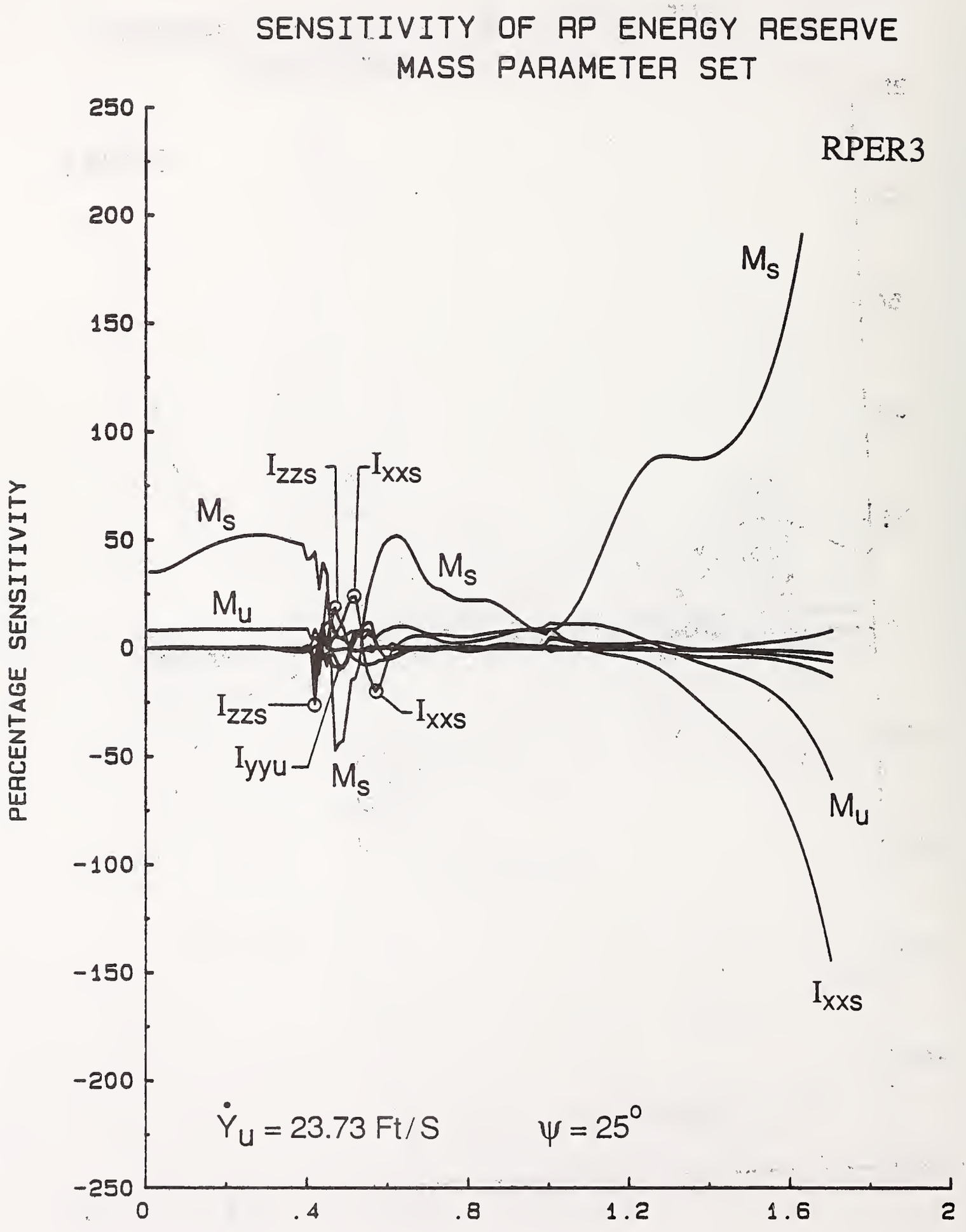
SENSITIVITY OF RP ENERGY RESERVE
MASS PARAMETER SET
RPER3
PERCENTAGE SENSITIVITY
250
200
150
100
50
0
-50
-100
-150
-200
-250
0
.4
.8
1.2
1.6
2
TIME (Sec.)
M_s
I_{zzs}
I_{xxs}
M_s
M_s
M_u
I_{zzs}
I_{xxs}
I_{yyu}
M_s
M_u
I_{xxs}
$\dot{Y}_u = 23.73$ Ft/S
$\psi = 25^\circ$

Figure 82.

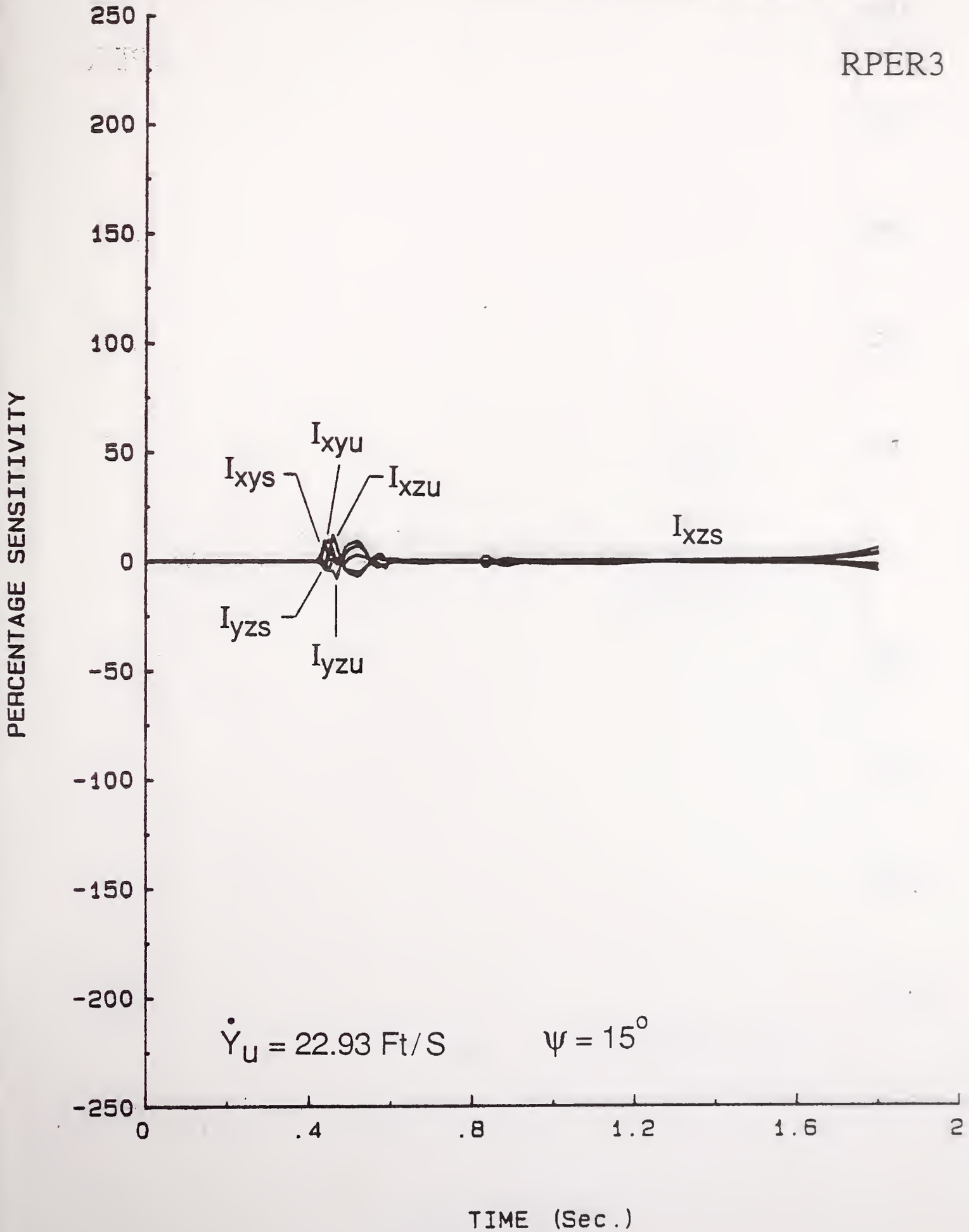
SENSITIVITY OF RP ENERGY RESERVE
PRODUCT OF INERTIA PARAMETER SET
RPER3
250
200
150
100
50
0
-50
-100
-150
-200
-250
PERCENTAGE SENSITIVITY
I_{xyu}
I_{xys}
I_{xzu}
I_{xzs}
I_{yzs}
I_{yzu}
$\dot{Y}_u = 22.93$ Ft/S
$\psi = 15^\circ$
0
.4
.8
1.2
1.6
2
TIME (Sec.)

Figure 83.

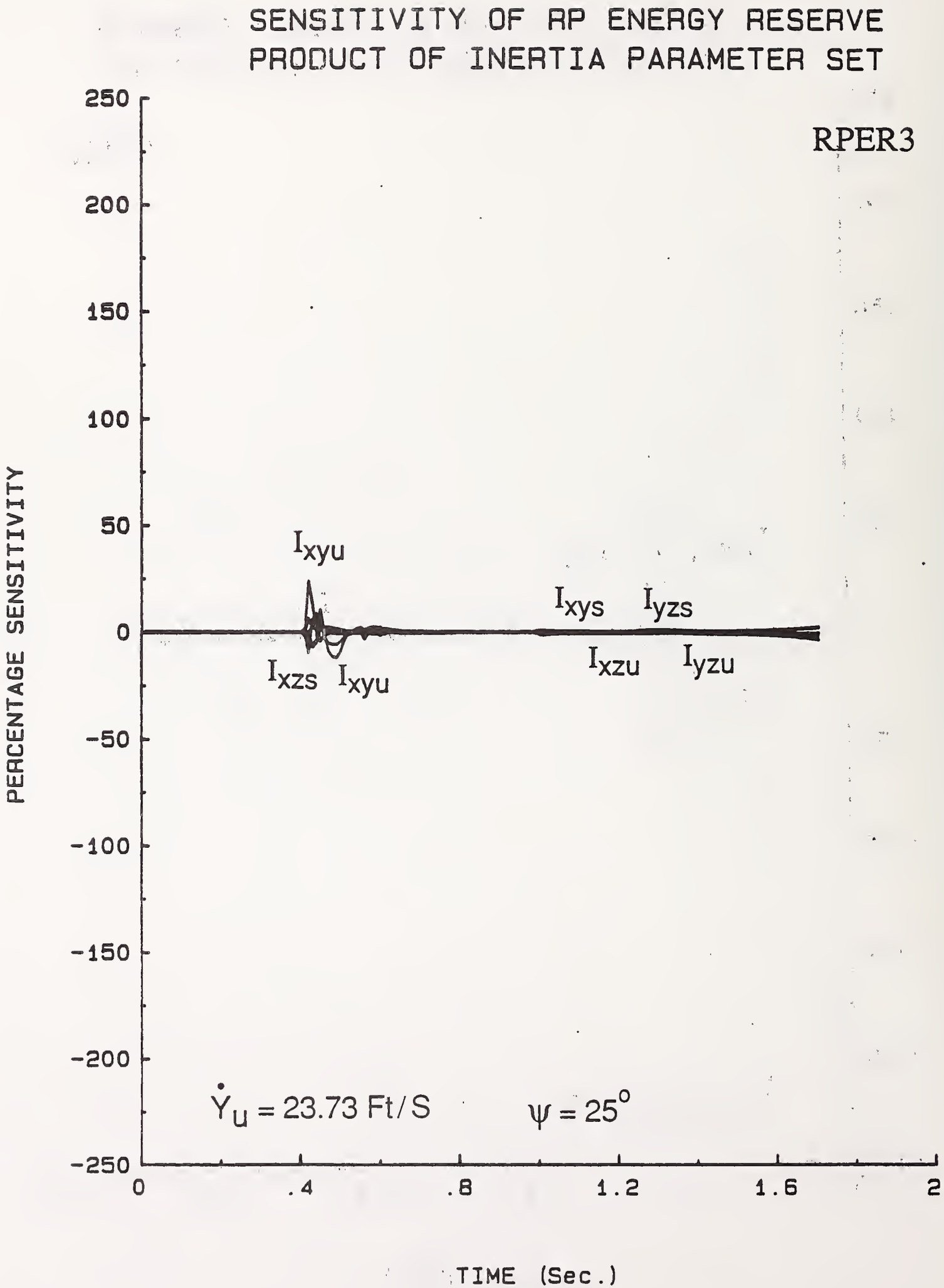
SENSITIVITY OF RP ENERGY RESERVE
PRODUCT OF INERTIA PARAMETER SET
RPER3
250
200
150
100
50
0
-50
-100
-150
-200
-250
PERCENTAGE SENSITIVITY
I_{xyu}
I_{xzs}
I_{xyu}
I_{xys}
I_{yzs}
I_{xzu}
I_{yzu}
$\dot{Y}_u = 23.73$ Ft/S
$\psi = 25^\circ$
0
.4
.8
1.2
1.6
2
TIME (Sec.)

Figure 84.

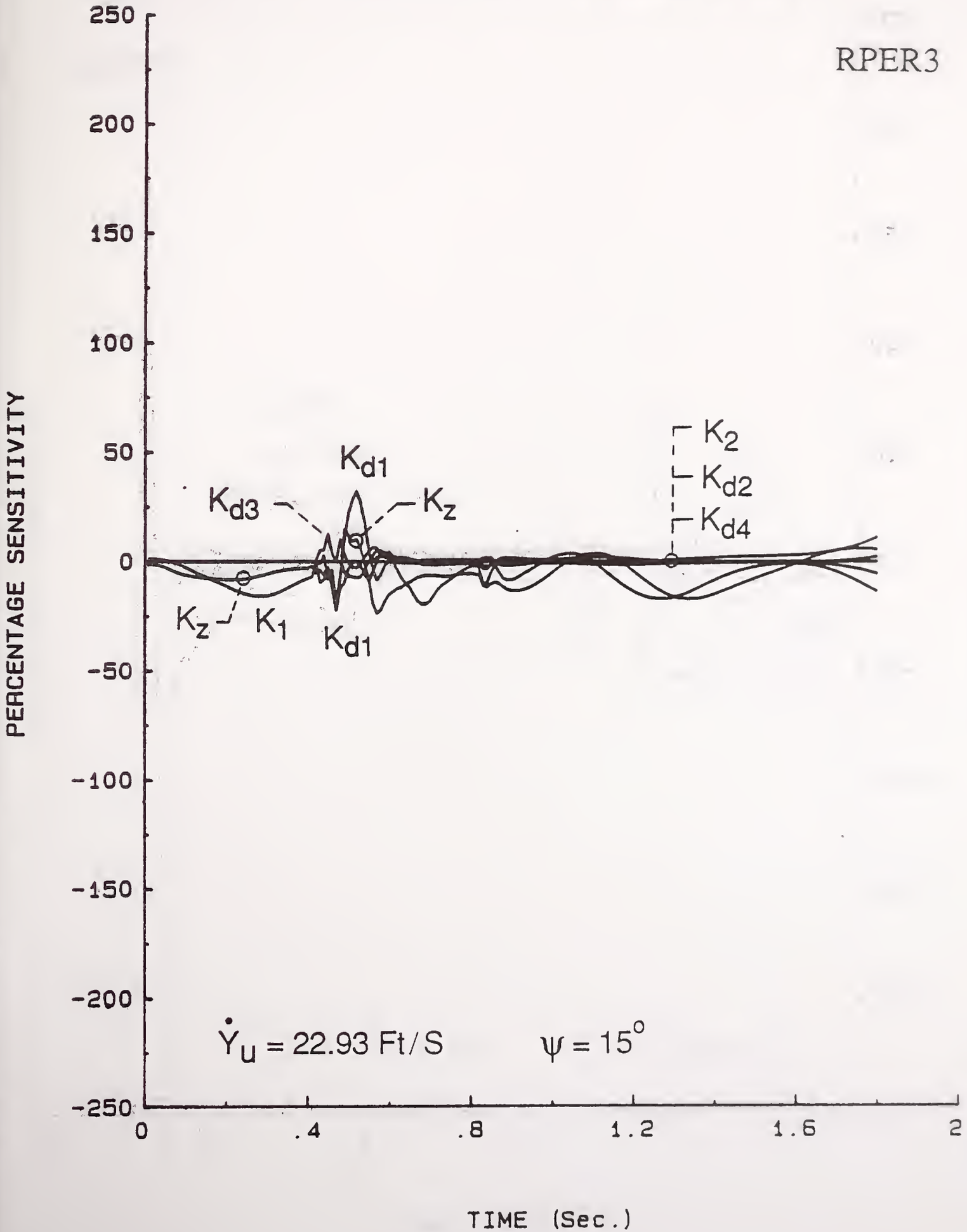
SENSITIVITY OF RP ENERGY RESERVE
STIFFNESS PARAMETER SET
RPER3
PERCENTAGE SENSITIVITY
250
200
150
100
50
0
-50
-100
-150
-200
-250
0
.4
.8
1.2
1.6
2
TIME (Sec.)
K_{d1}
K_{d3}
K_z
K_2
K_{d2}
K_{d4}
K_z
K_1
K_{d1}
$\dot{Y}_u = 22.93$ Ft/S
$\psi = 15^\circ$

Figure 85.

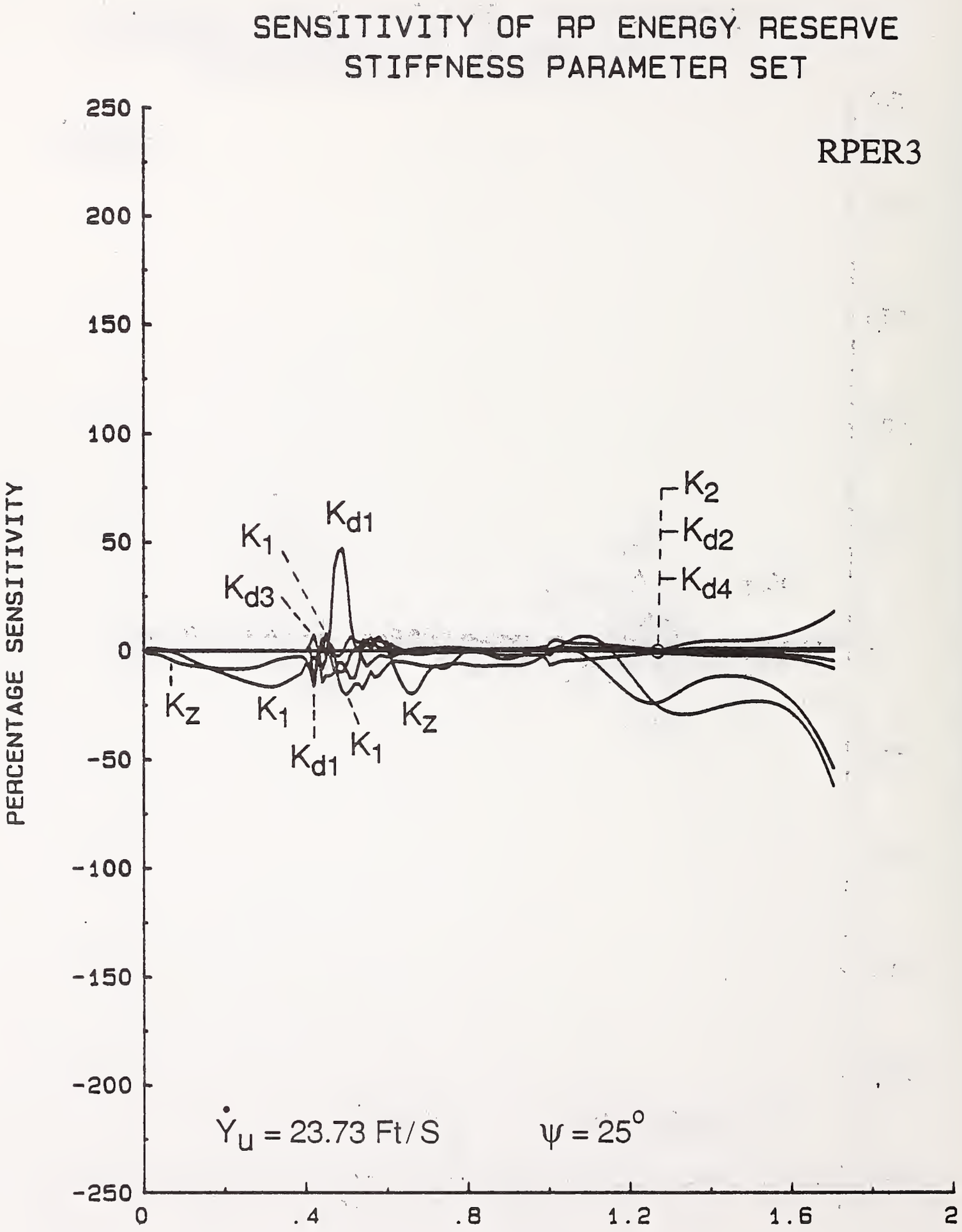
SENSITIVITY OF RP ENERGY RESERVE
STIFFNESS PARAMETER SET
RPER3
PERCENTAGE SENSITIVITY
250
200
150
100
50
0
-50
-100
-150
-200
-250
0
.4
.8
1.2
1.6
2
TIME (Sec.)
K_1
K_{d1}
K_{d3}
K_2
K_{d2}
K_{d4}
K_z
K_1
K_{d1}
K_1
K_z
$\dot{Y}_u = 23.73$ Ft/S
$\psi = 25^\circ$

Figure 86.

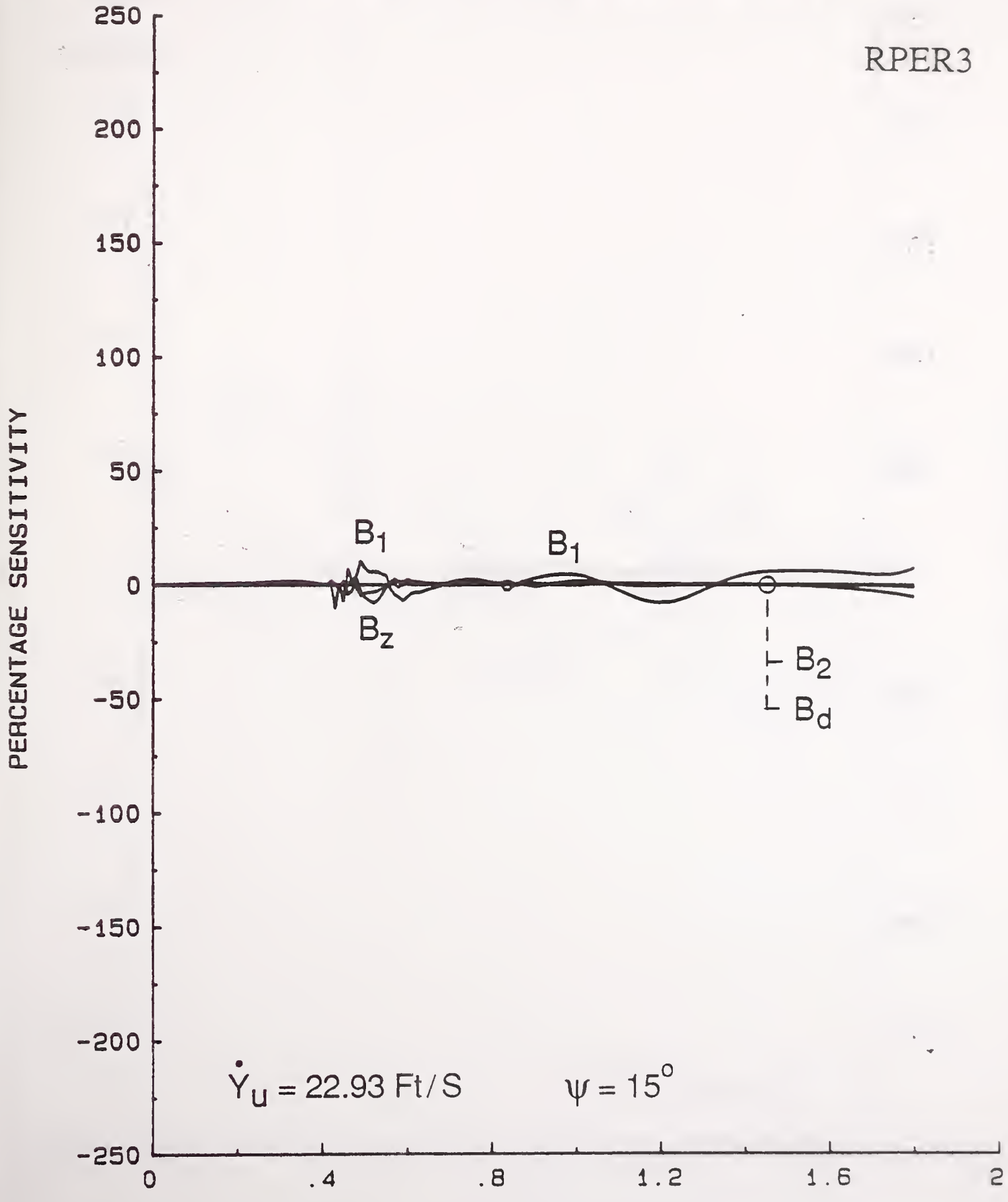
SENSITIVITY OF RP ENERGY RESERVE
DAMPING PARAMETER SET
RPER3
PERCENTAGE SENSITIVITY
250
200
150
100
50
0
-50
-100
-150
-200
-250
0
.4
.8
1.2
1.6
2
B1
B1
Bz
B2
Bd
Ẏu = 22.93 Ft/S
ψ = 15°
TIME (Sec.)

Figure 87.

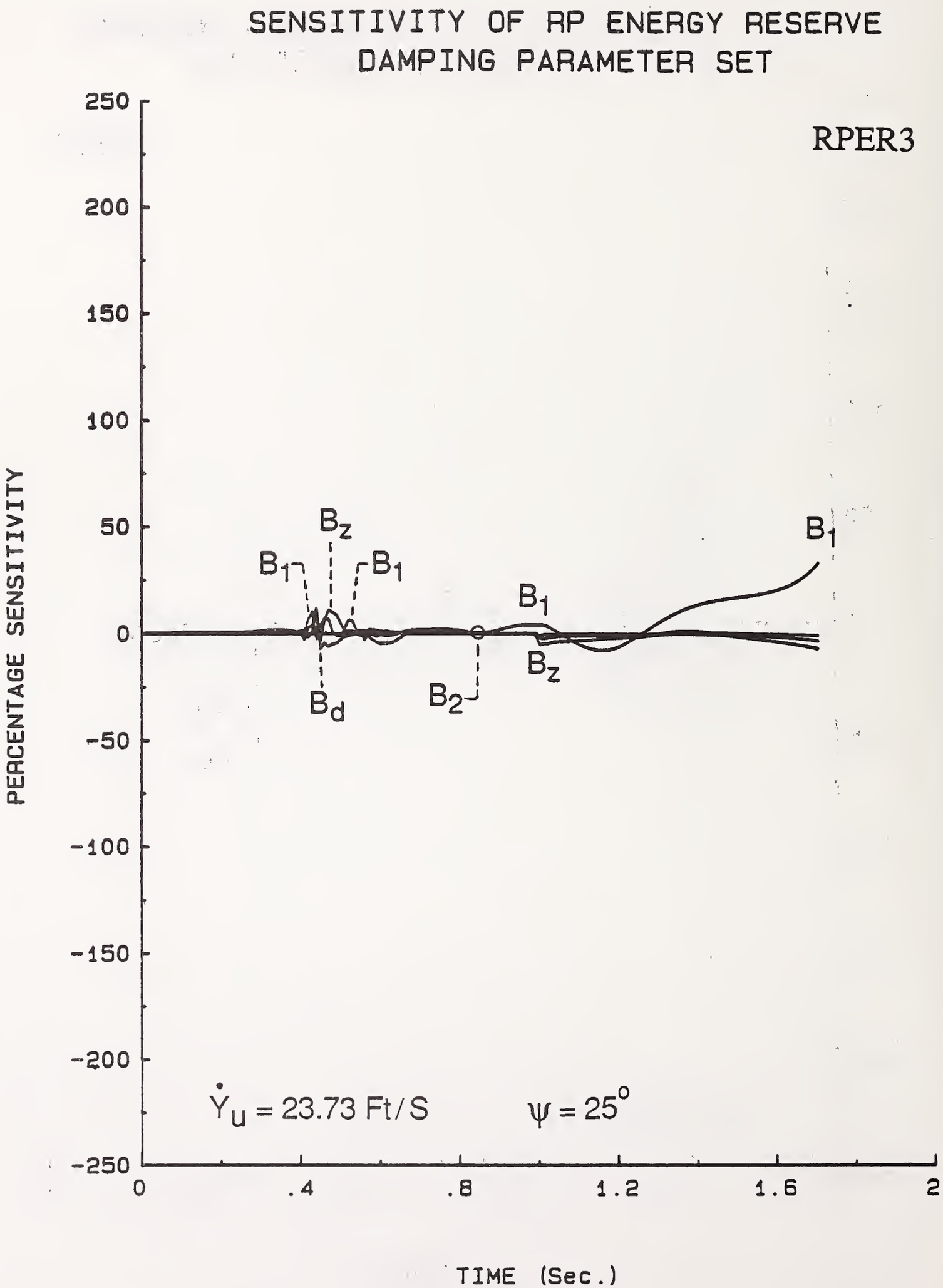
SENSITIVITY OF RP ENERGY RESERVE
DAMPING PARAMETER SET
RPER3
PERCENTAGE SENSITIVITY
250
200
150
100
50
0
-50
-100
-150
-200
-250
0
.4
.8
1.2
1.6
2
TIME (Sec.)
B_z
B_1
B_1
B_1
B_1
B_z
B_d
B_2
$\dot{Y}_u = 23.73$ Ft/S
$\psi = 25^\circ$

Figure 88.

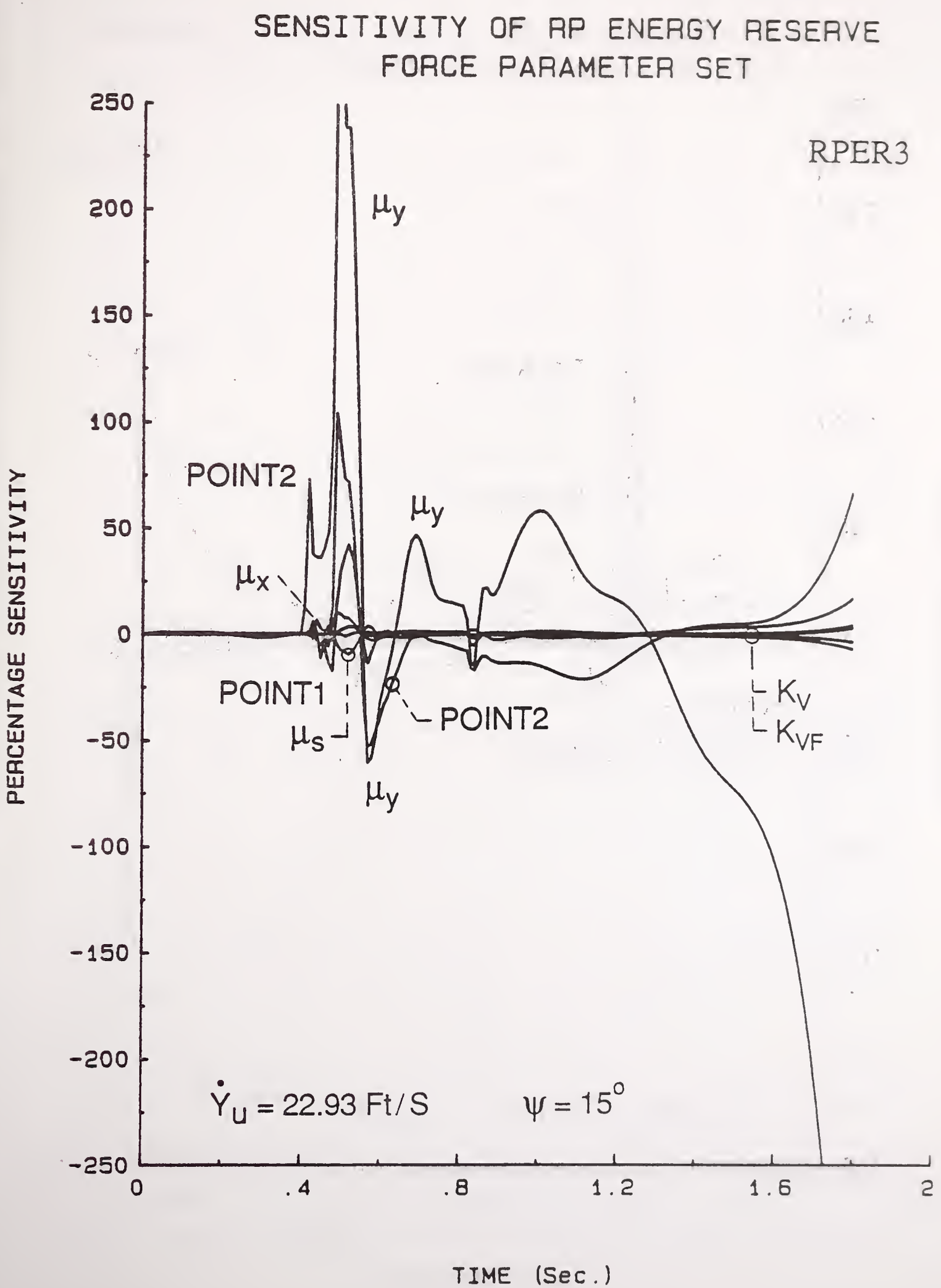
SENSITIVITY OF RP ENERGY RESERVE
FORCE PARAMETER SET
RPER3
PERCENTAGE SENSITIVITY
TIME (Sec.)
250
200
150
100
50
0
-50
-100
-150
-200
-250
0
.4
.8
1.2
1.6
2
μ_y
μ_x
μ_s
POINT1
POINT2
K_V
K_{VF}
$\dot{Y}_u = 22.93$ Ft/S
$\psi = 15^\circ$

Figure 89.

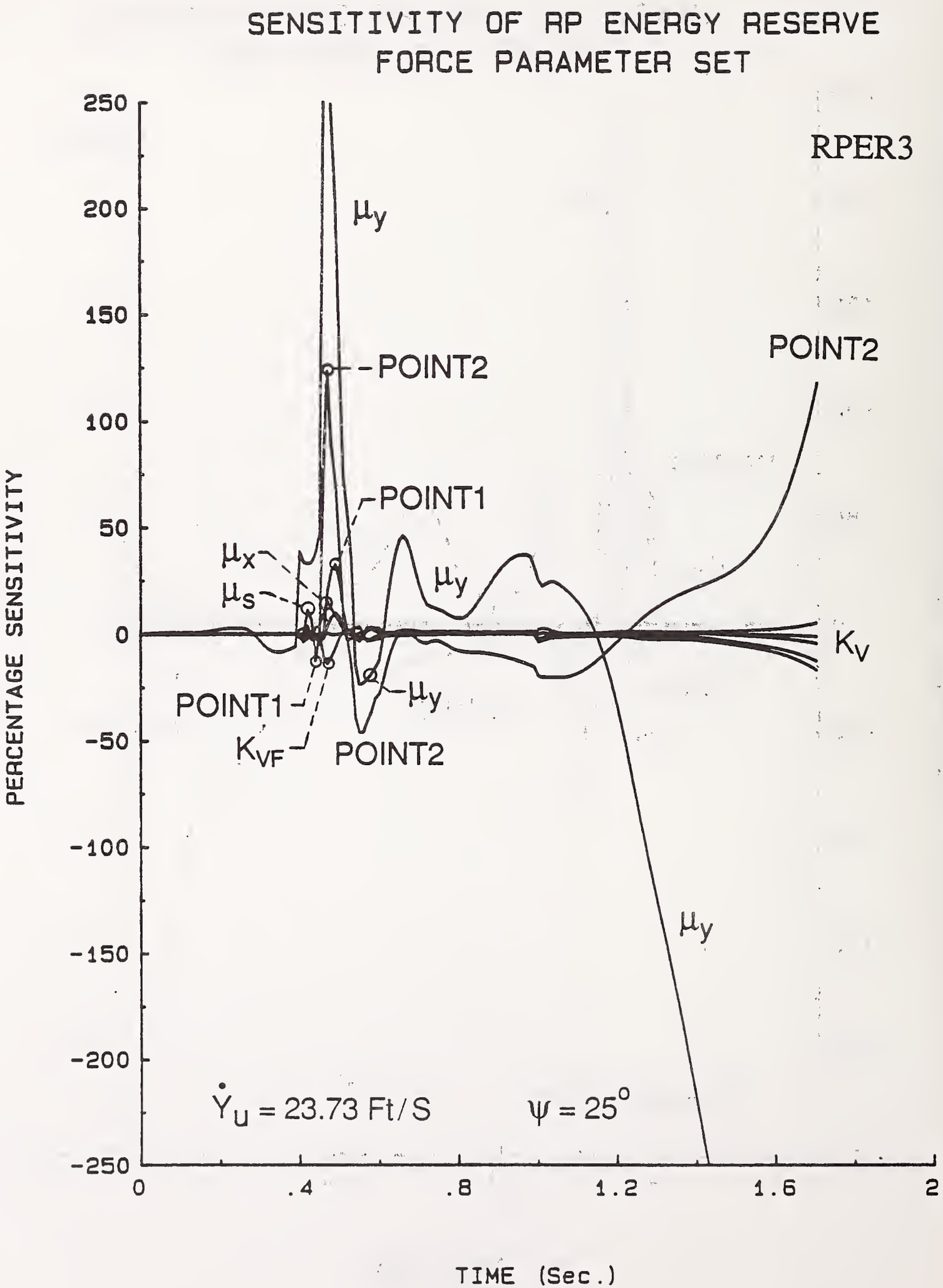
SENSITIVITY OF RP ENERGY RESERVE
FORCE PARAMETER SET
RPER3
PERCENTAGE SENSITIVITY
TIME (Sec.)
250
200
150
100
50
0
-50
-100
-150
-200
-250
0
.4
.8
1.2
1.6
2
μ_y
POINT2
POINT1
μ_x
μ_s
μ_y
K_V
POINT1
K_{VF}
POINT2
μ_y
μ_y
POINT2
$\dot{Y}_U = 23.73$ Ft/S
$\psi = 25^\circ$

Figure 90.

6. GENERAL CONCLUSIONS

It has been demonstrated throughout this report that the ITRS is a very useful simulation which is capable of predicting a vehicle's tripped rollover during side and oblique impacts with the curb. The ITRS fulfills the shortcomings of the STI's tripped rollover model [7], [14] among which, neglecting the vehicle's forward dynamics and an inability to simulate oblique curb impact are the most unfortunate. The ITRS vehicle model accounts for all dynamic couplings in the equations of motion in accordance with the mechanical representation of the vehicle dynamic system. This allows investigation of tripped rollover behavior of a vehicle under a wide range of initial conditions which also include the various rotational velocities of the vehicle.

The ITRS vehicle model has been thoroughly examined for the energy exchange between vehicle components and for the energy dissipation during the entire vehicle motion. Based on energy analyses, two dynamic functions of the Rollover Prevention Energy Reserve, RPER and RPER3, were developed. The RPER, which does not directly include the deformations encountered upon striking a curb, is equivalent to the rollover prevention energy reserve which was first used in [7]. The refined RPER3 function accounts for both elastic and plastic deformations of the vehicle, and the variation in the vehicle's CG height due to relative motions of the sprung and unsprung masses. Also, the Instantaneous Rollover Stability Factor (IRSF) was introduced and utilized in the RPER3 instead of, the previously used, static rollover stability factor (SRSF).

Investigation into the RPER and RPER3 under the same initial conditions revealed that both functions can successfully be used to assess the rollover propensity of vehicles during side and oblique impacts with the obstacle. The superiority of the RPER3 function lies with the fact that the vehicle deformations, which occur during the impact and can significantly alter the amount of energy necessary to

bring the vehicle to the static tip-over position, are accounted for. It has been observed, however, that RPER3 exhibits a greater sensitivity to initial conditions than does RPER.

Both RPER and RPER3 use the same dynamic criteria for rollover prediction of vehicles. The detailed investigation of RPER and RPER3 performed for a variety of tripped rollover scenarios has resulted in the following important observations regarding rollover occurrence and rollover prevention energy reserve:

(1) <u>If a vehicle rolls over, its RPER (or RPER3) must have become negative</u>

(2) <u>If the value of RPER (or RPER3) remains positive, the vehicle cannot rollover.</u>

It should be noted that none of the observations is a consequence of another and that both observations are valid in side as well as oblique impact with the curb.

RPER and RPER3 can effectively be used to assess the rollover propensity of various vehicles by examining the minimum values of RPER (or RPER3) attained by the vehicles in identical non-rollover situations. A comparison of rollover prevention energy reserve values in non-rollover cases (situations in which RPER, RPER3 remain positive) will indicate which vehicles are more prone to rollover under more severe impact conditions. The vehicle which achieved the lowest value of RPER (or RPER3) would be the first to rollover under more dangerous conditions. By comparing the time histories of RPER (RPER3) generated by vehicles in several different situations, the vehicles' overall dynamic rollover propensity can be evaluated.

From the time histories of RPER and RPER3, and the system response it has been found that, if the tripped rollover is to occur at critical speed, the dynamic criteria for rollover are satisfied when the unsprung mass absolute roll angle equals 9.5 and 11.5 degrees for impact angles of 0 and 25 degrees, respectively. For the speeds higher than critical rollover velocity, the dynamic criteria for vehicle rollover are satisfied at even smaller roll angles. This is very useful information, particularly for designing experimental tests, in which the rollover propensity of vehicles could be assessed without a need of rolling them over to the static tip-over position.

This report presents a thorough investigation into the effects of vehicle design characteristics on tripped rollover behavior. The results obtained using the percentage sensitivity functions are rational and agree with existing information and experience regarding tripped rollover behavior and vehicles' propensity to roll over. It has been demonstrated that the sensitivity curves of RPER to parameter changes follow patterns similar to RPER3. The only difference is that RPER3 displays more oscillations due to increased sensitivity to initial conditions than does RPER. However, the sensitivity analyses of both functions lead to the same general conclusions regarding the parameters' influence on a vehicle's rollover stability.

The sensitivity results reveal that geometrical, mass and impact deformation characteristics have the largest influence on vehicle rollover propensity in both side and oblique tripped rollover situations. The vehicle`s rollover stability can be best enhanced by increasing vehicle track width, roll moment of inertia and distance between suspension springs, or by reducing vehicle c.g. height, sprung mass and impact force deformation rate in elastic region. The vehicle's rollover prevention energy reserve can also be increased (thus improving rollover stability) by allowing a larger plastic deformation of the vehicle (wheel) to occur during impact with the curb. This is particularly important when the vehicle's impact velocity with a curb is increased or under oblique impact conditions.

A comparison of sensitivity results obtained in side and oblique impacts showed that a positive influence of a vehicle roll moment of inertia on RPER and RPER3 decreases when the angle of impact increases. At the same time, the negative influence of vehicle sprung mass on rollover stability increases as the impact angle increases. The vehicle damping characteristics were found to have very little influence on tripped rollover stability during both side and oblique impacts.

It should be noted that the results presented in this report were obtained for a one set of vehicle data representing a medium size passenger car. For the sake of completeness of analysis it is recommended that the sensitivity methods used in this report be applied to investigate a tripped rollover behavior of other vehicle data sets with varying initial conditions. The vehicle data sets should be representative of vehicles in different classes such as minivans, vans, light and full size utility vehicles, small and standard pickup trucks, and should reflect current and future design trends.

In this project the vehicle was skidding sideways prior to the impact with the curb. Although this study included a variation in initial position of the vehicle, so that side and oblique impacts could occur, it did not examine the cases in which a vehicle had a meaningful forward speed. Future research should also include the analysis of parameters' influences on the rollover stability of vehicles which accidentally run over a curb at various angles in a stable manner, both in a straight line and in a curve. The vehicle model to be used in the proposed research should account for the impact deformations in longitudinal and vertical directions in addition to lateral deformation.

Finally, accident statistics have shown that a significant number of rollover accidents occur when a vehicle skids into a soil or soft shoulder. It would therefore be beneficial to investigate the vehicle rollover behavior caused by a tripping mechanism generated

by the soil resistance and plowing forces in particular, when the vehicle crosses pavement/soil discontinuity in a skid and a turn under a high lateral acceleration.

REFERENCES

1. DeLeys, N. J.,Parada, L. O., "Rollover Potential of Vehicles on Embankments, Sideslopes and Other Roadside Features", FHWA - U.S. DOT Final Report No. FHWA/RD - 86/164, 1986.

2. National Accident Sampling System (NASS) 1985 Data Base, National Center for Statistics and Analysis, NHTSA, Washington D.C., 1985.

3. Griffin, L.I., III, "Probability of Overturn in Single Vehicle Accidents as a Function of Road Type and Passenger Car Curb Weight", Traffic Accident Research and Evaluation Program, Texas Transportation Institute, Texas A&M University System, November 1981.

4. Garrot, W. R., Monk, M. W., "Vehicle Inertial Parameters-Measured Values and Approximations", SAE Paper No. 881767, 1988.

5. Jones, I.S., "Vehicle Stability Related to Frequency of Overturning for Different Models of Cars", Proc. Australian Road Research Board, Vol. 7, Part 5, 1974.

6. Rosenthal, T. J., et al.,"User's Guide and Program Description for a Tripped Roll Over Vehicle Simulation", NHTSA- U.S. DOT Report No. DOT HS 807 140, 1987.

7. Nalecz, A.G., et al., "Sensitivity Analysis of Vehicle Tripped Rollover Model", NHTSA - U.S. DOT Final Report No. DOT HS 807 300, July 1988.

8. Nalecz, A.G., Bindemann, A.C., "Sensitivity Analysis of Vehicle Design Attributes that Affect Vehicle Response in Critical Accident Situations - Part I: User's Manual", NHTSA - U.S. DOT Final Report No. DOT HS 807 229, December 1987.

9. Nalecz, A.G., Bindemann, A.C., "Sensitivity Analysis of Vehicle Design Attributes that Affect Vehicle Response in Critical Accident Situations - Part II: Technical Report", NHTSA - U.S. DOT Final Report No. DOT HS 807 230, December 1987.

10. Nalecz, A.G., Wicher, J., "Design Sensitivity Analysis of Mechanical Systems in Frequency Domain", Journal of Sound and Vibration., Vol. 120, No. 3, 1988, pp. 517 - 526.

11. Wicher, J., Nalecz, A.G., "Second Order Sensitivity Analysis of Lumped Mechanical Systems in the Frequency Domain", International Journal for Numerical Methods in Engineering, Vol. 24, No. 12, 1987, pp. 2357 - 2366.

12. Nalecz, A.G., "Sensitivity Analysis of Vehicle Design Attributes in Frequency Domain", International Journal of Vehicle Mechanics and Mobility (Vehicle System Dynamics), Vol. 17, No. 3, 1988, pp. 141 - 163.

13. Nalecz, A.G., "Application of Sensitivity Methods to Analysis and Synthesis of Vehicle Dynamic Systems", State of the Art Paper at 11th IAVSD-IUTAM Symposium, International Journal of Vehicle Mechanics and Mobility (Vehicle System Dynamics), Vol. 18, No. 1-3, 1989, pp. 1 - 45.

14. Nalecz, A.G., "Influence of Vehicle and Roadway Factors on the Dynamics of Tripped Rollover", International Journal of Vehicle Design, Vol. 10, No. 3, 1989, pp. 321 - 347.

15. Nalecz, A.G., et al., "Dynamic Analysis of Vehicle Rollover", Proceedings of the 12th International ESV Conference, Goteborg, Sweden, May 1989.

16. Nalecz, A.G., "Intermediate Maneuver Induced Rollover Simulation (IMIRS) and Sensitivity Analysis", TSC - U.S. DOT Contract No. DTRS57-88-P-82668, Final Report, 1989.

17. Nalecz, A.G., et al., "Advanced Dynamic Rollover Model", NHTSA - U.S. DOT Contract No. DTNH-87-D-27174, Final Report , 1989.

SUBSCRIPT NOTATION

The following subscript notations are used in this report:

l : left side
r : right side
F : front
R : rear
s : sprung mass
u : unsprung mass

NOMENCLATURE

ABSDEF : vertical distance from axle to bump stop
a : distance from vehicle C.G. to front axle
b : distance from vehicle C.G. to rear axle
B_1 : suspension shock absorber damping rate per wheel
B_2 : bump stop damping rate per wheel
B_d : vehicle structural damping rate
B_z : single tire radial damping rate
F_{dF} : front lateral impact force
F_{dR} : rear lateral impact force
F_{dsF} : front impact scrubbing force
F_{dsR} : rear impact scrubbing force
F_{dxF} : front longitudinal impact force
F_{dxR} : rear longitudinal impact force
F_F : front lateral pin reaction force
F_R : rear lateral pin reaction force
F_t : longitudinal pin reaction force
F_{slF} : combined spring and shock absorber force on left front
F_{slR} : combined spring and shock absorber force on left rear
F_{srF} : combined spring and shock absorber force on right front

F_{srR} : combined spring and shock absorber force on right rear

F_{xlF} : left front tire longitudinal force

F_{xlR} : left rear tire longitudinal force

F_{xrF} : right front tire longitudinal force

F_{xrR} : right rear tire longitudinal force

F_{ylF} : left front tire lateral force

F_{ylR} : left rear tire lateral force

F_{yrF} : right front tire lateral force

F_{yrR} : right rear tire lateral force

F_{zlF} : left front tire normal reaction

F_{zlR} : left rear tire normal reaction

F_{zrF} : right front tire normal reaction

F_{zrR} : right rear tire normal reaction

h : distance from sprung mass pivot point to unsprung mass c.g.

h_{curb} : curb height

h_{ra} : distance from pivot point to sprung mass c.g.

h_s : distance from sprung mass c.g. to bottom of sprung mass

h_u : distance from axle center to unsprung mass c.g.

IRSF : instantaneous rollover stability factor

I_{xxs} : sprung mass roll moment of inertia

I_{yys} : sprung mass pitch moment of inertia

I_{zzs} : sprung mass yaw moment of inertia

I_{xxu} : unsprung mass roll moment of inertia

I_{yyu} : unsprung mass pitch moment of inertia

I_{zzu} : unsprung mass yaw moment of inertia

I_{xys} : sprung mass x-y product of inertia

I_{xzs} : sprung mass x-z product of inertia

I_{yzs} : sprung mass y-z product of inertia

I_{xyu} : unsprung mass x-y product of inertia

I_{xzu} : unsprung mass x-z product of inertia

I_{yzu} : unsprung mass y-z product of inertia

K_1 : single suspension spring rate

K_2 : single bump stop spring rate

K_{d1} : impact force deformation rate - 1st region

K_{d2} : impact force deformation rate - 2nd region

K_{d3} : impact force unloading/reloading rate

K_{d4} : impact force deformation rate - 3rd region

K_V : tire lateral velocity for constant force

K_{VF} : tire longitudinal velocity for constant force

K_z : single tire radial spring rate

L : vehicle wheelbase

M_s : sprung mass

M_u : unsprung mass

POINT1 : lateral crush distance to enter 2nd impact region

POINT2 : lateral crush distance to enter 3rd impact region

s : half distance between left and right suspension forces

SPRLNG : undeflected length of suspension springs

SRSF : ratio of half track width to c.g. height

T_r : undeformed tire radius

TRW : vehicle track width

TRWF : front half track width - impact side

TRWR : rear half track width - impact side

Y_u : initial distance between right front tire and curb

x : vehicle longitudinal position in absolute reference system

y : vehicle lateral position in absolute reference system

z_s : sprung mass vertical position in absolute reference system

z_u : unsprung mass vertical position in absolute reference system

ϕ_s : sprung mass absolute roll angle

ϕ_u : unsprung mass absolute roll angle

q : vehicle pitch angle

y : vehicle yaw angle

μ_s : tire/curb scrubbing coefficient of friction

μ_x : longitudinal tire/surface coefficient of friction

μ_y : lateral tire/surface coefficient of friction

$\Delta\phi$: relative roll angle between sprung and unsprung masses

APPENDIX A

Transformation coefficients from absolute reference system OXYZ to unsprung mass NIRS $o_u x_u y_u z_u$:

$$T_{xaxu} = \cos\theta \cos\psi$$
$$T_{xayu} = \sin\phi_u \sin\theta \cos\psi - \cos\phi_u \sin\psi$$
$$T_{xazu} = \cos\phi_u \sin\theta \cos\psi + \sin\phi_u \sin\psi$$

Transformation coefficients from unsprung mass NIRS $o_u x_u y_u z_u$ to NIRS oxyz:

$$T_{xuz} = - \sin\theta$$
$$T_{yuz} = \sin\phi_u \cos\theta$$
$$T_{zuz} = \cos\theta \cos\phi_u$$

Transformation coefficients from NIRS oxyz to unsprung mass NIRS $o_u x_u y_u z_u$:

$$T_{xxu} = \cos\theta$$
$$T_{xyu} = \sin\phi_u \sin\theta$$
$$T_{xzu} = \cos\phi_u \sin\theta$$
$$T_{yyu} = \cos\phi_u$$
$$T_{yzu} = - \sin\phi_u$$
$$T_{zxu} = - \sin\theta$$
$$T_{zyu} = \sin\phi_u \cos\theta$$
$$T_{zzu} = \cos\phi_u \cos\theta$$

Transformation coefficients from sprung mass NIRS $o_s x_s y_s z_s$ to unsprung mass NIRS $o_u x_u y_u z_u$:

$T_{xsxu} = 1$
$T_{ysyu} = \cos \Delta\phi$
$T_{yszu} = \sin \Delta\phi$
$T_{zsyu} = - \sin \Delta\phi$
$T_{zszu} = \cos \Delta\phi$

Transformation coefficients from unsprung mass NIRS $o_u x_u y_u z_u$ to sprung mass NIRS $o_s x_s y_s z_s$:

$T_{xuxs} = 1$
$T_{yuys} = \cos \Delta\phi$
$T_{yuzs} = - \sin \Delta\phi$
$T_{zuys} = \sin \Delta\phi$
$T_{zuzs} = \cos \Delta$

APPENDIX B

Vehicle Data Used in Sensitivity Analysis

a	4.45	ft
L	9.25	ft
h_{ra}	0.8667	ft
h_s	1.2	ft
h_u	0.2	ft
T_r	1.0	ft
TRW	5.0	ft
ABSDEF	0.25	ft
h_{curb}	0.5	ft
s	1.75	ft
SPRLNG	0.6667	ft
M_s	105.0	lb s^2/ft
M_u	16.7	lb s^2/ft
I_{xxs}	240.0	lb ft/s^2
I_{yys}	2000.0	lb ft/s^2
I_{zzs}	2400.0	lb ft/s^2
I_{xxu}	132.0	lb ft/s^2
I_{yyu}	380.0	lb ft/s^2
I_{zzu}	320.0	lb ft/s^2
I_{xys}	1.954	lb ft/s^2
I_{xzs}	-30.62	lb ft/s^2
I_{yzs}	10.82	lb ft/s^2
I_{xyu}	0.4	lb ft/s^2
I_{xzu}	-6.0	lb ft/s^2
I_{yzu}	2.0	lb ft/s^2
$K1_{susp}$	3450.0	lb/ft
$K2_{susp}$	16500.0	lb/ft
KD1	24000.0	lb/ft
KD2	0.0	lb/ft
KD3	96000.0	lb/ft
KD4	96000.0	lb/ft

K_z	12000.0	lb/ft
B1	162.5	lb-sec/ft
B2	16.5	lb-sec/ft
B_d	0.25	lb-sec/ft
B_z	80.0	lb-sec/ft
μ_x	0.75	
μ_y	0.75	
μ_s	0.72	
K_V	1.0	ft/s
K_{VF}	1.0	ft/s
POINT1	0.1667	ft
POINT2	0.6667	ft

APPENDIX C

Initial Conditions Used in Tripped Rollover Maneuvers

$\dot{x}(0)$	0.00	ft/s
$\dot{y}(0)$	varied	ft/s
$\dot{z}_s(0)$	0.00	ft/s
$\dot{z}_u(0)$	0.00	ft/s
$\dot{\phi}_s(0)$	0.00	rad/s
$\dot{\phi}_u(0)$	0.00	rad/s
$\dot{\theta}(0)$	0.00	rad/s
$\dot{\psi}(0)$	0.00	rad/s
$x(0)$	0.00	ft
$y(0)$	7.50	ft
$z_s(0)$	-1.6652	ft
$z_u(0)$	-1.11	ft
$\phi_s(0)$	varied	rad
$\phi_u(0)$	varied	rad
$\theta(0)$	0.00	rad
$\psi(0)$	varied	rad

ITRS POSITION

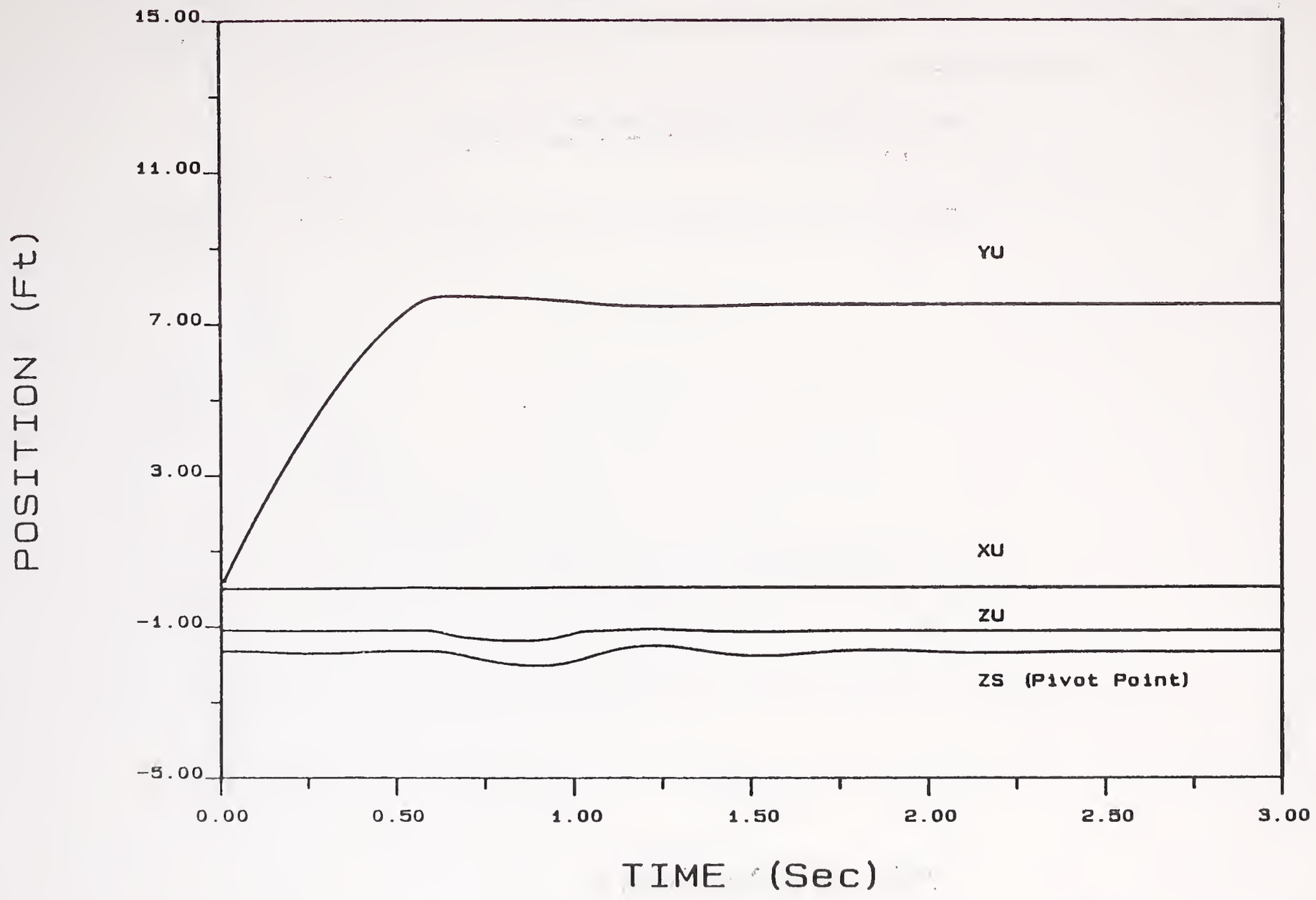

YUD=20 Ft/S : YA=7.5 Ft : PSI=0 Deg

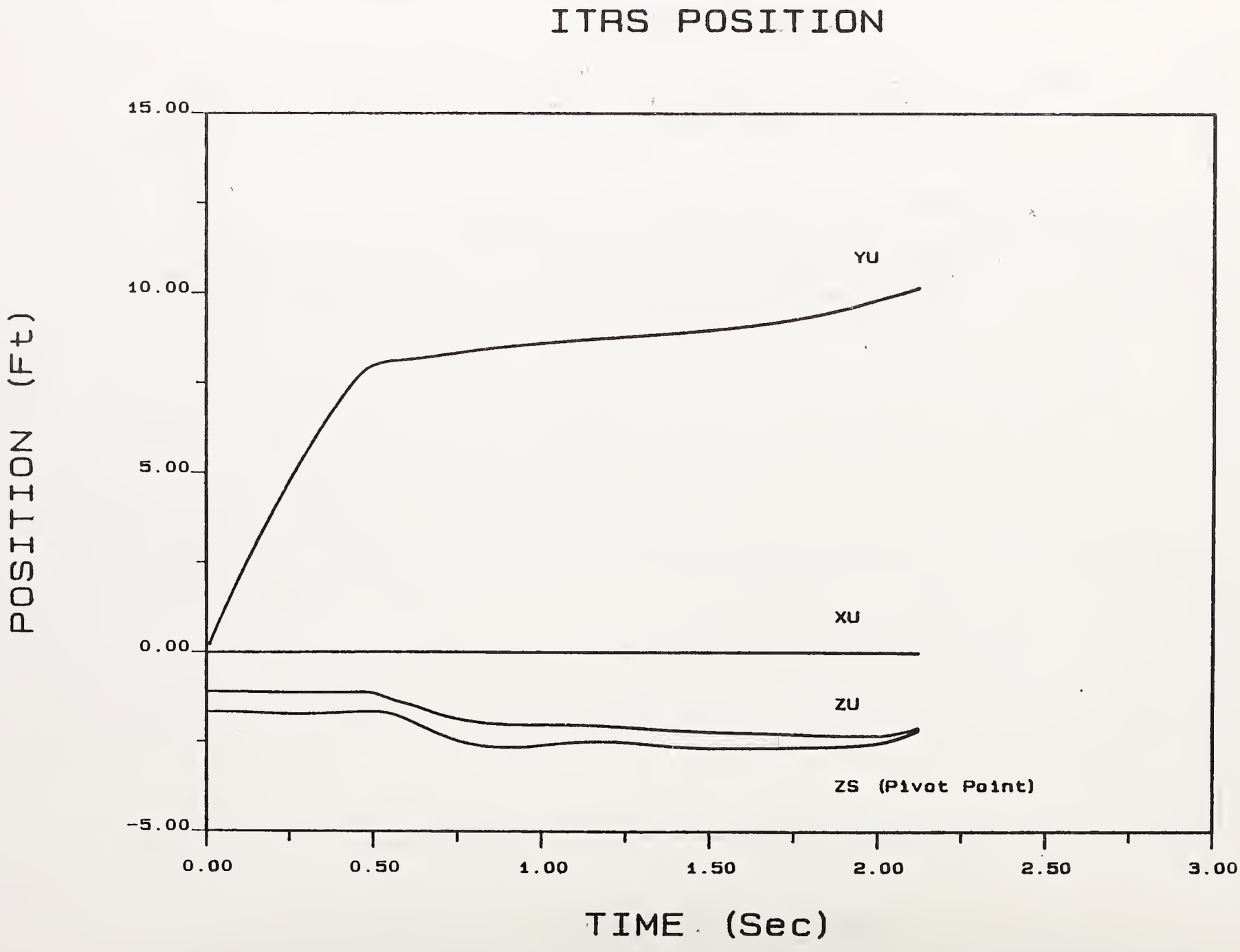
ITRS POSITION
15.00
10.00
5.00
0.00
-5.00
POSITION (Ft)
YU
XU
ZU
ZS (Pivot Point)
0.00
0.50
1.00
1.50
2.00
2.50
3.00
TIME (Sec)
YUD=22.13 Ft/S : YA=7.5 Ft : PSI=0 Deg

ITRS POSITION

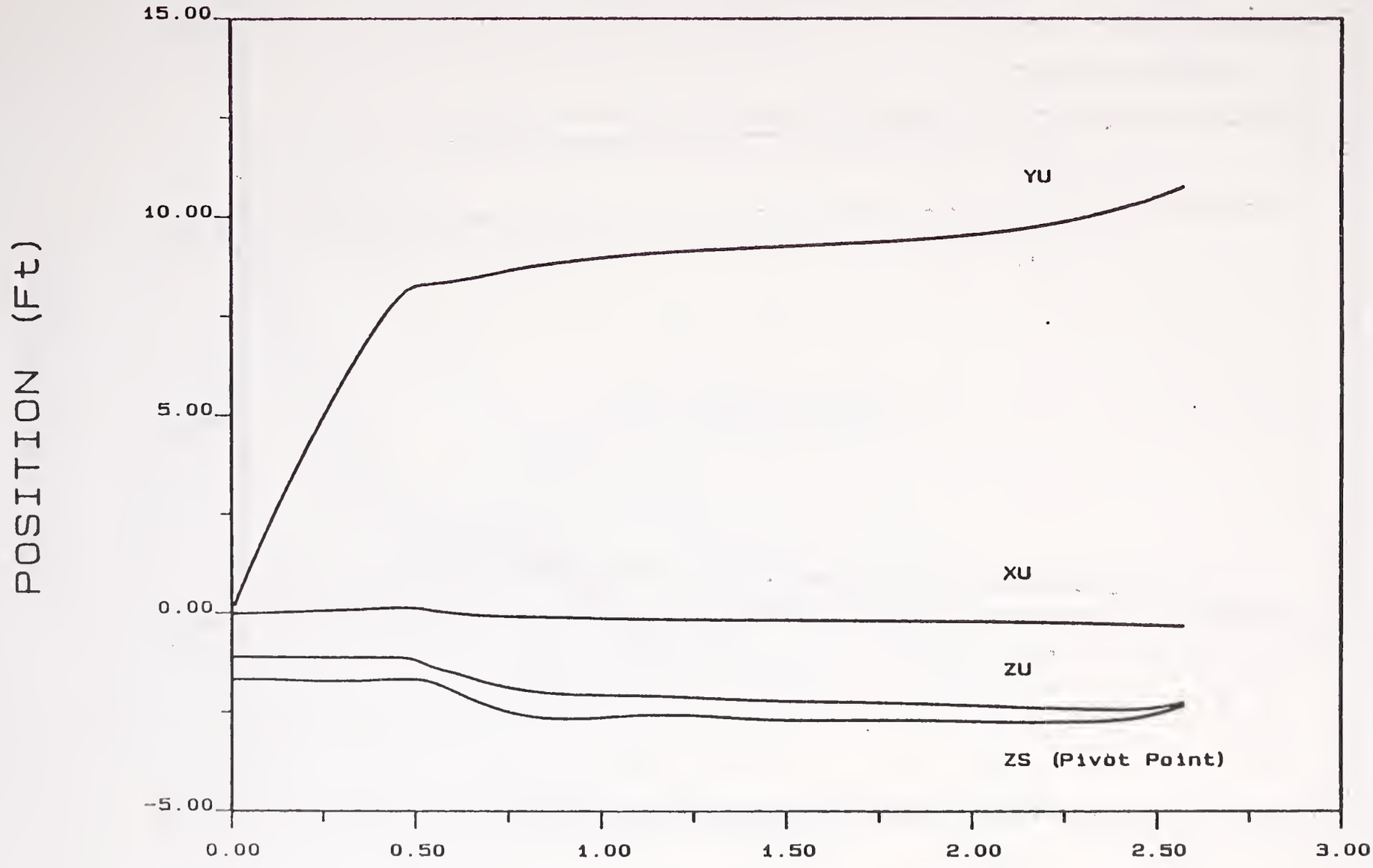

YUD=22.93 Ft/S : YA=7.5 Ft : PSI=15 Deg

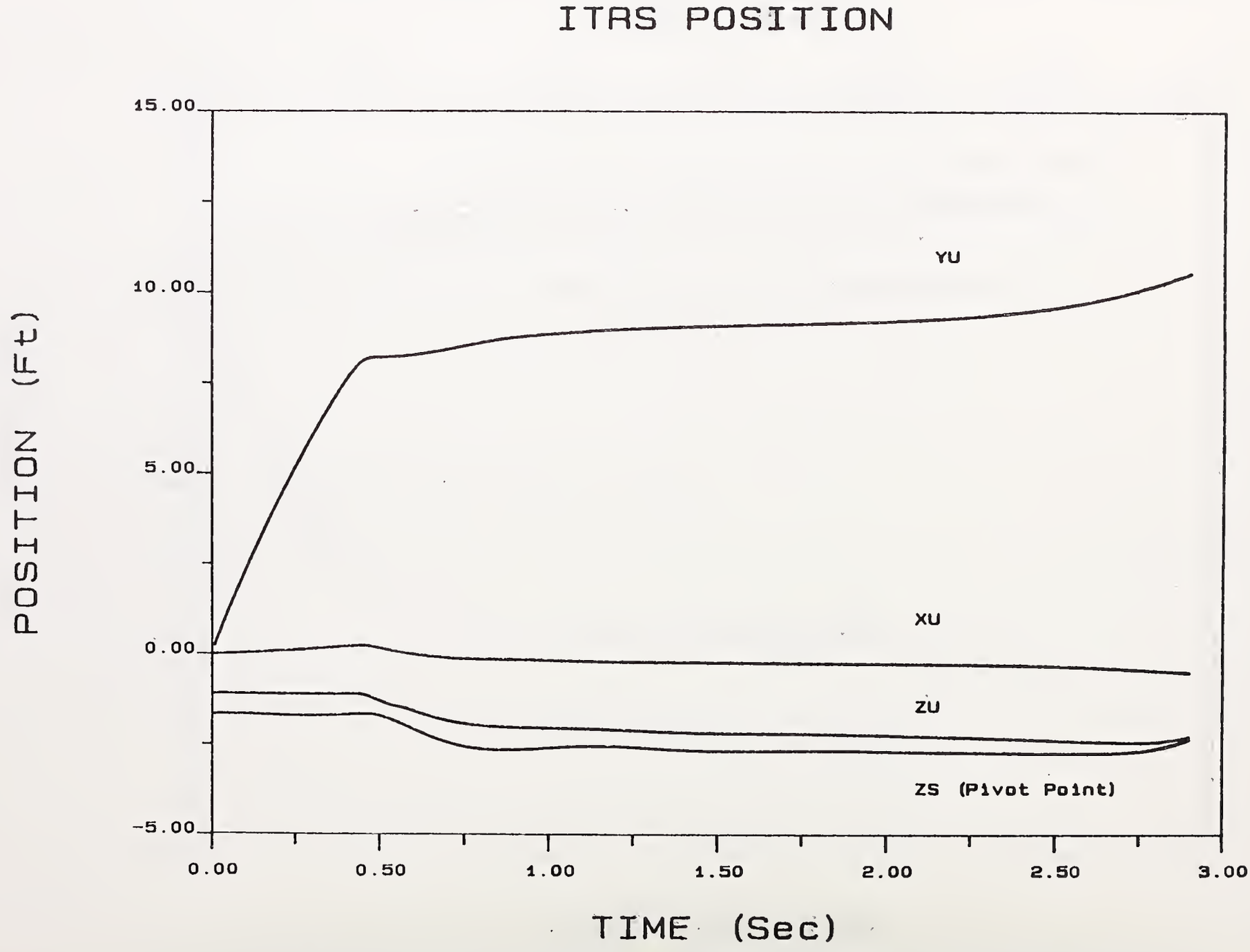

YUD=23.73 Ft/S : YA=7.5 Ft : PSI=25 Deg

ITRS ORIENTATION

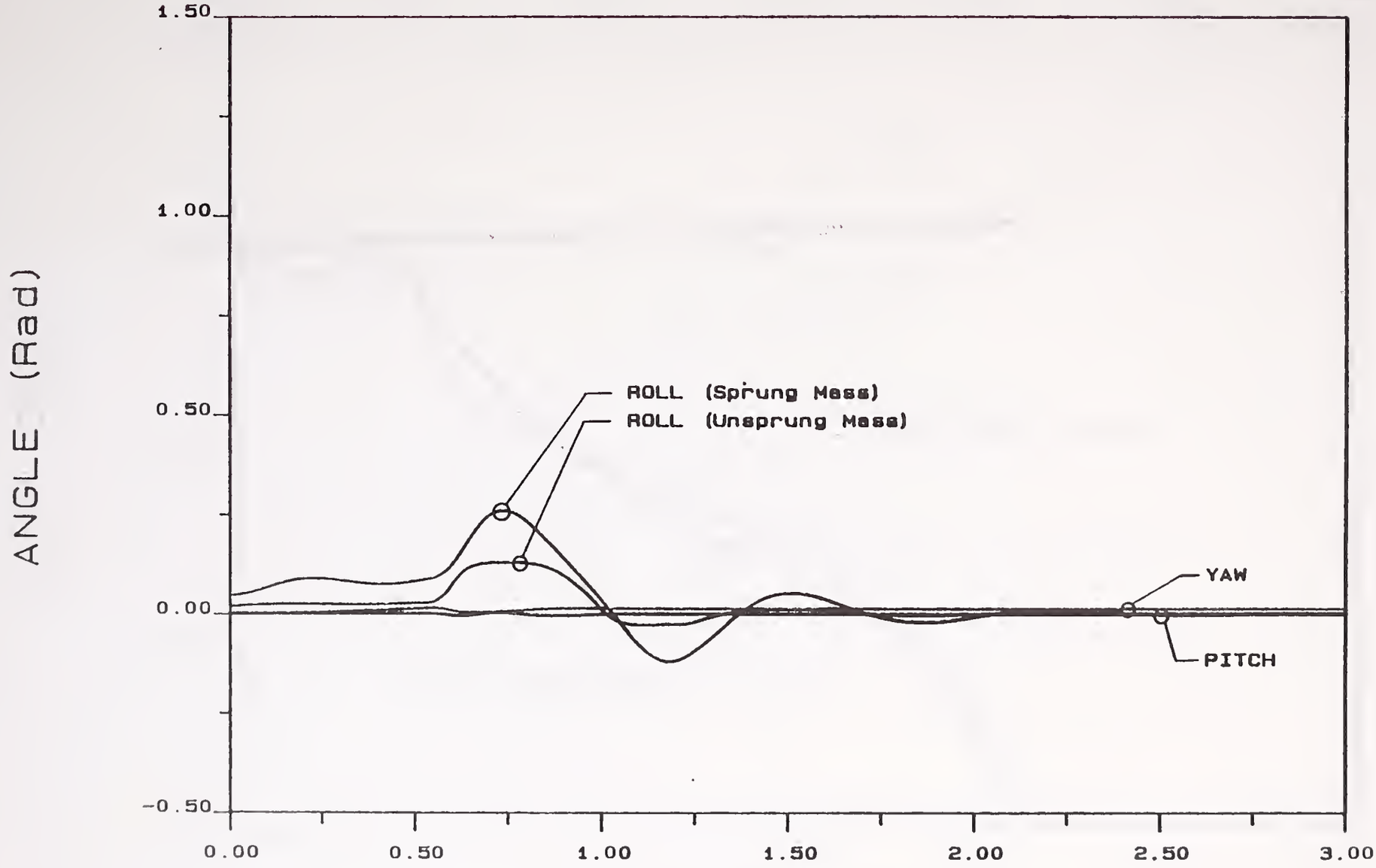

YUD=20 Ft/S : YA=7.5 Ft : PSI=0 Deg

ITRS ORIENTATION

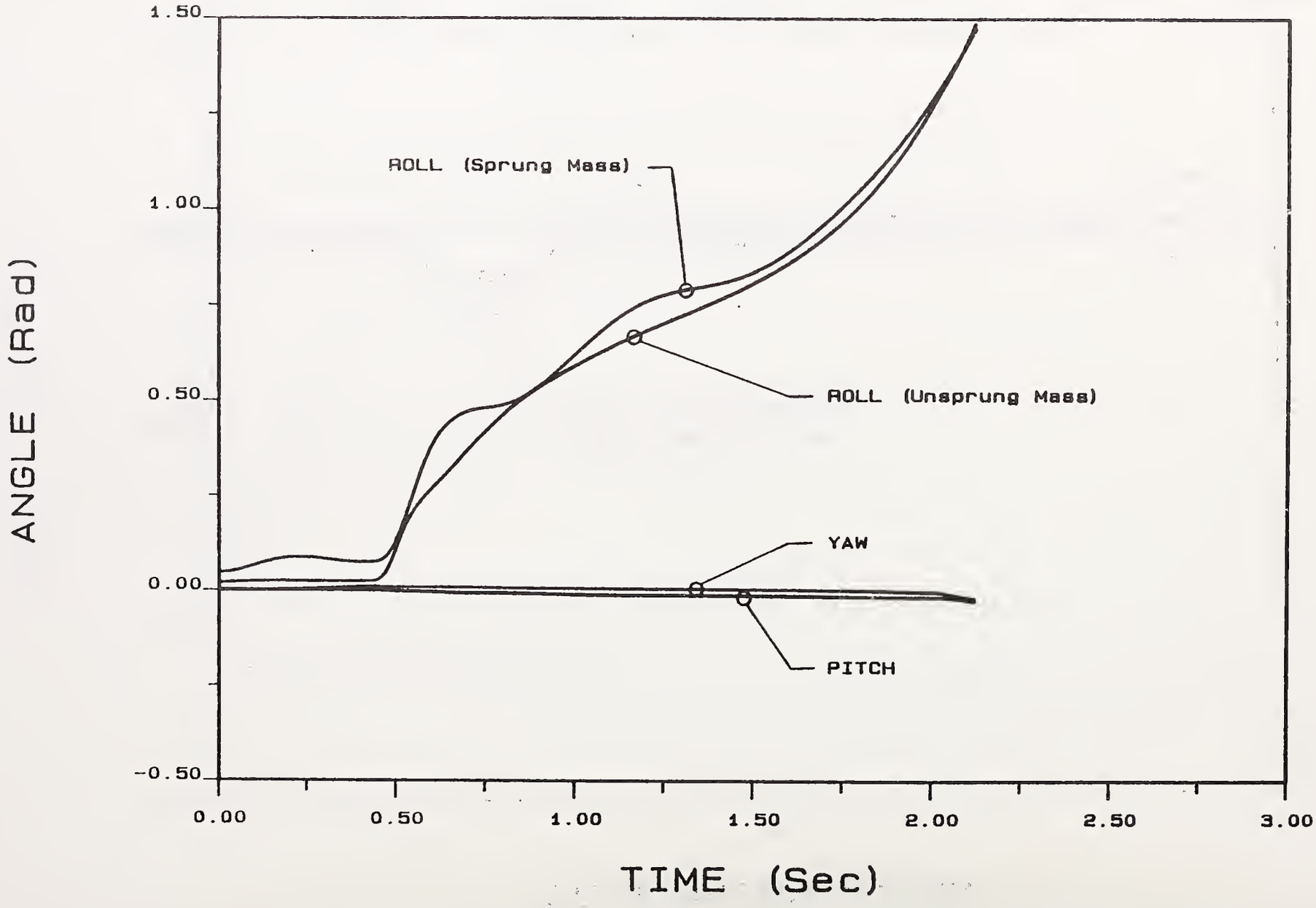

YUD=22.13 Ft/S : YA=7.5 Ft : PSI=0 Deg

ITRS ORIENTATION

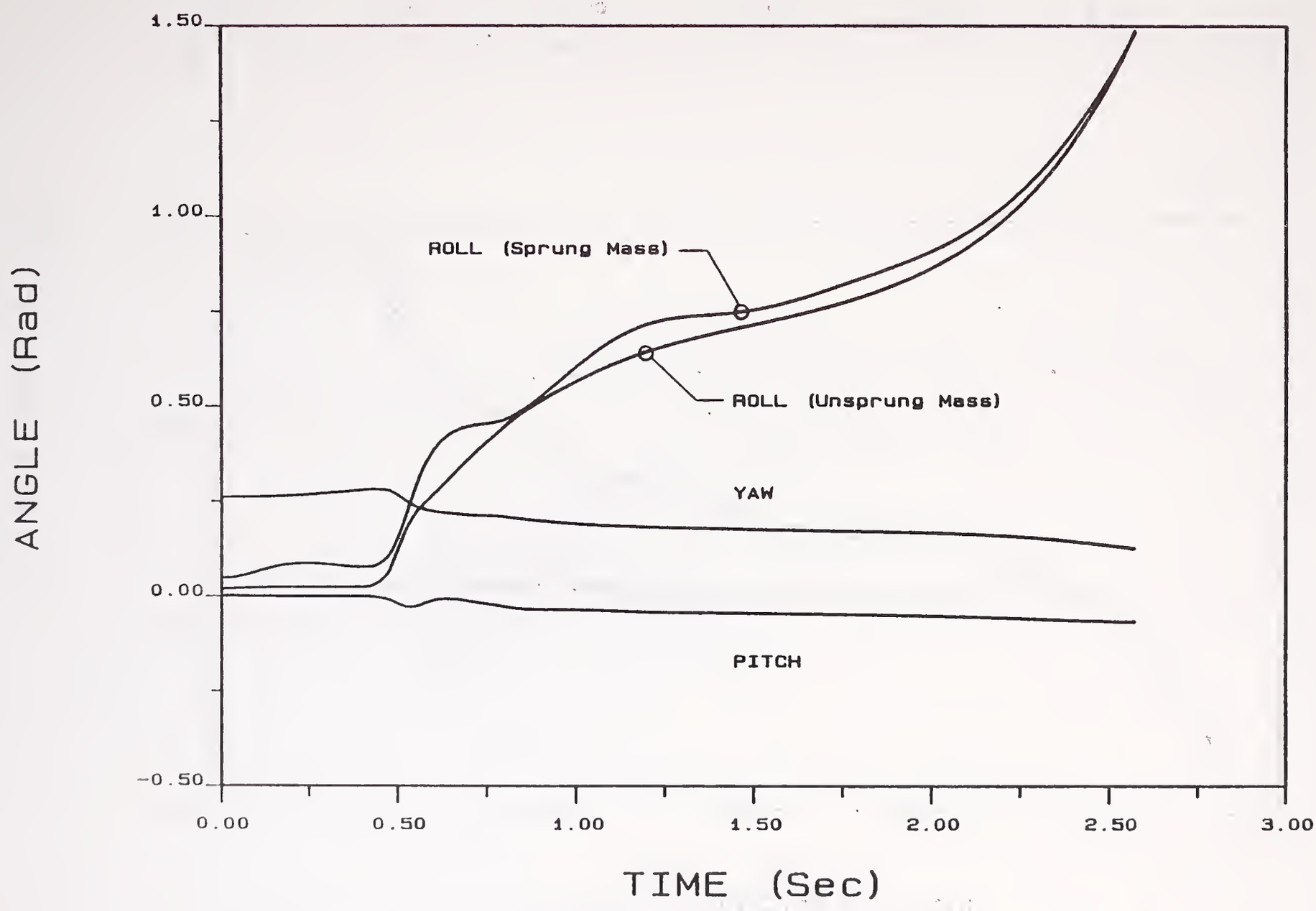

YUD=22.93 Ft/S : YA=7.5 Ft : PSI=15 Deg

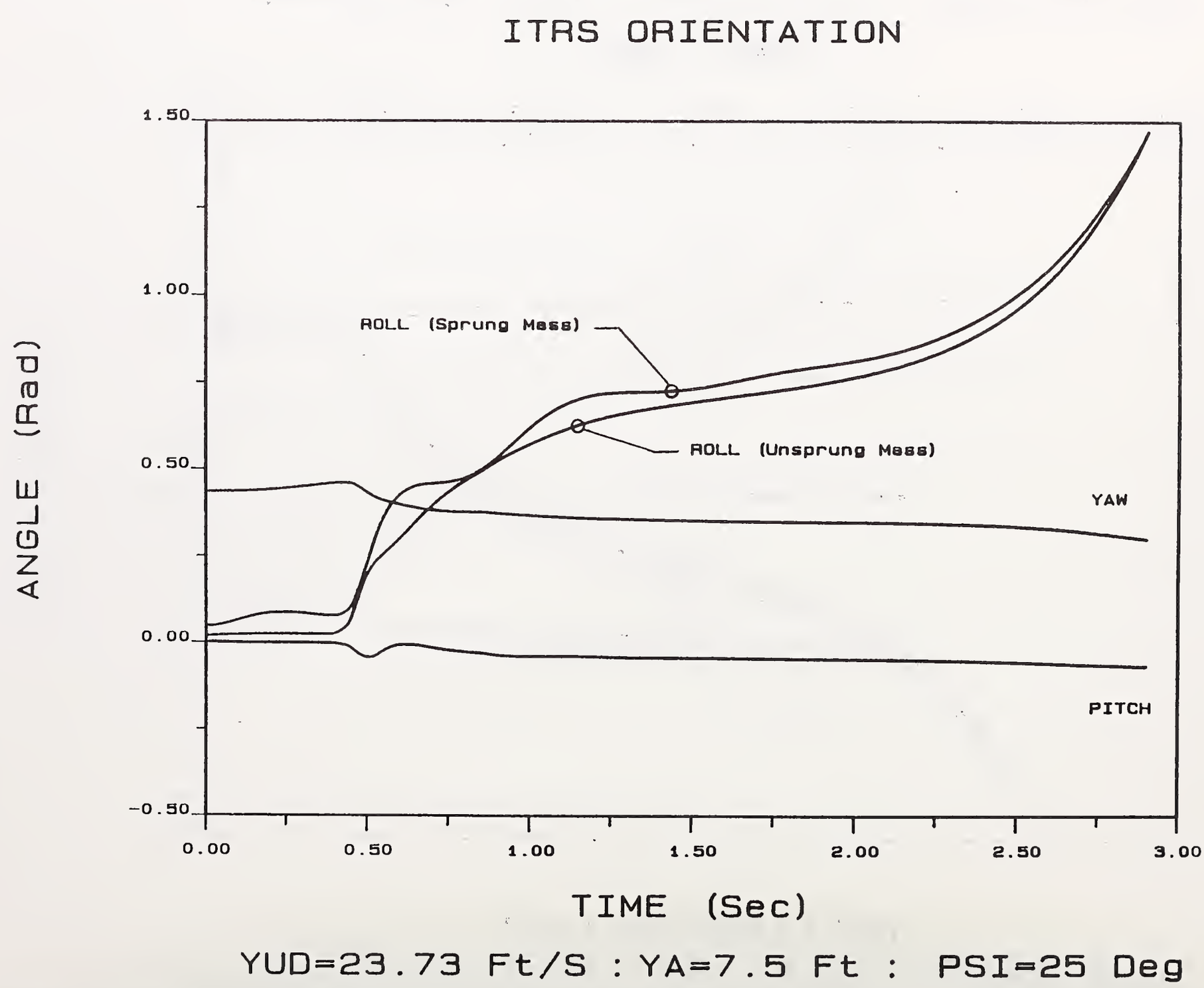
ITRS ORIENTATION
1.50
1.00
0.50
0.00
-0.50
ANGLE (Rad)
ROLL (Sprung Mass)
ROLL (Unsprung Mass)
YAW
PITCH
0.00
0.50
1.00
1.50
2.00
2.50
3.00
TIME (Sec)
YUD=23.73 Ft/S : YA=7.5 Ft : PSI=25 Deg

ITRS TRANSLATIONAL VELOCITIES

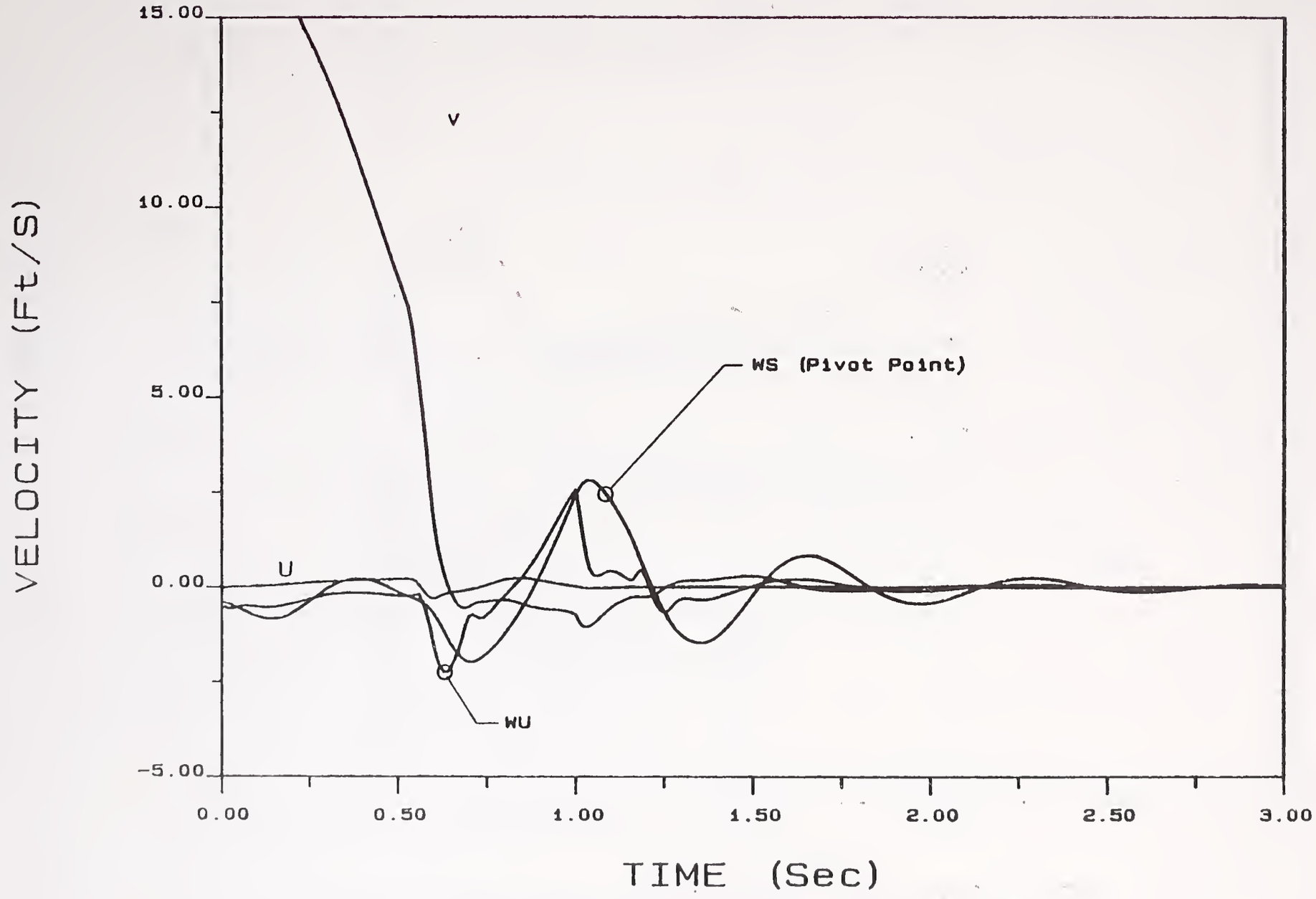

YUD=20 Ft/S : YA=7.5 Ft : PSI=0 Deg

ITRS TRANSLATIONAL VELOCITIES

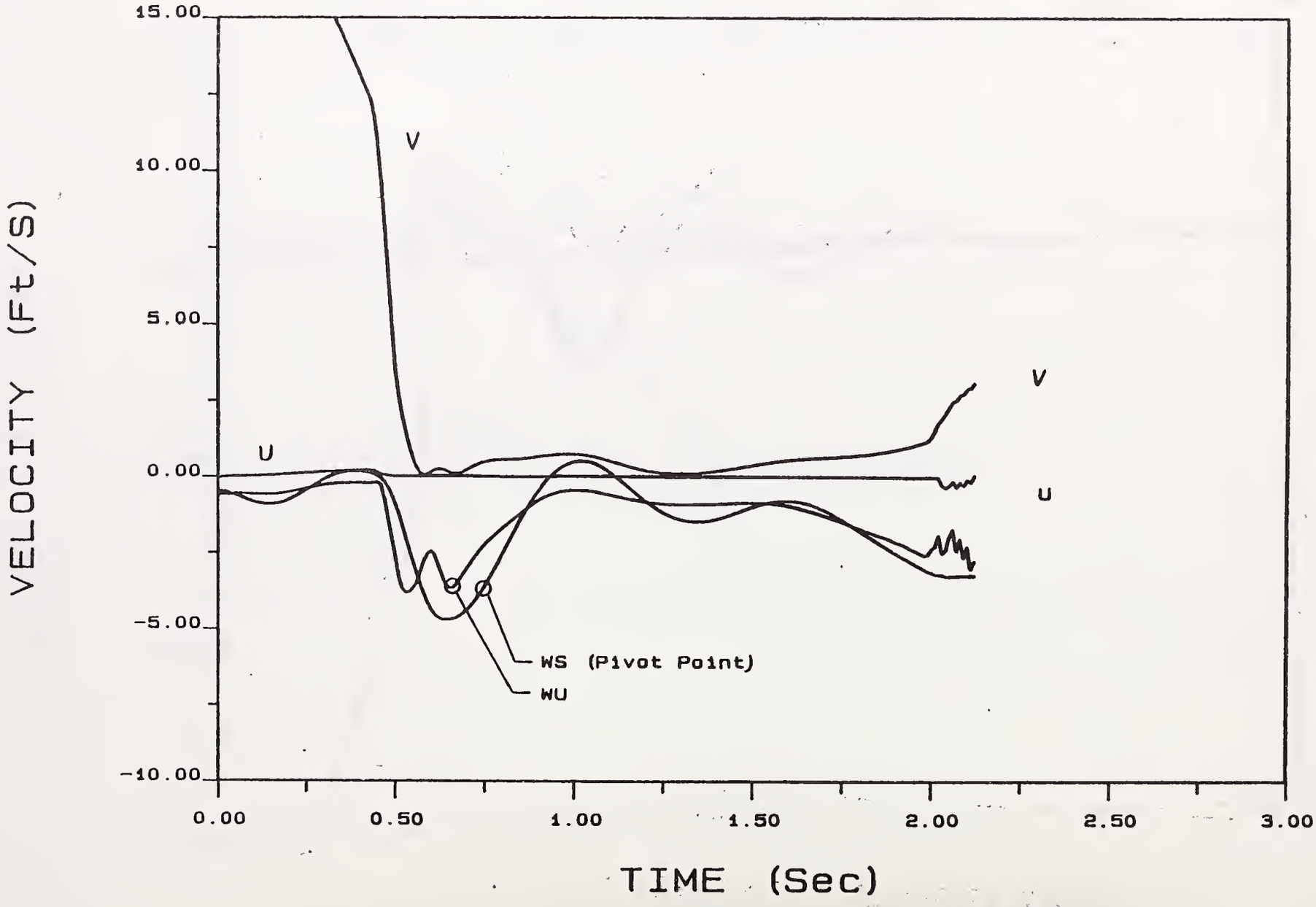

YUD=22.13 Ft/S : YA=7.5 Ft : PSI=0 Deg

ITRS TRANSLATIONAL VELOCITIES

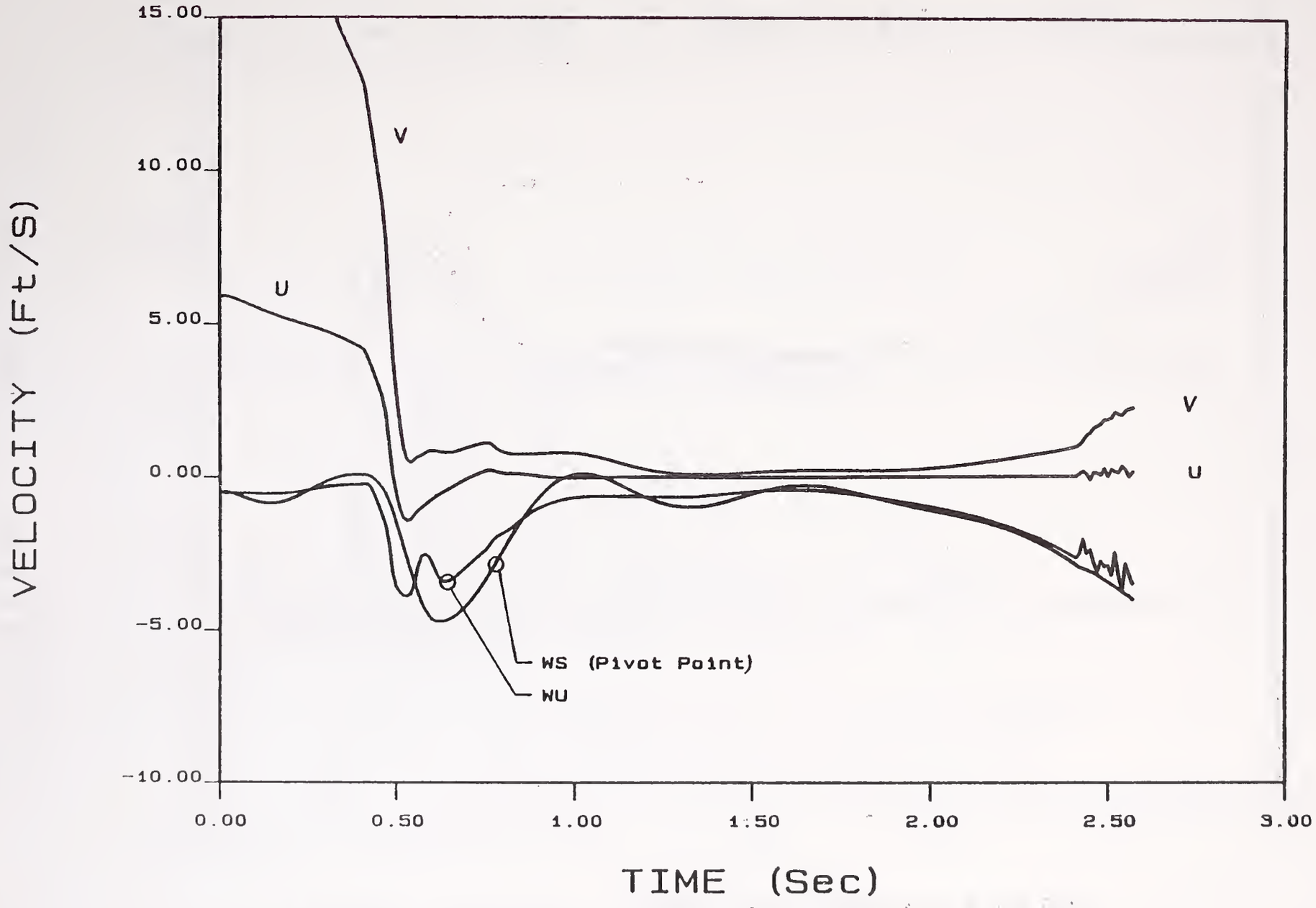

YUD=22.93 Ft/S : YA=7.5 Ft : PSI=15 Deg

ITRS TRANSLATIONAL VELOCITIES

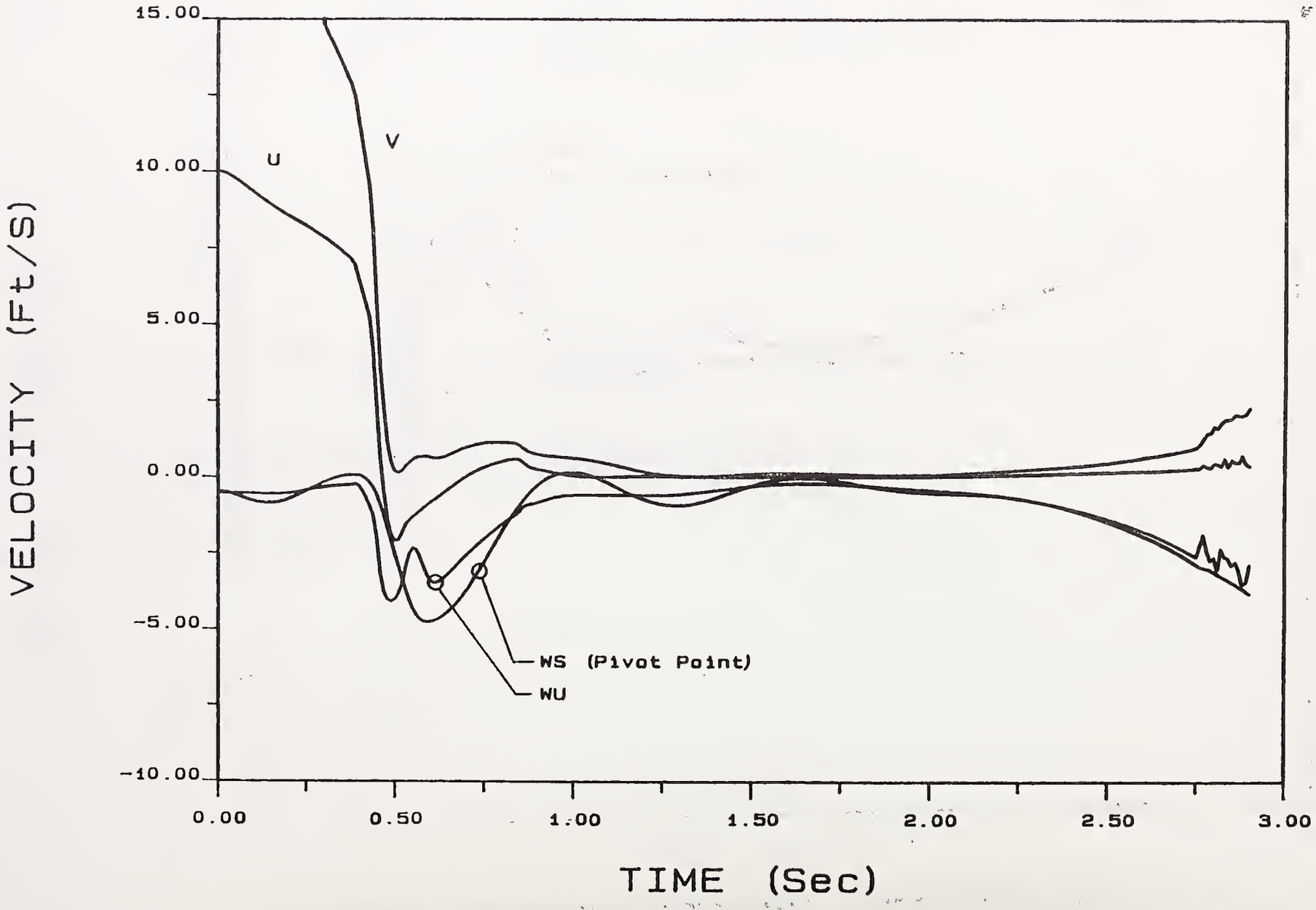

YUD=23.73 Ft/S : YA=7.5 Ft : PSI=25 Deg

ITRS ROTATIONAL QUASI-VELOCITIES

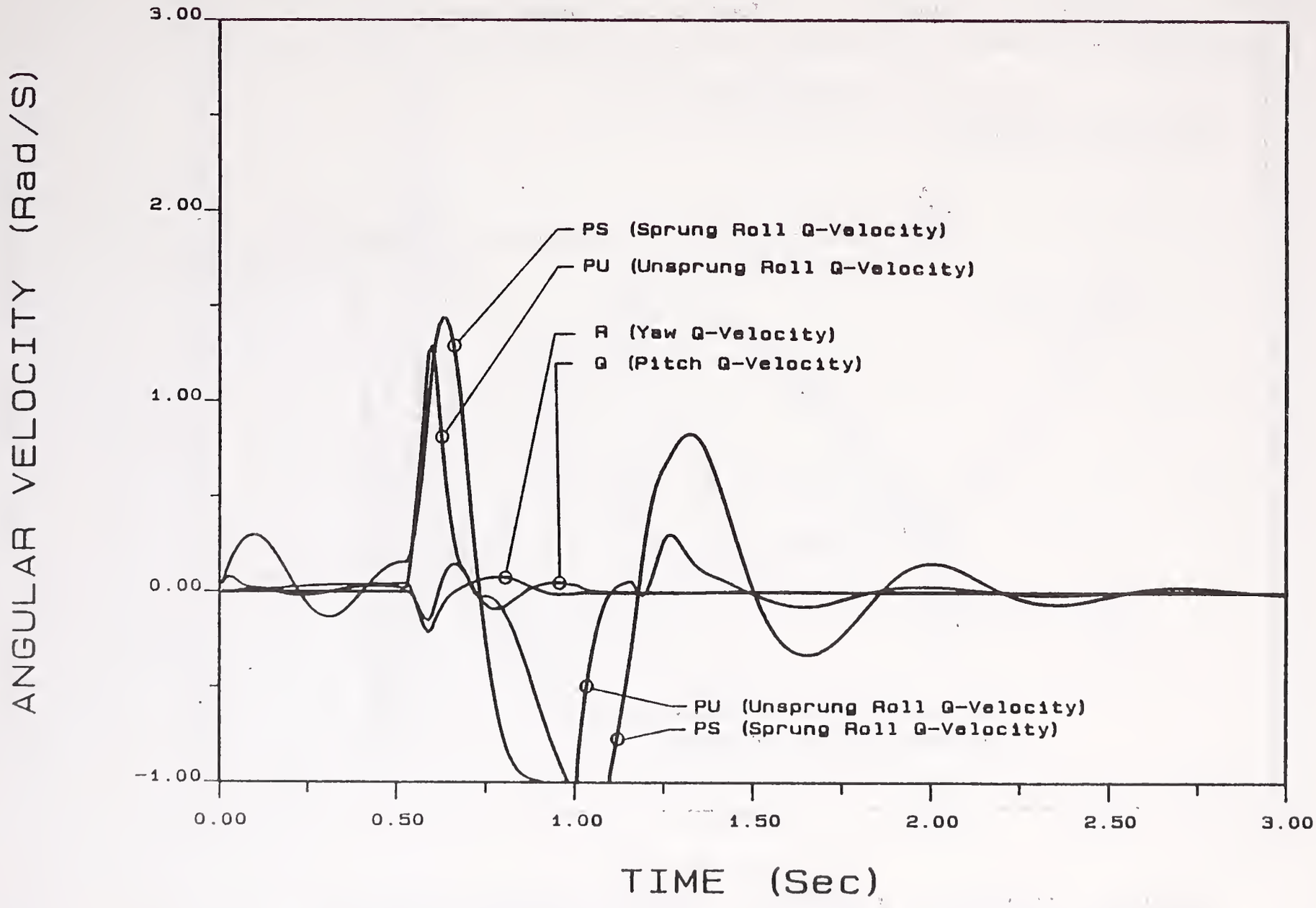

YUD=20 Ft/S : YA=7.5 Ft : PSI=0 Deg

ITRS ROTATIONAL QUASI-VELOCITIES

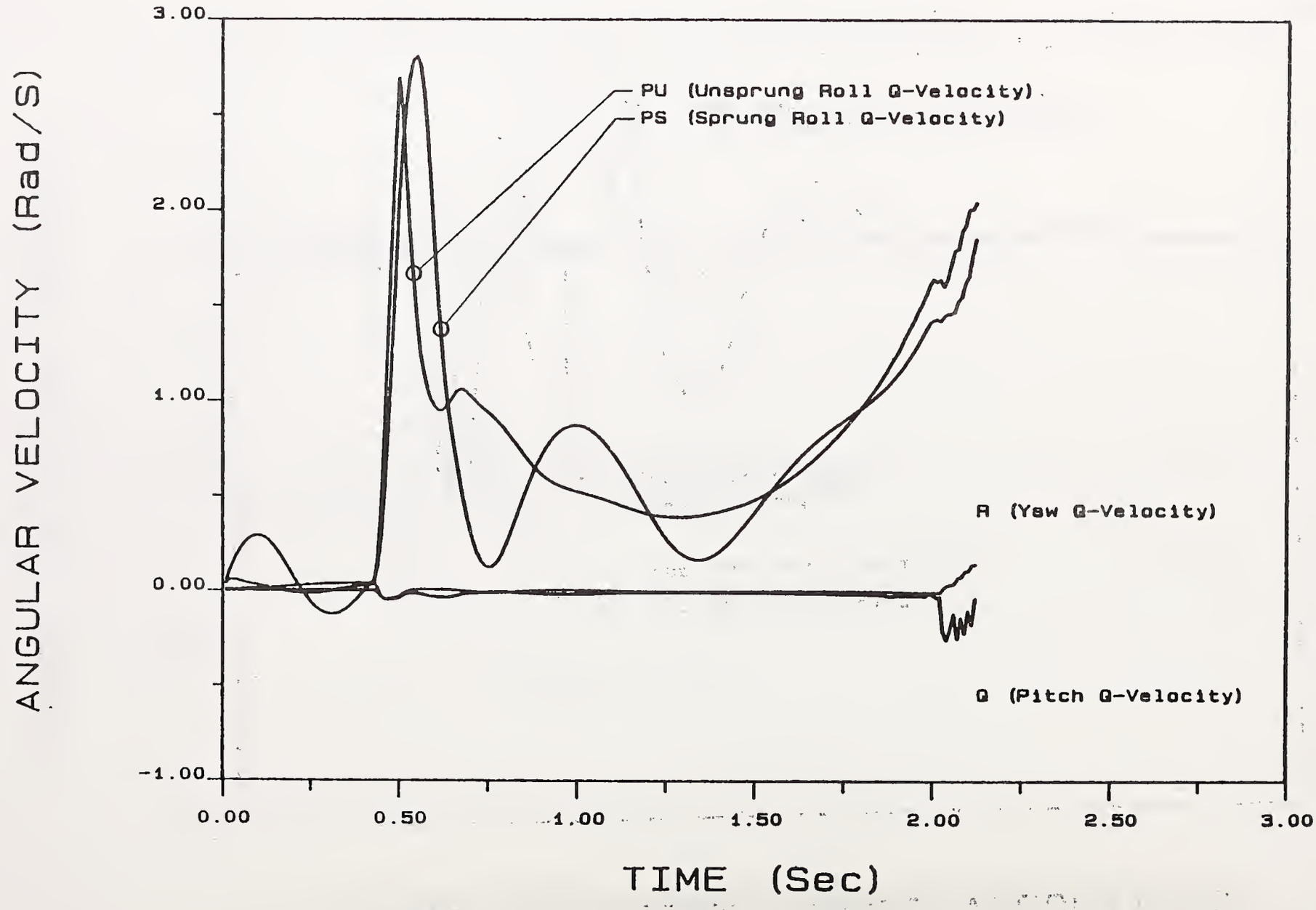

YUD=22.13 Ft/S : YA=7.5 Ft : PSI=0 Deg

ITRS ROTATIONAL QUASI-VELOCITIES

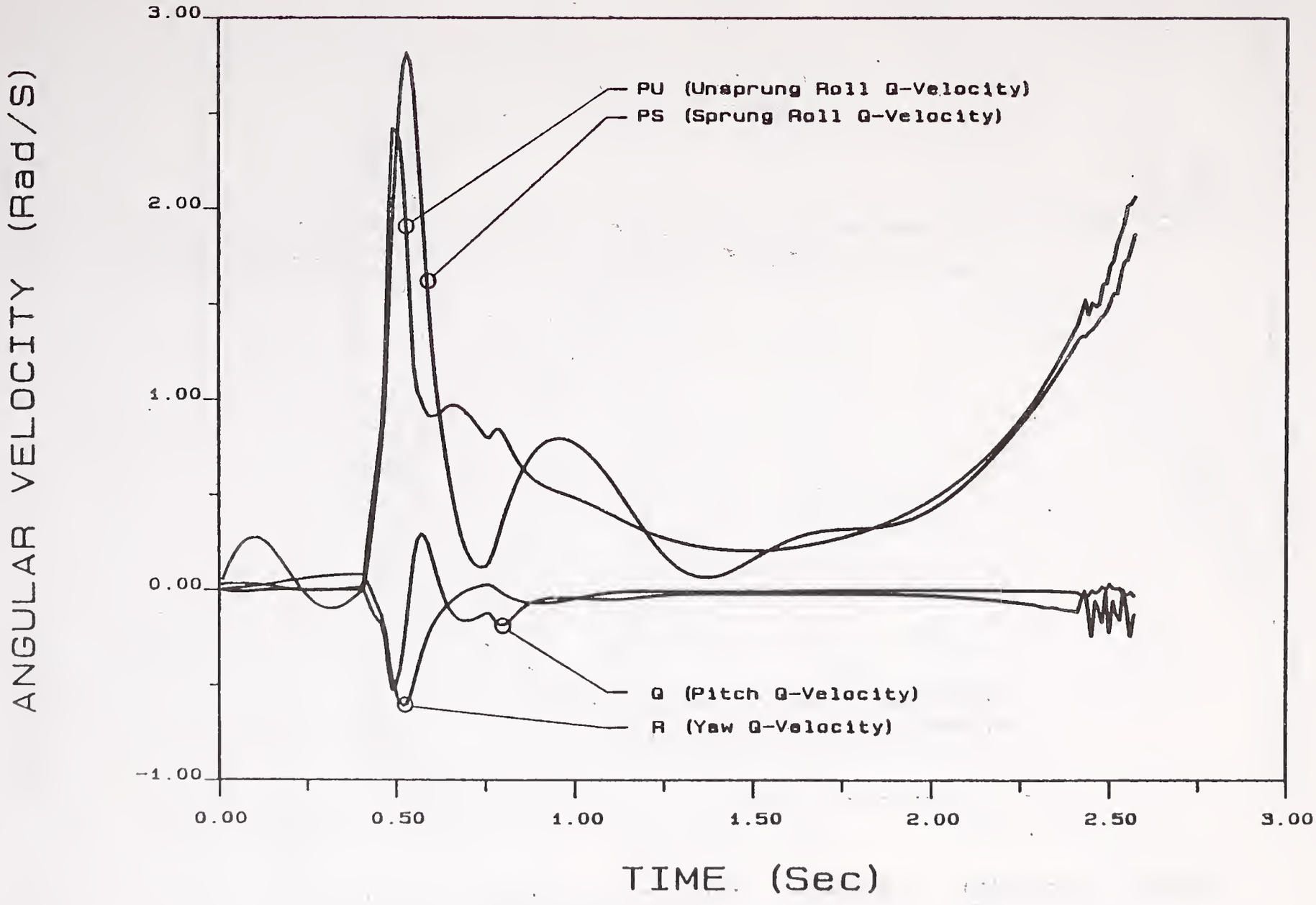

YUD=22.93 Ft/S : YA=7.5 Ft : PSI=15 Deg

ITRS ROTATIONAL QUASI-VELOCITIES

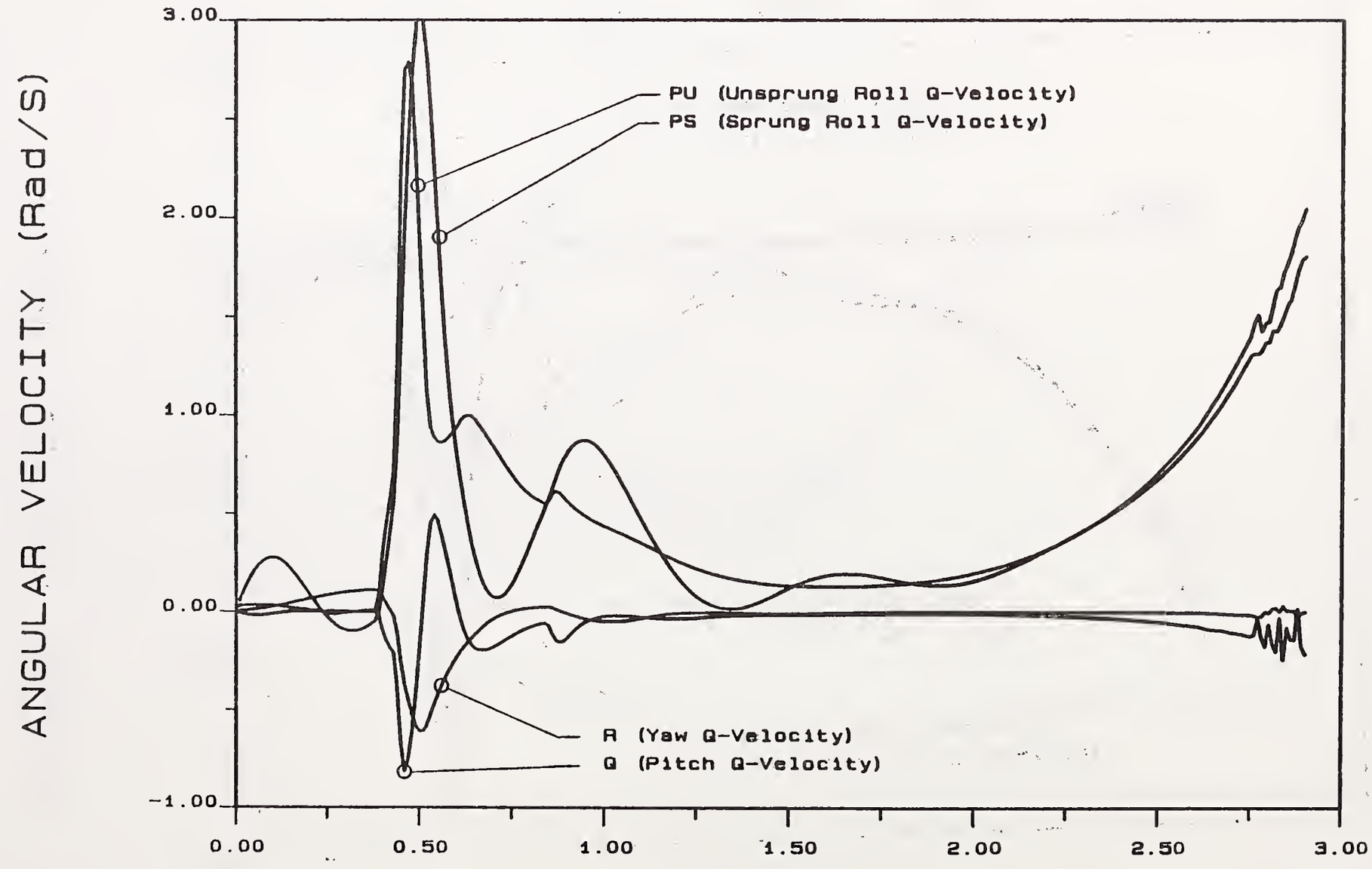

YUD=23.73 Ft/S : YA=7.5 Ft : PSI=25 Deg

APPENDIX E

User's Manual

The Intermediate Tripped Rollover Simulation (ITRS) is a FORTRAN subroutine developed to simulate a vehicle's skidding motion, impact of the front and rear wheels with a roadside curb, and the subsequent tripped rollover motion. The ITRS was developed to be used in conjunction with the sensitivity programs developed earlier by UMC. For more information regarding the use of vehicle model subroutines, such as ITRS, and the sensitivity programs refer to the example subroutines shown in the NHTSA reports:

(1) "Sensitivity Analysis of Vehicle Design Attributes that Affect Vehicle Response in Critical Accident Situations - Part 1: User's Manual", Nalecz A. G., et al., Report No. DOT HS 807 229, December 1987.

(2) "Sensitivity Analysis of Vehicle Design Attributes that Affect Vehicle Response in Critical Accident Situations - Part 2: Technical Report", Nalecz A. G., et al., Report No. DOT HS 807 230, December 1987.

A familiarity with both of these reports will facilitate use of the ITRS model subroutine.

The ITRS model subroutine can be utilized in two separate Fortran programs. The first program, ROLGEAR, can be used to find the time response of a vehicle in a rollover situation. The second program, TRANS, can be used to find the time domain sensitivity of vehicle parameters on system response. A program called PREPROC is used by both ROLGEAR and TRANS to generate a set of initial conditions needed to run the simulation.

1.0 Installation of ITRS Programs

The files needed to utilize the ITRS come on a single 360K floppy disk. This disk contains the following programs:

ROLGEAR. FOR	Main integration program
PREPROC. FOR	Data preprocessor program
ITRS. FOR	ITRS model subroutine
GAUSS. FOR	Simultaneous equation subroutine
INPUTI. FOR	Subroutine to read initial conditions file
VDATA. FOR	Subroutine to read vehicle data file
DRVT. FOR	Subroutine to compute numeric derivatives
FCN. FOR	Function subprogram required by IMSL routine DGEAR
FCNJ. FOR	Function subprogram required by IMSL routine DGEAR
TEST. INI	Sample initial conditions data file
VDAT. DAT	Sample vehicle data file
LIB. COM	DCL com file used to build an object library

1.1 Hardware and Software Requirements

To install and use the ITRS model the user must have access to the following hardware and software:

1. VAX Mini computer running under the VMS operating system and FORTRAN 77 compiler.
2. An IBM PC or compatible with a connection, such as a modem or direct port, to the VAX mainframe.
3. Version 9.2 of the Double Precision IMSL Library.
4. Sensitivity programs referenced above.

1.2 Generating Executable Versions of the ITRS on a VAX

The source code for the ITRS model should be uploaded from the IBM PC to VAX by using a suitable communication program of the user's choice (such as KERMIT or PROCOMM).

After the software has been uploaded onto the VAX, the user should create and build the object library which will contain the object

codes used for the ITRS subroutines. This library, which will be given the name TRNS, can be created by issuing the following VMS command:

```
$ LIBRARY/CREATE TRNS
```

The source codes are compiled and inserted into the library TRNS by issuing the following commands:

```
$ @LIB TRNS ITRS
$ @LIB TRNS GAUSS
$ @LIB TRNS FNC
$ @LIB TRNS FCNJ
$ @LIB TRNS INPUT1
$ @LIB TRNS VDATA
```

To compile the data preprocessor (PREPROC. FOR) and the main ITRS programs (ROLGEAR.FOR and TRANS.FOR), type the following commands.

```
$ FORTRAN PREPROC
$ FORTRAN ROLGEAR
$ FORTRAN TRANS
```

The three programs can then be linked to the necessary subroutine and run-time libraries by issuing the following commands:

```
$ LINK PREPROC,TRNS/LIB
$ LINK ROLGEAR,TRNS/LIB,IMSLIBD/LIB
$ LINK TRANS,TRNS/LIB,IMSLIBD/LIB
```

These commands will create the following executable files:

```
ROLGEAR.EXE
PREPROC.EXE
TRANS.EXE
```

(Note: If problems are encountered during this step consult your system manager to find the command syntax necessary to link with Version 9.2 of the IMSL math library)

Once the programs have been successfully linked they are in executable form and are ready to run.

2.0 Finding Initial Conditions for the ITRS Using PREPROC

The ITRS model consists of a system of simultaneous first order differential equations of motion which are integrated in order to determine the response of the vehicle. These differential equations require initial conditions for integration. Because the ITRS simulation typically begins with the vehicle sliding toward the curb at a large slide slip angle it is necessary to obtain an estimate of sprung and unsprung roll angles in order to reduce oscillations in these state variables during the initial phases of the simulation. The data preprocessing program PREPROC was developed to determine suitable values for the initial conditions of the differential equations of motion and facilitate the creation of the the initial condition data file. The user enters the values of position and velocity which are necessary to define the conditions of the simulation and PREPROC generates a file containing a set of initial conditions which represents an initial quasi-static equilibrium state of the vehicle. It is not mandatory that the preprocessing program PREPROC is used to obtain the quasi-static initial condition values, however, use of the preprocessor will reduce initial oscillations in simulation results. The vehicle position and velocity data required by PREPROC are summarized below.

XU - Initial longitudinal position (usually 0.0).

YU - Initial lateral position (usually 0.0). Note: this is not the distance to the curb but the distance from the origin of the inertial reference system to the unsprung mass CG.

ZU - Initial unsprung mass vertical position (usually a negative number). This is the unsprung mass CG height.

ZS - Initial pivot point vertical position (usually a negative number). This is <u>not</u> the sprung mass CG, but CG height minus HRA.

YAW - Initial yaw angle (in radians, usually ranges from -0.78 to 0.78).

THE - Initial pitch angle (usually 0.0).

H - Initial distance between unsprung mass CG and pivot point (given as a positive number for a pivot point above the unsprung mass CG).

codes used for the ITRS subroutines. This library, which will be given the name TRNS, can be created by issuing the following VMS command:

```
$ LIBRARY/CREATE TRNS
```

The source codes are compiled and inserted into the library TRNS by issuing the following commands:

```
$ @LIB TRNS ITRS
$ @LIB TRNS GAUSS
$ @LIB TRNS FNC
$ @LIB TRNS FCNJ
$ @LIB TRNS INPUT1
$ @LIB TRNS VDATA
```

To compile the data preprocessor (PREPROC. FOR) and the main ITRS programs (ROLGEAR.FOR and TRANS.FOR), type the following commands.

```
$ FORTRAN PREPROC
$ FORTRAN ROLGEAR
$ FORTRAN TRANS
```

The three programs can then be linked to the necessary subroutine and run-time libraries by issuing the following commands:

```
$ LINK PREPROC,TRNS/LIB
$ LINK ROLGEAR,TRNS/LIB,IMSLIBD/LIB
$ LINK TRANS,TRNS/LIB,IMSLIBD/LIB
```

These commands will create the following executable files:

```
ROLGEAR.EXE
PREPROC.EXE
TRANS.EXE
```

(Note: If problems are encountered during this step consult your system manager to find the command syntax necessary to link with Version 9.2 of the IMSL math library)

Once the programs have been successfully linked they are in executable form and are ready to run.

2.0 Finding Initial Conditions for the ITRS Using PREPROC

The ITRS model consists of a system of simultaneous first order differential equations of motion which are integrated in order to determine the response of the vehicle. These differential equations require initial conditions for integration. Because the ITRS simulation typically begins with the vehicle sliding toward the curb at a large slide slip angle it is necessary to obtain an estimate of sprung and unsprung roll angles in order to reduce oscillations in these state variables during the initial phases of the simulation. The data preprocessing program PREPROC was developed to determine suitable values for the initial conditions of the differential equations of motion and facilitate the creation of the the initial condition data file. The user enters the values of position and velocity which are necessary to define the conditions of the simulation and PREPROC generates a file containing a set of initial conditions which represents an initial quasi-static equilibrium state of the vehicle. It is not mandatory that the preprocessing program PREPROC is used to obtain the quasi-static initial condition values, however, use of the preprocessor will reduce initial oscillations in simulation results. The vehicle position and velocity data required by PREPROC are summarized below.

XU - Initial longitudinal position (usually 0.0).

YU - Initial lateral position (usually 0.0). Note: this is not the distance to the curb but the distance from the origin of the inertial reference system to the unsprung mass CG.

ZU - Initial unsprung mass vertical position (usually a negative number). This is the unsprung mass CG height.

ZS - Initial pivot point vertical position (usually a negative number). This is not the sprung mass CG, but CG height minus HRA.

YAW - Initial yaw angle (in radians, usually ranges from -0.78 to 0.78).

THE - Initial pitch angle (usually 0.0).

H - Initial distance between unsprung mass CG and pivot point (given as a positive number for a pivot point above the unsprung mass CG).

XUD - Initial longitudinal velocity in absolute reference system (usually 0.0). This is the velocity of the vehicle parallel to the curb.

YUD - Initial lateral velocity in absolute reference system (varies). This is the velocity of the vehicle toward the curb.

ZUD - Initial unsprung mass vertical velocity in absolute reference system (usually 0.0).

ZSD - Initial pivot point vertical velocity in absolute reference system (usually 0.0).

YAWD - Initial yaw angular velocity (usually 0.0).

THED - Initial pitch angular velocity (usually 0.0).

PHIUD - Initial unsprung mass roll angular velocity (usually 0.0).

PHISD - Initial sprung mass roll angular velocity (usually 0.0).

The vehicle data parameter set is located in a separate data file (VDAT.DAT). This file is divided into two parts. The first part contains the parameter values used to describe the vehicle. The second part, which starts after the line labeled ENDSP contains a list of the state variables, as well as other program output. Each line of the vehicle data file has three fields. The first field represents a flag used during sensitivity analysis. This field is used only when the model is being used in conjunction with program TRANS in order to determine sensitivity functions. If program ROLGEAR is used to obtain the system response of a vehicle in a tripped rollover situation then the values contained in this field are irrelevant. The second field contains a description of the parameter or variable associated with that line. The third field contains the numerical value of each parameter. For more details concerning the VDAT.DAT file and the flagging of variables and parameters see the Sensitivity Analysis User's Manual.

```
0,'{A}      DISTANCE - CG TO FRT AXLE ',4.45D0
1,'{L}      WHEELBASE                 ',9.25D0
0,'{HRA}    DIST - PIN TO MS CG       ',0.8667D0
0,'{HS}     DIST - MS BOTTOM TO MS CG ',1.2D0
```

```
0,'{HU}      DIST - AXLE TO MU CG       ',0.2D0
0,'{TRW}     VEHICLE TRACK WIDTH        ',5.0D0
0,'{ABSDEF}  DIST - AXLE TO BUMP STOPS  ',0.25D0
0,'{HCURB}   HEIGHT OF CURB             ',0.5D0
1,'{TRAD}    TIRE RADIUS                ',1.0D0
0,'{S}       HALF DIST OF SPRING BASE   ',1.75D0
0,'{SPRLNG}  UNLOADED SPRING LENGTH     ',0.6667D0
0,'{YO}      LATERAL POSITION OF CURB   ',07.5D0
0,'{MS}      SPRUNG MASS                ',105.0D0
0,'{MU}      UNSPRUNG MASS              ',16.7D0
0,'{IXXS|    SPRUNG ROLL INERTIA        ',240.0D0
0,'{IYYS}    SPRUNG PITCH INERTIA       ',2000.0D0
0,'{IZZS}    SPRUNG YAW INERTIA         ',2400.0D0
0,'{IXXU}    UNSPRUNG ROLL INERTIA      ',132.0D0
0,'{IYYU|    UNSPRUNG PITCH INERTIA     ',380.0D0
0,'{IZZU}    UNSPRUNG YAW INERTIA       ',320.0D0
0,'{IXYS}    SPRUNG PDT OF INERTIA      ',1.954D0
0,'{IXZS}    SPRUNG PDT OF INERTIA      ',-30.62D0
0,'{IYZS}    SPRUNG PDT OF INERTIA      ',10.82D0
0,'{IXYU}    UNSPRUNG PDT OF INERTIA    ',0.4D0
0,'{IXZU}    UNSPRUNG PDT OF INERTIA    ',-6.0D0
0,'{IXZU}    UNSPRUNG PDT OF INERTIA    ',2.0D0
0,'{SUSK1}   SUSPENSION SPRING CONST    ',3450.0D0
0,'{SUSK2}   BUMP STOP SPRING CONST     ',16500.0D0
0,'{KD1}     IMPACT MODEL - REGION 1    ',24000.0D0
0,'{KD2}     IMPACT MODEL - REGION 2    ',000.0D0
0,'{KD3}     IMPACT MODEL - UNLOADING   ',96000.0D0
0,'{KD4}     IMPACT MODEL - REGION 3    ',96000.0D0
0,'{KZ}      SINGLE TIRE SPRING CONST   ',12000.0D0
0,'{B1}      SUSPENSION DAMPING CONST.  ',62.50D0
0,'{B2}      BUMP STOP DAMPING CONST.   ',16.50D0
0,'{BD}      CURB FORCE DAMPING CONST'  ',.25D0
0,'{BZ}      SINGLE TIRE DAMPING CONST  ',80.0D0
0,'{MUX}     LONGIT. FRICTIONAL CONST   ',0.750D0
0,'{MUY}     LATERAL FRICTIONAL CONST.  ',0.75D0
0,'{MUS}     TIRE/CURB FRICT CONST      ',0.720D0
0,'{KV}      VEL. OF SIDE VEL. FUNCTN   ',0.0D0
0,'{KVF}     VEL. OF FORW. VEL FUNCTN   ',1.0D0
0,'{POINT1}  CHANGE OF SLOPE IN IMPACT  ',0.1667D0
0,'{POINT2}  CHANGE OF SLOPE IN IMPACT  ',0.6667D0
0,'{DUMMY}   DUMMY PARAMETER            ',1.0D0
0,'ENDPP                                ',0.0D0
0,' SRSF     - PC1                      ',1.0D0
0,' IRSF     - PC2                      ',1.0D0
0,'ENDSP                                ',0.0D0
0,'1  XU   - LONGITUDINAL POSITION      ',0.0D0
0,'2  YU   - LATERAL POSITION           ',0.0D0
0,'3  ZU   - UNSPRUNG MASS VERTICAL     ',0.0D0
0,'4  ZS   - SPRUNG MASS VERTICAL       ',0.0D0
0,'5  PHIU - UNSPRUNG ROLL ANGLE        ',0.0D0
1,'6  PHIS - SPRUNG ROLL ANGLE          ',0.0D0
0,'7  YAW  - VEHICLE YAW ANGLE          ',0.0D0
0,'8  THE  - VEHICLE PITCH ANGLE        ',0.0D0
0,'9  YA   - FRONT RIGHT TIRE POST.     ',0.0D0
0,'10 H    - RELATIVE VERTICAL POST.    ',0.0D0
0,'11 UU   - FORW.   VELOCITY           ',0.0D0
0,'12 VV   - LATERAL   VELOCITY         ',0.0D0
0,'13 WU   - MU VERTICAL Q-VELOCITY     ',0.0D0
```

```
0,'14 WS    - MS VERTICAL Q-VELOCITY    ',0.0D0
0,'15 PU    - MU ROLLING Q-VELOCITY     ',0.0D0
0,'16 PS    - MS ROLLING Q-VELOCITY     ',0.0D0
0,'17 RR    - YAWING  Q-VELOCITY        ',0.0D0
0,'18 QQ    - PITCHING Q-VELOCITY       ',0.0D0
0,'18 YR    - REAR TIRE LATERAL POSITI  ',0.0D0
0,'20 TRAN     - TOTAL TRANSLAT ENERGY  ',0.0D0
0,'21 TROT     - TOTAL SYSTEM ROT ENERG',0.0D0
0,'22 POTEN    - TOTAL SYSTEM POTEN ENE',0.0D0
0,'23 ELAS     - TOTAL ELASTIC ENERGY   ',0.0D0
0,'24 ENERG    - TOTAL SYSTEM ENERGY    ',0.0D0
0,'25 DGRAV    - GRAV ENERGY CHANGE     ',0.0D0
0,'26 DELAST   - ELAST ENERGY CHANGE    ',0.0D0
0,'27 TNR      - NONCENTROIDAL ROLL KE  ',0.0D0
0,'28 NO VARIABLE                       ',0.0D0
0,'29 NO VARIABLE                       ',0.0D0
0,'30 DE_TI    - TIRE ELAS ENER CHANGE  ',0.0D0
0,'31 DE_SP    - SUSP ELAS ENER CHANGE  ',0.0D0
0,'32 DE_IM    - IMPA ELAS ENER CHANGE  ',0.0D0
0,'32 RPER     - ORIGINAL VERSION       ',0.0D0
0,'34 VCRITM   - INSTAST MODIF RPER     ',0.0D0
0,'35 TRANSP   - KE RELATIVE TRAN       ',0.0D0
0,'36 NO VARIABLE                       ',0.0D0
0,'37 VCRIT    - GRAV ENER FOR ROLL     ',0.0D0
0,'38 RPER3    - VERSION 4              ',0.0D0
0,'ENDOV                                ',0.0D0
```

All vehicle data and initial conditions should be entered in English units, angles are entered in radians.

To execute PREPROC type:

```
$ run preproc
```

Then answer the following questions as shown below:

```
   SENSITIVITY ANALYSIS IN THE TIME DOMAIN

        C COPYRIGHT DECEMBER 1987 BY
  THE CURATORS OF THE UNIVERSITY OF MISSOURI,
            A PUBLIC CORPORATION


INITIAL VEHICLE DATA IN THE ABSOLUTE REFERENCE SYSTEM
ENTER DATA AS A DOUBLE PRECISION NUMBER (EX. 1.0D0)

PLEASE INPUT VEHICLE INITIAL YAW ANGLE (rad)
0.0d0

PLEASE INPUT VEHICLE INITIAL PITCH ANGLE (rad)
0.0d0
```

```
PLEASE INPUT VEHICLE INITIAL X POSITION (Ft)
0.0d0

PLEASE INPUT VEHICLE INITIAL Y POSITION (Ft)
0.0d0

PLEASE INPUT VEHICLE INITIAL UNSPRUNG MASS Z POSITION (Ft)
-1.11d0

PLEASE INPUT VEHICLE INITIAL PIVOT POINT Z POSITION (Ft)
-1.6633d0

PLEASE INPUT VEHICLE INITIAL VEHICLE YAW RATE (rad/s)
0.0d0

PLEASE INPUT VEHICLE INITIAL PITCH RATE (rad/s)
0.0d0

PLEASE INPUT VEHICLE INITIAL LONGITUDINAL VELOCITY (Ft/s)
0.0d0
PLEASE INPUT VEHICLE INITIAL LATERAL VELOCITY (Ft/s)
25.0d0

PLEASE INPUT VEHICLE INITIAL UNSPRUNG MASS VERTICAL VELOCITY (Ft/s)
0.0d0

PLEASE INPUT VEHICLE INITIAL PIVOT POINT VERTICAL VELOCITY (Ft/s)
0.0d0

PLEASE INPUT INITIAL RELATIVE HEIGHT OF THE TWO MASSES
IN THE UNSPRUNG NIRS (Ft)
.5533d0
```

The user is free to vary any of the initial conditions shown above. In most cases, however, different tripped rollover events are investigated by varying the initial lateral or longitudinal vehicle velocity, or initial yaw angle.

```
Y( 1) =    0.0000
Y( 2) =    0.0000
Y( 3) =   -1.1100
Y( 4) =   -1.6633
Y( 5) =    0.0000
Y( 6) =    0.0000
Y( 7) =    0.0000
Y( 8) =    0.0000
Y( 9) =    0.0000
Y(10) =    0.5533
Y(11) =    0.0000
Y(12) =   24.9949
Y(13) =   -0.5052
Y(14) =   -0.5052
Y(15) =    0.0000
Y(16) =    0.0000
```

```
Y(17) =     0.0000
Y(18) =     0.0000
Y(19) =     0.0000


*** Data Required By IMSL Routine DGEAR ****

Default Values

H     = .5D-03
TOL   = .1D-06
METH =1
MITER=2
INDEX=1

Do you wish to change any of these parameters (Y/N)
n


Input the Number of State Variables

39

*** Program Parameters ***

Derivative Method - Central Difference With 3 Points
Percent used in Central Difference - 1.0D-2

Do You Wish to Change These Parameters (Y/N)
n

*** Simulation Duration and Output Increment ***

Input Total Run Time (Double Precision)
3.5d0

Input Output Time Increment (Double Precision)
.5d0

Input Filename For Output Data
test.out

Would You Like the Program to Create a Plotting Output File (Y/N)
y

Input Storage Time Increment for Plot (Double Precision)
.01d0

Input Filename For Plotting Data
test.plt

Do You Want to Store This Data in a File (Y/N)
y

What Filename Do You Wish to Give the Input Data
test.ini

FORTRAN STOP
```

The set of quasi-static initial conditions, along with all other required simulation parameters are stored in file named TEST.INI.

3.0 Running the ITRS Simulation ROLGEAR

Once the user has created an initial conditions file (TEST.INI) he may compute the time history of a tripped rollover by entering the following sequence of commands:

Note: If PREPROC was not used to generate the initial condition file (TEST.INI) then the user must select Data Entry option 1 (Enter From Keyboard) and answer the questions shown above in the description of PREPROC. After answering the questions the user may store their responses in a file. If the user chooses to run the simulation in this manner he should be aware that the initial conditions to the differential equations of motion may not represent an quasi-static equilibrium state and the simulation results may contain initial oscillations, especially in the roll angle of the vehicle.

```
$ RUN ROLGEAR


        C COPYRIGHT DECEMBER 1987 BY
  THE CURATORS OF THE UNIVERSITY OF MISSOURI,
            A PUBLIC CORPORATION


*** Data Entry ***

1.) Enter From Keyboard
2.) Read From File

2

Input Filename
test.ini

TIME =  .01
TIME =  .02
        .
        .
        .
        .
TIME =  3.5
FORTRAN STOP
```

If, during the simulation run, the rollover criteria is satisfied (when the vertical projection of the unsprung mass CG lies outside the vehicle track) or if the vehicle yaws through an angle greater than 90 degrees the simulation will inform the user of the condition and will then terminate.

Vehicle system response and other output data is stored in column form in 7 files. The first column in all files is time. The dashes signify a dummy variable no longer stored by the simulation and should contain a column of zeros. A brief explanation of all primary and secondary variables is contained in the VDAT.DAT file. An explanation of all primary and secondary variables stored in the output files is shown below.

File Name	Variables (In Column Order)								
	1	2	3	4	5	6	7	8	9
RG1.OUT -	T	XU	YU	ZU	ZS	PHIU	PHIS	YAW	THETA
RG2.OUT -	T	YA	H	UU	VV	WU	WS	PU	PS
RG3.OUT -	T	RR	QQ	YR					
ENERGY.OUT -	T	TRAN	TROT	POTEN	ELAS	ENERG			
ELASTIC.OUT -	T	DE_TI	DE_SP	DE_IM	TRANSP	DELAST	--		
COMP.OUT -	T	VCRIT	DE_TI	DE_SP	DE_IM	VCRITM	TRANSP	TNR	
RPER.OUT -	T	RPER	--	--	RPER3	--			

The results stored in these files can be down-loaded onto an IBM PC and plotted using available software packages such as Tech*Graph*Pad.

List and Description of Variables Stored in Vehicle Output Data Files

T	-	Time
XU	-	Longitudinal position of unsprung mass in absolute reference system
YU	-	Lateral position of unsprung mass in absolute reference system
ZU	-	Vertical position of unsprung mass in absolute reference system
ZS	-	Vertical position of sprung mass pivot point in absolute reference system
PHIU	-	Unsprung mass roll angle
PHIS	-	Sprung mass roll angle
YAW	-	Vehicle yaw angle
THE	-	Vehicle pitch angle
YA	-	Distance traveled by front right tire (perpendicular to the curb)
H	-	Vertical position of unsprung mass CG relative to sprung mass pivot point in the unsprung mass NIRS
UU	-	Vehicle forward velocity in the unsprung mass NIRS
VV	-	Vehicle lateral velocity in the unsprung mass NIRS
WU	-	Unsprung mass vertical velocity in the unsprung mass NIRS
WS	-	Sprung mass pivot point velocity in the unsprung mass NIRS
PU	-	Unsprung mass roll quasi-velocity
PS	-	Sprung mass roll quasi-velocity
RR	-	Vehicle yaw quasi-velocity
QQ	-	Vehicle pitch quasi-velocity
YR	-	Distance traveled by rear right tire (perpendicular to curb)
TRAN	-	Total vehicle translational energy
TROT	-	Total vehicle rotational energy
POTEN	-	Total vehicle gravitational potential energy
ELAS	-	Total vehicle elastic potential energy

ENERG - Total vehicle energy

DE_TI - Change in tire elastic energy

DE_SP - Change in suspension elastic energy

DE_IM - Change in impact elastic energy

TRANSP - Kinetic energy of relative translational motion

DELAST - Total vehicle elastic energy change

VCRIT - Energy required to bring vehicle to static tip-over angle

VCRITM - Energy term to account for changes in VCRIT due to Track width deformation and spring deflection

TNR - Vehicle non-centriodal rolling energy (about tire-curb contact point)

RPER - Rollover prevention energy reserve (VCRIT - TNR)

RPER3 - A modified rollover prevention energy reserve (includes terms for elastic potential energy, yawing kinetic energy, and track width deformation)

4.0 Running the Time Domain Sensitivity Algorithm

Before the user begins running the time domain sensitivity algorithm TRANS he must first decide which vehicle parameters and variables are of interest and flag these items in the vehicle data file VDAT.DAT. Each line of the vehicle data file consists of three fields. In the first half of the vehicle data file (the section containing the vehicle parameter data) this field contains a flag which is used to signal that sensitivity functions will be computed with respect to that parameter. These flags are set by replacing the value of 0 with 1. The second half of the vehicle data file contains the variables which are used to measure the vehicle's response to external inputs. If the user is interested in the sensitivity of one or more variables to changes in system parameters then he may select each parameter by placing a 1 in the field containing the sensitivity flag. The example data file shown in section 2.0 is flagged so that the sensitivity program will find the influence of wheelbase and tire radius on the roll angle of the sprung mass.

After the user has selected the parameters and variables of interest, the sensitivity program will compute the influence of each parameter

on each variable and store the results in printer and plotter output files. The names of the output files are those entered by the user while building the initial data file. After the user has generated an initial data file using program PREPROC then he may execute the Time Domain Sensitivity Algorithm as shown below:

```
$ RUN TRANS


   SENSITIVITY ANALYSIS IN THE TIME DOMAIN

        C COPYRIGHT DECEMBER 1987 BY
  THE CURATORS OF THE UNIVERSITY OF MISSOURI,
             A PUBLIC CORPORATION


*** Data Entry ***

1.) Enter From Keyboard
2.) Read From File

2

Input Filename
test.ini

FORTRAN STOP
```

After execution is completed, the results may be examined by printing out the results stored in the output data file (in the example run this file was named TEST.OUT). If the user requires graphs he may download the plotter data file (e.g. TEST.PLT) to an IBM PC and plot the results on either a screen, or a HP7475A plotter using the program SENSPLT. If the user desires a plotter output, the plotter must be connected to the PC's COM1 serial port.

For further information into the interpretation of the sensitivity results, the user may refer to the reports cited at the beginning of this manual.